THE UNIVERSITY
of EDINBURGH

Behavioural Testing and General Phenotyping of Mice with Mutations in *Eef1a2* to Investigate Autism, Intellectual Disability and Epilepsy

Jilly Evelyn Hope

THE UNIVERSITY *of* EDINBURGH

A thesis submitted for the degree of
Doctor of Philosophy

The University of Edinburgh
2018

Declaration

I declare that this thesis was composed by myself and that all work presented within is my own unless stated otherwise. All sources of information and other individuals' contributions have been appropriately acknowledged. This work has not been submitted for any other degree or professional qualification.

Jilly Evelyn Hope

I dedicate this thesis to my late biology teacher, Gordon Suttie, who guided me down this path.

Acknowledgements

There are so many people who have helped me in the last four years that I don't even know where to begin. First and most importantly, I'd like to give a huge thank you to my primary supervisor Professor Cathy Abbott. Your support, both on a scientific and a personal level, has been invaluable to me and I honestly couldn't have wished for a better mentor. I would also like to thank my second supervisor Dr Mandy Jackson along with my thesis committee Dr Kathy Evans and Professor Ian Jackson for great ideas and support along the way. Thanks also to BBSRC Eastbio DTP for providing me with the funding to complete this PhD project.

To the members of the Abbott lab: Amaka, Anna, Faith, Fiona, Francis and Vesa, you have made this such a lovely place to work. Thank you for all the laughter that kept me going through the tough times and all of your kind help with experiments. I couldn't have found a better group of people to work with if I tried. Many thanks also to past lab members Jennifer and Shannon and to all of the students: Charlie, James, James and Laura, who helped me with my project. I couldn't have done this without all of you. To the "dream team" girls: Amaka, Elena, Marion and Rodanthi, thank you for being such great friends.

I am hugely grateful to the staff at the BRF for all of their help with the mice. Especially the two Johns, Robert, Scott and Simon. Thank you so much for making me laugh during long days of behavioural experiments and being so accommodating when I needed things done with the mice. You always made me feel very welcome. Thanks also to the staff at the Evans unit for your help with the CRISPR experiments. I'd also like to give a big thank you to Dr Oliver Hardt, Dr Tine Pooters and Dr Emma Wood for giving me lots of advice and allowing me to borrow equipment for behavioural experiments. Thanks also to Richard Wroblewski at the HGU workshop for making apparatus for me.

I couldn't have gotten through the last four years without love and support from my friends and family. A massive thank you to my friends, Keir and Darryl, for meeting up with me regularly to have fun and take my mind off of work. It was nice to have two friends at the same stage of their PhD who understood how tough it could be. Thanks also to my friend Nora for always keeping me entertained! To my family, especially my mum Pam, my dad Colin, my stepdad George, my stepmum Stacey, my brother Craig and my better half James. You're all absolutely fantastic and incredibly supportive. I'm so lucky to have all of you in my life. Mum, you've always believed that I could do this and shown me more support and encouragement than I could ever have asked for. Thank you, I love you lots.
Finally, to my stepbrother, Mikey, who I lost during my PhD; you will always be missed.

List of Contents

List of Figures

List of Tables

Abstract

Eukaryotic Elongation Factor 1A (eEF1A) plays a key role in protein synthesis by delivering aminoacylated tRNAs to the A site of the ribosome. In higher vertebrates, two isoforms of eEF1A exist called eEF1A1 and eEF1A2, with eEF1A2 being expressed in adult brain, heart and skeletal muscle. Since 2012, several different *de novo* heterozygous missense mutations in *EEF1A2* have been identified in humans and these cause epilepsy, intellectual disability and autism. Before considering treatment options, it is vital to determine whether these mutations cause loss or gain of protein function.

I performed a battery of behavioural tests using two mouse lines with heterozygous loss of function mutations in eEF1A2. The aim was to determine whether there were any behavioural phenotypes consistent with intellectual disability and/or autism. Using heterozygous wasted mice (*Eef1a2*$^{+/wst}$), I analysed the effects of aging on behaviour and found that *Eef1a2*$^{+/wst}$ mice showed reduced marble burying activity and reduced movement in the open field test with age. In a test of social behaviour, *Eef1a2*$^{+/wst}$ mice showed a significantly reduced preference for social novelty at all ages tested.

The second heterozygous null line, Del22.ex3, was generated on a pure C57BL/6J genetic background. This new line was made in order to reduce the level of variation observed in data from the wasted line, which was on a mixed genetic background. The genetic background was shown to have an influence on behaviour as the results differed between this line and the wasted line. Del22.ex3 *Eef1a2*$^{+/-}$ mice showed significantly reduced engagement in repetitive behaviours compared with wild-type littermates and normal preference for social novelty.

Using CRISPR/Cas9, a mouse line with the D252H missense mutation was generated and I repeated my behavioural testing on heterozygotes from this line. I found no behavioural abnormalities in this line suggesting a mouse-human difference in the ability to tolerate eEF1A2 missense mutations. Previous attempts to make a line with

the G70S missense mutation were unsuccessful but as a product of this experiment, it was found that mice expressing G70S eEF1A2 had a comparable phenotype to and died at the same age as complete knockouts. This suggested that the G70S protein is non-functional and cannot compensate for loss of wild-type eEF1A2.

These experiments have improved our understanding of the phenotypic effects of *Eef1a2* mutations in mice and have shown, for the first time, that mutations in *Eef1a2* affect mouse behaviour.

Lay Summary

Cells have a constant need to make new proteins. These are molecules which carry out all of the tasks needed for the cell to function, grow and survive. All of the cells in the body contain a protein called eEF1A which is responsible for making new proteins. There are two different forms of eEF1A called eEF1A1 and eEF1A2 and these work to make new proteins in different cells from each other. I worked on eEF1A2 for my PhD project and this form is present inside cells of the brain, muscle and heart. Every cell in these tissues has two copies of eEF1A2.

eEF1A2 is essential for survival in mice. Mice that do not have any eEF1A2 develop severe degeneration of their nervous system and muscle and die by four weeks of age. Humans who have mutations in one copy of *EEF1A2* present with epilepsy, intellectual disability and autism. It is important that we find out how these mutations lead to disease so that we can consider treatment options.

In my PhD project, I used mice with different mutations in *Eef1a2* to look for changes that might explain what is happening in humans. The main aim of my project was to study mouse behaviour to check if this was abnormal in the mutant mice and whether we could link any abnormalities to the intellectual disability and autism we see in humans. I found that these mice have abnormal social behaviour which seems to fit with the clinical features identified in patients. The mice I used for this part of my project had one normal copy and one mutated copy of eEF1A2 (in a 50:50 ratio).

I also managed to show that these mutant eEF1A2 proteins are unable to function properly in mice. Mice that have two mutated copies of eEF1A2 (no normal copies) die at the same age as the mice that have no eEF1A2 described above. Therefore, having mutated eEF1A2 is just as detrimental as having no eEF1A2 at all. These mutant eEF1A2 proteins can be identified in cells using certain analysis techniques post-mortem but at much lower levels than we find the normal protein suggesting

that the cell is degrading these mutant proteins. Therefore, the cell is able to recognise these proteins as “the wrong thing” and discard them.

Our team also found that mice that don’t have any eEF1A2 at all experience seizures in response to sound. This shows that losing the correct balance of eEF1A2 in both humans and mice can result in seizures.

All in all, my research shows that mice with *Eef1a2* mutations develop some of the clinical features we see in humans and therefore these mice provide a valuable tool for us to find out how these mutations lead to disease and to develop treatments.

List of Abbreviations

5-HTT	Serotonin transporter
Acra-4	Alpha-4 nicotinic receptor (mouse gene)
AD	Alzheimer's disease
ADHD	Attention deficit hyperactivity disorder
ADNP	Activity dependent neuroprotector homeobox
Akt	Protein kinase B
AMPS	Ammonium persulphate
ANOVA	Analysis of variance
ARID1B	AT-rich interaction domain 1B
ASD	Autism spectrum disorder
BAC	Bacterial artificial chromosome
bp	Base pairs
BRF	Biomedical Research Facility
cDNA	Complementary DNA
CNV	Copy number variant
CRISPR	Clustered regularly interspaced short palindromic repeats
CV	Coefficient of variation
dB	Decibels
DF	Degrees of freedom
dH_2O	Distilled water
DNA	Deoxyribonucleic acid
dNTP	Deoxyribonucleoside triphosphate
DR	Discrimination ratio
DYRK1A	Dual-specificity tyrosine phosphorylation-regulated kinase 1A
EDTA	Ethylenediaminetetraaceticacid
eEF1A	Eukaryotic elongation factor 1A
EEF1A1	Eukaryotic elongation factor 1A1 (human gene)
EEF1A2	Eukaryotic elongation factor 1A2 (human gene)
Eef1a1	Eukaryotic elongation factor 1A1 (mouse gene)
Eef1a2	Eukaryotic elongation factor 1A2 (mouse gene)

eEF1A1	Eukaryotic elongation factor 1A1 (protein)
eEF1A2	Eukaryotic elongation factor 1A2 (protein)
eEF1B	Eukaryotic elongation factor 1B
EF	Elongation factors
EPSP	Excitatory post-synaptic potential
ERK	Extracellular signal-regulated kinase
ES cells	Embryonic stem cells
Fmr1	Mutated gene in fragile X syndrome (mouse)
FMRP	Fragile X mental retardation protein
GAPDH	Glyceraldehyde-3-phosphate dehydrogenase
GDP	Guanosine diphosphate
GFAP	Glial fibrillary acidic protein
GluR	Glutamate receptor
GRIN2B	Glutamate receptor subunit epsilon-2
GTP	Guanosine triphosphate
gRNA	Guide RNA
H_2O_2	Hydrogen peroxide
HCl	Hydrogen chloride
HDR	Homology directed repair
HM	Henry Molaison
HPA	Hypothalamic-pituitary adrenal
ID	Intellectual disability
IF	Initiation factors
IP	Immunoprecipitation
iPSC	Induced pluripotent stem cells
IQ	Intelligence quotient
ITI	Inter-trial interval
KO	Knock-out
LTD	Long-term depression
LTP	Long-term potentiation
$MgCl_2$	Magnesium chloride
mGluR5	Metabotropic glutamate receptor 5

mRNA	Messenger ribonucleic acid
mTOR	Mammalian target of rapamycin
N/A	Not applicable
NaCl	Sodium chloride
NaF	Sodium fluoride
NaOH	Sodium hydroxide
NHEJ	Non-homologous end joining
NRXN1	Neurexin 1
P	Postnatal day
PAM	Protospacer adjacent motif
PBS	Phosphate buffered saline
PBS-T	Phosphate buffered saline with tween 20
PCR	Polymerase chain reaction
PD	Parkinson's disease
PI3K	Phosphoinositide-3-kinase
PIKE	Phosphoinositide-3-kinase enhancer
PTEN	Phosphatase and tensin homolog
PVDF	Polyvinylidene difluoride
qPCR	Quantitative PCR
Ra	Ragged (mouse gene)
RF	Release factors
RNA	Ribonucleic acid
RT	Reverse transcriptase
RT-PCR	Reverse transcriptase PCR
SCN2A	Sodium voltage-gated channel alpha subunit 2
SD	Standard deviation
SDS	Sodium dodecyl sulphate
SEM	Standard error of the mean
SHANK	SH3 and multiple ankyrin repeat domains protein
shRNA	Small hairpin ribonucleic acid
SNV	Single nucleotide variant
SUDEP	Sudden unexpected death in epilepsy

SYNGAP1	Synaptic Ras GTPase-activating protein 1
TBE	Tris borate EDTA buffer
TEMED	Tetramethylethylenediamine
TGS	Tris/Glycine/SDS
TRIS	Tris(hydroxymethyl)aminomethane
TSC	Tuberous sclerosis complex
tRNA	Transfer RNA
UBE3A	Ubiquitin E3 ligase
USV	Ultrasonic vocalisation
v/v	Volume/volume
WES	Whole exome sequencing
WGS	Whole genome sequencing
Wst	Wasted
WT	Wild-type
w/v	Weight/volume

Chapter 1: Introduction

1.1. Protein synthesis

1.1.1. Overview

Each and every cell needs to carry out *de novo* protein synthesis in order to survive. The process of translating mRNA into protein is divided into three main stages: initiation, elongation and termination. Initiation is controlled by proteins called initiation factors (IFs) which form a complex with the ribosomal subunits and mRNA to begin the translation process. Elongation is controlled by elongation factors (EFs) and is the process by which amino acids are added to the growing peptide chain. This occurs through recognition of complementary codon and anticodon sequences on the mRNA and tRNA, respectively. Termination is controlled by release factors (RFs) and signifies the end of protein synthesis. The presence of a stop codon: UAA, UGA or UAG allows the mRNA to be released from the ribosome which allows recycling of mRNA and ribosomes for subsequent translation (Merrick, 1992, Clark *et al*., 1999).

1.1.2. Eukaryotic elongation factor 1A (eEF1A)

eEF1A participates in the elongation stage of protein synthesis by bringing aminoacylated-tRNAs to the A site of the ribosome. This is a GTP-dependent process mediated by the GTP exchange eEF1B. After each amino acid is added to the growing protein chain, GTP is hydrolysed to GDP and eEF1A is released to bring the next tRNA (Sasikumar, Perez and Kinzy, 2012) (Figure 1.1).

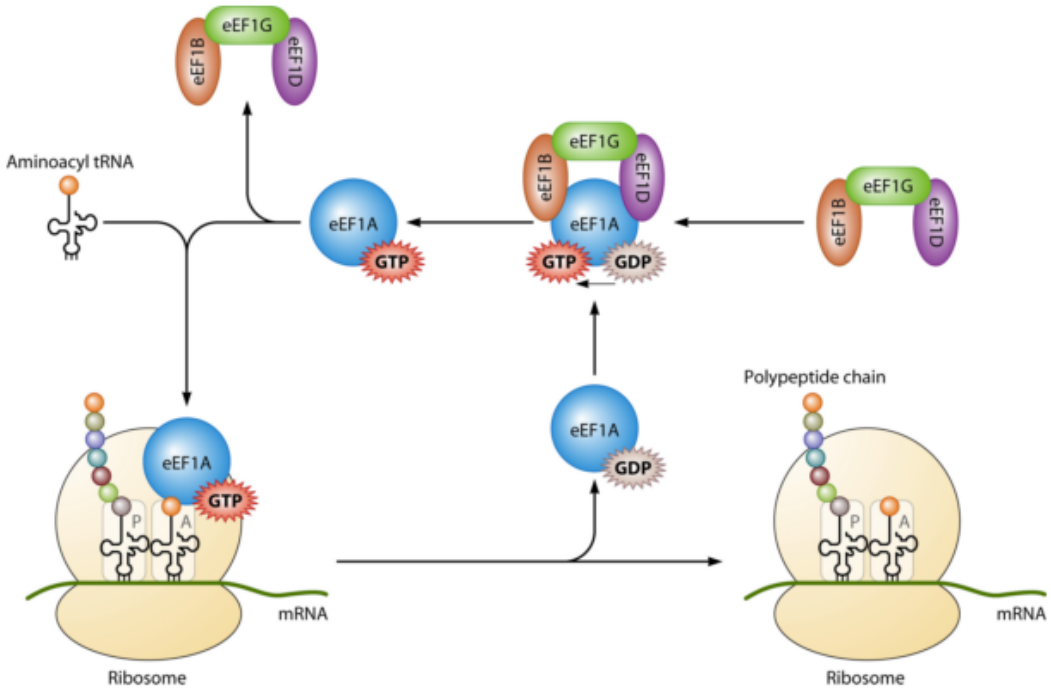

Figure 1.1. The role of eEF1A in protein synthesis. *eEF1B, which exists as three subunits (eEF1B in orange, eEF1G in green and eEF1D in purple), binds to eEF1A (blue) and converts GDP to GTP. The eEF1B complex is then released and eEF1A collects an aminoacyl tRNA and brings it to the A site of the ribosome. Once the amino acid bound to the tRNA is added to the protein chain, GTP is hydrolysed to GDP and eEF1A is released from the ribosome. Taken from Li et al., 2013.*

1.2. eEF1A isoforms in higher vertebrates

1.2.1. The two isoforms

eEF1A exists as two isoforms in higher vertebrates which are encoded on different chromosomes. In humans, *EEF1A1* maps to chromosome 6q14 and *EEF1A2 t*o 20q13.3 whereas in mouse *Eef1a1* maps to chromosome 9 and *Eef1a2* to chromosome 2 (Lund *et al*., 1996).

There is little difference in amino acid composition between the two isoforms, specifically these are 92% identical and 98% similar. Soares *et al* (2009) compared the amino acid differences between the isoforms and found that most of the differences lie in two clusters on one side of the molecule away from the binding sites that are important for protein synthesis (Figure 1.2A). This suggests that the ability of each isoform to participate in protein synthesis is probably similar and that any differences are more likely to relate to differences in the non-canonical functions of eEF1A alluded to later in this section. Interestingly, some of the amino acid residues that vary between the isoforms lead to differences in the potential of each isoform to be phosphorylated (Soares *et al*., 2009) and differences in post-translational modifications (Soares and Abbott, 2013). It is important to note that the amino acid substitutions don't appear to affect overall protein structure (Soares *et al*., 2009) (Figure 1.2B).

Differences in the molecular dynamics i.e. flexibility and mobility of the isoforms have also been observed, leading to differences in conformation between the two isoforms and differences in binding affinities for calmodulin (Kanibolotsky *et al*., 2008). eEF1A1 is also more hydrophobic and is more likely to bind to itself than eEF1A2 is (Timchenko *et al*., 2013). The two isoforms also have different affinities for GTP with eEF1A1 having a higher affinity than eEF1A2. This means that eEF1A1 binds GTP more strongly than GDP but eEF1A2 binds GDP more strongly than GTP. However, this difference in GTP affinity does not appear to have any effect on translation as measured using an *in vitro* assay. GTPase activity is also identical between the isoforms (Kahns *et al*., 2008).

The non-canonical roles of eEF1A include a role in the heat shock response (eEF1A1 only) (Vera *et al*., 2014), the ability to bind and bundle actin (Liu *et al*., 1996, Vlasenko *et al*., 2015), a role in the export of proteins from the nucleus (Khacho *et al*., 2008), a role in protein degradation through interactions with the proteasome (Chuang *et al*., 2005), a role in apoptosis (eEF1A1 pro-apoptotic, eEF1A2 anti-apoptotic) (Duttaroy *et* al., 1998, Ruest *et* al., 2002, Lamberti *et al*., 2004) and a role in oncogenesis (eEF1A2 only) (Anand *et al*., 2002, Tomlinson *et al*., 2005, Li *et al*., 2006, Schlaeger *et al*., 2008, Cao *et al*., 2009). The reason for differences in the structure and function of the two isoforms described above may be related to these functions, especially as translational activity appears to be similar.

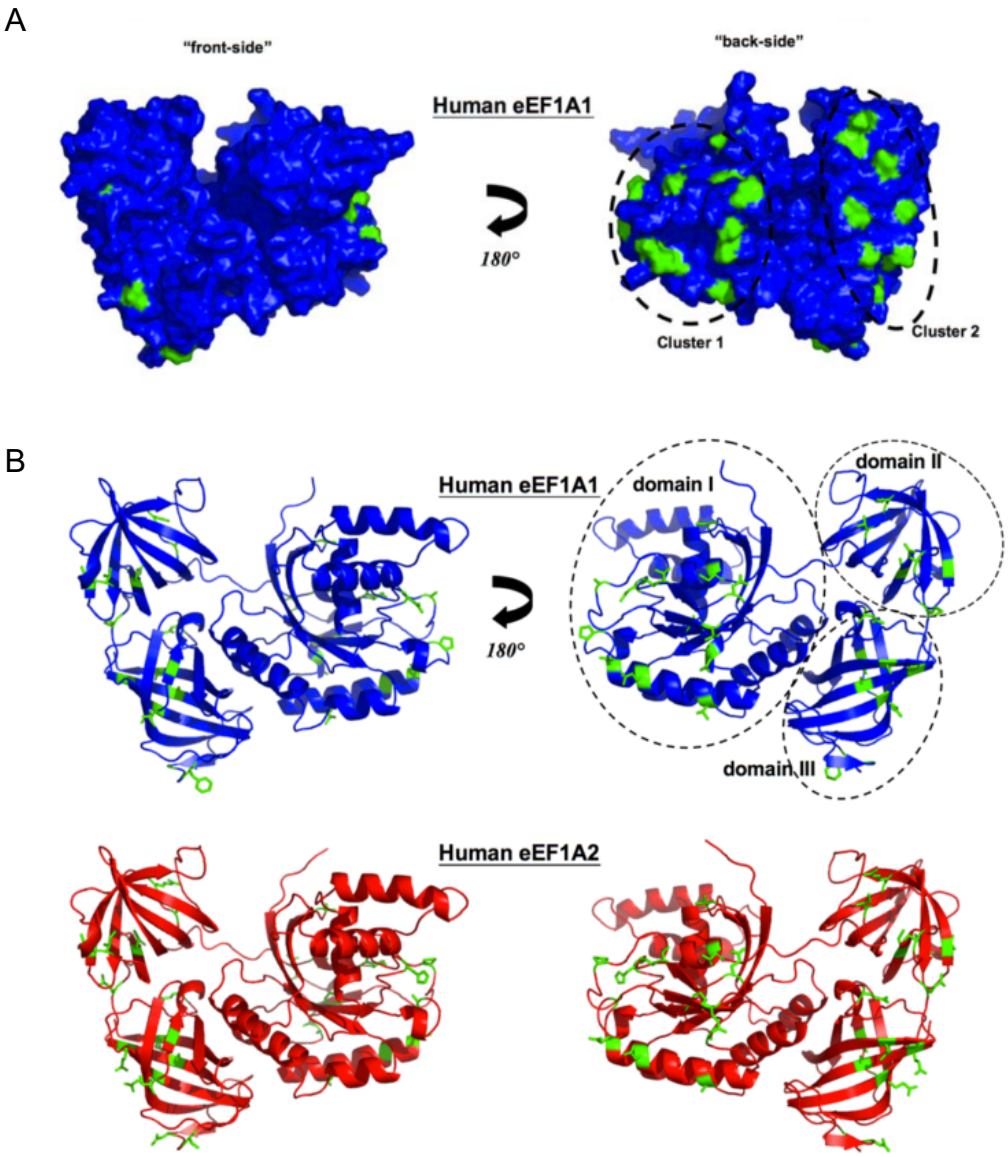

Figure 1.2. Structural differences between eEF1A1 and eEF1A2. ***A.*** *3D models of each side of the human eEF1A1 molecule with the amino acid residues that differ between this isoform and the eEF1A2 isoform mapped in green. These differences appear in two distinct clusters labelled "cluster 1" and "cluster 2".* ***B.*** *Diagrams showing the overall structure of each side of the eEF1A1 (blue) and eEF1A2 (red) molecules. Each isoform contains the same three domains, called domain I, II and III, the overall structure of which remain identical despite the differences in amino acid residues. The side chains that differ between the two isoforms are shown in green. Taken from Soares et al., 2009.*

1.2.2. eEF1A undergoes a developmental expression switch

eEF1A1 and eEF1A2 are differentially expressed. In several studies of adult human, mouse, rat and more recently pig eEF1A, eEF1A2 has been shown to be highly expressed in brain, spinal cord, heart and skeletal muscle whereas eEF1A1 is expressed in all other tissues tested (placenta, lung, liver, kidney, pancreas, spleen, testis, bladder, stomach and thymus).

eEF1A1 is expressed ubiquitously throughout development but is down-regulated postnatally in neurons, heart and skeletal muscle and is replaced by eEF1A2 (Lee *et al* 1992, Knudsen *et al*., 1993, Chambers, Peters and Abbott, 1998, Khalyfa *et al*., 2001, Newbery *et al*., 2007, Svobodová *et al*., 2015). eEF1A2 has also been identified postnatally in islet cells in the pancreas and enteroendocrine cells in the gut. In adult brain, eEF1A1 continues to be expressed but only in glial cells and some small neurons. eEF1A1 is also expressed in glial cells and white matter in the spinal cord (Khalyfa *et al*., 2001, Newbery *et al*., 2007).

In mouse skeletal muscle at P21, eEF1A1 is undetectable at both the RNA level (Chambers, Peters and Abbott, 1998) and at the protein level (Khalyfa *et al*., 2001) having been completely replaced by eEF1A2. In mouse brain at P20, Khalyfa *et al* (2001) showed, using double immunofluorescence labelling, that eEF1A1 co-localised with a glial-specific marker and eEF1A2 with a neuronal-specific marker, suggesting that the expression switch was complete by this time point. Notably, weak eEF1A1 staining was also detectable in a few unspecified neuronal cells. Pan *et al* (2004) confirmed the timing of this switch in the brain but analysed the expression changes in more detail by looking at changes at specific time points using double-label immunofluorescence in neurons. It was found that at P14, eEF1A1 was expressed at very low levels whilst eEF1A2 had just become detectable. eEF1A2 then showed a gradual increase in expression until P26, where a plateau was reached. Importantly, at P20, eEF1A1 was undetectable in neurons, as found by Khalyfa *et al* (2001). No eEF1A2 expression was detected in glial cells. The developmental expression profile in neurons is summarised in table 1.1.

Table 1.1. Summary of developmental expression switch in neurons.

	E16	**P1**	**P14**	**P20**	**P26**
eEF1A1	High	High	Low	Undetectable	Undetectable
eEF1A2	Undetectable	Undetectable	Moderate (rising)	High (rising)	High (plateau)

The reason for having two differentially expressed isoforms of eEF1A with slightly differing roles is not fully understood. Maybe, following early development, certain cell types (neurons, heart, skeletal muscle) switch to eEF1A2 as some of the functions performed by eEF1A1 are no longer needed or are potentially detrimental. The cells that express eEF1A2 are robust, established and long-living, being terminally differentiated.

1.3. eEF1A in disease

1.3.1. The wasted mouse model and neurodegeneration

In 1972, a spontaneous deletion in the *Eef1a2* gene arose in a mouse line housed in the Jackson laboratory. This deletion results in complete loss of eEF1A2 expression (Shultz *et al*., 1982). This *Eef1a2* knockout (KO) line has a 15.8 kilobase deletion that spans the promoter and first non-coding exon of the gene (Chambers, Peters and Abbott, 1998).

This mouse line has been well characterised over the years and is referred to as "wasted" due to a severe degenerative phenotype starting at around 21 days postnatal (P21). Homozygous wasted mice develop tremors, ataxia and weight loss which, over the course of a few days, leads to paralysis and early death at around P28 (Shultz *et al*., 1982). Heterozygous mice are phenotypically normal (Griffiths *et al*., 2012).

In 1984, the gene responsible for the wasted phenotype was mapped to the distal end of chromosome 2, 1 centiMorgan from the Ragged (*Ra*) gene (Sweet, 1984). The ragged mutation also arose spontaneously, however, it is semi-dominant meaning that homozygotes and heterozygotes manifest with different phenotypes from one another. Heterozygotes simply present with ragged coats whereas homozygotes are much more severely affected, being almost completely hairless and failing to survive post-weaning (Carter and Phillips, 1956). Subsequently, interspecific backcrosses were used to map the ragged and wasted genes relative to other genes on the distal end of chromosome 2 in order to identify potential candidate genes that may be responsible for the phenotypes and to lay the foundation for a positional cloning approach. It was found that the gene responsible for the wasted phenotype is positioned 3cM distal to *Acra-4*, the molecular marker closest to the telomere. The ragged gene was also successfully mapped relative to the same markers and was found to be no further than 2.19cM from *Acra-4* and *D2Mit74* and further from the telomere than the wasted gene (Abbott *et al*., 1994). No potential candidate genes were identified for the wasted phenotype through this mapping approach, therefore, a positional cloning approach was necessary to identify the gene responsible. A positional cloning/positional candidate approach was used whereby *Eef1a2* was selected as a candidate gene. Amplification of mouse *Eef1a2* by PCR showed a difference in product size between wild-type and wasted mice and analysis of 247 mice showed that *Eef1a2* and the wasted gene did not recombine. Subsequent PCR amplification across the boundaries of the deletion and sequencing of the product revealed that the deletion is 15.8kb and spans the promoter and first non-coding exon of the gene (Chambers, Peters and Abbott, 1998). The sequence analysis of the deletion is shown in Figure 1.3.

In 2007, work in our laboratory confirmed that *Eef1a2* is the only gene responsible for the wasted phenotype. Transgenic mice were generated with a bacterial artificial chromosome (BAC) containing the *Eef1a2* gene and the *C20orf149* gene, the mouse homologue of a human gene of unknown function. These mice were crossed with mice from the wasted line to give rise to wasted homozygotes that carried the transgene. These mice showed none of the phenotypes normally seen in wasted mice,

were fertile and had a normal lifespan showing that the BAC was able to rescue the wasted phenotype. It was therefore reasonable to assume that *Eef1a2* and/or *C20orf149* are responsible for the wasted phenotype. To investigate whether one or both genes are involved, a deletion was introduced into the BAC to inactivate *Eef1a2*. When crossed into the wasted line, this BAC failed to correct the phenotype showing that *Eef1a2* is solely responsible (Newbery *et al*., 2007).

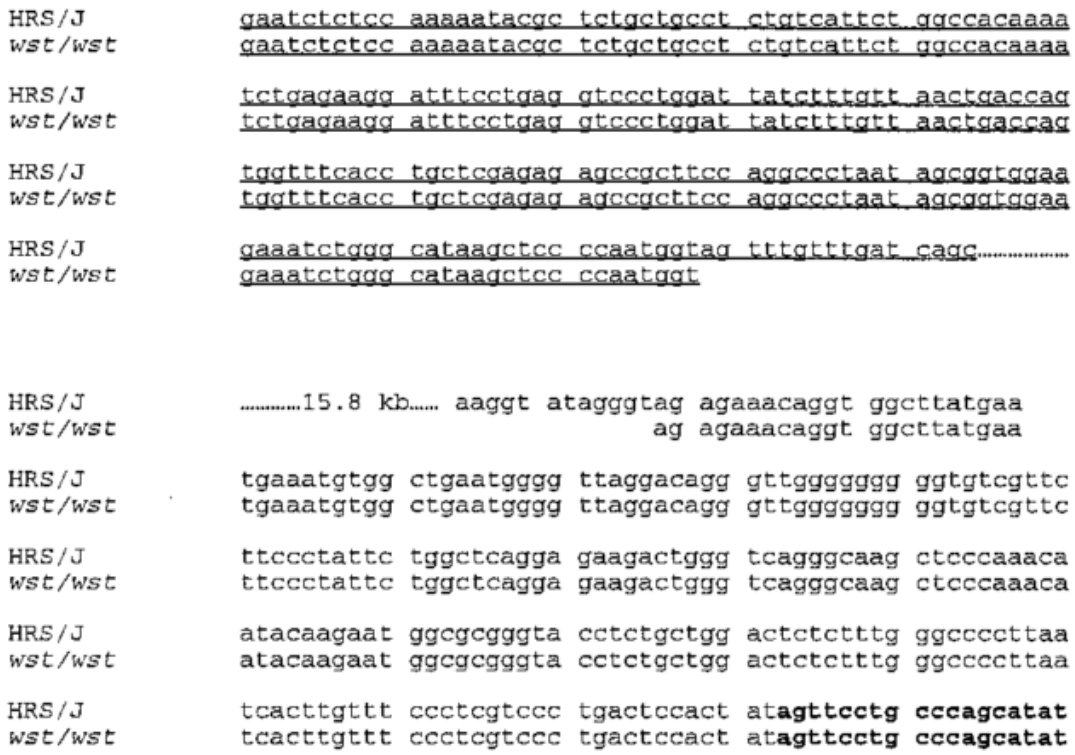

Figure 1.3. Sequence analysis of wasted (wst/wst) and wild-type (HRS/J) mice revealing position and size of wasted deletion in Eef1a2. *Underlined = IAP element, non-underlined = intron 1, bold = exon 2. The dotted line represents the 15.8kb deletion in wasted mice. Taken from Chambers, Peters and Abbott (1998).*

The first signs of neuromuscular pathology can be identified in wasted mice at P17. At this early time point, there is retraction of motor nerve terminals from motor end plates, leaving both unoccupied and partially occupied endplates which results in weak synaptic transmission by P23. At P23, wasted homozygous mice weigh significantly less than their heterozygous littermates due to loss of muscle bulk (Figure 1.4A). In terms of spinal cord pathology, gliosis and accumulation of phosphorylated neurofilaments can be seen inside motor neurons of the anterior horn at P19, followed by vacuolation of these motor neurons at P25 (Figure 1.4B) (Newbery *et al*., 2005). Motor impairments and muscle weakness can be assessed using the rotarod and grip strength tests respectively. Wasted mice perform significantly worse than their littermates in the rotarod test from P21 (Newbery *et al*., 2005) and in the grip strength test from P20 (Griffiths *et al*., 2012).

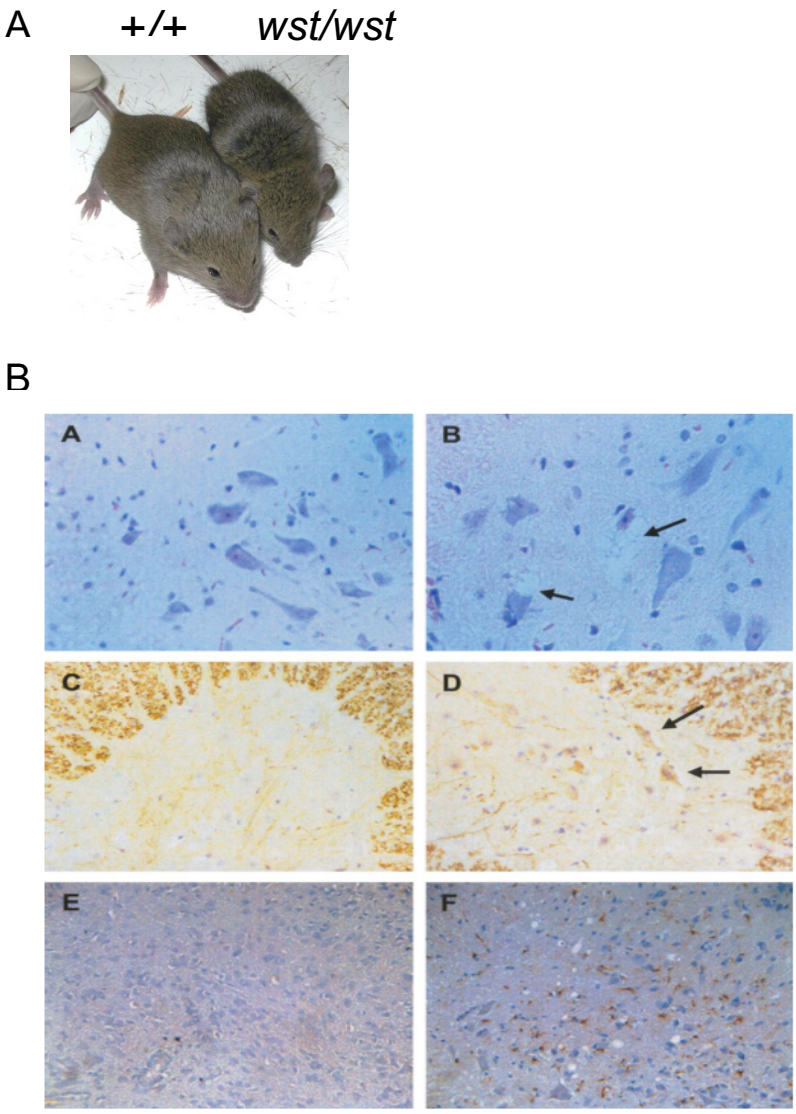

Figure 1.4. Phenotypic abnormalities in homozygous wasted mice. ***A.*** *An image showing the size difference between a +/+ mouse (left) and its wst/wst littermate (right).* ***B.*** *Pathology of wasted mice in the anterior horn of the cervical spinal cord. The top panel shows haematoxylin and eosin staining of a +/wst (A) and a wst/wst mouse (B). Arrows show areas of vacuolation which can be seen as 'holes' in the tissue. The middle panel shows staining of phosphorylated neurofilaments by immunohistochemistry. Shown is a section from a +/wst mouse (C) and a wst/wst mouse (D). Arrows show accumulation of phosphorylated neurofilaments in the cytoplasm of motor neurons. The bottom panel shows gliosis measured by immunohistochemistry with an antibody against glial fibrillary acidic protein (GFAP) in +/wst (E) and wst/wst (F) sections. The high level of staining in the wasted mouse section indicates neuronal damage (brown puncta). Taken from Newbery et al., 2005.*

The onset of the wasted phenotype coincides with the loss of eEF1A1 expression in muscle (Chambers, Peters and Abbott, 1998). Since there is no eEF1A2 to compensate, muscle tissue ends up with no eEF1A which, as evidenced by the phenotype, clearly has detrimental effects. This is also around the same time that eEF1A1 expression is lost from neurons and again there is no eEF1A2 to compensate (Pan *et al*., 2004). Furthermore, it has been shown that there is no compensatory up-regulation of eEF1A1 in the absence of eEF1A2 (Khalyfa *et al*., 2001).

Doig *et al* (2013) aimed to determine whether the muscle atrophy seen in wasted mice is due to loss of eEF1A2 in muscle or whether it is neurogenic in origin. To achieve this, they generated transgenic wasted mice expressing eEF1A2 only in muscle and compared them with non-transgenic wasted mice by measuring weight, survival, grip strength and limb muscle atrophy by post-mortem histology. The levels of eEF1A2 expression in the muscle of transgenic wasted mice were confirmed as being comparable to wild-type mice. They found that wasted mice carrying the transgene were indistinguishable from non-transgenic wasted mice which shows that expression of eEF1A2 in muscle is not sufficient to rescue the phenotype. This suggests that the muscle atrophy seen in wasted mice is of a neurological origin. The authors also attempted to generate transgenic wasted mice expressing eEF1A2 only in neurons, but this was unsuccessful as all founAders unexpectedly expressed eEF1A2 both in neurons and muscle.

1.3.2. Human *EEF1A2* mutations cause intellectual disability and epilepsy

Since 2012, 20 different *EEF1A2* mutations have been identified over 40 individuals which cause intellectual disability, epilepsy or abnormal EEG and in some cases autism. It is worth noting that a diagnosis of autism is not always possible as, in some cases, the intellectual disability is too severe. Autistic behaviours that have been identified in these patients include repetitive hand twisting, finger sucking, rocking and self-injury behaviours. All of these mutations are *de novo* heterozygous

missense mutations and were discovered using trio-based exome sequencing of the individuals and their unaffected parents. It is important to note that a number of the cases are currently unpublished. The mutations are summarised in table 1.2.

In most cases, these mutations are very severe as most of the patients cannot speak at all and some can only communicate using signs. If they can speak, they have very limited language capabilities. Their motor skills are also severely under-developed. Some of the patients are unable to sit, stand or walk at all whilst others are able to do some or all of these tasks with assistance. Ataxia has been observed in those that can walk independently.

The first case was identified in 2012, a 22-year-old female with a missense mutation that changes the amino acid glycine to serine at position 70 on the protein (G70S). Her clinical profile stated that she had neonatal hypotonia, seizures from 4 months of age, severely delayed motor and language development, autistic features and aggressive behaviours. Height, weight, head circumference and facial features were normal (de Ligt *et al*., 2012). A second G70S case was identified in 2013 which increased confidence that *EEF1A2* was the causative gene as there was now two patients with the same mutation sharing similar clinical features. This 10-year-old male had clinical features of West syndrome, neonatal hypotonia, seizures starting at 10 weeks of age, severe developmental delay, gait abnormalities and microcephaly with no mention of whether or not there were any autistic features. Language development was absent in this individual as he was completely non-verbal (Veeramah *et al*., 2013).

Two more cases were discovered in 2014. These were the first two patients to be identified as having characteristic facial features thought to be associated with the mutation (Nakajima *et al*., 2014). Specifically, these features are a broad nasal bridge, a tented upper lip, an everted lower lip and downturned corners of the mouth. Lam *et al* (2016) presented seven new cases and reported that six of these seven patients showed the facial features described above. Therefore, this may be a helpful diagnostic for identifying patients with *EEF1A2* mutations in the future.

It is interesting to note that disease severity varies depending on the mutation. One of the most severe cases is a female with a F98L mutation who was 9-years-old at diagnosis and has daily seizures that cannot be controlled with medication, cannot sit, has no head control, is non-verbal and has severe global developmental delay (Lam *et al*., 2016). By contrast, the mildest case is a female with an E124K mutation who was 10-years-old at diagnosis and has seizures that are controlled by medication. She can walk independently, speaks in sentences and only has mild intellectual disability. She attends a mainstream primary school but will attend a special secondary school (Lam *et al*., 2016).

Table 1.2. Human EEF1A2 mutations and their corresponding clinical features

Mutation	Seizure type and age of onset	Intellectual disability phenotype	Autism?	Hypotonia?	Motor phenotype	Speech phenotype	Facial features?	Defects on brain scan?	Reference
A92T	Undefined from 1 month	Severe	Y					Y	Lopes *et al*., 2016
D252H	GTCS from 8 years	Moderate	Y	Y	Cannot walk	Non-verbal	Y	Y	Nakajima *et al*., 2014
D252H		Severe						Y	DDD
D91N	Eye rolling, head dropping and arm extensions from 2 years	Severe		Y	Can walk assisted	Non-verbal	Y		Lam *et al*., 2016
E122K	Infantile seizures from undefined age	Severe	Y	Y	Can walk unassisted but ataxic		Y	Y	Nakajima *et al*., 2014
E122K	Atypical, myoclonic and absence from 10 months	Severe			Cannot walk	Non-verbal	Y		Inui *et al*., 2016
E122K	Myoclonic and myoclonic-atonic from 8 months	Severe			Cannot walk	Non-verbal	Y	Y	Inui *et al*., 2016
E122K	Infantile spasms from 10 weeks	Severe	N	Y	Can walk unassisted but ataxic	Non-verbal but uses signs	Y	Y	Lam *et al*., 2016
E124K	Myoclonic followed by absence from 3 months	Mild	N	N		Verbal	N	N	Lam *et al*., 2016
F98C	Abnormal EEG only	Moderate	Y	Y		Non-verbal		N	Personal commun-ication
F98L	Focal seizures followed by tonic, myoclonic, tonic-clonic from undefined age	Severe		Y	Cannot walk	Non-verbal	Y	Y	Lam *et al*., 2016
G70S	Absence, myoclonic and GTCS from 4 months	Severe	Y	Y		Non-verbal	N		De Ligt *et al*., 2012
G70S	Infantile spasms, tonic, myoclonic and GTCS from 8 months	Severe		Y	Can walk but ataxic (assisted or unassisted not specified)	Non-verbal		Y	Veeramah *et al*., 2013
G70S	Myoclonic and clonic-tonic followed by	Severe		Y			Y		Lam *et al*., 2016

Mutation	Seizure type and age of onset	Intellectual disability phenotype	Autism?	Hypotonia?	Motor phenotype	Speech phenotype	Facial features?	Defects on brain scan?	Reference
G70S	Absence, tonic, myoclonic and GTCS from 18 months	Severe	Y	Y		Non-verbal		Y	Personal communication
G70S	Absence, atypical and myoclonic from 1 month	Moderate	N	Y		Non-verbal		N	Personal communication Helbig *et al*., 2016
I71L	Undefined seizure type and age of onset	Severe			Can walk unassisted	Non-verbal but uses signs	Y	Y	Lam *et al*., 2016
M102V	Febrile, hemiclonic and GTCS from undefined age	Moderate	N	N				N	Personal communication
R266W	Absence, hemiclonic and GTCS from undefined age	Severe	N	Y				Y	Personal communication
R266W	Undefined seizure type and age of onset	Severe	Y				Y		DDD
R423C	Infantile spasms, tonic and myoclonic from undefined age	Moderate		Y		Non-verbal	Y	Y	Personal communication Lam *et al*., 2016
T432M		Severe							DDD

GTCS = Generalised tonic-clonic seizures, DDD = Deciphering Developmental Disorders study. Red dot = patient died from respiratory failure. Blank boxes indicate that the information was unavailable. Defects on brain scans include microcephaly, generalised brain atrophy, atrophy of the cerebrum and ventriculomegaly. Adapted from Davies (2017).

The human missense mutations have been mapped onto a 3D model of the eEF1A2 protein (Figure 1.5). Most of the mutations are clustered around the sites that are important for protein synthesis suggesting that alteration of this process might lead to the disease phenotype. For example, the Glu122Lys mutation involves substitution of an amino acid residue that is involved in binding the GTP-exchange factor eEF1B (Nakajima *et al*., 2014). Similarly, the Asp252His mutation is in the GDP/GTP binding domain (Nakajima *et al*., 2014) and it has been shown that mutating this residue in yeast eEF1A reduces translational fidelity (Sandbaken and Culbertson, 1988). Interestingly, the patient that has the mildest phenotype (described above) has a mutation that is further away from the binding sites important for protein synthesis (Lam *et al*., 2016).

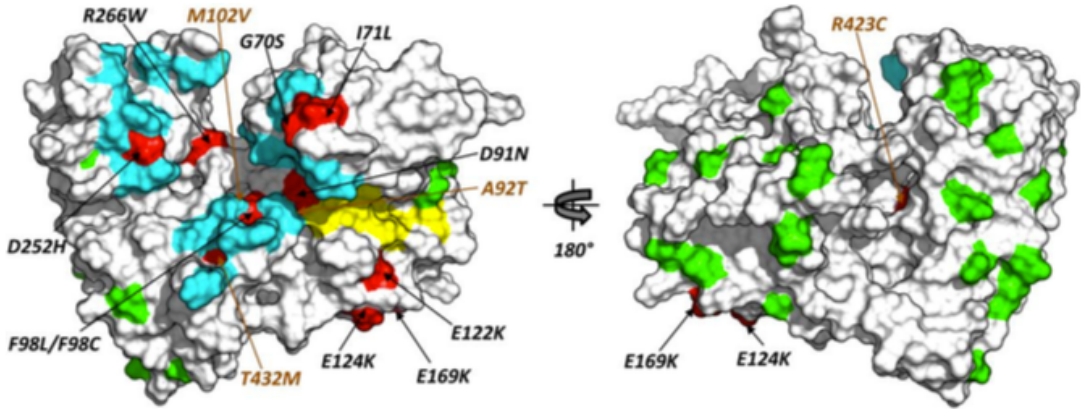

Figure 1.5. Human EEF1A2 mutations mapped onto a 3D model of the protein to show proximity of mutations to sites crucial for protein synthesis. *Both sides of the human eEF1A2 protein are shown. Highlighted are the eEF1B binding site (blue), the GDP/GTP binding site (yellow), the human mutations (red) and the amino acid residues that vary between eEF1A1 and eEF1A2 (green). Residues with side chains that are buried within the molecule are labelled in brown. Mutations that are close to or overlap with eEF1B or GDP/GTP binding sites are A92T, D252H, D91N, E122K, E124K, F98L, F98C, G70S, I71L, M102V, R266W and T432M. 3D modelling by Dinesh Soares.*

1.3.3. eEF1A and other nervous system disorders

Dysregulation of protein synthesis and eEF1A have been implicated in other neurological disorders in several studies. The majority of these studies analyse total eEF1A levels without distinguishing between the two isoforms. For example, in studies investigating protein expression, eEF1A antibodies which are not isoform-specific are commonly used. However, in some studies, it is possible to decipher whether eEF1A1 or eEF1A2 are being studied. For example, expression of eEF1A in adult neurons can be assumed to be eEF1A2. However, studies of eEF1A in whole tissue will include both isoforms. In the studies described below, specific isoforms have been referred to where possible.

Using a combination of western blotting and immunohistochemistry, eEF1A protein expression levels have been shown to be down-regulated in Alzheimer's disease (AD), a neurodegenerative disease characterised by memory impairments. In post-mortem brain samples from patients with the disease, eEF1A2 levels are significantly reduced specifically in hippocampal neurons in the CA1 and dentate gyrus. eEF1A

levels are also significantly lower in the hippocampus of TG2576 AD model mice compared with controls (Beckelman *et al*., 2015, Beckelman *et al*., 2016). The hippocampus is an important area for memory formation and eEF1A is known to contribute to the maintenance of LTP, the physiological process that is hypothesised to underlie the formation of new memories (Tsokas *et al*., 2005). Therefore, perhaps it is unsurprising that we find this link between eEF1A and AD. In transgenic AD mice, LTP is impaired and it has been found that this can be rescued by up-regulation of eEF1A (Beckelman *et al*., 2016). It has been speculated that eEF1A dysregulation might be one of the mechanisms underlying AD pathogenesis and could potentially contribute to the memory loss that is a hallmark of the disease.

It has been shown that protein synthesis machinery is altered in human Parkinson's disease (PD) post-mortem brain samples. With regards to eEF1A, there is a reduction in protein expression in the frontal cortex that correlates with disease progression, shown by western blotting. This means that individuals with more severe disease have lower levels of eEF1A (Garcia-Esparcia *et al*., 2015). Another PD study investigated the relationship between the PI3K/Akt/mTOR pathway, which is dysregulated in PD, and eEF1A. An MPP^+-induced SH-SY5Y cellular model of PD was used in which cells were treated with MPP, a compound that is toxic to dopaminergic neurons. Using qPCR, both eEF1A isoforms were found to be significantly up-regulated at the mRNA level in non-differentiated MPP^+ treated cells compared with control cells that had not been treated. In differentiated MPP^+ treated cells, only eEF1A2 was up-regulated. Up-regulation of eEF1A2 was also observed in both non-differentiated and differentiated cells at the protein level, however, only one sample per group was analysed (Khwanraj *et al*., 2016).

Altered eEF1A expression has also been observed using mass spectrometry in human iPSC-derived forebrain neural progenitor cells from schizophrenia patients. A significant 2.4-fold increase in levels of global protein synthesis accompanied by an increase in components of the translational machinery was observed. This included a significant increase in eEF1A1 and eEF1A2 protein expression compared with healthy controls (Topol *et al*., 2015).

Changes in eEF1A have been observed in Fragile X syndrome, an X-linked disorder which is the most common genetic cause of intellectual disability. Fragile X syndrome is caused by mutations in the *FMR1* gene which encodes the Fragile X Mental Retardation Protein (FMRP) (Verkerk *et al*., 1991). The normal function of FMRP is to suppress translation of specific mRNAs, however, many of the mRNA targets remain unidentified (Bagni and Greenough, 2005). Sung *et al* (2003) sought to identify mRNA targets of FMRP and found an interaction with eEF1A. In PC12 cells transfected with human FMRP, a direct interaction between FMRP and eEF1A mRNA was confirmed by immunoprecipitation (IP) and subsequent northern blotting of the associated mRNAs. It was shown that PC12 cells expressing lower levels of FMRP express higher levels of eEF1A through western blotting. Finally, western blotting showed that eEF1A protein expression is increased 2-fold in Fragile X lymphocytes compared with control cell lines. A direct interaction between FMRP and both eEF1A1 and eEF1A2 mRNA has also been shown using crosslinking IP followed by high-throughput sequencing of isolated mRNAs (Darnell *et al*., 2011). These data suggest that FMRP regulates translation of both eEF1A isoforms.

There is an excess of immature dendritic spines in the brains of individuals with Fragile X syndrome and *Fmr1* knockout mice and subsequent research suggests that this is caused by impaired synapse elimination (Pfeiffer *et al*., 2010). Tsai *et al* (2012) investigated synapse elimination in *Fmr1* KO mice using neuronal cultures and hippocampal slice cultures. Silencing of eEF1A1 in these cultures using specific shRNAs was found to rescue defects in synapse elimination, suggesting that elevated levels of eEF1A1 may contribute to impaired synapse elimination in Fragile X syndrome.

1.4. Autism, intellectual disability and epilepsy: common molecular pathways affected

1.4.1. Co-occurrence of autism, intellectual disability and epilepsy

Autism, intellectual disability and epilepsy commonly co-occur. Therefore, there is a lot of interest in determining which pathways are affected in these disorders and where they converge. Individuals with autism have an increased risk of developing epilepsy, with 25% of people with autism having a seizure disorder. A striking 70% of people with autism also have an intellectual disability (Zoghbi and Bear, 2012). In children with autism, IQ is negatively correlated with epilepsy meaning that epilepsy is more likely to present itself in those who also have an intellectual disability (Jeste and Tuchman, 2015). In cases where these disorders co-occur, it is debated as to whether these manifest due to the same common mechanism or whether epilepsy disrupts cortical connections which then leads to autism and intellectual disability. However, the interplay of both of these mechanisms is likely to be causative.

1.4.2. Genetics

There have been many identified genetic causes of autism in which individuals also present with epilepsy and intellectual disability including well-characterised inherited single-gene disorders, such as Fragile X syndrome, Rett syndrome and Tuberous Sclerosis Complex (Jeste and Tuchman, 2015, Ronemus *et al*., 2014). Genetic studies have shown that hundreds of different genes are linked to autism (Vorstman *et al*., 2017). Variants in these autism-associated genes are often rare and can include both single nucleotide variants (SNVs) and copy number variants (CNVs). Additionally, *de novo* genetic variants i.e. those that are not present in the parents are more common in individuals with autism than their unaffected siblings. Advances in genetic methods such as whole genome sequencing (WGS) and whole exome sequencing (WES) have improved the ability of scientists to identify novel causes of autism. Genes with SNVs that have been shown to be associated with ASD through sequencing studies include ADNP, ARID1B, SCN2A, DYRK1A, SYNGAP1 and GRIN2B. The variants identified in these genes have also been found to be associated with ID and epilepsy (Vorstman *et al*., 2017).

Many genes associated with autism, epilepsy and intellectual disability are involved in the regulation of synapse structure and function (Jeste and Tuchman, 2015). Examples of these are shown in Table 1.3.

Table 1.3. Examples of genes mutated in autism, epilepsy and intellectual disability that function at synapses

Syndrome (if applicable)	Relevant genes	Epilepsy features	Developmental features
Fragile X syndrome	FMR1	Focal epilepsy, often with centrotemporal spikes	Comorbid ID with ASD severity linked to IQ, anxiety, sleep impairment
Tuberous sclerosis complex	TSC1/2	Infantile spasms, generalised and multifocal epilepsy	Comorbid ID, anxiety and ADHD
	NRXNI	Early onset, severe, both focal and generalised epilepsy	Profound ID, ADHD
	UBE3A	Generalised and partial, multifocal, infantile spasms	Hypotonia, comorbid ID and ASD, profound language impairment
	SHANK3	Generalised, focal, absence	Hypotonia, comorbid ID and ASD, profound language impairment
	PTEN	Focal and generalised	Macrocephaly, comorbid ID

ID = intellectual disability, ASD = autism spectrum disorder, ADHD = attention deficit hyperactivity disorder, IQ = intelligence quotient. Adapted from Jeste and Tuchman (2015).

All of the genes described in Table 1.3 are involved in regulating protein synthesis at excitatory glutamatergic synapses (Zoghbi and Bear, 2012). Therefore, there appears to be a link between dysregulation of synaptic protein synthesis and disorders that feature autism, epilepsy and intellectual disability.

1.4.3. Extracellular signal-regulated kinase pathway

Regulation of specific processes within the synapse, including translation, involves the activation of the extracellular signal-regulated kinase (ERK1/2) pathway (Figure 1.6). ERK 1/2 form part of the MAPK signalling cascade that is involved in synaptic plasticity and memory formation. Downstream targets of ERK1/2 signalling regulate processes including synaptic receptor docking and dendritic spine stabilisation (Subramanian *et al*., 2015). This pathway is commonly affected in disorders that are characterised by autism, epilepsy and intellectual disability. Two examples based on the mutations in Table 1.3 are described below.

In post-mortem brain tissue from patients with Fragile X syndrome, it has been shown that levels of phosphorylated ERK are increased 17.5-fold compared with controls (Wang *et al*., 2012). A similar increase has also been observed in *Fmr1* knockout mice. SL327, a selective inhibitor of ERK activity, can abolish audiogenic seizure activity in these mice (Wang *et al*., 2012). These data suggest that the ERK1/2 signalling is altered in Fragile X syndrome and that this contributes to some of the phenotypes of the disease.

Osterweil *et al* (2013) tested whether inhibition of Ras, an upstream component of the pathway which acts on ERK1/2, can rescue disease phenotypes in the *Fmr1* knockout mouse. Lovastatin, a drug used to lower cholesterol, happens to be an inhibitor of Ras and the team showed that this can rescue the exaggerated levels of protein synthesis and prevent epileptiform activity in hippocampal slices from *Fmr1* knockout mice. Strikingly, this drug is also able to significantly reduce audiogenic seizure incidence and severity in *Fmr1* knockout mice *in vivo* (Osterweil *et al*., 2013).

There is evidence to suggest that TSC1/2, the genes mutated in Tuberous Sclerosis, interact with the ERK1/2 signalling pathway. In transgenic mouse models of the disease, elevated ERK phosphorylation and an increase in ERK signalling have been observed in the hippocampus. Furthermore, inhibiting the ERK pathway with the antagonist U0126 can rescue disease phenotypes in these mice including restoration of synaptic plasticity impairments (Chévere-Torres *et al*., 2012).

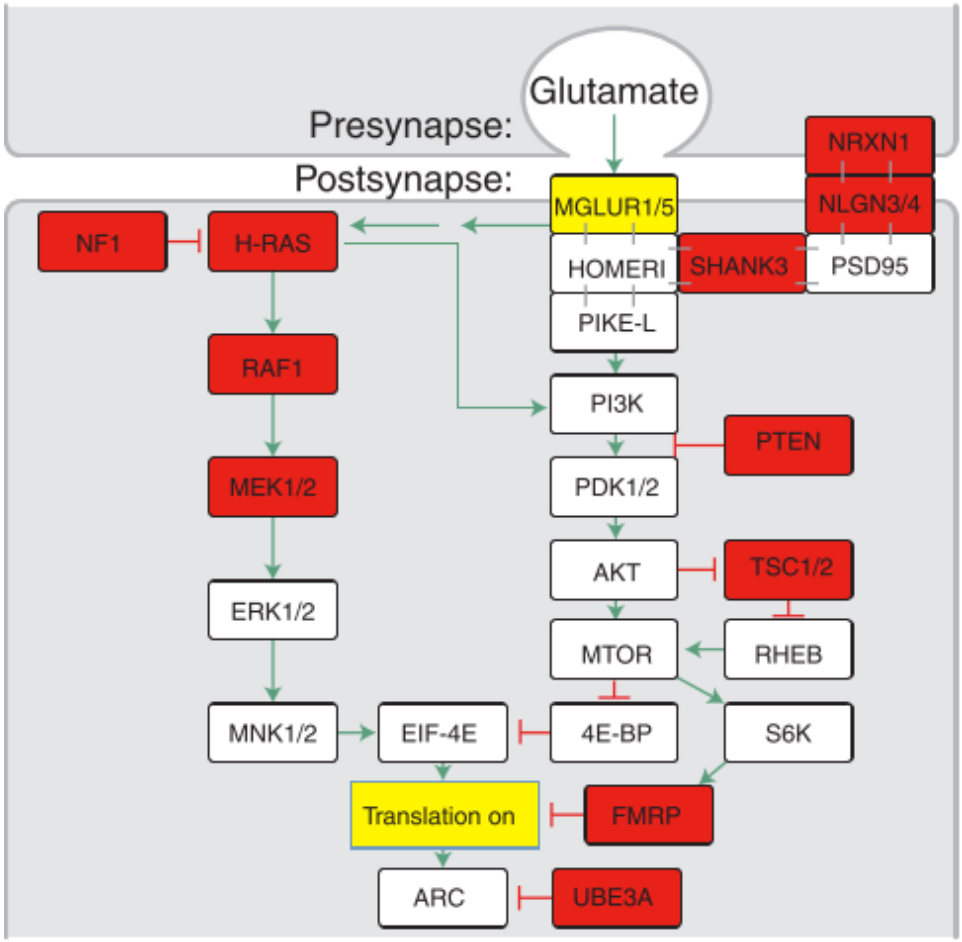

Figure 1.6. Signalling at the excitatory glutamatergic synapse involves ERK1/2. *This signalling is necessary for the control of protein synthesis. Autism-related genes are shown in red. Taken from Zoghbi and Bear (2012).*

1.4.4. Mammalian target of rapamycin pathway

In neurons, the mammalian target of rapamycin (mTOR) signalling pathway is involved in the control of protein synthesis, growth and morphogenesis and is controlled by metabotropic glutamate receptor 5 (mGluR5) (Subramanian *et al*., 2015). Like ERK1/2 signalling, there is much evidence to suggest that the mTOR pathway is altered in disorders that are characterised by autism, epilepsy and intellectual disability. There is cross-talk between the ERK1/2 pathway and the mTOR pathway, as shown in Figure 1.6, so, unsurprisingly, the same mutations have been found to affect both pathways. Two examples of mTOR pathway dysfunction in disease are given below, based on the mutations in Table 1.3.

The mTOR pathway is overactive in *Fmr1* knockout mice. This is evidenced by an increase in phosphorylation of mTOR and its downstream targets in the hippocampus, shown using western blotting and IP. This is coupled with increased protein expression of upstream pathway components PIKE-S and PI3K, the former of which is a confirmed target of FMRP (Sharma *et al*., 2010a). The hypothesised action of FMRP on the mTOR pathway, proposed by Sharma *et al* (2010a), is shown in Figure 1.7. Selective knockdown of PI3K mRNA in the prefrontal cortex of *FmrI* knockout mice abolishes specific behavioural deficits and reduces audiogenic seizure frequency (Gross *et al*., 2015). Additionally, this inhibition restores the increase in protein synthesis observed in the KO, measured by incorporation of radiolabelled amino acids, to wild-type levels. Finally, dendritic spine density is restored to wild-type levels, shown by golgi staining and subsequent imaging of dendrites.

As can be seen from Figure 1.7, PTEN forms part of the mTOR pathway by inhibiting PI3K and mutations in this gene have been found to cause epilepsy, intellectual disability and autism (Table 1.3). The mTOR pathway is overactive in mice with a conditional knockout of PTEN in the brain and inhibiting mTOR activity using rapamycin in these mice alleviates some of the disease phenotypes. These mice have macrocephaly but treatment with rapamycin restores brain size to wild-type levels. Suppression of mTOR activity with rapamycin also rescues behavioural

deficits in tests of anxiety and social behaviour and reduces spontaneous seizure activity (Zhou *et al*., 2009).

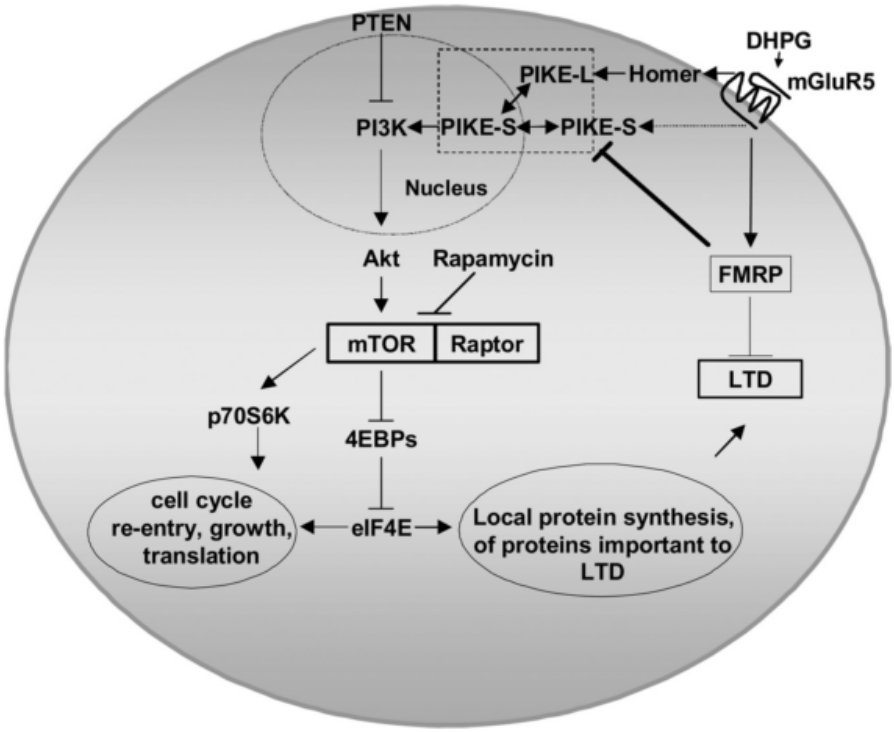

Figure 1.7. A schematic of the mTOR pathway showing its proposed interaction with FMRP. *FMRP is thought to inhibit PIKE-S. This downregulates PI3K and Akt signalling resulting in negative regulation of mTOR signalling. Supplying the agonist DHPG to activate mGluR5 up-regulates mTOR signalling via complex formation with Homer and PIKE-L. An increase in mTOR signalling stimulates translation of synaptic proteins leading to mGluR-dependent-LTD. In Fragile X, this LTD is exaggerated due to over-activation of the mTOR pathway. The pathway is overactive because FMRP is lost and is therefore unable to suppress PIKE-S. The control of protein synthesis is also lost resulting in an imbalance of synaptic proteins. Taken from Sharma et al (2010a).*

1.5. eEF1A and aging

Protein synthesis has been shown to slow down with age in many species, including human, rodents and *Drosophila* (Webster and Webster, 1983, Gonskikh and Polacek, 2017) and several lines of evidence suggest that elongation is the most rate-limiting step. Specifically, the rate of this step has been shown to be reduced by up to 80% by measuring translation elongation *in vitro* using cell-free extracts from aged *Drosophila*, nematode and rodent organs. Similarly, *in vivo* studies using rat liver and brain have shown that the rate of polypeptide chain assembly can be reduced by up to 50% with age (Rattan and Clark, 1996).

Several studies have shown a link between eEF1A and aging with convincing evidence for an age-related decline in eEF1A activity. One such study in *Drosophila* shows that eEF1A activity declines with aging due to a reduction in eEF1A synthesis and that this precedes a drop in global protein synthesis (Webster and Webster, 1983). It was thought that providing another copy of eEF1A through genetic engineering could increase survival age of *Drosophila* by 41% (Shepherd *et al*., 1989) but it was later shown that these genetically engineered flies did not actually overexpress eEF1A (Shikama, Ackermann and Brack, 1994). However, it has been shown that transgenic fungi containing eEF1A high-fidelity mutations live longer which suggests that eEF1A may act to increase lifespan by preventing errors in peptide elongation (Silar and Picard, 1994).

Moldave *et al* (1979) studied protein synthesis in rat brain and liver, and found that the rate was 30% less in 30-month-old rats compared with 3-month old rats and that this was accompanied by a 30-40% decrease in eEF1A activity. A 35-45% decrease in eEF1A protein expression levels and activity has also been observed in cell-free extracts from senescent human fibroblasts (Rattan *et al*., 1996).

eEF1A has also been studied in an attempt to find links with age-related disease. Griffiths *et al* (2012) studied an aging cohort of wasted heterozygous mice to look for signs of late-onset neurodegeneration. They used the rotarod and grip strength tests to study motor function and muscle function, respectively, and stained spinal

cords from 21 month old animals to look for signs of motor neuron degeneration. Perhaps surprisingly, they found that the performance of heterozygous mice in the rotarod and grip strength tests were comparable with wild-type mice and found no signs of neurodegeneration in the spinal cord. This shows that a presumed 50% decrease in eEF1A2 expression is compatible with normal function and survival in mice. As discussed in Section 1.3.3, eEF1A levels have also been shown to be reduced in AD (Beckelman *et al*., 2015, Beckelman *et al*., 2016).

1.6. Learning and memory

1.6.1. The basic neuroscience of learning and memory

Neuroscientists still do not fully understand the molecular processes underlying learning and memory, however, recent advances in technology have aided our understanding substantially. In the 19th century, many scientists thought that the processes involved in learning and memory were carried out by the brain as a whole, but lesion studies showed that different parts of the brain controlled different memory functions (Queenan *et al*., 2017). For example, a patient called Henry Molaison ("HM") had his anterior hippocampus, amygdala and surrounding cortex removed from both hemispheres to cure his intractable epilepsy. Unfortunately, as a product of this, he ended up with a very specific type of memory impairment. This memory loss was specific for episodic memories (memories for events) and HM had a complete inability to form new memories and a severe impairment in memory recall. However, his procedural memory (memory for skills e.g. riding a bike) remained intact (Squire, 2009). The different types of memory, including those mentioned above, are shown in figure 1.8.

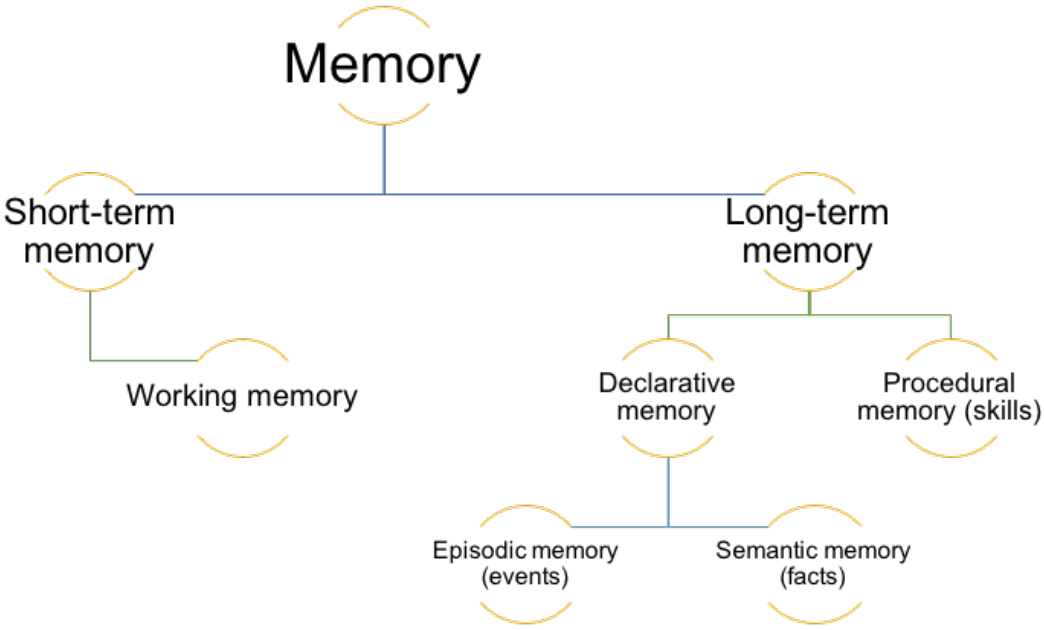

Figure 1.8. The different types of memory. *First of all, memory is divided into short-term and long-term memory. Short-term memory has limitations in duration and capacity. Short-term memory can hold a finite number of items temporarily (generally agreed to be around 7 items in adults). Generally, short-term memory is the memory for the "here and now". Working memory is a type of short-term memory that is used to plan and execute an action. Working memory is required to perform mental arithmetic or to cook without introducing the same ingredient more than once. Long-term memory is a form of memory whereby memories are stored and are able to be recalled later. Long-term memory formation requires new protein synthesis. Procedural memory is unconscious memory for skills such as reading, writing and riding a bicycle i.e. processes that don't require thinking about in order to perform them. Declarative memory is conscious memory for either events that have happened in a person's life e.g. remembering lunch with a friend last week (episodic) or memory for facts e.g. knowing who is the Prime Minister (semantic). Constructed from information in Shanks and John, 1994, Cowan, 2008 and Queenan et al., 2017.*

Synaptic plasticity is generally accepted to be the cellular mechanism underlying learning and memory. This concept was introduced by Donald Hebb in 1949 who stated that neurons that "fire together, wire together". By this, Hebb hypothesised that connections between co-activated cells are altered by synaptic activity (Hebb, 1949, Queenan *et al*., 2017). This idea was expanded by Bliss and Lomo (1973) who

identified that repetitive stimulation of the perforant path fibres to granule cells in the hippocampus lead to specific changes. They found that this repeated stimulation caused a potentiated response from the granule cells lasting up to 10 hours, characterised by a reduction in population spike latency and an increase in excitatory-post-synaptic-potential (EPSP) and population spike amplitude. This meant that there was an elevation in the efficiency of synaptic transmission.

This strengthening of synaptic connections and therefore increase in the efficacy of synaptic transmission is known as long-term potentiation (LTP). When populations of cells fire asynchronously, there is a decrease in the efficacy of synaptic transmission and a weakening of synaptic connections known as long-term depression (LTD). It is thought that these two types of change in synaptic strength underlie memory formation, and may confer learning and forgetting, respectively. Changes in synaptic strength and connectivity have been observed in specific subsets of neurons during memory formation and it is thought that this is required to store information. The maintenance of LTP and LTD requires new protein synthesis (Martin, Grimwood and Morris, 2000, Queenan *et al*., 2017).

The specific molecular alterations occurring at the synapse that accompany these changes are not fully understood but there are known alterations in neurotransmitter receptors, mRNA expression, protein expression, post-translational modifications and the structure of the extracellular matrix (Queenan *et al*., 2017).

1.6.2. The role of eEF1A in learning and memory

Since the maintenance of LTP and LTD require new protein synthesis, local synthesis of proteins at synapses is likely to be important. Much of the recent work towards understanding the molecular basis of learning and memory has focussed on identifying mRNAs that are expressed at synapses and understanding how translation is regulated at these sites.

There is evidence to suggest that eEF1A is translated locally at synapses and plays a role in LTP and LTD. In rat hippocampus, eEF1A has been identified as part of a

group of mRNAs transported from the soma to the dendrites (Zhong, Zhang and Bloch, 2006). In a pull-down experiment using adult rat brain extracts, eEF1A protein was identified as a binding partner of the alpha-2 subunit of the glycine receptor. This interaction was confirmed in rat spinal cord, specifically for eEF1A2. Subsequent immunofluorescence experiments in cultured rat hippocampal and spinal cord neurons showed that eEF1A protein co-localised with the alpha-2 subunit at inhibitory synapses (Bluem *et al*., 2007).

It has been found that induction of LTP at rat hippocampal synapses results in both an increase in eEF1A protein expression and increased activation of the mTOR pathway. This increase in eEF1A can be observed in dendrites that have been severed from the cell body, showing that the increase is due to local protein synthesis. Both the increase in eEF1A and the maintenance of LTP are blocked by rapamycin, an mTOR inhibitor, showing that activation of the mTOR pathway is crucial for the maintenance of LTP. It is hypothesised that synaptic stimulation activates mTOR signalling which then enhances translation allowing maintenance of LTP (Tsokas *et al*., 2005). This study highlights a role for eEF1A in the maintenance of LTP.

Similarly, local translation of eEF1A has been observed at synapses in response to LTD. Induction of LTD by metabotropic glutamate receptor (mGluR) activation results in an increase in eEF1A protein expression in the dendrites of rat hippocampal neurons. Induction of LTD also increases ERK phosphorylation suggesting that there is activation of the ERK signalling pathway in response to LTD. Interestingly, the same group found that eEF1A mRNA is highly expressed in developing dendrites suggesting that eEF1A may play a role in synaptic development (Huang, Chotiner and Steward., 2005). This study suggests that eEF1A plays a role in the synaptic mechanisms underlying LTD.

1.7. Project aims

The majority of my PhD project involved behavioural testing of mice with different mutations in *Eef1a2*. I studied two lines with heterozygous null mutations on different genetic backgrounds and a third line with the D252H missense mutation identified in humans. The aim of this was to determine whether these mice showed any phenotypes that were consistent with the intellectual disability and autism observed in humans with *EEF1A2* mutations. Another part of my project was to assist with genotypic and phenotypic characterisation of mice with the *Eef1a2*/G70S missense mutation that were generated using CRISPR/Cas9.

My individual aims according to chapter are as follows:

- **Chapter 3** - To characterise mice with the *Eef1a2*/G70S missense mutation with an aim to better understand the mechanisms underlying the human phenotype.
- **Chapter 4** – To determine the effects of age and genetic background on the behaviour of heterozygous *Eef1a2*-null mice.
- **Chapter 5** – To investigate the effects of the *Eef1a2*/D252H missense mutation on mouse behaviour.

Chapter 2: Materials and Methods

2.1. Materials

All laboratory chemicals and primers are from Sigma-Aldrich unless otherwise stated. Recipes for all buffers and solutions are shown in Table 2.1.

Buffer or solution	**Recipe for working solution**
25% AMPS	0.25g Ammonium Persulphate (AMPS) dissolved in 1ml dH_2O
Betaine	7.44g Betaine Monohydrate dissolved in 10ml dH_2O
Deoxyribonucleoside triphosphates (dNTPs)	10µl of each 25µM dNTP (dATP, dCTP, dGTP, dTTP) (Invitrogen) diluted in 60µl dH_2O
Laemmli loading buffer	12ml 0.5M Tris-HCl pH6.8, 0.1g bromophenol blue, 10ml 100% glycerol, 10ml 20% SDS and 68ml dH_2O
Phosphate buffered saline (PBS)	1 Phosphate Buffered Saline tablet (PBS) tablet dissolved in 100ml dH_2O and autoclaved
Phosphate buffered saline with Tween 20 (PBS-T)	1ml Tween 20 (Thermo Fisher Scientific) mixed with 1L PBS
Primers for Polymerase Chain Reaction (PCR) and Reverse-Transcriptase Polymerase Chain Reaction (RT-PCR)	10µl of forward **or** reverse 100µM primer diluted in 90µl dH_2O to make 10µM aliquots
Primers for Quantitative RT-PCR (qPCR)	6µl of both forward **and** reverse 100µM primer diluted in 88µl dH_2O to make 6µM aliquots

Protein extraction buffer	50µl 100mM EDTA, 2.5ml 1M Hepes pH7.6, 7.5ml 1M NaCl, 500µl 1M NaF, 500µl Triton X and 39ml dH_2O
10% separating gel	8ml 1.5M Tris pH8.8, 10.4ml 30% acrylamide/bis (Bio-Rad), 160µl 20% SDS, 20µl TEMED, 80µl 25% AMPS and 13.4ml dH_2O
4.3% stacking gel	5ml 0.5M Tris-HCl pH6.8, 2.9ml 30% acrylamide/bis (Bio-Rad), 100µl 20% SDS, 10µl TEMED, 100µl 25% AMPS and 11.9ml dH_2O
20x TBE buffer stock	216g Tris Base, 110g Boric Acid, 80ml 0.5M EDTA (pH 8.0) and 920ml dH_2O
Western running buffer	100ml 10x TGS (Bio-Rad) diluted in 900ml dH_2O
Western transfer buffer	100ml 10x TGS (Bio-Rad), 200ml methanol and 700ml dH_2O

Table 2.1. Recipes for buffers and solutions used in experiments

2.2. General equipment

All behavioural apparatus was crafted in-house by Richard Wroblewski at the MRC Human Genetics Unit workshop. The Macintosh computer with Blackmagic Media Express software for mouse behaviour video acquisition was kindly provided by Dr Oliver Hardt from the Centre for Cognitive and Neural Systems, George Square. Following recording, videos were compressed using Handbrake software. A 30-day trial of the Any Maze program was downloaded to analyse the open field test. All other videos were scored manually. A small set of the objects used for novel object recognition were kindly provided by Dr Tine Pooters from the Centre for Integrative Physiology. The digital lux meter LX1010B was used to measure light levels in the behavioural apparatus. Animals were weighed using standard scales that gave measurements in grams (g) to two decimal places.

2.3. Mouse models

2.3.1. Husbandry and general practice

Mice were housed in the Biomedical Research Facility (BRF), University of Edinburgh. All maintenance and procedures were carried out in accordance with Home Office regulations. Mice were kept on a 12-hour light/dark cycle with *ad libitum* access to standard chow and water. Homozygous wasted mice, homozygous *Eef1a2*/del22.ex2 mice and homozygous *Eef1a2*/D252H mice were fed with diet gel (Clear H_2O) from P14. Mice were normally ear notched for genotyping and identification purposes at P14 and weaned at P21. When necessary, mice were culled using schedule 1 methods.

2.3.2. Details of mutations

The mouse models used in this project are shown in Table 2.2.

Name of mouse line	Mutation in *Eef1a2*	Genetic background	Breeding information
Wasted	15.8kb deletion removing promoter and first non-coding exon	Mixed (predominantly C57BL/6J, HRS/J and C3H/HeH)	Outbred
Eef1a2/del22.ex3	22bp deletion in exon 3	C57BL/6J	Inbred
Eef1a2/D252H	D252H missense mutation identified in patients: single base change from guanine (G) to cytosine (C) in exon 5 causing amino acid 252 to change from aspartic acid (D) to histidine (H)	C57BL/6J	Inbred
Eef1a2/G70S	G70S missense mutation identified in patients: single base change from guanine (G) to adenine (A) in exon 3 causing amino acid 70 to change from glycine (G) to serine (S)	C57BL/6J	N/A

Table 2.2. Details of mouse models used in this project

2.4. DNA methods

2.4.1. DNA extraction from ear notches

Ear notches were boiled for 10 minutes in 300µl 15mM NaOH, vortexed briefly, 25µl Tris 1M pH8 was added and the samples were shaken by hand to mix.

2.4.2. DNA extraction from tissue

DNA was extracted from mouse brain using the DNeasy Blood and Tissue Kit (Qiagen) following manufacturer's instructions.

2.4.3. Genotyping of wasted mice

Two sets of primers were used to genotype the wasted line. One primer pair amplified the wild-type allele and the other amplified the wasted allele. The primers used in the reaction are shown in Table 2.3. The primers named P2F and P2R (Khalyfa *et al*., 2001) were used to amplify the wild-type allele giving a 452bp product. The primers named wstspanF and wstspanR (Newbery *et al*., 2005) were used to amplify the wasted allele giving a 200bp product.

Each PCR reaction contained:

Component	Volume (µl)
10x PCR buffer (Invitrogen)	2.5
$MgCl_2$ (Invitrogen)	1
Taq DNA polymerase (Invitrogen)	0.2
10mM dNTPs (Invitrogen)	0.5
10µM primers	1
Betaine	7.5
dH_2O	8.3
Ear notch DNA	1
Total	25

Samples were run in the Bio-rad C1000 Touch Thermal Cycler using the program shown in Table 2.4.

Primer name	Sequence 5'-3'
P2F	TAG TGG CTC CTT GGA ACA G
P2R	CTA CTC TCC CTG AAT GCC TT
wstspanF	ATA AGC TCC CCA ATG GTA GAG AA
wstspanR	CGC GCC ATT CTT GTA TTG TT

Table 2.3. Sequences of primers used to genotype the wasted line

Step	Temperature	Time
Initial denaturation	95ºC	3 minutes
30 cycles	95ºC	1 minute
	62ºC	1 minute
	72ºC	1 minute
Final extension	72ºC	5 minutes

Table 2.4. PCR program for genotyping the wasted line

2.4.4. Genotyping of *Eef1a2*/del22.ex3 mice

A single set of primers was used to genotype the *Eef1a2*/del22.ex3 line to give a 208bp product when amplifying the wild-type allele and an 186bp product when amplifying the mutant allele. The primers used in the reaction are shown in Table 2.5.

Each PCR reaction contained:

Component	Volume (µl)
10x PCR buffer (Invitrogen)	2.5
$MgCl_2$ (Invitrogen)	1
Taq DNA polymerase (Invitrogen)	0.2
10mM dNTPs (Invitrogen)	0.5
10µM primers	1
Betaine	7.5
dH_2O	10.3
Ear notch DNA	1
Total	25

Samples were run in the Bio-rad C1000 Touch Thermal Cycler using a touchdown PCR program optimised in our laboratory by Faith Davies. This is shown in Table 2.6.

Primer name	Sequence 5'-3'
CRISPR *Eef1a2* null genotyping F	TGA GTT GTG CCT CTA CCC TT
CRISPR *Eef1a2* null genotyping R	TAC AGG CAC ATC CCA GGT GT

Table 2.5. Sequences of primers used to genotype the del22.ex3 line

Step	Temperature	Time
Initial denaturation	98ºC	5 minutes
7 cycles	98ºC	10 seconds
	68ºC, -1ºC/cycle	30 seconds
	72ºC	45 seconds
22 cycles	98ºC	10 seconds
	61ºC	30 seconds
	72ºC	45 seconds
Final extension	72ºC	7 minutes

Table 2.6. PCR program for genotyping *Eef1a2*/del22.ex3 mice

2.4.5. Genotyping of *Eef1a2*/D252H mice

A single set of primers was used to genotype this line to give a 442bp product. The primers used in the reaction are shown in Table 2.7.

Each PCR reaction contained:

Component	Volume (µl)
5x platinum super-fi buffer (Thermo Fisher Scientific)	4
Platinum super-fi polymerase (Thermo Fisher Scientific)	0.2
10mM dNTPs (Invitrogen)	0.4
10µM primers	1
Betaine	4
dH_2O	9.15
Ear notch DNA	0.25
Total	20

Samples were run in the Bio-rad C1000 Touch Thermal Cycler using the PCR program shown in Table 2.8.

Following PCR, samples were digested using Hin1II restriction enzyme. A digest of the wild-type allele produced two products: one of 330bp and one of 112bp. A digest of the allele containing the D252H mutation produced three products: one of 202bp, one of 128bp and a third of 112bp.

Each digest contained:

Component	**Volume (µl)**
Fast digest green buffer (Thermo Fisher Scientific)	2.5
Hin1II restriction enzyme (Thermo Fisher Scientific)	0.5
PCR product	15
dH_2O	7
Total	25

Samples were incubated at 37ºC for 5 minutes in the Bio-rad C1000 Touch Thermal Cycler.

Primer name	**Sequence 5'-3'**
1F primer	AGG CTA CCC CTT AGG CAG GT
1R primer	TGA ACA AAT GGT AGG TGG GAG G

Table 2.7. Sequences of primers used to genotype the *Eef1a2*/D252H line

Step	**Temperature**	**Time**
Initial denaturation	98ºC	60 seconds
30 cycles	98ºC	5 seconds
	58ºC	10 seconds
	72ºC	15 seconds
Final extension	72ºC	10 minutes

Table 2.8. PCR program for genotyping *Eef1a2*/D252H mice

2.4.6. Genotyping of *Eef1a2*/G70S mice

A single set of primers was used to genotype mice from the G70S CRISPR/Cas9 experiment, giving a 487bp wild-type product. The primers are shown in Table 2.9.

Each PCR reaction contained:

Component	Volume (µl)
10x PCR buffer (Invitrogen)	2.5
$MgCl_2$ (Invitrogen)	1
Taq DNA polymerase (Invitrogen)	0.2
10mM dNTPs (Invitrogen)	0.5
10µM primers	1
Betaine	7.5
dH_2O	10.3
Ear notch DNA	1
Total	25

Samples were run in the Bio-rad C1000 Touch Thermal Cycler using the touchdown PCR program shown in Table 2.10.

PCR products were digested using the restriction enzyme AciI. A digest of the wild-type allele produced two products: one of 274bp and one of 213bp. A digest of the G70S allele produced a full-length 487bp product as the only AciI site had been destroyed by a PAM site mutation.

Each digest contained:

Component	Volume (µl)
Cutsmart buffer (NEB)	1.5
Restriction enzyme (NEB)	0.5
PCR product	5
dH_2O	8
Total	15

Samples were incubated at 37ºC for 2 hours in the Bio-rad C1000 Touch Thermal Cycler.

Primer name	Sequence 5'-3'
G70S mice long F	ATC AAC ACC AGA GAG ATG GGA C
G70S mice long R	TCT TGA GGG ACT CTA TGC CCA AC

Table 2.9. Sequences of primers used to genotype *Eef1a2*/G70S mice

Step	Temperature	Time
Initial denaturation	98ºC	5 minutes
7 cycles	98ºC	10 seconds
	68ºC, -1ºC/cycle	30 seconds
	72ºC	45 seconds
22 cycles	98ºC	10 seconds
	61ºC	30 seconds
	72ºC	45 seconds
Final extension	72ºC	7 minutes

Table 2.10. PCR program for genotyping *Eef1a2*/G70S mice

2.5. RNA methods

2.5.1. RNA extraction from tissue

RNA was extracted from mouse brain using the RNeasy Mini Kit (Qiagen), following manufacturer's instructions. RNA concentration and quality was measured using the Nanodrop 1000 (Thermo Fisher Scientific).

2.5.2. DNase digestion

The DNase digestion was performed on-column during RNA extraction using the RNase-free DNase Set (Qiagen), following manufacturer's instructions.

2.5.3. RNA clean-up

To make sure the RNA was pure and free of contaminants, RNA clean-up was performed using the RNeasy Mini Kit (Qiagen), following manufacturer's instructions. RNA concentration and quality was measured using the Nanodrop 1000 (Thermo Fisher Scientific).

2.5.4. cDNA synthesis

cDNA was synthesised from RNA using the Affinity Script cDNA Synthesis Kit (Agilent Genomics), following manufacturer's instructions.

A "minus RT" (-RT) control was made in which 1µl of each RNA sample was mixed together and run in the reaction without reverse transcriptase to check for genomic DNA contamination. A "minus RNA" control was also made in which all components were added to the reaction except RNA.

2.5.5. Reverse-transcriptase PCR (RT-PCR)

All samples were run in triplicate with primers that amplified the *Eef1a2* gene and primers that amplified the reference gene, actin, in separate reactions. The *Eef1a2* primers amplified a 246 product and the actin primers amplified a 152bp product. The primers are shown in Table 2.11.

Each PCR reaction contained:

Component	Volume (µl)
10x PCR buffer (Invitrogen)	2.5
$MgCl_2$ (Invitrogen)	1
Taq DNA polymerase (Invitrogen)	0.2
10mM dNTPs (Invitrogen)	0.5
10µM primers	1
Betaine	7.5
dH_2O	10.3
cDNA	1
Total	25

Samples were run in the Bio-rad C1000 Touch Thermal Cycler on a PCR program shown in Table 2.12. For actin, the program was identical except the second cycling step was run for 20 cycles instead of 14 cycles (highlighted in bold in Table 2.12).

Primer name	Sequence 5'-3'
Eef1a2 RT-PCR F	GCC ACG ATC AGC ACT GCG
Eef1a2 RT-PCR R	CAA GCG GAC CAT CGA GAA GT
Actin F	TCC ATC ATG AAG TGT GAC GT
Actin R	GAG CAA TGA TCT TGA TCT TCA

Table 2.11. eEF1A2 and actin primers used in the RT-PCR reaction

Step	Temperature	Time
Initial denaturation	98ºC	5 minutes
10 cycles	98ºC	10 seconds
	69ºC, -1ºC/cycle	30 seconds
	72ºC	45 seconds
14 cycles	98ºC	10 seconds
	61ºC	30 seconds
	72ºC	45 seconds
Final extension	72ºC	7 minutes

Table 2.12. RT-PCR program for G70S mouse brain samples

2.5.6. Restriction enzyme digestion

RT-PCR products amplified using the protocol shown in Section 2.5.5 were digested with two restriction enzymes: AciI and MnlI. Using AciI, a digest of the wild-type allele produced four products: 127bp, 90bp, 25bp and 4bp whereas a digest of the G70S allele produced three products: 217bp, 25bp and 4bp as one AciI site had been destroyed by a PAM site mutation. Using MnlI, a digest of the wild-type allele produced four products: 112bp, 73bp, 39bp and 22bp whereas a digest of the G70S allele produced three products: 112bp, 112bp and 22bp as one MnlI site was destroyed by the G70S point mutation.

AciI and MnlI digests contained:

Component	Volume (µl)
Cutsmart buffer (NEB)	1.5
Restriction enzyme (NEB)	0.5
PCR product	5
dH_2O	8
Total	15

Samples were incubated at 37ºC for 2 hours in the Bio-rad C1000 Touch Thermal Cycler.

2.5.7. Quantitative RT-PCR (qPCR)

The following method was used to quantify eEF1A2 mRNA expression. Absolute quantification was performed using two reference genes – actin and GAPDH – the primer sequences for which are shown in Table 2.13 along with those for the eEF1A2 primers. The Brilliant II SYBR Green QPCR Master Mix (Agilent) was used to make the reaction mix as follows:

Component	Volume (µl)
2x Brilliant II SYBR green	5µl
6µM primer mix	0.5µl
Reference dye	0.375 (diluted 1:50 in dH_2O)
RNase free water	0.125
cDNA	4 (diluted 1:10 in dH_2O)
Total	10

Samples were run in the Light Cycler HT7900 (Roche) using the program outlined in Table 2.14.

Note that cDNA and controls were amplified using the RT-PCR protocol shown in Section 2.5.5 and run on a 2% agarose gel before proceeding with the qPCR to ensure that there was no contamination (see Section 2.5.4 for information on controls and Section 2.6 for information on agarose gel electrophoresis). The gel images are shown in Appendix A. For qPCR, each sample was run in triplicate and quantity means were calculated using Ct values along with the slope and Y-intercept from the standard curve for each gene. Melting curves and standard curves are shown in Appendix A.

Primer name	Sequence 5'-3'
eEF1A2 RT-PCR F	GCC ACG ATC AGC ACT GCG
eEF1A2 RT-PCR R	CAA GCG GAC CAT CGA GAA GT
Actin F	TCC ATC ATG AAG TGT GAC GT
Actin R	GAG CAA TGA TCT TGA TCT TCA
GAPDH F	GGA AGG GCT CAT GAC CAC A
GAPDH R	CCG TTC AGC TCT GGG ATG AC

Table 2.13. Primer sequences for qPCR

Cycles	Temperature	Time
1	95ºC	10 minutes
40	95ºC	30 seconds
	60ºC	1 minute

Table 2.14. Cycling program for qPCR

2.6. Agarose gel electrophoresis

2g of agarose (Invitrogen) was added to 100ml 0.5x TBE buffer and microwaved for 2 minutes to make a 2% w/v gel. Then 6µl SYBR safe (Invitrogen) was added to the gel mix and the mix was poured into a tray containing combs to make the wells. Once left to set for 30 minutes, the gel was transferred to a tank containing 0.5x TBE buffer and the PCR samples were loaded into the wells after addition of 5µl 6x purple gel loading dye (NEB). The first well was loaded with either hyperladder I (Bioline), low molecular weight marker (NEB) or 100bp DNA ladder (NEB) to visualise band sizes. The gel was run at a maximum voltage of 140V until band sizes could be accurately determined. All gels were imaged using either the Fujifilm FLA-5100 imager or using a standard transilluminator.

2.7. Protein analysis

2.7.1. Protein extraction from tissue

Tissue was weighed and placed in 2ml tubes containing 1.4 and 2.8mm ceramic beads (VWR). 10ml protein extraction buffer was aliquoted and 1 Complete Mini EDTA-free protease inhibitor tablet was added (Roche). This buffer was then added to the tissue at a volume of 10µl/mg and samples were homogenised using a Precellys 24 homogeniser. Samples were centrifuged for 10 minutes at 17,000g at a temperature of 4ºC in a Heraeus Fresco 17 centrifuge (Thermo Fisher Scientific). 100µl supernatant was then pipetted into a clean micro-centrifuge tube and mixed with 100µl laemmli loading buffer containing 5% v/v beta-mercaptoethanol. Samples were then boiled for 5 minutes, placed on ice for 2 minutes and stored at -20ºC until use.

2.7.2. SDS polyacrylamide gel electrophoresis

Gels were made in the laboratory using equipment from Bio-Rad: Mini-Protean Gel Casting Stand, glass plates, clamps and combs. The 10% separating gel was prepared in a 50ml Falcon tube and 4-5ml was pipetted between the glass plates, overlaid with 1ml isopropanol (Thermo Fisher Scientific) and left to set for 45 minutes. The isopropanol was then poured off and the plates were filled to the top with the 4.3% stacking gel mix which had been pre-prepared in a 50ml Falcon tube. Combs were inserted between the plates to make wells and the stacking gel was left to set for 30 minutes. Gels were wrapped in tissue paper, wet using water from the tap, wrapped in cling film and stored at 4ºC until use.

Gels were run in a Bio-Rad Protean III tank filled with Western running buffer. 10µl Full-Range Rainbow Molecular Weight Marker (Amersham) was loaded into the first well and 10µl of each sample was loaded into the other wells. The gel was run at 100V through the stacking gel and 150V through the separating gel until the samples had run to the bottom.

2.7.3. Membrane transfer

Following step 2.7.2, protein was transferred to an Immobilon-FL polyvinylidene difluoride (PVDF) membrane (Millipore). This was carried out using a Bio-Rad Mini Trans-Blot Electrophoretic Transfer Cell in a Bio-Rad Protean III tank containing Western transfer buffer for 1 hour at 400mA.

2.7.4. Immunoblotting

Membranes were blocked for 1 hour in Odyssey Blocking Buffer (Licor Biosciences) diluted 1:1 in PBS. Membranes were incubated overnight at 4ºC with primary antibodies diluted to an appropriate concentration in Odyssey blocking buffer 1:1 PBS-T. Antibody dilutions are given in the figure legends for each Western blot. The primary antibodies used were rabbit anti-eEF1A2 (50kDa) (Abcam) and mouse anti-GAPDH (38kDa) (Millipore). Membranes were washed 3 times with PBS-T for 5 minutes and incubated for 1 hour with secondary antibodies diluted 1:1000 in Odyssey blocking buffer 1:1 PBS-T. The secondary antibodies used were donkey anti-rabbit for eEF1A2 and donkey anti-mouse for GAPDH (Licor Biosciences). Membranes were washed 2 times with PBS-T for 5 minutes and photographed using the Licor Odyssey FC imager.

2.7.5. Western blot quantification

Western blots were quantified using Image Studio Lite Version 4.0 software. Values from the band of interest were normalised to values from the GAPDH loading control band.

2.8. Behaviour and motor testing

2.8.1. General information

All mice used for behavioural testing were male and were tested from 9 weeks of age. Female mice were excluded from testing due to the potential for results to vary across different phases of the oestrus cycle. The age groups tested for each mouse line are shown in Table 2.15. Mice were habituated to the test room for at least 15 minutes immediately prior to every test. Following data collection, analysis was performed with the experimenter blind to the genotype. Timelines showing the order that behavioural tests were carried out for each mouse line are shown in Figure 2.1.

Mouse line	Young	Middle aged	Older
Wasted mixed genetic background	2-6 months	7-11 months	12-18 months
Eef1a2/del22.ex3 C57BL/6 genetic background	2-5 months	N/A	N/A
Eef1a2/D252H	2-4 months	N/A	N/A

Table 2.15. Age groups of mice used in behavioural tests

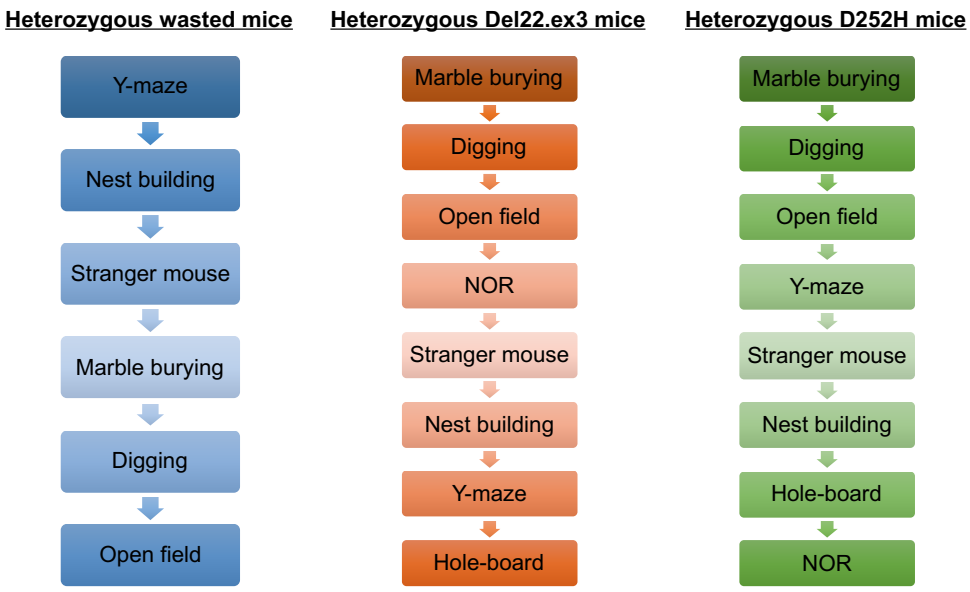

Figure 2.1. Order of behavioural tests for each mouse line. *The Y-maze test was always performed before the stranger mouse test to ensure that mice had no prior memory for the Y-shaped apparatus. For the heterozygous wasted line, a second cohort of mice was used for the marble burying, digging and open field tests. For these three tests, five of the mice tested at 2-6 months were also tested at 12-18 months. For the Del22.ex3 line, a second cohort of mice was used for the Y-maze and hole-board tests. For the D252H line, a second cohort of mice was used for the hole-board and novel object recognition (NOR) tests.*

2.8.2. Open field

The open field box was made of white Perspex and measured 50cm x 50cm. The light level was set to 100 lux in the centre of the box and the mouse was placed inside and allowed to explore for 5 minutes. The box was cleaned with 70% ethanol and rinsed with dH_2O between mice and at the end of each test day. Data was analysed using Any Maze software. Videos were scored for the total distance travelled, the total time spent freezing and the total time spent exploring the centre vs the outside of the arena. These measurements were taken across the full 5-minute test to assess locomotor activity and anxiety. A 30cm square superimposed onto the middle section of the apparatus was counted as the centre for scoring anxiety.

2.8.3. Y-maze

The Y-maze was made of Perspex, with three arms at 120 degrees to each other. The Y-maze was filled with fresh bedding and a handful of bedding from each cage of test mice. Light levels were set to 100 lux at the end of each arm using the lux meter. The test mouse was placed in one arm of the maze facing the wall and habituated to two arms for 5 minutes. After a 15-minute or 120-minute inter-trial interval (ITI), the gate closing the third arm was removed and the mouse was placed back in the same start arm and allowed to explore all 3 arms for 2 minutes. The bedding was mixed and gate and maze walls were cleaned with 1% Conficlean between trials. The maze was emptied, cleaned with 1% Conficlean and rinsed with dH_2O at the end of each test day. Videos were scored for the time spent in each arm during the test phase.

2.8.4. Novel object recognition in Y-maze

This test was carried out in the Y-maze apparatus (Image shown in Figure 4.20). The maze was filled with fresh bedding and a handful of bedding from each cage of test mice. The start arm was closed using a gate and gates were placed halfway along the other two arms. The light level was set to 100 lux in front of each gate using the lux meter. Mice were habituated to the maze for 5 minutes in two sessions separated by a 24-hour delay.

Testing began 24 hours after the second habituation session. In the sample phase, two identical objects were placed in front of the gates located halfway along the maze arms and the mouse was allowed to explore for 5 minutes. In the choice phase, one of the objects from the sample phase was swapped with a completely new, or "novel", object the test mouse had not interacted with before. The test mouse was allowed to explore the objects for 2 minutes. The choice phase took place 5 minutes after the sample phase and the position and identity of the novel object was counterbalanced between mice.

The bedding was mixed and gate and maze walls were cleaned with 1% Conficlean between mice and between phases. The maze was emptied, cleaned with 1% Conficlean and rinsed with dH_2O at the end of each test day. Videos were scored for

the time spent exploring each object during the choice phase. Exploration was defined as the mouse being in close proximity to and facing the object. Rearing against the objects was counted as exploration but climbing was not. Mice that explored for less than 10 seconds in the first minute of the choice phase were excluded from analysis. The discrimination ratio (DR) was calculated as the time spent exploring the novel object minus the time spent exploring the familiar object all divided by the total exploration time (N-F)/(N+F).

2.8.5. Novel object recognition in arena

The open field box was used for this test. The open field box was made of white Perspex and measured 50cm x 50cm. The light level was set to 100 lux in the centre of the apparatus using the lux meter. Mice were habituated to the box either once per day for 5 minutes on 2 consecutive days or twice per day for 5 minutes on 3 consecutive days depending on the experiment.

Testing began 24 hours after the final habituation session. In the sample phase, two identical objects were placed 5cm from the walls and the mouse was allowed to explore for 5 minutes. In the choice phase, one of the objects from the sample phase was swapped with a completely new, or "novel", object the test mouse has not interacted with before. The test mouse was allowed to explore the objects for either 2 minutes or 5 minutes depending on the experiment. The choice phase took place 5 minutes after the sample phase and the position and identity of the novel object was counterbalanced between mice.

The arena was cleaned with 70% ethanol between mice, between phases and at the end of each test day. Videos were scored for the time spent exploring each object during the choice phase. Exploration was defined as the mouse being in close proximity to and facing the object. Rearing against the objects was counted as exploration but climbing was not. Mice that explored for less than 25 seconds in the choice phase were excluded from analysis. The discrimination ratio (DR) was calculated as the time spent exploring the novel object minus the time spent exploring the familiar object all divided by the total exploration time (N-F)/(N+F).

2.8.6. Hole-board

The hole-board arena was made of white Perspex and measured 40cm x 40cm. An insert measuring 39.5cm x 39.5cm and containing 16 holes of 1.5cm diameter was placed inside the box. The light level was set to 100 lux in the centre of the box and the mouse was placed in and allowed to explore for 5 minutes. The box was cleaned with 70% ethanol and rinsed with dH_2O between mice and at the end of each test day. Videos were scored for hole exploration during the full 5-minute test.

2.8.7. Nest building

Fresh mouse bedding was added to a clean cage and a square of nest material was weighed and placed in the centre. The test mouse was placed in one corner of the cage facing the wall, the lid was placed on and the mouse was left overnight from 5pm-9am. The nestlet was removed from the cage and allowed to dry overnight and then it was scored according to the scale devised by (Deacon, 2006a, Figure 4.2) and weighed to calculate the percentage of shredded nestlet. Between mice, cages were cleaned with 70% ethanol and fresh bedding was added.

2.8.8. Marble burying

Fresh mouse bedding was added to a clean cage at a depth of 5cm and flattened by hand to make it level. Then, 20 marbles were placed in the cage in 4 rows of 5. The mouse was placed in the cage and left for 30 minutes. Videos were recorded to score the total number of marbles buried after the 30-minute test. A marble counted as buried if covered 2/3 by bedding. Bedding was mixed but was reused for subsequent mice (Deacon, 2006b). Marbles were cleaned with 70% ethanol, rinsed with dH_2O and dried between mice.

2.8.9. Digging

Fresh mouse bedding was added to a clean cage and the test mouse was placed in for 3 minutes in order to observe digging behaviour. Bedding was mixed but was reused for subsequent mice (Deacon, 2006b). Videos were scored for digging behaviour during the 3-minute test.

2.8.10. Stranger mouse social behaviour test

The stranger mouse test was carried out in the Y-maze apparatus (Images shown in Figures 4.5 and 4.6). The maze was filled with fresh bedding and a handful of bedding from each cage of test mice. The start arm was closed using a gate and two wire mesh gates were placed halfway along the other two arms. Light levels were set to 100 lux in front of each gate using the lux meter. The test mouse was habituated to the apparatus for 10 minutes. Following this, the mouse was removed briefly and a novel male mouse unrelated to the test mouse was placed between the mesh gates at one side of the apparatus. The test mouse was placed back in the maze and allowed to explore for 10 minutes. Then the test mouse was again removed and another novel mouse was placed between the mesh gates at the other side of the apparatus. The test mouse was then placed back in and allowed to explore for a further 10 minutes.

The position of novel mouse 1 was counterbalanced between mice. The bedding was mixed and gate and maze walls were cleaned with 1% Conficlean between mice and between habituation, test 1 and test 2 for a given mouse. The maze was emptied, cleaned with 1% Conficlean and rinsed with dH_2O at the end of each test day. Videos were scored for time spent with the novel mouse vs. the empty mesh gate in test 1 and time spent with the novel vs. the familiar mouse in test 2. Exploration was defined as the test mouse being in close proximity to and facing the stranger mouse/gate.

2.8.11. Olfaction

For three consecutive days prior to the test, ¼ Cadbury's chocolate button was placed in the home cage for 15 minutes to introduce the mouse to the food reward (habituation). 12 hours before the test, all food was removed from the home cage to stimulate hunger and therefore motivate the mouse to find the chocolate button in the testing phase. For testing, the mouse was placed in a clean cage with fresh bedding in which the food reward had been buried in one corner. The latency (s) for the mouse to find the buried food was measured and the test was stopped if the mouse failed to find the food after 15 minutes. The bedding was changed and the cage cleaned with 70% ethanol between mice.

2.8.12. Power calculations

Post-hoc power calculations were performed on behaviour results using online software (https://www.stat.ubc.ca/~rollin/stats/ssize/n2.html). Scores for wild-type and mutant mice from the literature were used to calculate sample size, taking the mean of three values for each where possible. The wild-type standard deviation values from my own set of experiments were used in the calculations to obtain sample sizes that were based on the variation in my mouse line. Details of each parameter in the calculation is shown in Table 2.16.

Parameter	Details
Mu1	Wild-type value from literature (mean of 3 independent values)
Mu2	Mutant value from literature (mean of 3 independent values)
Sigma	My wild-type standard deviation
Test type	Two sided
Alpha	0.05 (default)
Power	0.80 (default)

Table 2.16. Details of parameters set in sample size power calculations

2.8.13. Grip strength

All mice used for grip strength testing were male. Limb muscle strength was measured using the grip strength meter (Bioseb). Grip strength from all four limbs and front limbs only was measured in triplicate with a 1-minute break in between to let the mouse rest. This meant that each mouse had six trials: three with all four limbs and three with front limbs only. For testing, the mouse was lowered onto the grid until it gripped either both front paws or all four paws (depending on the test) and pulled from the grid by holding the tail. The maximum force (Newtons (N)) generated by the mouse was recorded. Scores were normalised to body weight.

Chapter 3: Characterisation of mice with the G70S *Eef1a2* mutation

3.1. Introduction

3.1.1. The G70S mutation

Five patients have been identified so far with a mutation in *EEF1A2* that changes glycine to serine at position 70 on the protein (G70S). This mutation is in exon 3 of the gene. These patients all present with epilepsy, intellectual disability and hypotonia. In some cases, there is also impaired motor development, autism, severe language impairment, abnormalities detected on brain scans and characteristic facial features. One of the G70S patients died from respiratory failure at 4 years old. This is all described in Section 1.3.2 and in Table 1.2.

3.1.2. Experimental design

It is important for us to model the human mutations in mice to investigate the underlying mechanisms that lead to disease. A mouse model would help us to understand whether the mutations result in loss or gain of protein function, an essential question that must be answered before we can think about developing therapeutic strategies. The work presented in this chapter is from a joint project performed by myself, Faith Davies, Fiona McLachlan and Francis Nuñez.

The G70S mutation was chosen to model in mice as it is the most frequently occurring mutation in humans. CRISPR/Cas9 was used to introduce the mutation because it is quick and easy to prepare the necessary guide RNAs (gRNAs) and repair templates, to generate mice with the desired mutation and to breed these mice to establish a colony. Due to the somewhat unpredictable nature of the technique and the possibility of creating multiple mutations, there is the chance that mice with the desired genotype will not be generated. However, this technique is at the forefront of molecular biology and is still remarkably quicker than other techniques.

The CRISPR/Cas9 mechanism of action is shown in Figure 3.1A. The gRNA (grey) contains a sequence complementary to the DNA region of interest and guides Cas9

here. Cas9 then introduces a double-stranded break into the DNA at the PAM site (red). The cell is able to repair this break in the DNA using one of two mechanisms: Non-homologous end joining (NHEJ) or homology directed repair (HDR). NHEJ is an error-prone process which can often introduce insertions or deletions into the DNA sequence during repair. In this experiment, this would give rise to mice with the genotypes *Eef1a2*$^{+/-}$ and *Eef1a2*$^{-/-}$. HDR is the desired repair method. This allows the region of interest to take up donor DNA in the form of repair templates. In this experiment, this would give rise to mice with the genotypes *Eef1a2*$^{G70S/+}$ and *Eef1a2*$^{G70S/G70S}$.

The gRNAs and repair templates were designed by Cathy Abbott (Figure 3.1B) and were cloned into pSpCas9n(BB)-2A-puro plasmids by Jennifer Doig. RNA was transcribed by Hemant Bengani and microinjected into single-cell stage mouse embryos by staff at the Evans Transgenic Unit, University of Edinburgh. Two repair templates were used: one of the repair templates had a G>A base change at the G70S site that would change glycine to serine in the protein, creating the G70S mutation, whilst the other repair template was wild-type at the G70S site. These two repair templates were used to increase the chance of producing heterozygous mice (*Eef1a2*$^{G70S/+}$). This genotype was predicted to have a high chance of survival and ability to breed, while homozygotes (*Eef1a2*$^{G70S/G70S}$) might have been expected to have too severe a phenotype.

With the human phenotype in mind, it was hypothesised that *Eef1a2*$^{G70S/+}$ mice might have seizures and behavioural impairments consistent with intellectual disability and autism. As for *Eef1a2*$^{G70S/G70S}$ mice, it was predicted that they may also present with seizures but would likely also show more severe phenotypes. For example, we know that *Eef1a2*-null wasted mice exhibit severe muscle wasting and motor neuron degeneration, dying by P28 (Shultz *et al*., 1982, Newbery *et al*., 2005). Therefore, it was possible that *Eef1a2*$^{G70S/G70S}$ mice might show a similar phenotype and, if more severe than null mice, may point towards gain of function as a disease mechanism. Conversely, expression of G70S eEF1A2 may have been sufficient to protect against neurodegeneration.

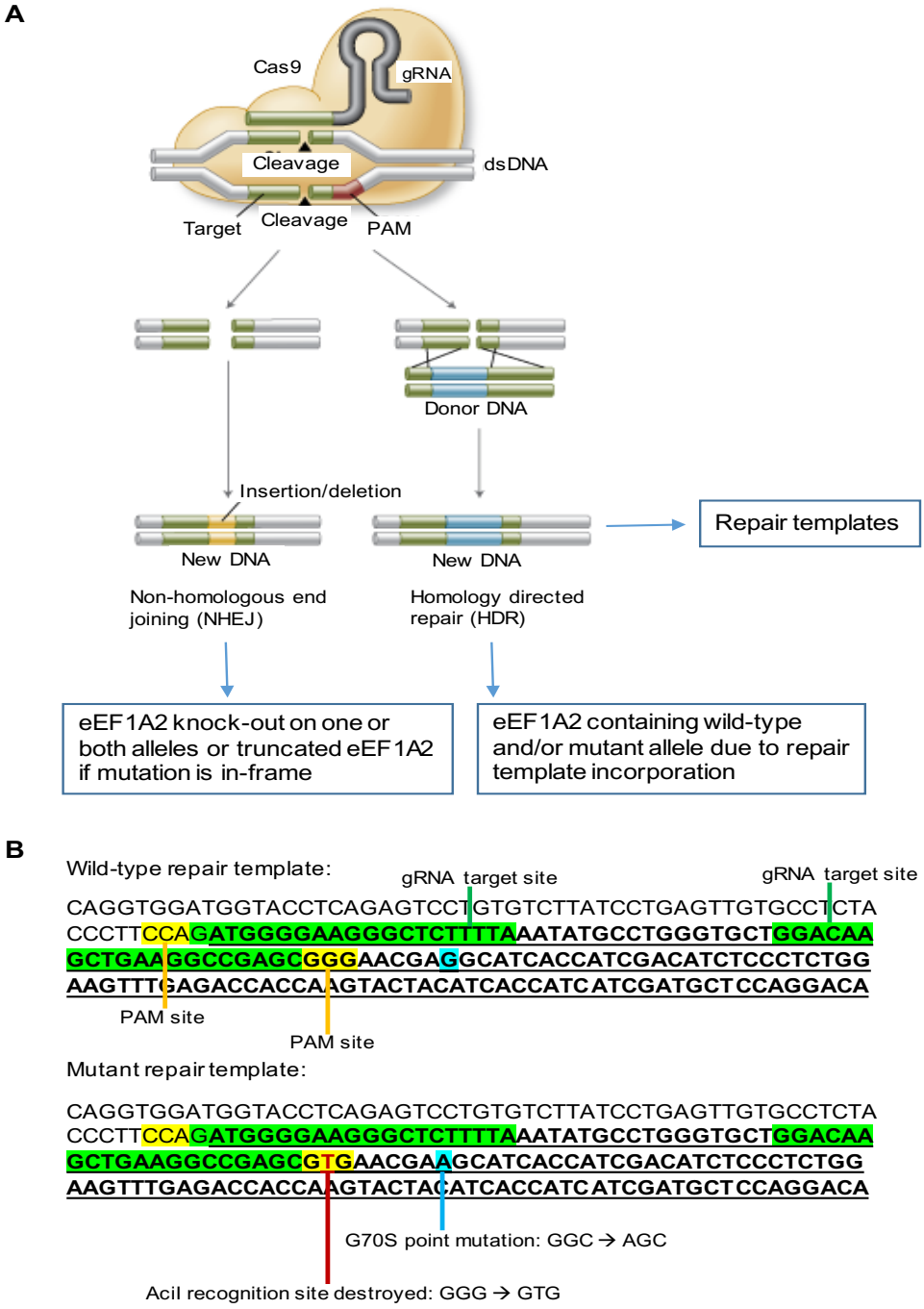

Figure 3.1. Design of CRISPR/Cas9 experiment. ***A.*** *CRISPR/Cas9 mechanism of action. Adapted from (Reis et al., 2014).* ***B.*** *Wild-type and mutant repair template design.* ***Exon 3*** *is shown in bold and underlined. The gRNA target sites are shown in green, the PAM sites in yellow and the G70S site in blue. A point mutation in the mutant repair template destroys an AciI restriction enzyme site (shown in red). The G>A point mutation at the G70S site in the mutant repair template destroys an MnlI restriction enzyme site.*

I was aware of the possibility that mice would be generated with the genotypes *Eef1a2*$^{+/-}$ and *Eef1a2*$^{-/-}$ as a product of the CRISPR/Cas9 experiment. The expectation was that *Eef1a2*$^{-/-}$ mice would have a phenotype similar to that of wasted mice and would not survive past P28. Therefore, mice were genotyped promptly to allow prediction of severe phenotypes early and to provide sufficient time to make any necessary decisions regarding the fate of particular mice.

Thirty-five mice were born from two rounds of microinjection. The process involved microinjecting gRNA and repair template RNA into the cytoplasm of C57BL/6J fertilised oocytes and implanting these into four pseudopregnant females. Once the mice were born, Faith Davies and Francis Nuñez performed the PCR genotyping from ear notch tissue. Following this, I performed specific restriction enzyme digests on the PCR products to detect repair template incorporation prior to sequencing. Faith Davies performed the sequencing experiments necessary to confirm the genotype of each mouse. Faith Davies and I phenotyped and collected tissue from the mice together. After tissue collection, I performed RNA expression analysis and Fiona McLachlan performed protein expression analysis on brain tissue.

The work in this chapter has been published in Nature Scientific Reports (Davies *et al*., 2017).

3.1.3. Aims

- **To characterise mice with the *Eef1a2*/G70S missense mutation with an aim to better understand the mechanisms underlying the human phenotype.**

1) To identify mice with incorporation of the G70S repair template in advance of sequencing using specific restriction enzyme digests.

2) To determine the effects of the G70S mutation on phenotype and survival.

3) To perform post-mortem expression analysis using specific restriction enzyme digests to determine whether G70S eEF1A2 is expressed at the RNA level and how expression relates to phenotype and survival.

3.2. Results

3.2.1. Restriction enzyme digests were used to detect G70S incorporation

Once *Eef1a2* from each mouse ear notch had been amplified by PCR, I digested the products using the restriction enzyme AciI (Figure 3.2) to check for incorporation of the mutant repair template. This was done in order to predict how many mice had a G70S allele prior to sequencing. It was impossible to determine this through PCR alone as the G70S change is a point mutation and therefore the PCR product did not differ in size from wild-type. These digests were necessary so that we could predict mutations quickly and therefore monitor specific mice closely and make informed decisions regarding their fate. DNA from two of the mice, #13 and #18, could not be successfully amplified and therefore were not included in my digests.

A PAM site mutation engineered into the mutant repair template (GGG>GTG) destroyed an AciI restriction enzyme site. This meant that if the mutant repair template was incorporated, there would be one less AciI site in the PCR product and the cutting pattern would be altered. The wild-type PCR product is shown in Figure 3.2A. The digest product sizes were predicted using Serial Cloner software and are shown in Figure 3.2B. PCR products were digested and run on an agarose gel to view band sizes (Figure 3.2C).

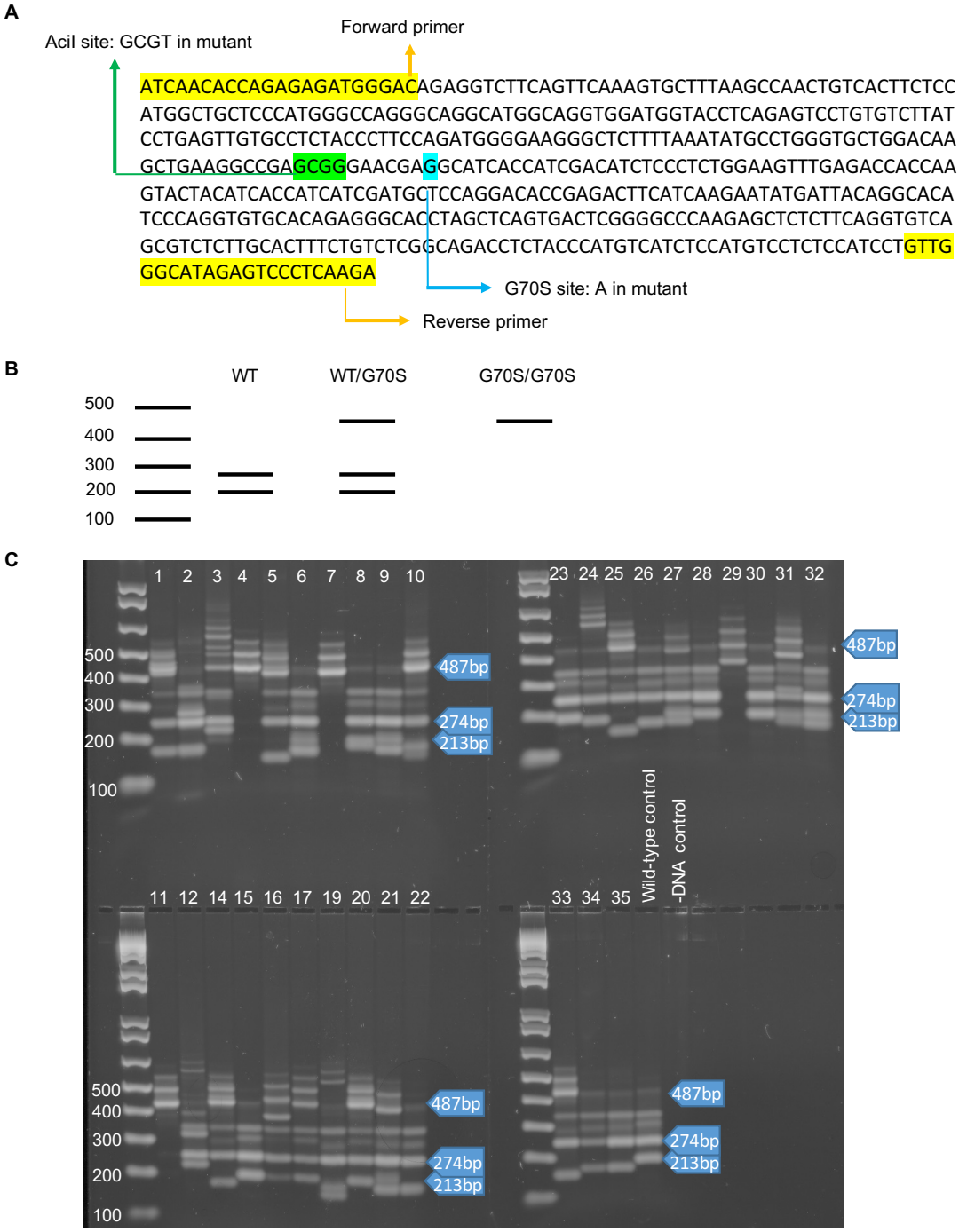

Figure 3.2. AciI genotyping digest. ***A.*** *WT PCR product showing the primers in yellow, the G70S site in blue and the AciI recognition site in green.* ***B.*** *Product sizes as predicted by Serial Cloner software. If the genotype is +/+ the sizes are 274bp and 213bp. If the genotype is G70S/+ the sizes are 487bp, 274bp and 213bp. If the genotype is G70S/G70S the product is a single, undigested band of 487bp.* ***C.*** *Agarose gel with AciI digest products run alongside a wild-type control to compare band sizes and a no DNA (-DNA) control to check for contamination. The positions of the bands of interest are indicated by the blue arrows.*

The AciI digest worked well and I was able to identify all three genotypes (+/+, G70S/+ and G70S/G70S). There were non-specific bands but these were higher than the bands that were specific and therefore the gel was able to be interpreted. Importantly, product sizes could be disrupted by the presence of indels and therefore it was not always possible to interpret band sizes with complete confidence. A full list of the genotype predictions from each mouse based on the digests is shown in Figure 3.3A. Figure 3.3B provides a summary, showing how accurate the digests were at predicting the genotypes based on the subsequent sequencing (carried out by Faith Davies). Note that mouse #12 was excluded from analysis as it could not be satisfactorily genotyped.

I analysed how accurate the AciI digest was at predicting G70S incorporation and the presence or absence of indels (Figure 3.3B). The digest was able to correctly predict the genotype of each allele based on G70S incorporation in 84% of samples. In addition, the digest showed a 66% match with the sequencing results when predicting the presence or absence of indels. The percentage match with sequencing based on predicting the correct genotype at the G70S locus and correctly predicting the presence or absence of indels was 59%. The digest predicted the genotypes incorrectly for some samples and this was likely due to disruption of restriction enzyme sites by the presence of indels. Another reason for inaccuracy was that small indels could not be detected on the gel.

A

Mouse ID	Predicted mutations from AciI digest	Are indels predicted from digests?	Actual mutations based on sequencing
1	Allele 1: WT Allele 2: G70S	Y	Allele 1: WT + 22bp del Allele 2: G70S
2	Allele 1: WT Allele 2: WT	Y	Allele 1: WT + 20bp del + 6bp sub Allele 2: WT + 19bp ins
3	Allele 1: WT Allele 2: G70S	Y	Allele 1: WT + large ins Allele 2: WT + 27bp ins
4	Allele 1: G70S Allele 2: G70S	N	Allele 1: G70S Allele 2: G70S
5	Allele 1: WT Allele 2: G70S	Y	Allele 1: WT + 43bp del + 1bp sub Allele 2: G70S + 1bp del
6	Allele 1: WT Allele 2: WT	Y	Allele 1: WT Allele 2: WT + 24bp del + 1bp sub
7	Allele 1: G70S Allele 2: G70S	N	Allele 1: G70S + 17bp del Allele 2: same as above or WT or both (mosaic)
8	Allele 1: WT Allele 2: WT	N	Allele 1: WT + 12bp del + 1bp del Allele 2: same as above or WT or both (mosaic)
9	Allele 1: WT Allele 2: WT	Y	Allele 1: WT Allele 2: WT + 14bp del
10	Allele 1: WT Allele 2: G70S	Y	Allele 1: WT + 16bp del Allele 2: G70S
11	Allele 1: G70S Allele 2: G70S	N	Allele 1: G70S + 10bp del Allele 2: same as above or WT or both (mosaic)
12	Allele 1: WT Allele 2: WT	Y	Unidentified – probable large insertions on both alleles
14	Allele 1: WT Allele 2: G70S	Y	Allele 1: WT + 22bp del Allele 2: G70S + 1bp del
15	Allele 1: WT Allele 2: WT	N	Allele 1: WT Allele 2: WT
16	Allele 1: WT Allele 2: G70S	N	Allele 1: WT + 125bp ins Allele 2: WT + 125bp ins
17	Allele 1: WT Allele 2: G70S	N	Allele 1: G70S + 1bp ins Allele 2: same as above or WT or both (mosaic)
19	Allele 1: WT Allele 2: WT	Y	Allele 1: WT + 25bp del Allele 2: WT + 40bp del
20	Allele 1: WT Allele 2: G70S	N	Allele 1: WT + 4bp del Allele 2: G70S
21	Allele 1: WT Allele 2: G70S	Y	Allele 1: WT + 22bp del Allele 2: G70S + 22bp del Allele 3: G70S + 1bp del
22	Allele 1: WT Allele 2: WT	Y	Allele 1: WT + 20bp del Allele 2: WT + 22bp del
23	Allele 1: WT Allele 2: WT	N	Allele 1: WT Allele 2: WT
24	Allele 1: WT Allele 2: WT	Y	Allele 1: WT + 180bp del Allele 2: WT + 10bp del
25	Allele 1: WT Allele 2: G70S	Y	Allele 1: WT Allele 2: WT + 42bp del
26	Allele 1: WT Allele 2: WT	Y	Allele 1: WT + 1bp del + 22bp del Allele 2: WT + 22bp del
27	Allele 1: WT Allele 2: G70S	Y	Allele 1: WT + 20bp del Allele 2: WT + 19bp del Allele 3: G70S + 19bp del
28	Allele 1: WT Allele 2: WT	N	Allele 1: WT Allele 2: WT + 1bp del Allele 3: WT + 45bp sub
29	Allele 1: G70S Allele 2: G70S	N	Allele 1: WT + 7bp del + 63bp del Allele 2: WT + 7bp del + 63bp del
30	Allele 1: WT Allele 2: WT	N	Allele 1: WT + 1bp del Allele 2: WT + 1bp del
31	Allele 1: WT Allele 2: G70S	N	Allele 1: WT + 7bp ins + 5bp sub Allele 2: G70S + 1bp del Allele 3: WT + 4bp del + 14bp sub Allele 4: WT + 10bp del Allele 5: G70S + 4bp del + 36bp del
32	Allele 1: WT Allele 2: WT	N	Allele 1: WT Allele 2: WT + 22bp del
33	Allele 1: WT Allele 2: G70S	Y	Allele 1: WT + 1bp del + 1bp del + 6bp del Allele 2: G70S
34	Allele 1: WT Allele 2: WT	Y	Allele 1: WT + 22bp del Allele 2: WT + 22bp del
35	Allele 1: WT Allele 2: WT	Y	Allele 1: WT + 23bp del Allele 2: WT + 48bp ins

B

	Match with sequencing		
	Alleles only	**Indels only**	**Alleles and indels**
Percentage match	84%	66%	59%

Figure 3.3. The accuracy of genotyping restriction digests based on the sequencing results. ***A.*** *Table showing the predicted mutations based on the results of the AciI digest compared with the results from the sequencing. Y = indels were predicted, N = indels were not predicted. Del = deletion, ins = insertion, sub = substitution. WT = wild-type for G70S.* ***B.*** *Table showing the percentage match of the AciI digests with the sequencing results and therefore the percentage of predictions that were accurate and showed the correct genotype. The results are summarised for alleles i.e. genotype based on presence or absence of G70S (+/+, G70S/+ or G70S/G70S) and for indels i.e. whether or not the digest correctly detected the presence of insertions and/or deletions. The "alleles and indels" group shows the percentage of digests that correctly predicted the right genotype based on both G70S incorporation and presence or absence of indels.*

3.2.2. A range of genotypes were obtained from the CRISPR/Cas9 experiment

The genotype of each mouse was confirmed by Faith Davies using a combination of Sanger sequencing, allele-specific sequencing and TOPO cloning (Table 3.1). Allele-specific sequencing and TOPO cloning were necessary where mice had indels on both alleles or had more than two alleles (mosaicism). All of the mice were successfully genotyped apart from mouse #12 and #13 which could not be genotyped with any certainty. However, all of the sequencing data that were obtained from these two mice pointed towards an *Eef1a2*$^{-/-}$ mosaic genotype.

Genotype	Number of mice	Mouse ID number
-/-	17	#2 #3 #5 #7 #11 #14 #16 #17 #18 #19 #22 #24 #26 #29 #30 #34 #35
+/-	5	#6 #9 #25 #32 #8
Mosaic	4	#21 #27 #28 #31
G70S/-	4	#1 #10 #20 #33
Unidentified	2	#12 #13
+/+	2	#23 #15
G70S/G70S	1	#4
G70S/+	0	-

Table 3.1. Summary of genotypes from the G70S CRISPR/Cas9 experiment. *Male mice are shown in blue and female mice are shown in orange. Mice with a null allele (-) had an indel in exon 3. Mice with a G70S allele had G70S incorporation on one or both alleles with no indels.*

Unfortunately, none of the mice had the G70S/+ genotype that was required to establish a new breeding line. However, one mouse was generated (#4) that had a G70S/G70S genotype but the phenotype was too severe for survival. Eight mice had G70S incorporation with an indel on the same allele. These alleles have been categorised as null or mosaic in Table 3.1. Only the five mice that had G70S allele(s)

containing no indels have been categorised as G70S/G70S or G70S/-. Expression analysis was required for each mouse to determine which alleles express RNA and protein.

3.2.3. The phenotype of *Eef1a2*$^{-/-}$ and *Eef1a2*$^{G70S/-}$ mice was comparable to the phenotype of wasted mice

The phenotype, fate and age at death for each mouse is shown in Table 3.2. Eighteen mice with the genotypes *Eef1a2*$^{-/-}$, *Eef1a2*$^{G70S/-}$ and *Eef1a2* mosaic showed a wasted phenotype characterised by tremor, ataxia, weight loss and early death by P28 (Shultz *et al*., 1982). These mice had to be culled after onset of phenotype as outlined on our project license. There was no difference in the timing of onset or severity of the wasted phenotype between *Eef1a2*$^{-/-}$ and *Eef1a2*$^{G70S/-}$ mice. Two of the mosaic mice that showed a wasted phenotype, #27 and #28, survived until P35 and P32 respectively. This is thought to be due to the assumption that some of the cells would have expressed wild-type eEF1A2.

The *Eef1a2*$^{G70S/G70S}$ mouse #4 was pointed out by the technician, who was blind to the genotype, at P18. This mouse had a tremor, was hunched and was visibly smaller than its littermates. It was also unable to right itself. It appeared to be displaying a wasted-like phenotype earlier than the onset in wasted mice which happens around P21. This mouse had to be culled at P18 due to the severity of the phenotype.

Wild-type mouse #15 was runted and had to be culled at P14. Inducing mutations using CRISPR/Cas9 can sometimes result in off-target mutations in other parts of the genome but no off-target mutations were detected in mouse #15 (the five most homologous gRNA sites were checked by Francis Nuñez). Therefore, the runted phenotype may have been due to either competition from other littermates in the womb/postnatal or a mutation, unrelated to the CRISPR/Cas9 process, located elsewhere in the genome. Competition from littermates is likely due to the large litter sizes and therefore limited availability of resources.

Mouse ID	Sex	Genotype	Phenotype	Fate	Age at death
1	M	G70S/-	Wasted	Culled	P25
2	M	-/-	Wasted	Culled	P22
3	M	-/-	AGS	Died	P18
4	M	G70S/G70S	Wasted	Culled	P18
5	M	-/-	AGS	Died	P18
6	M	+/-	Wild-type	-	-
7	M	-/-	AGS	Died	P18
8	M	+/-	AGS	Died	P18
9	M	+/-	Wild-type	-	-
10	F	G70S/-	Wasted	Culled	P25
11	F	-/-	AGS	Died	P18
12	F	Unidentified	Wasted	Culled	P25
13	F	Unidentified	Wasted	Culled	P29
14	F	-/-	AGS	Died	P18
15	M	+/+	Runted	Culled	P14
16	M	-/-	Found dead	Died	P23
17	M	-/-	Wasted	Culled	P25
18	M	-/-	Wasted	Culled	P25
19	F	-/-	Found dead	Died	P23
20	F	G70S/-	Wasted	Culled	P23
21	F	Mosaic	Found dead	Died	P23
22	M	-/-	Wasted	Culled	P23
23	M	+/+	Wild-type	-	-
24	F	-/-	Wasted	Culled	P23
25	F	+/-	Wild-type	-	-
26	M	-/-	Wasted, AGS	Died	P23
27	M	Mosaic	Wasted	Culled	P35
28	M	Mosaic	Wasted	Culled	P32
29	M	-/-	Wasted, AGS	Culled	P23
30	F	-/-	Found dead	Died	P23
31	F	Mosaic	Wasted	Culled	P23
32	F	+/-	Wild-type	-	-
33	F	G70S/-	Wasted	Culled	P23
34	F	-/-	Found dead	Died	P23
35	F	-/-	Wasted	Culled	P23

Table 3.2. Summary of phenotype, fate and age of death for each mouse in the G70S CRISPR/Cas9 experiment. *AGS = audiogenic seizure (described in Section 3.2.4), P = postnatal day. '-' indicates that a mouse was phenotypically normal and therefore had a normal lifespan.*

Mice were weighed regularly from P17-P30 (Figure 3.4). Unfortunately, the *Eef1a2*$^{G70S/G70S}$ mouse could not be included in the weight analysis as it was culled at P18 due to its severe phenotype. As only one healthy wild-type mouse was generated through the CRISPR/Cas9 experiment, another set of age-matched wild-type C57BL/6J mice were weighed to add to the dataset. *Eef1a2*$^{+/+}$ and *Eef1a2*$^{+/-}$ mice gained weight, as predicted, based on the evidence that heterozygous wasted mice are phenotypically normal (Griffiths *et al*., 2012). *Eef1a2*$^{-/-}$ and *Eef1a2*$^{G70S/-}$ mice failed to gain weight, a phenotype which is characteristic of wasted mice, albeit a non-specific one.

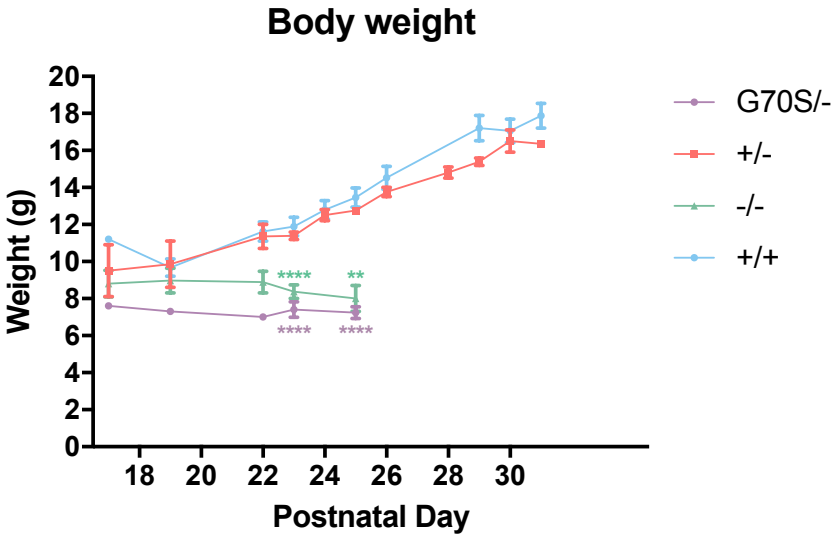

Figure 3.4. Weights of mice born from the G70S CRISPR/Cas9 experiment. *Weights were measured from P17-P30. Each genotype is represented by a different coloured line. The graph shows the mean weight for each genotype on each day with error bars showing SEM. At P23 and P25, the weights of Eef1a2*$^{-/-}$ *and Eef1a2*$^{G70S/-}$ *mice were significantly lower than those of Eef1a2*$^{+/+}$ *mice (One-way ANOVA: F = 13.9, DF = 3, 14, p = <0.0001. Tukey's multiple comparison test: at P23 p = <0.0001 for both genotype comparisons. At P25 p = <0.0001 for Eef1a2*$^{G70S/-}$ *vs. Eef1a2*$^{+/+}$ *and 0.0017 for Eef1a2*$^{-/-}$ *vs. Eef1a2*$^{+/+}$*. Weights of Eef1a2*$^{-/-}$ *vs Eef1a2*$^{G70S/-}$ *mice and of Eef1a2*$^{+/+}$ *vs Eef1a2*$^{+/-}$ *mice were not significantly different.*

3.2.4. *Eef1a2*$^{-/-}$ mice had seizures in response to environmental sounds

At P18, a loud sound of 90 decibels (dB) in the room next door was caused by collection of liquid nitrogen. This caused six mice to die from seizures (#3, #5, #7, #8, #11 and #14). They displayed wild running followed by tonic-clonic seizure and did not recover. At P23, the sound of a door banging caused mice #26 and #29 to have audiogenic seizures. Mouse #29 recovered but was subsequently culled due to a wasted phenotype.

All of the mice that had audiogenic seizures were *Eef1a2*$^{-/-}$, apart from mouse #8 which was *Eef1a2*$^{+/-}$. However, the sequencing results from mouse #8 were complicated (see Figure 3.3A) and it was later found to have very low expression of eEF1A2 in muscle and no expression in brain. The other genotypes that were exposed to the sound stimuli were *Eef1a2*$^{+/-}$, *Eef1a2*$^{G70S/-}$, *Eef1a2*$^{G70S/G70S}$ and *Eef1a2* mosaic but none of these mice had seizures. It should be noted, however, that the group sizes were very small and that these seizures were accidental and were not performed under controlled conditions. Therefore, results should be interpreted with caution and further study will be required to determine whether missense mutations in *Eef1a2* increase audiogenic seizure susceptibility in mice.

It is noteworthy that five other mice had sudden unexplained deaths at P23: #16 (*Eef1a2*$^{-/-}$), #19 (*Eef1a2*$^{-/-}$), #21 (*Eef1a2* mosaic), #30 (*Eef1a2*$^{-/-}$) and #34 (*Eef1a2*$^{-/-}$). Mice #30 and #34 were found dead in their home cage in the morning, having seemed healthy when checked the previous afternoon at P22. Mice #16, #19 and #21 were being moved from the Evans Transgenic Unit to the Biomedical Research Facility (BRF) next door for housing purposes but died during transfer. The reasons for these sudden deaths could not be resolved and it is entirely possible that the mice may have had fatal seizures. However, this remains undetermined.

3.2.5. G70S eEF1A2 was expressed in brain but unable to compensate for loss of wild-type protein

To investigate the effects of the G70S mutation on eEF1A2 function at the mRNA and protein level and to gain insight into whether the mutation may lead to loss or gain of protein function, expression analysis was performed. After mice were culled, brain and muscle tissue was collected. Western blots to examine eEF1A2 protein expression in brain are shown overleaf (performed by Fiona McLachlan, Figure 3.5A) and RT-PCR gels to examine eEF1A2 mRNA expression in brain are shown in Figure 3.5B (performed by myself). Following the RT-PCR, I performed restriction enzyme digests using AciI and MnlI to determine which alleles were expressing RNA and protein. This was an important step to determine whether or not G70S eEF1A2 was being expressed. If G70S eEF1A2 was not expressed, this would point towards loss of function as a disease mechanism. However, if G70S eEF1A2 was expressed, gain of function would remain possible.

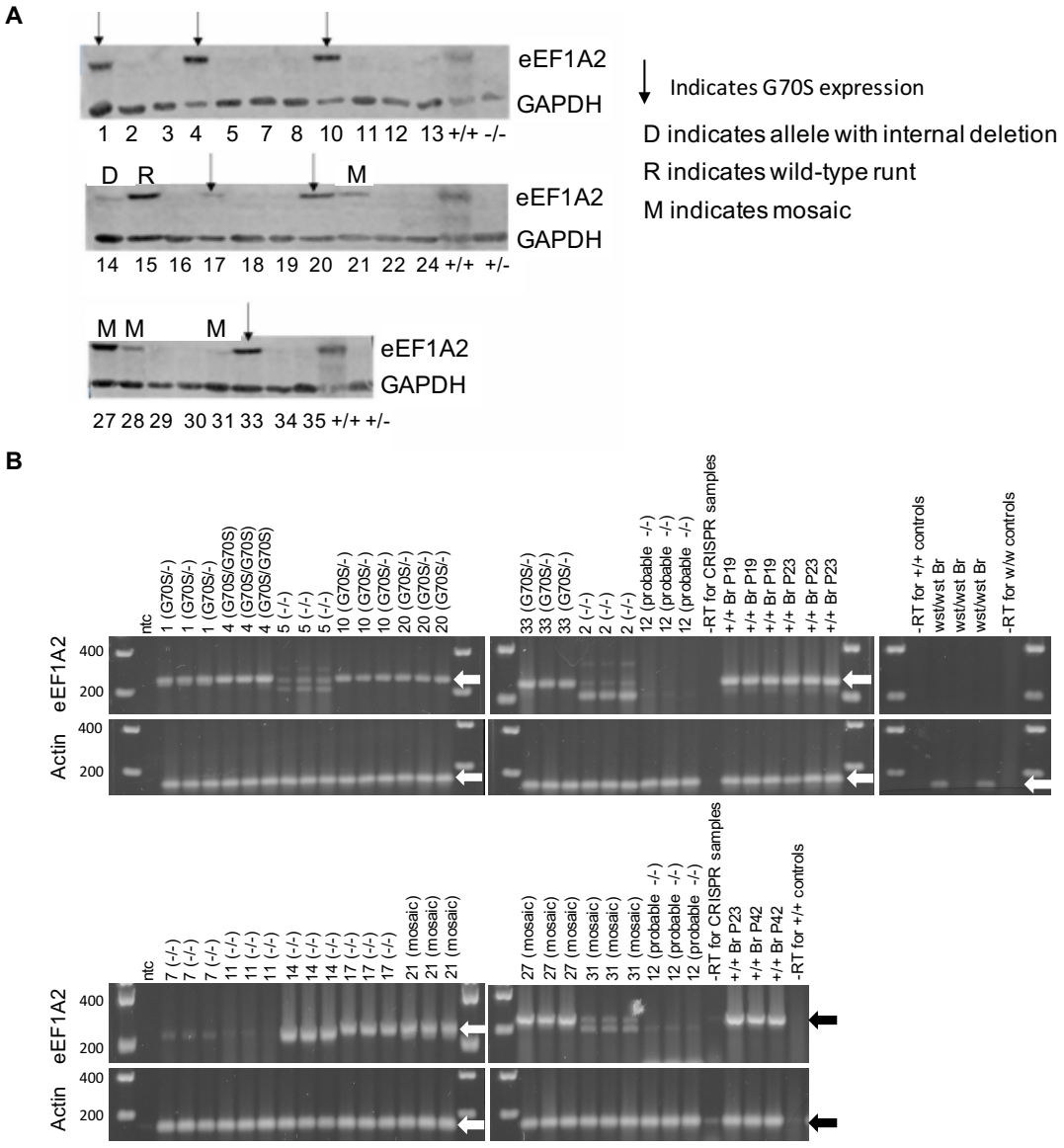

Figure 3.5. eEF1A2 expression in the brains of mice from the G70S CRISPR/Cas9 experiment. A. *Western blots probed with an eEF1A2 antibody and a GAPDH antibody as a control. Arrows indicate mice that were subsequently found to express eEF1A2 containing the G70S mutation. Experiment by Fiona McLachlan, adapted from Davies et al., 2017.* ***B.*** *RT-PCR using cDNA from brain tissue with primers amplifying Eef1a2 and actin as a reference gene. The 200bp and 400bp ladder bands are shown (Bioline Hyperladder I). Arrows show the positions of the bands for eEF1A2 at 246bp and actin at 152bp. ntc = no template control, -RT control = no reverse transcriptase control, +/+ Br = wild-type brain positive control, wst/wst Br = wasted brain negative control. Mice #2 and #12 were also included as negative controls.*

Based on the Western blot results (Figure 3.5A), mouse #1, #4, #10, #14, #15, #17, #20, #21, #27, #28 and #33 were expressing eEF1A2 protein. This Western showed whether or not eEF1A2 was expressed in brain tissue from each mouse but did not allow us to distinguish between wild-type eEF1A2 and G70S eEF1A2 as there is no reason to assume that the presence of the mutation would affect protein size. To determine which allele(s) were expressing RNA and protein, I performed RT-PCR (Figure 3.5B) and digested the products using the restriction enzymes MnlI and AciI (Figure 3.6).

For the RT-PCR, the initial analysis was on samples that had G70S incorporation on one or both alleles with no indels (Top gel – mouse #1, #4, #10, #20, #33). Mouse #5 was initially suspected to have G70S incorporation on one allele with no indels but was subsequently found to have a 1bp deletion on the same allele. Therefore, it was, in fact, a null (*Eef1a2*$^{-/-}$). It can be seen that all of the samples on this gel were expressing eEF1A2 (arrows), apart from mouse #5, showing that all of the mice with a clean G70S allele were expressing RNA. All of the mice, apart from #5, were also shown to express eEF1A2 protein on the Western. Mouse #4 could only be expressing RNA and protein containing the G70S mutation as this mouse had the mutation on both alleles with no indels. For the other mice, restriction digests were required to determine whether or not they were expressing eEF1A2 with the G70S mutation.

Subsequent RT-PCR analysis was carried out on samples that had G70S incorporation with an indel on the same allele (Bottom gel - #7, #11, #14, #17, #21, #27, #31) since these mice could be expressing G70S eEF1A2. Mice #17, #21 and #27 were found to express eEF1A2 RNA and protein. Mouse #14 also had a strong band indicating RNA expression but it was slightly smaller than the expected size for eEF1A2. This mouse showed a slightly smaller band on the Western too indicating that it may express a truncated protein. This fits with sequencing data showing that mouse #14 had a 21bp in-frame deletion. Mice #7 and #11 did not express eEF1A2 at the RNA or protein level, however, mouse #31 showed a faint band both in the RT-PCR and in the Western.

The two RT-PCR analyses also provided insight into the nature of the mutations in some of the samples that did not express G70S. In the sample from mouse #2, a strong band smaller in size than that would be expected for eEF1A2 was observed. This was despite the fact that the mutations on both alleles (a 20bp deletion and a 19bp insertion) were out of frame and were therefore predicted to cause a premature stop codon and lead to nonsense-mediated decay of the mRNA product. The band observed in the RT-PCR is much stronger than that would be expected if the mRNAs were undergoing nonsense-mediated decay. There are a few possible explanations for this: there was an error in the sequencing results and one of the mutations is actually in frame, the frameshift on one of the alleles may not actually lead to a premature stop codon or one of the alleles is resistant to nonsense-mediated decay as observed previously with mutations in other genes (Neu-Yilik *et al*., 2011). This mouse was not expressing eEF1A2 at the protein level despite the strong mRNA expression, therefore it's likely that the mRNA was translated but the protein was subsequently degraded. Mouse #31 shows two bands in the RT-PCR and one faint band in the western indicating expression of eEF1A2 at the RNA and protein level. It is curious that this mouse expresses eEF1A2 protein, albeit at a very low level, despite the fact that none of the mutations were in frame. The same possibilities highlighted for mouse #2 also apply here. Mice #7 and #11 also yielded interesting results as the sequencing from these mice was difficult to interpret and it appeared that both mice might have a wild-type allele (Figure 3.3A). However, the lack of eEF1A2 expression both in the RT-PCR and the western blot indicates that neither mouse had a wild-type allele and therefore were not mosaics.

To summarise the expression results in Figure 3.5. it can be seen that mice #1, #4, #10, #20, #33, #17, #21 and #27 were expressing high levels of eEF1A2 RNA and protein. Mouse #14 was also expressing RNA and protein but the size was slightly smaller than that expected for eEF1A2. Note that mouse #28 expressed protein on the Western but was not included in the RT-PCR as there was no evidence of G70S incorporation in the sequencing. I next performed restriction enzyme digests on the RT-PCR products using AciI and MnlI to determine which alleles were expressing RNA and protein (Figure 3.6).

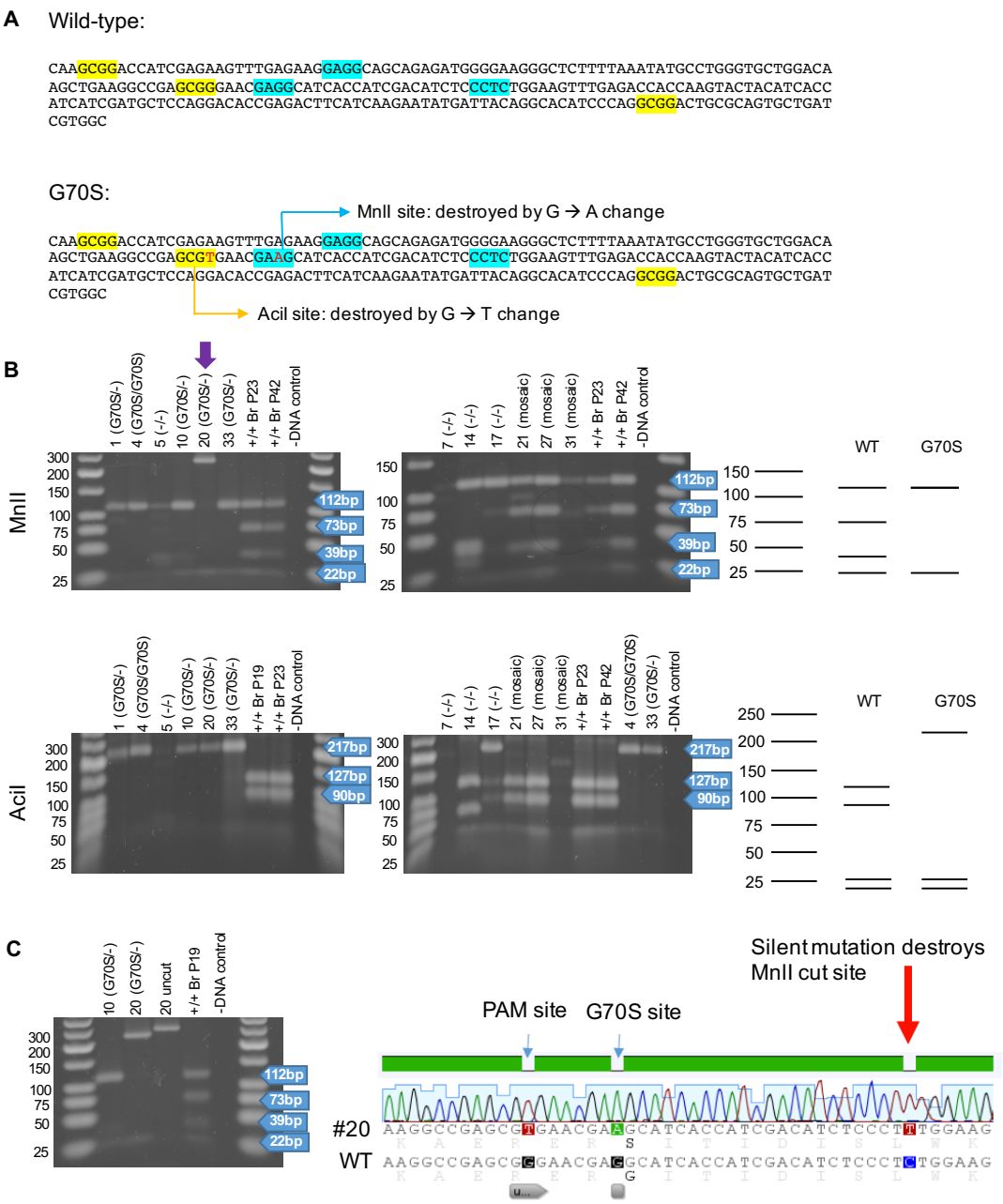

Figure 3.6. eEF1A2 RT-PCR products digested with restriction enzymes. ***A.*** *RT-PCR products showing cut sites for AciI and MnlI.* ***B.*** *MnlI and AciI digests with product sizes predicted by Serial Cloner software. MnlI (top) - wild-type band sizes: 112bp, 73bp, 39bp and 22bp. G70S band sizes: 112bp, 112bp and 22bp. The purple arrow indicates the sample from mouse #20 failed to digest in the predicted way. AciI (bottom) - wild-type band sizes: 127bp, 90bp, 25bp and 4bp. G70S band sizes: 217bp, 25bp and 4bp.* ***C.*** *Repeated MnlI digest on sample #20 and corresponding sequencing trace showing that the cut pattern was changed by a silent mutation that destroyed an MnlI site (red arrow).*

The MnlI and AciI digest results are shown in Figure 3.6B. With MnlI, digest of the wild-type allele produced bands of 112bp, 73bp, 39bp and 22bp whereas digest of the G70S allele produced bands of 112bp, 112bp and 22bp as one of the MnlI sites had been destroyed by the G70S change. With AciI, digest of the wild-type allele produced bands of 127bp, 90bp, 25bp and 4bp whereas digest of the G70S allele produced bands of 217bp, 25bp and 4bp as one AciI site had been destroyed by a silent mutation engineered into the repair template. A caveat of the MnlI digest was the inability to tell whether G70S RNA was also expressed in mice that expressed wild-type RNA due to overlapping bands. Mice #1, #4, #10 and #33 showed only the G70S cut pattern in both the MnlI and AciI digest indicating that the only allele that was being expressed, at both the mRNA and protein level, contained the G70S mutation.

Mouse #20 contained an additional silent C>T point mutation that destroyed the last recognition site for MnlI. The sequencing trace showing this mutation is presented in Figure 3.6C along with the repeated MnlI digest showing the 22bp difference between the undigested sample and the largest digest product. In the AciI digest (Figure 3.6B), sample #20 was digested giving a G70S cut pattern only. This shows that, as with mouse #1, #4, #10 and #33, this mouse was expressing only eEF1A2 RNA and protein containing the G70S mutation.

As mentioned, mouse #14 showed a smaller than expected product on both the RT-PCR and on the Western (Figure 3.5). Therefore, it was thought that this mouse could be expressing a truncated protein. From the sequencing results, this mouse had a known 21bp deletion one one allele and a 1bp deletion with G70S incorporation on the other. The cut pattern on both the MnlI and AciI digests was wild-type but specific bands were smaller than the predicted size. This could be observed most clearly in the AciI digest where the 127bp band was the correct size but the predicted 90bp band was smaller than expected and sat around the 75bp marker on the ladder. This pattern was consistent with expression of a truncated wild-type protein with a

21bp deletion. Absence of a G70S cut pattern shows that the other allele was not expressing.

Unexpectedly, mouse #17 seemed to be expressing RNA and protein from the G70S allele despite this allele containing an 1bp deletion. The MnlI and AciI digests both showed a strong G70S cut pattern with a faint wild-type cut pattern suggesting expression from both alleles. The sequencing from this mouse was hard to interpret but the G70S allele contained a single insertion. However, this did not seem to affect expression.

Mice #21 and #27 were mosaics each with at least one wild-type allele containing an indel and at least one G70S allele containing an indel. The cut pattern on both the MnlI and AciI digests was wild-type with no G70S cut pattern present suggesting expression from a wild-type allele only.

Lastly, mice #5, #7 and #31 showed faint bands in both digests that did not fit with either a wild-type or a G70S cut pattern. In summary, mice #1, #4, #10, #17, #20 and #33 expressed eEF1A2 protein containing the G70S mutation. Table 3.3 provides a summary of the Western blotting, RT-PCR and digest results described in Figure 3.5 and 3.6.

Mouse ID	Protein expression?	Alleles expressing mRNA and protein based on digest results	Notes
1 (G70S/-)	Y	G70S	
4 (G70S/G70S)	Y	G70S	
5 (-/-)	N	None	Originally thought to have clean G70S on one allele but found later to have an indel
7 (-/-)	N	None	
10 (G70S/-)	Y	G70S	
14 (-/-)	Y	WT	Truncated protein - also has a G70S mutation on the other allele but there's an indel which leads to no expression
17 (G70S/-)	Y	WT, G70S	Has a G70S mutation with an indel on the same allele but this doesn't seem to affect expression
20 (G70S/-)	Y	G70S	
21 (mosaic)	Y	WT	Also has a G70S mutation on another allele but there's an indel which leads to no expression
27 (mosaic)	Y	WT	Also has a G70S mutation on another allele but there's an indel which leads to no expression
31 (mosaic)	N	None	
33 (G70S/-)	Y	G70S	

Table 3.3. Summary of Western blot, RT-PCR and digest results showing which alleles were expressing eEF1A2 for each mouse of interest. *WT = wild-type.*

3.3. Discussion

The aims of this chapter were as follows:

1) To identify mice with incorporation of the G70S repair template in advance of sequencing using specific restriction enzyme digests.

2) To determine the effects of the G70S mutation on phenotype and survival.

3) To perform post-mortem expression analysis using specific restriction enzyme digests to determine whether G70S eEF1A2 is expressed at the RNA level and how expression relates to phenotype and survival.

My first aim was successful in that I was able to clearly identify products that represented wild-type and G70S alleles using the AciI digest. However, my genotype predictions were not accurate for every sample, likely due to disruption of restriction enzyme sites by indels. Despite this, the digest correctly predicted the alleles in 84% of samples, indicating a high success rate.

Unfortunately, we did not generate mice of the desired genotype (G70S/+) that were required to set up a new breeding line due to the high frequency of indels. A high number of indels arose due to inefficient repair template design caused by the position of the G70S mutation. Ideally, both PAM sites would have been mutated to prevent further cutting after repair template incorporation and this would have prevented the build-up of indels. However, the 5' PAM site was located near a splice site and therefore could not be mutated without risking changes to splicing and gene expression. Future attempts to generate a G70S mouse model may require the use of different methodology. One potential approach is to generate a knock-in mouse by introducing the mutation to mouse embryonic stem (ES) cells. These genetically modified ES cells can then be microinjected into a mouse blastocyst and the blastocyst implanted into the uterus of a female mouse. The resulting offspring can then be bred, eventually giving rise to homozygous G70S mice (Babinet and Cohen-Tannoudji, 2001).

Despite the lack of success in generating this model, valuable data was obtained regarding the phenotype and survival of mice with a G70S mutation in *Eef1a2*. This

allowed us to better understand the effects of the G70S mutation on eEF1A2 function. I was able to determine which alleles were expressing RNA and protein for all mice tested and successfully identified mice that were expressing G70S eEF1A2. This information was essential in order to relate phenotypes to changes in eEF1A2.

We successfully generated four *Eef1a2*$^{G70S/-}$ mice that had G70S on one allele with no indels (#1, #10, #20 and #33). All of these mice showed a phenotype and age of survival comparable to that of wasted mice, which are *Eef1a2*-null, including weight loss, tremor and gait abnormalities. In addition, all of these mice were shown to express eEF1A2 from the G70S allele in brain and muscle (muscle analysis by Faith Davies, not shown). The above evidence suggests that G70S eEF1A2 is functionally impaired and unable to compensate for loss of wild-type protein. This points towards loss of protein function as a disease mechanism.

However, interestingly, the mouse that had clean G70S incorporation on both alleles (#4) showed a more severe phenotype than the four G70S/- mice. This mouse showed a wasted phenotype characterised by tremor and weight loss and had to be culled at P18 due to the severity. The onset of the phenotype in wasted mice starts at P21 (Shultz *et al*., 1982), therefore the onset of the phenotype in this mouse was three days earlier. Although there is only evidence from one mouse, this suggests that the G70S mutation may not simply lead to loss of protein function and that a gain-of-function mechanism may also be at play. It is possible that this mutation may lead to gain of novel protein functions, such as a gain of new binding partners, as well as the loss of particular functions. However, it must be noted that the number of mice in this experiment was low (4 G70S/- and 1 G70S/G70S) and therefore a repeated experiment is necessary to confirm these results.

Unexpectedly, eight *Eef1a2*$^{-/-}$ mice had audiogenic seizures in response to environmental sounds out of the seventeen mice of that genotype that were exposed. Therefore, the seizure incidence was 47%. None of the four G70S/- or the one G70S/G70S mice exposed to the sound had seizures, however, it must be noted that this is a very low number of mice. Therefore, further experiments with a larger

cohort under controlled conditions would be required to determine whether mice with missense mutations in *Eef1a2* are susceptible to audiogenic seizures. If these experiments confirmed that G70S/- mice are not susceptible to audiogenic seizures, this would be in contrast to G70S/+ patients who have epilepsy. This would suggest either a species difference or perhaps an interaction between wild-type and mutant protein is required to cause seizures. This is entirely possible based on evidence that eEF1A is able to act as a dimer (Bunai *et al*., 2006). The discovery of audiogenic seizure susceptibility in *Eef1a2*-null mice is unexpected considering that seizures have never been observed in wasted mice which have been bred since 1972. An investigator in our laboratory experienced two incidents in which a wasted mouse died during handling (personal communication). However, whether or not these were seizures remains unconfirmed. One hypothesis to explain why wasted mice seem to be resistant is that their mixed genetic background is somehow protective against seizures.

Five of the mice had sudden unexplained deaths at P23. Four of these were *Eef1a2*-null and the other a mosaic. These mice did not look severely wasted at P22 and were certainly capable of surviving another few days. Therefore, neurodegeneration was not a likely cause of death. It is suspected that these mice may have died from seizures, however, there is no way to confirm this. Audiogenic seizures were entirely possible since three of the mice died while being transferred between facilities, meaning that they would have been exposed to novel sounds. An alternative hypothesis is that these mice died from sudden unexpected death in epilepsy (SUDEP) which can occur in humans with epilepsy. The biological mechanisms underlying SUDEP are not clear but it is more common in drug resistant epilepsies and in people with high seizure frequency (Donner *et al*., 2017).

These experiments have been invaluable in allowing us to understand the effects of mutations, and in particular the G70S mutation, on eEF1A2 function. Generating a mouse line with a missense mutation in *Eef1a2* would be beneficial and the next, successful, attempt is discussed in Chapter 5.

Chapter 4: Investigating the effects of age and genetic background on the behaviour of heterozygous *Eef1a2*-null mice

4.1. Introduction

4.1.1. Why study the effects of eEF1A2 mutations on behaviour?

All of the patients with missense mutations in *EEF1A2* have intellectual disability and/or developmental delay of varying severity. Eight of the cases outlined in Table 1.2 have been reported as showing clinical features characteristic of autism. These eight cases have the following mutations: G70S (De Ligt *et al*., 2012), D252H, E122K (Nakajima *et al*., 2014), F98C, R266W (personal communication) and A92T (Lopes *et al*., 2016). The autistic-like phenotypes observed in these individuals include repetitive hand twisting, finger sucking, rocking and also self-injury behaviours including pulling hair out and hitting oneself (Nakajima *et al*., 2014). For the majority of the cases, autism has not been reported because the intellectual disability is too severe for testing.

Based on the above evidence, it is entirely possible that mice with mutations in *Eef1a2* may show impairments in behavioural tests that are correlates for intellectual disability and autism in humans. In addition, it has been shown that eEF1A plays a role in the maintenance of LTP, the physiological process underlying the formation of new memories. It has been shown that local translation of eEF1A at the synapse is important for this process (Tsokas *et al*., 2005) Therefore, it can be hypothesised that changes in eEF1A2 expression and/or function will have a negative effect on learning and memory.

4.1.2. Why investigate aging?

For the aging studies in this chapter, I used heterozygous wasted mice (*Eef1a2*$^{+/wst}$). These mice are heterozygous null for *Eef1a2*. I chose this line because they were readily available in our laboratory, well studied and phenotypically normal on a gross observational level i.e. do not show any of the neurodegenerative phenotypes observed in wasted homozygotes (Griffiths *et al*., 2012). This made them an ideal

model to study the effects of eEF1A2 mutations on behaviour as there were predicted to be no phenotypes that would affect the ability of the mice to perform the tasks.

Griffiths *et al* (2012) analysed *Eef1a2*$^{+/wst}$ mice up to the age of 21 months to detect signs of late-onset motor neuron degeneration using grip strength and rotarod tests and by analysing spinal cord pathology post-mortem. They found that the mice were phenotypically normal and collected tissue post-analysis to measure eEF1A2 expression levels in brain, spinal cord and muscle. Strikingly, it was observed that eEF1A2 expression levels in the brains of male mice at 21 months were much lower than the expected 50% of wild-type levels. In some cases, the level of expression was as low as 7.5% (Figure 4.1).

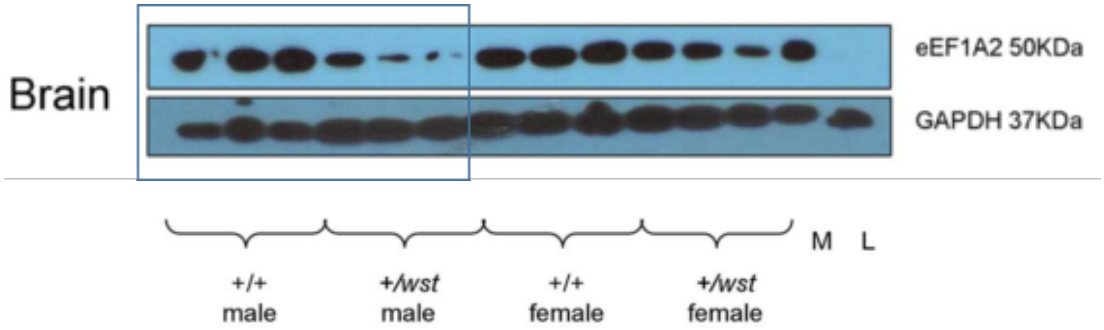

Figure 4.1. Western blot showing eEF1A2 expression levels in the brains of heterozygous wasted mice at 21 months. *Blots probed for eEF1A2 and GAPDH as a loading control. Three samples are shown for each group. M = muscle positive control, L = liver negative control. The rectangle highlights the* *Eef1a2*$^{+/wst}$ *samples that had low eEF1A2 expression and their corresponding Eef1a2*$^{+/+}$ *controls. Adapted from Griffiths et al., 2012.*

The data presented in this paper suggests that testing young mice in my behavioural assays would provide an eEF1A2 dosage of 50% whilst studying older mice may provide the opportunity to test an even lower dose. I hypothesised that older *Eef1a2*$^{+/wst}$ mice might be more impaired in behavioural tests than their younger counterparts due to lower eEF1A2 expression levels.

4.1.3. Heterozygous-null mice as a model of loss of function

It is currently unknown whether the human heterozygous missense mutations in *EEF1A2* result in loss or gain of protein function. As heterozygous wasted mice have a deletion on one allele of *Eef1a2* resulting in protein expression from only the other allele, these mice provide a good model of loss of function. We can use these mice to reliably investigate the effects of having ≤50% levels of eEF1A2 on behaviour. However, if these mice do not show behavioural deficits this could point towards either a mouse-human difference in the levels of eEF1A2 that are necessary for normal function or a gain of function mechanism as the cause of disease. If the mechanism is found to be gain of function, then a mouse model with one of the human missense mutations would be an invaluable tool for future behavioural research.

4.1.4. Behavioural testing in mouse models of neurological disease

Behaviour abnormalities are routinely identified mouse models that have mutations in genes associated with intellectual disability and autism in humans. These include, but are certainly not limited to, mutations in *Fmr1*, *Tsc1/2*, *Cntnap2* and *Shank2*.

Fmr1 knockout mice are hyperactive, which can be shown by increased movement in an open field test (Ding, Sethna and Wang, 2014). In terms of autism-like phenotypes, they display changes in repetitive behaviours by burying more marbles than wild-type mice in the marble burying test and abnormalities in social behaviour as they prefer to spend time with an object rather than another mouse in the three-chamber social test (Dahlhaus and El-Husseini, 2010, Spencer *et al*., 2011). These mice also show evidence of anxiety, as some groups have found that they spend less time in the centre of an open field arena and less time in the open arms of an elevated plus maze (Restivo *et al*., 2005, Bilousova *et al*., 2009). In terms of learning and memory, *Fmr1* knockout mice show hippocampal working memory deficits in the Morris water maze during reversal i.e. when the platform is moved to a new location (Baker *et al*., 2010). They also show deficits in hippocampal-dependent contextual fear conditioning and in object recognition (Paradee *et al*., 1999, Ventura *et al*., 2004). It is important to note that conflicting results have been found in some of

these tests and the deficits seem to vary depending on genetic background (Spencer *et al*., 2011, Kazdoba *et al*., 2014).

Mutations in *TSC1* and *TSC2* cause Tuberous Sclerosis (TSC) in humans, a disorder that affects multiple organs including the brain, lung, kidney, heart and skin. Clinical features of TSC can include intellectual disability, autism and epilepsy (Caban *et al*., 2016). Mice with mutations in *Tsc1/2* exhibit impaired social behaviour by avoiding spending time with novel mice during direct contact tasks and by building poor nests in a group nest building task (Goorden *et al*., 2007). They also have social impairments in the three-chamber test by preferring to spend time with an object over another mouse and showing no preference for a novel mouse compared with a previously encountered mouse. Similar to *Fmr1* knockout mice, these mice display changes in repetitive behaviours by burying more marbles than wild-type mice in the marble burying test (Reith *et al*., 2013). *Tsc1/2* mice also show learning and memory impairments in hippocampal-dependent tasks including the Morris water maze and contextual fear conditioning (Goorden *et al*., 2007, Kirschstein, 2012), a phenotype which has also been observed in *Fmr1* knockout mice.

The *CNTNAP2* gene, which encodes a neurexin-family receptor and cell adhesion protein, can be knocked out in mice to produce behavioural deficits (Peñagarikano *et al*., 2011). These mice show increased locomotion in the open field test, similar to *Fmr1* knockout mice. They also display abnormal social behaviour when allowed direct contact with novel mice in the juvenile play test and indirect contact in the three-chamber test. *Cntnap2* knockout mice also show changes in repetitive behaviours including excessive digging and grooming, which are correlates for autism in humans. Like *Tsc1/2* mutant mice, *Cntnap2* mutants building significantly poorer nests than wild-type mice in a group nest building task. Interestingly, these mice show a hippocampal-dependent working memory deficit in the Morris water maze as observed in *FmrI* and *Tsc1/2* mutants (Peñagarikano *et al*., 2011).

Mutations in mouse *Shank* genes (*Shank1/2/3)*, which encode synaptic scaffold proteins, result in similar behavioural impairments to those described above. For

example, mice with *Shank2* deletions show reduced sociability and lower preference for social novelty in the three-chamber test. These mice also show changes in repetitive behaviours, including excessive digging and grooming. In addition, they display increased locomotion in the open field test, similar to *Fmr1* and *Cntnap2* knockout mice (Schmeisser *et al*., 2012, Won *et al*., 2012).

In light of the above studies, the following point is worth noting. In mouse models that display hyperactivity coupled with an increase in repetitive behaviours, results must be interpreted carefully. This is because the increase in repetitive behaviours may in fact be due to the hyperactivity phenotype and therefore not indicative of autistic-like behaviour. For example, a significant increase in marble burying behaviour in a hyperactive mouse may actually be caused by a high level of movement resulting in marbles being buried inadvertently. In addition, repetitive body movements regularly co-occur with hyperactivity making it more difficult to disentangle the two processes (Kim, Lim and Kaang, 2016).

Based on the above evidence, consistently observed behavioural deficits in mice with mutations in genes that cause intellectual disability and autism in humans include social impairments, changes in repetitive behaviours, hyperactivity and impaired hippocampal learning and memory.

4.1.5. Aims

- **To determine the effects of age and genetic background on the behaviour of heterozygous *Eef1a2*-null mice.**

1) To characterise the behavioural phenotype of heterozygous wasted (*Eef1a2*$^{+/wst}$) mice and to determine whether phenotype is affected by age.

2) To determine, through protein expression analysis, whether any age-specific effect on behaviour found through aim 1 is accompanied by a dosage of eEF1A2 lower than 50%.

3) To characterise the behavioural phenotype of heterozygous mice from a new *Eef1a2*-null mouse line (Del22.ex3) which, in contrast to the mixed background of wasted mice, is on an inbred C57BL/6J genetic background.

4.2. Results

4.2.1. Investigating the effects of aging on the behaviour of *Eef1a2*$^{+/wst}$ mice

4.2.1.1. The aging cohort

Mice were bred from heterozygote x heterozygote matings or wild-type x heterozygote matings and were housed in male-only cages of mixed genotypes. All mice were housed in groups to avoid any confounding effects of single housing on behaviour. Female mice were excluded from testing due to the potential for results to vary across different phases of the oestrus cycle. These experiments were not completed in a single time frame and multiple cohorts were used throughout the course of my project to generate the final dataset. Mice were tested in behavioural assays from 9 weeks (2 months) of age. The age of the mice tested ranged from 2 months to 18 months. For analysis, mice were split into age groups ranging from 2-6 months, 7-11 months and 12-18 months. These age groups were chosen firstly to split the mice tested between 2 months and 11 months into two equal sizes groups. Secondly, mice are considered aging after 12 months and therefore all mice tested from this age were put into a third group to analyse the effects of aging on behaviour. Behavioural testing was performed with assistance from James Innes (summer student) and James Vipond (Honours project student). Data for each test are presented as mean values in the bar graphs and as individual scores for each mouse in the dot plots. The bar graphs allow the means to be observed and compared with ease whilst the dot plots show the spread of data and therefore the variability in scores within genotypes. Correlations of behaviour score with age are shown in Appendix B.

4.2.1.2. *Eef1a2*$^{+/wst}$ mice showed no evidence of changes in repetitive behaviours compared with *Eef1a2*$^{+/+}$ mice

Mice naturally exhibit stereotyped repetitive behaviours such as digging, grooming, circling and jumping. However, these behaviours are considered to be abnormal when a mouse engages in them for long periods of time or when the frequency of these behaviours increases. These persistent behaviours are often identified in mouse

models of autism (Silverman *et al*., 2010). These behaviours are considered to be a correlate for autism in humans and can be analysed accordingly. As previously mentioned, many mouse models of autism have shown a significant increase in repetitive behaviours including *Fmr1* knockout mice, *Tsc1/2* mutants, *Cntnap2* knockout mice and *Shank2* mutants (Peñagarikano *et al*., 2011, Spencer *et al*., 2011, Reith *et al*., 2013, Kazdoba, Leach and Crawley, 2016). However, others have shown a significant reduction. For example, mice with deletion of *Pten* in a subset of neurons showed a significant decrease in the number of marbles buried and number of head dips in the hole-board test compared with their wild-type littermates (Lugo *et al*., 2014). It is noteworthy that mice with other mutations in *Pten* have shown an increase in repetitive behaviours, for example, heterozygous null *Pten* mice have shown a significant increase in repetitive digging behaviour compared with wild-type mice (Clipperton-Allen and Page, 2015).

There are several established assays to measure changes in repetitive behaviours in mice. Digging behaviour can simply be observed in a clean cage for a defined length of time or can be measured using the marble burying assay. These assays aim to determine whether mutant mice dig significantly more (or less) than wild-type mice. In the marble burying test, this is determined by the number of marbles buried in a set period of time (Deacon, 2006b, Angoa-Pérez *et al*., 2013). The individual nest building assay can also be used to investigate repetitive behaviour as mice with mutations linked to autism will often shred more nestlet and/or build higher quality nests than wild-type mice (Deacon, 2012, Angoa-Pérez *et al*., 2013). The results of this are in contrast to those of group nest building tasks in which mutants often build poorer quality nests (Goorden *et al*., 2007, Peñagarikano *et al*., 2011).

Firstly, I tested *Eef1a2*$^{+/+}$ and *Eef1a2*$^{+/wst}$ mice in the nest building assay to determine whether *Eef1a2*$^{+/wst}$ mice show changes in repetitive behaviours (Figure 4.2). Mice were housed individually in clean cages containing a square of nest material overnight. Following testing, nest material was weighed to calculate the percentage shredded and was scored according to a scale devised by Deacon (2006a) (shown in Figure 4.2). There were no statistically significant differences in the

percentage of nestlet shredded (Figure 4.2A) or in nest building score (Figure 4.2B) between genotypes or age groups. The dot plots in Figure 4.2 show the individual data points for each mouse and it can be seen that the results within groups are very variable.

For other tests described later in this chapter, a 7-11-month age group was included. However, this group was not included in the nest building assay as there were only 3 *Eef1a2*$^{+/+}$ and 4 *Eef1a2*$^{+/wst}$ mice of this age available at the time of testing.

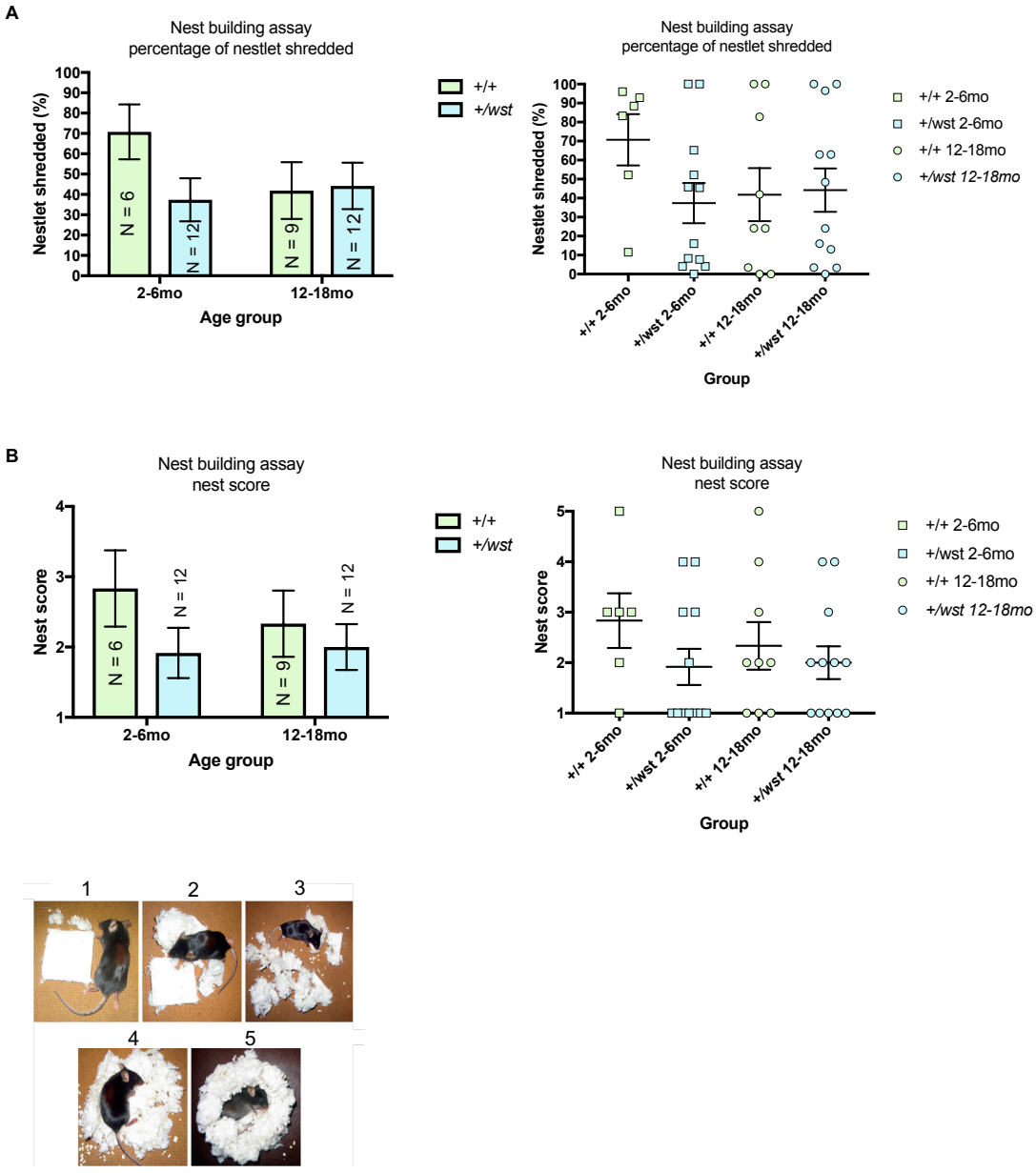

Figure 4.2. Data from Eef1a2$^{+/+}$ and Eef1a2$^{+/wst}$ mice in the nest building assay. *Error bars for all graphs show SEM.* ***A.*** *Percentage of nestlet shredded for +/+ and +/wst mice at 2-6 months and 12-18 months. There was no significant difference between genotypes or age groups (Two-way ANOVA).* ***B.*** *Nest score for +/+ and +/wst mice at 2-6 months and 12-18 months. The scoring criteria used is shown in the images labelled 1-5 (Deacon, 2006a). There was no significant difference between genotypes or age groups (Kruskal-Wallis test).*

Further testing was necessary to establish whether or not these mice show changes in repetitive behaviours. Therefore, I performed the marble burying test to complement the nest building data. Initially, this test was performed with 12 marbles, however, wild-type mice buried a high number of marbles (mean = 8) making it difficult to observe differences between genotypes (data not shown). Therefore, the test was repeated with 20 marbles. Mice were placed in clean cages containing 20 marbles for 30 minutes and the number of marbles buried was scored. The results are shown in Figure 4.3.

There were no significant differences in the number of marbles buried between the genotypes for any age group, however, *Eef1a2*$^{+/wst}$ mice at 12-18 months buried significantly fewer marbles than *Eef1a2*$^{+/wst}$ mice at 2-6 months. This was shown using a two-way ANOVA with post-hoc Tukey's multiple comparisons test. Despite the reduction in marble burying behaviour with age, there was no evidence to suggest that *Eef1a2*$^{+/wst}$ mice showed any changes in repetitive behaviours compared with *Eef1a2*$^{+/+}$ mice.

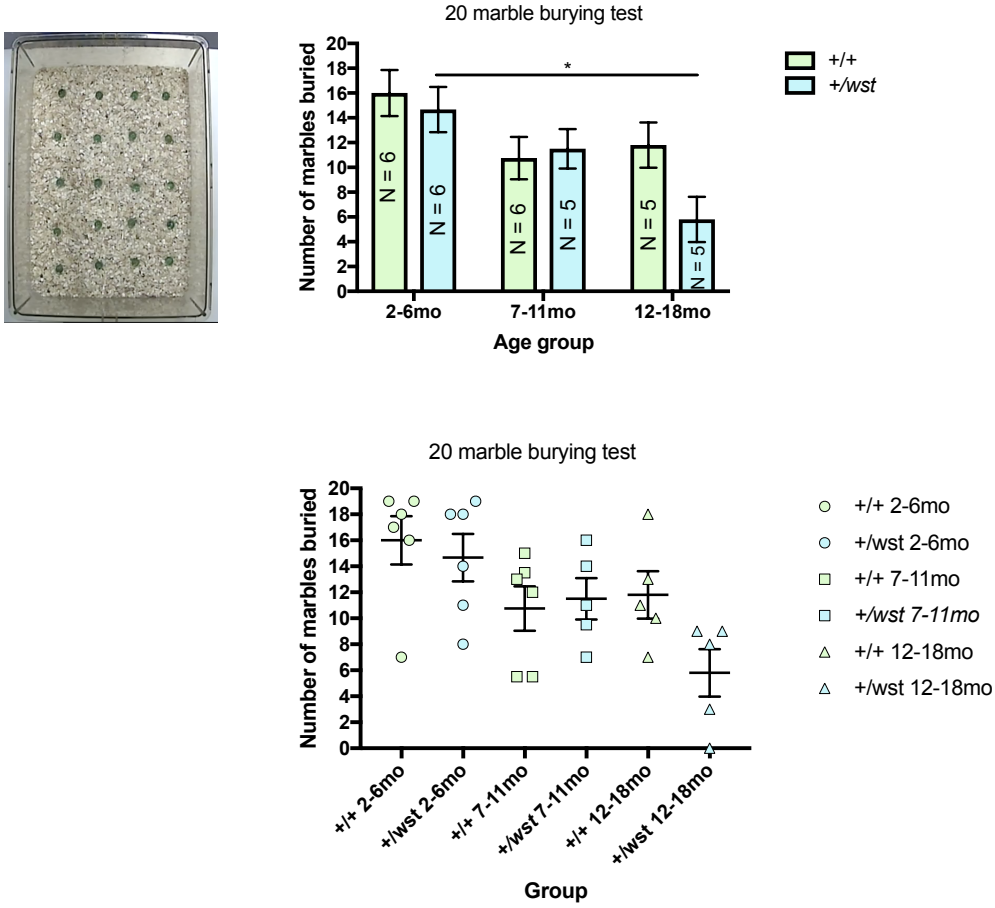

Figure 4.3. Data from Eef1a2$^{+/+}$ and Eef1a2$^{+/wst}$ mice in the marble burying assay. *Number of marbles buried for +/+ and +/wst mice at 2-6 months, 7-11 months and 12-18 months. A photograph of the apparatus is shown. Error bars for all graphs show SEM. +/wst mice at 12-18 months buried significantly fewer marbles than +/wst mice at 2-6 months (Two-way ANOVA showed significant effect of age: F = 6.796, DF = 2, 27, p = 0.0041. Tukey's multiple comparisons test p = 0.0187). There were no significant differences between any of the other groups.*

Based on the nest building and marble burying data, it seemed that +/*wst* mice did not show the changes in repetitive behaviours seen in other mouse models of autism. To test this hypothesis, I performed a third and final test, the digging assay. Mice were placed individually in clean cages containing fresh bedding and digging behaviour was recorded for 3 minutes. The results are shown in Figure 4.4.

There was no statistically significant difference in the latency to start digging (Figure 4.4A), the number of digging bouts (Figure 4.4B) or the total duration of digging (Figure 4.4C) between genotypes or age groups. Therefore, *Eef1a2*$^{+/wst}$ showed no evidence of changes in repetitive behaviours in this test. As with the nest building assay, the dot plots show that the spread of data within groups is large.

To summarise, *Eef1a2*$^{+/wst}$ mice did not differ from *Eef1a2*$^{+/+}$ mice in the percentage of nestlet shredded and quality of nests built in the nest building assay, the number of marbles buried in the marble burying assay or the extent of digging in the digging assay. These mice showed no evidence of changes in repetitive behaviours compared with wild-type mice in any of the three tests performed.

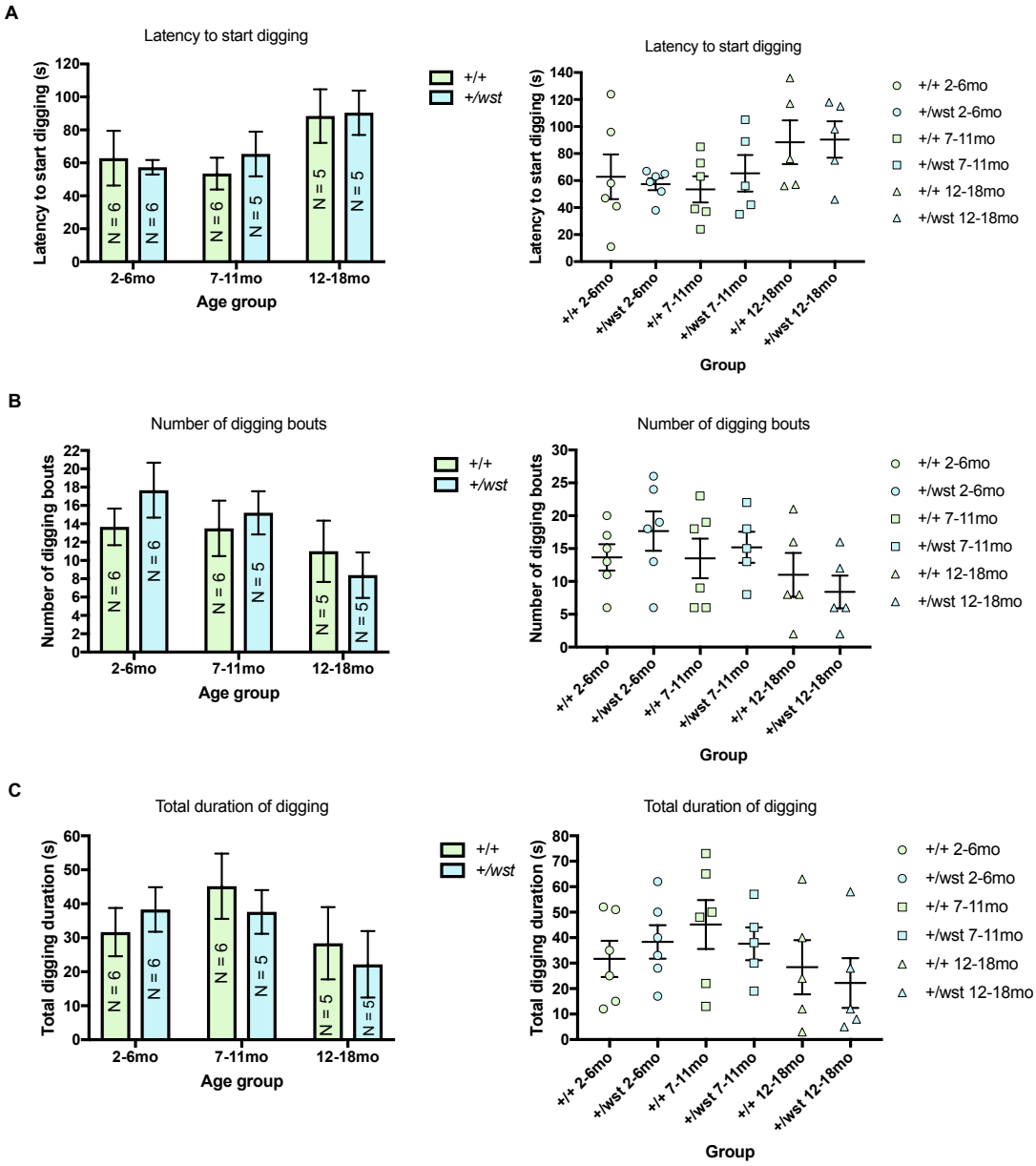

Figure 4.4. Data from Eef1a2$^{+/+}$ and Eef1a2$^{+/wst}$ mice in the digging assay. *Error bars for all graphs show SEM.* ***A.*** *Latency to start digging for +/+ and +/wst mice at 2-6 months, 7-11 months and 12-18 months. There was no significant difference between genotypes or age groups (Two-way ANOVA).* ***B.*** *Number of digging bouts for +/+ and +/wst mice at 2-6 months, 7-11 months and 12-18 months. There was no significant difference between genotypes or age groups (Two-way ANOVA).* ***C.*** *Total duration of digging for +/+ and +/wst mice at 2-6 months, 7-11 months and 12-18 months. There was no significant difference between genotypes or age groups (Two-way ANOVA).*

4.2.1.3. *Eef1a2*$^{+/wst}$ mice showed no preference for social novelty

For mice, social interactions and social recognition are important for establishing a social hierarchy and choosing a mate. The three-chamber test (or stranger mouse test) is a well established assay to investigate social behaviour in mice (Crawley, 2007). In the first stage of this assay, the test mouse is given the choice between spending time with another mouse or spending time alone/with an object. This allows the experimenter to assess whether mice with specific mutations show reduced sociability by avoiding spending time with the other mouse. A second stage of this test can also be performed which involves assessing whether a test mouse prefers to spend time with the mouse presented in stage one, which is now familiar, or with a novel mouse. This allows the experimenter to determine whether mice with specific mutations show preference for social novelty by spending more time with the novel mouse. Wild-type mice are expected to show preference for social novelty in this test (Kaidanovich-Beilin *et al*., 2011). Both stages of this test are used as correlates for autism in humans as mice with mutations in autism-related genes, including *Fmr1* (Dahlhaus and El-Husseini, 2010), *Cntnap2* (Peñagarikano *et al*., 2011), *Shank2* (Kazdoba, Leach and Crawley, 2016), and *Tsc1/2* (Reith *et al*., 2013) have been found to show reduced sociability and/or reduced preference for social novelty.

This test is usually performed in a rectangular arena with three chambers. For example, in stage one, the chambers contain: the mouse for the test mouse to interact with (left), an empty "decision making chamber" (middle) and a chamber which is empty or contains an object (right). In stage two, the chamber on the right is taken up by the novel mouse (Kaidanovich-Beilin *et al*., 2011). I used an adapted version of this apparatus to assess the social behaviour of *Eef1a2*$^{+/wst}$ mice. Rather than a rectangular arena, a Y-shaped maze was used. The setup is shown in Figure 4.5A and 4.6A.

The results of stage 1, where the test mouse was given the choice between spending time alone or with a mouse, is shown in Figure 4.5. Figure 4.5A shows an image of the Y-shaped apparatus containing the stranger mouse in the left arm between wire

mesh gates, empty wire mesh gates with no mouse in between in the right arm ("cage') and the test mouse in the middle.

Figure 4.5B shows the data for the time spent exploring the mouse vs the empty cage for *Eef1a2*$^{+/+}$ and *Eef1a2*$^{+/wst}$ mice in each age group. For all age groups, both *Eef1a2*$^{+/+}$ and *Eef1a2*$^{+/wst}$ mice spent significantly more time exploring the mouse than the empty cage. This was shown using a two-way ANOVA with Holm-Sidak's multiple comparisons test. The total exploration time did not differ between genotypes at any age, shown using a two-way ANOVA (data not shown). Therefore, there is no evidence that *Eef1a2*$^{+/wst}$ mice show the reduced sociability that is observed in other mouse models of autism.

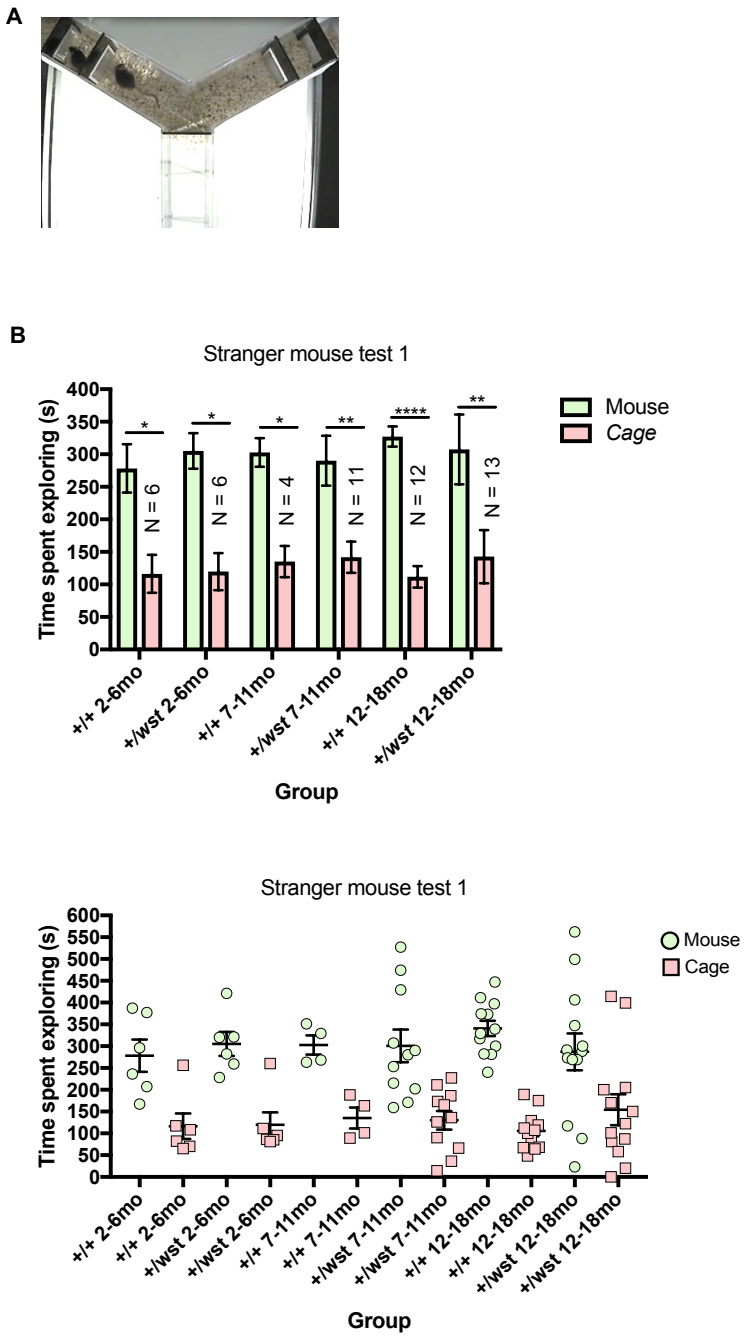

Figure 4.5. Data from Eef1a2$^{+/+}$ and Eef1a2$^{+/wst}$ mice in the stranger mouse test stage 1. *Error bars for all graphs show SEM.* ***A.*** *Image of the Y-shaped apparatus.* ***B.*** *Time spent exploring the mouse vs the empty cage for +/+ and +/wst mice at 2-6 months, 7-11 months and 12-18 months. Asterisks on the bar graph show statistically significant differences (Two-way ANOVA showed significant effect of stimulus (mouse vs cage): F = 53.39, DF = 1, 92, p = <0.0001. Holm Sidak's multiple comparisons test: from left to right, p = 0.0255, 0.0137, 0.0348, 0.0089, <0.0001, 0.0013.*

The results of stage 2, whether the test mouse was provided the option of spending time with a familiar mouse vs a novel mouse, are shown in Figure 4.6. Figure 4.6A shows an image of the Y-shaped apparatus containing the familiar mouse in the left arm between wire mesh gates, the novel mouse in the right arm between wire mesh gates and the test mouse in the middle.

Figure 4.6B shows the data for the time spent exploring the familiar mouse vs the novel mouse for *Eef1a2*$^{+/+}$ and *Eef1a2*$^{+/wst}$ mice in each age group. *Eef1a2*$^{+/+}$ mice in each age group spent significantly more time exploring the novel mouse compared with the familiar mouse, shown by a two-way ANOVA with Holm-Sidak's multiple comparisons test. Interestingly, *Eef1a2*$^{+/wst}$ mice showed no preference for the novel mouse at any age indicating that they show a lack of preference for social novelty which is not age-specific. The total exploration time did not differ between genotypes at any age, shown using a two-way ANOVA (data not shown). This social impairment has been observed in other mouse models with mutations in autism-related genes including mice with mutations in *Tsc1/2* and *Shank2* (Reith *et al*., 2013, Kazdoba, Leach and Crawley, 2016).

To ensure that the social novelty impairment found in *Eef1a2*$^{+/wst}$ mice was not due to olfactory deficits, I performed the buried food test (Reith *et al*., 2013). This test involved burying a small piece of food under fresh bedding in a clean cage and measuring the time taken for the test mouse to find the food. The mean latency to find the food was not significantly different between genotypes (unpaired t-test) and both genotypes located the food after a mean of approximately one minute (Figure 4.6C). Therefore, the apparent lack of preference for the novel mouse observed in *Eef1a2*$^{+/wst}$ mice is not likely to be due to olfactory deficits. In summary, the impairment appears to be due to a reduced preference for social novelty rather than an inability to distinguish between the mice through olfaction.

For both stages of this test, it is important to note that the number of mice tested for the '*Eef1a2*$^{+/+}$ 7-11mo' age group is low (N = 4). These were the only mice available

at this age at the time of testing as it was particularly important to test littermates due to the mixed genetic background of the wasted line. Due to the low N, results from this group should be interpreted with caution. However, as there are groups both younger and older that provide consistent results this was not a particular issue.

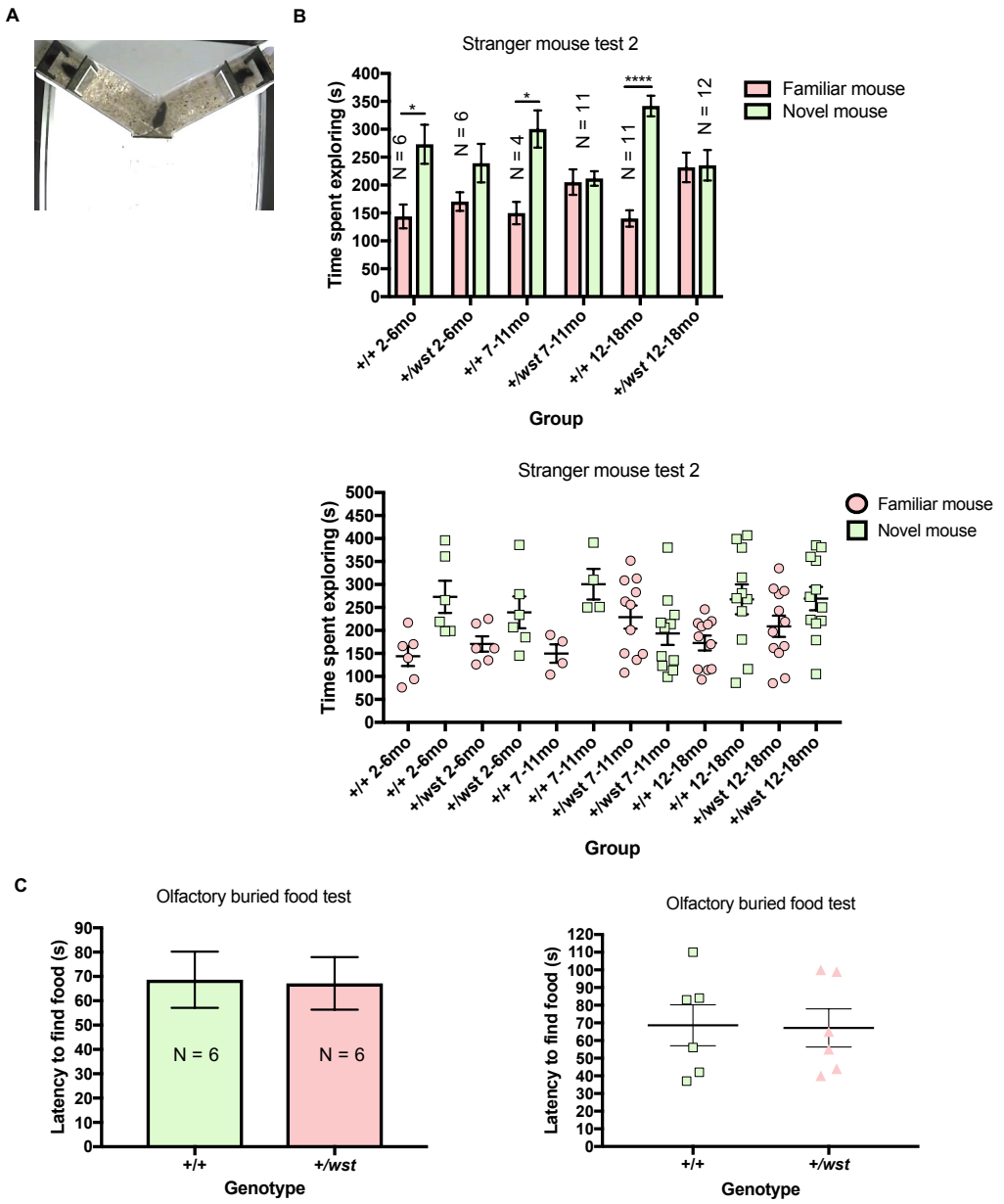

Figure 4.6. Data from Eef1a2$^{+/+}$ and Eef1a2$^{+/wst}$ mice in the stranger mouse test stage 2. *Error bars for all graphs show SEM.* ***A.*** *Image of the Y-shaped apparatus.* ***B.*** *Time spent exploring the familiar mouse vs the novel mouse for +/+ and +/wst mice at 2-6 months, 7-11 months and 12-18 months. Asterisks on the bar graph show statistically significant differences. Two-way ANOVA showed significant effect of stimulus (familiar vs novel mouse): F = 36.92, DF = 1, 88, p = <0.0001. Holm Sidak's multiple comparisons test: from left to right, p = 0.0107, 0.0136, <0.0001.* ***C.*** *Olfactory buried food test results for +/+ and +/wst mice. There was no significant difference between the genotypes (unpaired t-test).*

4.2.1.4. Locomotor activity of *Eef1a2*$^{+/wst}$ mice decreased with age

The open field test is routinely used to assess locomotor and anxiety phenotypes in mice. This test also provides useful baseline data to interpret other behavioural tests that involve locomotion, including the marble burying test. The test involves placing a mouse in an opaque, square arena, usually measuring 50cm x 50cm, and recording exploration in the arena for a set period of time. Locomotor activity is commonly used as an indicator of hyperactivity in mouse models, with a significant increase in movement compared with wild-type mice indicating hyperactivity. A defined square area is set as the centre of the apparatus and the time spent in the centre vs the outside is routinely used to assess anxiety. Anxious mutant mice will spend significantly less time in the centre than their wild-type counterparts. Freezing can also be used as a measure of anxiety with more time spent freezing indicating higher anxiety (Seibenhener and Wooten, 2015). As outlined in section 4.1.4, particular mouse models with mutations in genes that cause autism in humans have shown hyperactivity and anxiety in the open field test including *Fmr1* knockout mice (Restivo *et al*., 2005, Ding, Sethna and Wang, 2014).

I performed the open field test to determine whether *Eef1a2*$^{+/wst}$ mice show any locomotor and/or anxiety phenotypes. In terms of motor analysis, it is important to note that *Eef1a2*$^{+/wst}$ mice have previously been tested on the rotarod and were shown to have a normal performance up to the age of 21 months (Griffiths *et al*., 2012). Mice were allowed to explore the 50cm x 50cm open field arena for 5 minutes. The total distance travelled was measured to determine whether these mice are hyperactive. The time spent freezing, the time spent in the outside zone and the time spent in the centre zone were used to assess the presence of anxiety phenotypes.

Figure 4.7A shows the data for the total distance travelled for *Eef1a2*$^{+/+}$ and *Eef1a2*$^{+/wst}$ mice in each age group. *Eef1a2*$^{+/wst}$ mice in the 12-18-month group travelled a significantly smaller distance than those in the 2-6-month group. This was shown using a two-way ANOVA with Tukey's multiple comparisons test. Hyperactive mice have been shown to travel significantly larger distances than wild-type mice in the open field (Peñagarikano *et al*., 2011, Ding, Sethna and Wang,

2014, Kazdoba, Leach and Crawley, 2016). However, this was not the case here for any age group. Therefore, +/*wst* mice do not appear hyperactive compared with wild-type mice.

Figure 4.7B shows the data for the total time spent freezing for *Eef1a2*$^{+/+}$ and *Eef1a2*$^{+/wst}$ mice in each age group. *Eef1a2*$^{+/wst}$ mice in the 12-18-month group spent significantly more time freezing than *Eef1a2*$^{+/wst}$ mice in the 2-6-month group. This was shown using a two-way ANOVA with Tukey's multiple comparisons test. However, there was no difference in the time spent freezing between the genotypes at any given age. Based on the data in Figure 4.7A and B, it appears that *Eef1a2*$^{+/wst}$ mice show decreased locomotion as they age.

Figure 4.7C shows the data for the time spent in the outside and centre zones of the open field box for *Eef1a2*$^{+/+}$ and *Eef1a2*$^{+/wst}$ mice in each age group. *Eef1a2*$^{+/+}$ mice at 2-6 months, *Eef1a2*$^{+/wst}$ mice at 2-6 months, *Eef1a2*$^{+/wst}$ mice at 7-11 months and *Eef1a2*$^{+/+}$ mice at 12-18 months spent significantly more time in the outside zone than in the centre zone (Two-way ANOVA with Tukey's multiple comparisons test). Therefore, generally, *Eef1a2*$^{+/+}$ and *Eef1a2*$^{+/wst}$ mice both preferred to spend time in the outside zone. There were no significant differences in the time spent in either zone between genotypes. Therefore, there was no indication of increased anxiety of *Eef1a2*$^{+/wst}$ mice compared with *Eef1a2*$^{+/+}$ mice based on the results of this analysis. It should be noted that one *Eef1a2*$^{+/+}$ mouse in the 12-18-month group and one *Eef1a2*$^{+/wst}$ mouse in the 12-18-month were excluded from analysis of this parameter as they did not move at all during the whole test and, as a result, spent the whole time in the centre zone. The dot plots show that there is a large spread of data for some groups (for wild-type mice at 2-6 months, for example).

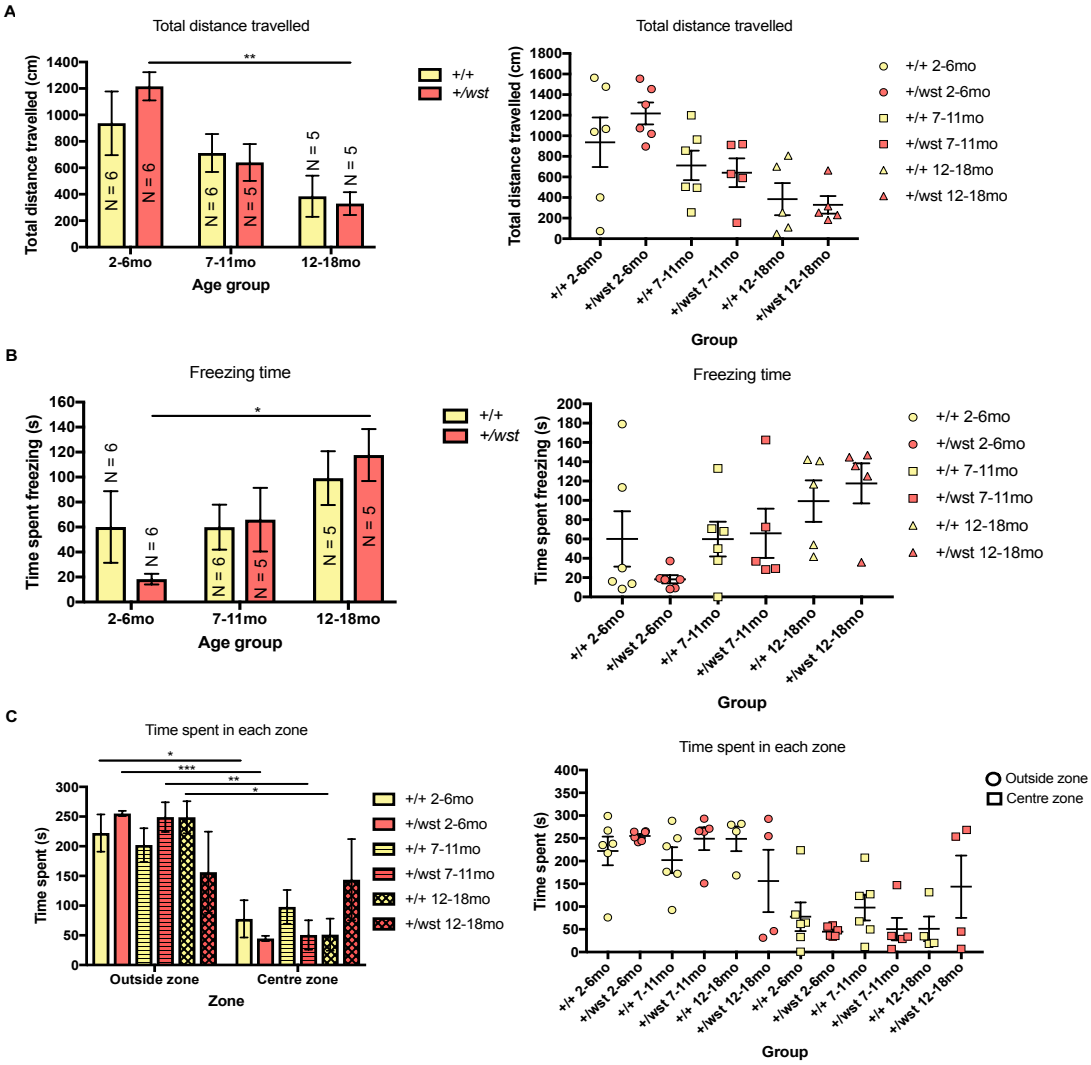

Figure 4.7. Data from Eef1a2$^{+/+}$ and Eef1a2$^{+/wst}$ mice in the open field test. *Error bars for all graphs show SEM.* ***A.*** *Total distance travelled for +/+ and +/wst mice at 2-6 months, 7-11 months and 12-18 months. Asterisks on the bar graph show statistically significant differences. Two-way ANOVA showed significant effect of age: F = 10.3, DF = 2, 27, p = 0.0005. Tukey's multiple comparisons test: p = 0.0061.* ***B.*** *Total time spent freezing for +/+ and +/wst mice at 2-6 months, 7-11 months and 12-18 months. Asterisks on the bar graph show statistically significant differences. Two-way ANOVA showed significant effect of age: F = 5.54, DF = 2, 27, p = 0.0096. Tukey's multiple comparisons test p = 0.00277.* ***C.*** *Time spent in outside and centre zone for +/+ and +/wst mice at 2-6 months, 7-11 months and 12-18 months. The numbers of mice are the same as for A and B, apart from for the 12-18-month group where n = 4 for each genotype. Asterisks on the bar graph show statistically significant differences. Two-way ANOVA showed significant effect of zone: F = 59.58, DF = 1, 50, p = <0.0001. Tukey's multiple comparisons test: from left to right p = 0.0473, 0.0004, 0.0038, 0.0156.*

4.2.1.5. *Eef1a2*$^{+/wst}$ mice showed normal spatial memory in a short ITI Y-maze test

The Y-maze is routinely used to assess spatial memory in mice, a process that is dependent on hippocampal function (Sharma, Rakoczy and Brown-Borg, 2010b). Mice with mutations in genes linked to intellectual disability and autism, including *Fmr1* (Paradee *et al*., 1999, Baker *et al*., 2010), *Tsc1/2* (Goorden *et al*., 2007, Kirschstein, 2012) and *Cntnap2* (Peñagarikano *et al*., 2011) have been found to show impairments in hippocampal-dependent memory tasks including the Morris water maze and contextual fear conditioning. There is minimal data on performance in the Y-maze but deficits in *Fmr1* knockout mice have been observed (Bilousova *et al*., 2009). The Y-maze has also been used to assess spatial memory in mouse models with mutations in genes related to learning and memory (Freudenberg *et al*., 2016).

I used the Y-maze in an attempt to assess spatial memory of *Eef1a2*$^{+/wst}$ mice. The Y-maze test consisted of two phases. In the first phase, one of the three arms was closed with a gate and the test mouse was allowed to explore the other two arms for 5 minutes (Figure 4.8A). These are commonly referred to as the 'start' and 'other' arm, the start arm being the arm that the mouse is placed in to begin the test. To assess spatial memory, the mouse was removed from the maze for a short ITI of 15 minutes. After 15 minutes, the second phase was begun. In this phase, the gate closing the third ('novel') arm was opened and the mouse was allowed to explore all three arms for 2 minutes. As mice show an innate preference for novelty, wild-type mice are expected to spend significantly more time exploring the novel arm than the two familiar arms.

Figure 4.8B shows the results of the Y-maze test. The bar graph shows the mean time spent in the familiar vs novel arms and the dot plot shows the individual scores for each mouse. Mice at 12-18 months were not included in this test as there were not enough mice of this age at the time of testing. Both *Eef1a2*$^{+/+}$ and *Eef1a2*$^{+/wst}$ mice at 2-6 months and 7-11 months showed a significant preference for exploring the novel arm compared with the familiar arms. This was shown using a two-way

ANOVA with Tukey's multiple comparisons test. Therefore, +/*wst* mice appeared to show preference for novelty and therefore normal spatial memory in the Y-maze after 15 minutes.

The implementation of this test with a longer ITI to further assess spatial memory is explored in Chapter 5.

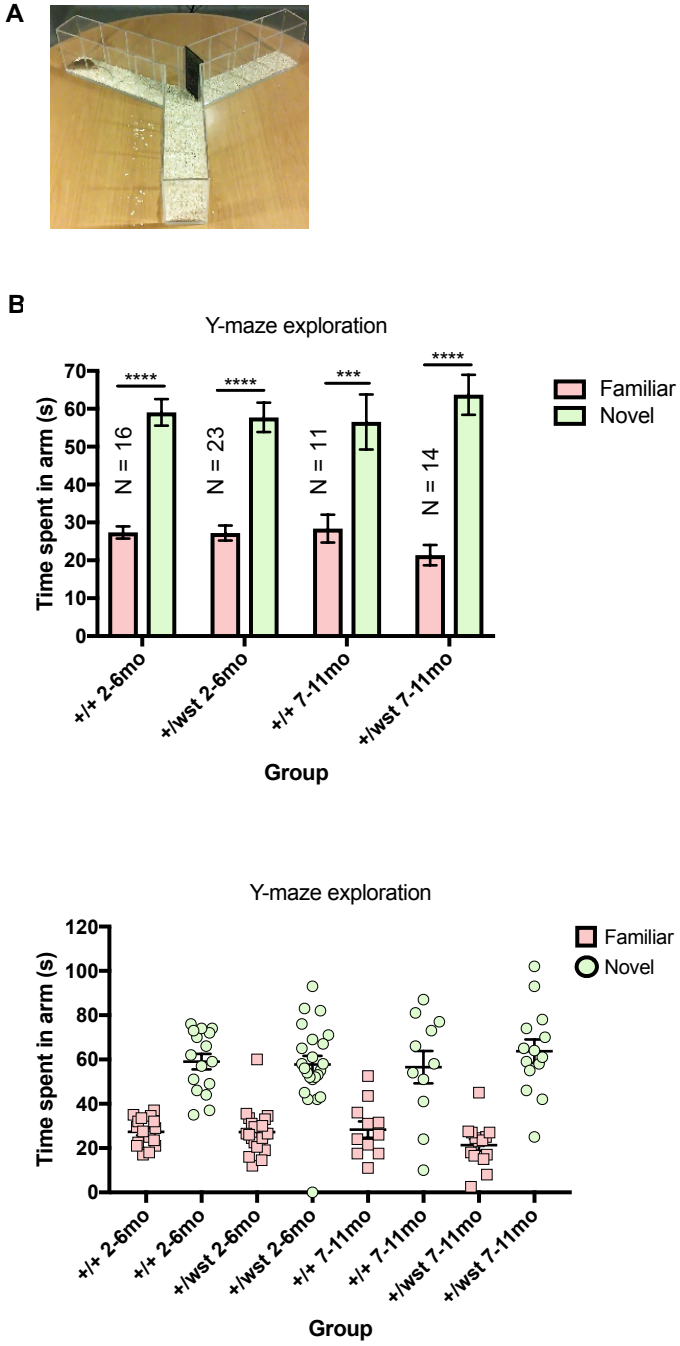

Figure 4.8. Data from Eef1a2$^{+/+}$ and Eef1a2$^{+/wst}$ mice in the Y-maze test. A. *Image of the Y-maze. This maze was also used for the stranger mouse test (Section 4.2.1.3) and the novel object recognition test (Section 4.2.2.7).* ***B.*** *Mean time spent exploring Y-maze arms for +/+ and +/wst mice at 2-6 months and 7-11 months. Familiar = mean of 'start' and 'other' arm. Asterisks on the bar graph show statistically significant differences. Two-way ANOVA showed significant effect of arm (familiar vs novel): F = 149.8, DF = 1, 124, p = <0.0001. Tukey's multiple comparisons test: from left to right p = <0.0001, <0.0001, 0.0006, <0.0001. Error bars show SEM.*

4.2.1.6. Variation in data was due to mixed genetic background of wasted line

After testing a small group of mice for some of the above behavioural tests, I performed post-hoc power calculations to determine the recommended number of mice for testing. The results of this analysis are shown in Figure 4.9. I used data from a set of young mice at 2-6 months (set 1) and an older set at 12 months (set 2). Power calculations were performed with an online calculator using standard deviations from my mice to take the variation in my mouse line into consideration. From Figure 4.9A, it can be seen that for some of the tests, power analysis recommended testing a very large, unfeasible number of mice. Examples of this are the stranger mouse test 1 and 2, with recommendations of 27 and 43 mice respectively and the marble burying test with a recommendation of 27 and 60 mice. From the behaviour results in this chapter, it can be seen that there is a large amount of variation within groups for some of the tests. It is noteworthy that I attempted to perform a power calculation on data from the digging assay, however, a value of 1 along with an error was received. This appeared to be due to the fact that the mean values from the literature (mu1 and mu2) used for the calculation were very different from the mean values I obtained in my experiment. Therefore, my standard deviation used as the value for sigma did not make sense with the data. I could not find other suitable values.

To determine whether the variability I observed might be due to the mixed genetic background of the wasted line, I performed a Y-maze exploration test on six wild-type mice from the wasted line (mixed background) and six wild-type mice on a pure C57BL/6J genetic background. This test involved a simple measurement of preference for the novel arm by allowing mice to explore two arms and subsequently three arms with a short 15-minute ITI (see Section 4.2.1.5). The results of this test are shown in Figure 4.9B. Both groups of mice spent significantly more time exploring the novel arm than the familiar arms. It can be seen that the standard deviations for mice on the mixed genetic background were higher than those for the C57BL/6 mice, especially for novel arm exploration (19 for mixed vs. 3 for C57BL/6) indicating higher variation in the mixed line. Therefore, it seems likely

that the high variability within certain groups in my analyses and the recommendation of testing large numbers of mice through the power calculations is due to the mixed genetic background of the wasted line.

A

	Set 1	Set 2
Y-maze	20	16
Stranger mouse test 1	27	19
Stranger mouse test 2	14	43
Nest building	7	9
Marble burying	27	60
Digging	1	1

B

	Mixed			C57BL/6	
	Familiar	**Novel**		**Familiar**	**Novel**
	17	86		25.5	68
	23.5	69		29	62
	24	66		28.5	63
	15.5	116		31	66
	24.5	66		31	58
	21.5	77		28	63
Mean	21	80		28.83	63.33
Standard Deviation	3.85	19.26		2.07	3.44

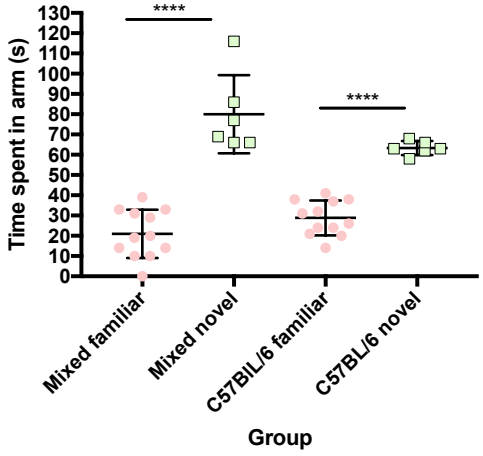

Figure 4.9. Tables showing evidence for high variability in data from the wasted line. ***A.*** *Results of post-hoc power calculations showing the recommended number of mice that should be tested. Set 1 = 2-6 month old mice, set 2 = 12 month old mice.* ***B.*** *Results of Y-maze analysis of wild-type mice from the wasted line (mixed) and wild-type mice on a pure C57BL/6 background. Familiar = mean of 'start' and 'other' arm, novel = novel arm. In the table, individual scores are shown for each mouse with the mean shown below. The standard deviation shows the spread of the data and has been used as an indicator of variability. In the graph, error bars show SD and asterisks represent statistically significant differences. Two-way ANOVA showed significant effect of arm (familiar vs novel): F = 130.6, DF = 1, 20, p = <0.0001. Tukey's multiple comparison's test: mixed p = <0.0001, C57BL/6 p = <0.0001.*

4.2.1.7. eEF1A2 protein expression levels in the brains of aging *Eef1a2*$^{+/wst}$ mice showed high levels of variability

After behavioural testing, I aimed to determine whether aging *Eef1a2*$^{+/wst}$ mice expressed eEF1A2 in the brain at levels lower than 50% of wild-type (Aim 2). Griffiths *et al* (2012) showed that eEF1A2 expression in the brain declines with age in *Eef1a2*$^{+/wst}$ mice but used a small number of animals. *Eef1a2*$^{+/wst}$ mice at 21 months expressed, in some cases, eEF1A2 at 7.5% of wild-type. Therefore, I wanted to determine whether age-specific effects on behaviour in the marble burying and open field tests were due to lower expression levels of eEF1A2 in aging mice, specifically in the animals in which I had carried out my behavioural analysis. I decided to analyse cortex and hippocampus as key brain regions important for behaviour in mice.

When a subset of the aging mice from the behaviour cohort reached 15-18 months, they were culled and brain tissue was dissected. Hippocampus and cortex were dissected with assistance from Dr Matthieu Vermeren. Protein was extracted from the samples and run on Western blots with an eEF1A2-specific antibody. Figure 4.10A shows the results for the cortex and Figure 4.10B shows the results for the hippocampus. Western blots show bands for eEF1A2 in red and the loading control, GAPDH, in green (arrows). The expression values for each mouse are shown in the graphs beneath the blots.

From the graphs, it can be seen that the expression levels were very variable within genotypes, especially in the cortex. This seems unlikely to represent an accurate measure of expression as, for several *Eef1a2*$^{+/+}$ mice, expression appeared to be lower than for *Eef1a2*$^{+/wst}$ mice. In addition, comparing the individual expression values for each mouse between cortex and hippocampus showed no correlation further suggesting that these values are not accurate. One reason for variable results could be the use of small amounts of tissue extract, especially for the hippocampus, in combination with the Licor method for Western blotting. Fluorescent detection methods are less sensitive than chemiluminescent methods, which can lead to

inaccurate quantification when using small amount of tissue. However, the Licor method was selected because the accuracy of quantification is improved by the ability to probe for the loading control simultaneously (Kurien and Scofield, 2006). To summarise, I was unable to quantify eEF1A2 protein expression in aging mice.

The mice used for behavioural analysis had been genotyped prior to the start of my project. Therefore, I extracted DNA from tissue and repeated the genotyping on these mice and was able to confirm that the genotypes were correct (results shown in Appendix C).

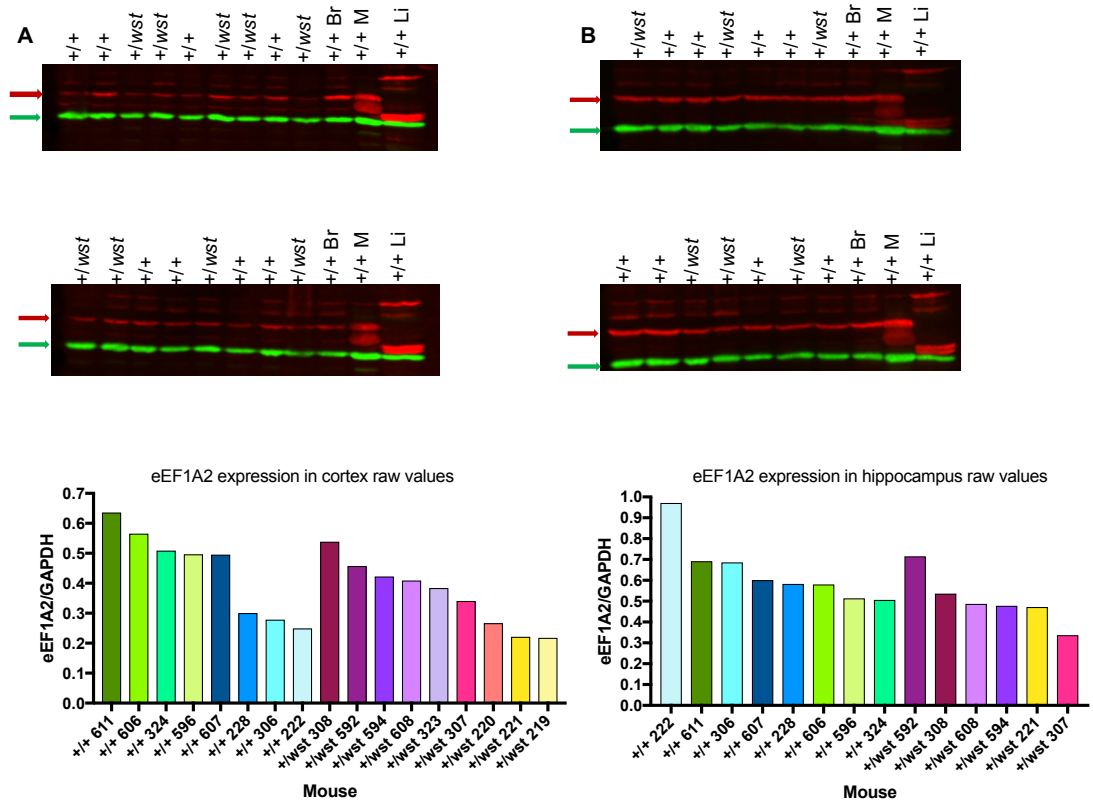

Figure 4.10. eEF1A2 protein expression in cortex and hippocampus of aging mice. *Blots were imaged using the Licor Odyssey FC with eEF1A2 in red (concentration = 1:1000) and GAPDH in green (concentration = 1:2000) and quantified using Image Studio Lite version 4.0. Br = wild-type brain positive control, M = wild-type muscle positive control, Li = wild-type liver negative control.* ***A.*** *eEF1A2 expression in cortex.* ***B.*** *eEF1A2 expression in hippocampus.*

4.2.2. Characterising the behavioural phenotype of a new *Eef1a2*-null mouse line on a C57BL/6J genetic background

4.2.2.1. Establishing the line

Due to the high variability in behavioural data as a result of the mixed genetic background of the wasted line, I decided to establish a new line. It was hypothesised that a line bred on a pure genetic background would reduce variation based on the results of the Y-maze test shown in Figure 4.9.

Heterozygous null mouse #9 from the G70S CRISPR/Cas9 experiment described in Chapter 3 was used to establish the new line (Table 3.2). The breeding process is shown in Figure 4.11A. Figure 4.11B shows part of the genotyping results from a litter which shows bands for a heterozygous, wild-type and homozygous mouse from left to right. Founder #9 contained a 22bp deletion on one allele of *Eef1a2* and this 22bp size difference between mutant and wild-type *Eef1a2* was used to identify the genotypes. Therefore, the genotyping results from heterozygous mice show two bands which are 22bp different in size. The wild-type product is 208bp and the mutant product is 186bp. As this line has a 22bp deletion in exon 3 of *Eef1a2*, it was named 'Del22.ex3'.

Figure 4.11C shows the weights of the first litter that contained wild-type, heterozygous and homozygous mice (F2 generation). Weight data was collected between P19 and P26. It is well established that homozygous wasted mice, which are complete nulls for *Eef1a2*, progressively lose weight from around P21 and do not survive past P28 (Shultz *et al*., 1982). Therefore, homozygous mice from this line were predicted to show the same phenotype. The heterozygous mice and the one wild-type mouse from the Del22.ex3 litter gained weight from P19-P26 and were phenotypically normal as expected. As predicted, the one homozygous mouse from this litter was unable to gain weight at the same rate as wild-type and heterozygous mice. This was apparent by P24 and the mouse had started to lose weight by P26. This mouse had to be culled at P26 due to low weight, a characteristic tremor and unsteady gait, phenotypes which are characteristic of homozygous wasted mice

(Shultz *et al*., 1982). Unfortunately, as there was only one homozygous mouse in the litter, statistical analysis could not be performed. It is important to note that the whole litter was very small at P19 (5.0-5.5g) but this was not the case for subsequent litters.

I collected brain and skeletal muscle from the wild-type and homozygous mouse at P26. Protein was extracted from the tissue and ran on a Western blot with antibodies specific to eEF1A2 and GAPDH as a loading control. This was performed in order to confirm that there was no eEF1A2 expression in the homozygous mouse and that the mutation resulted in complete loss of expression. The results are shown in Figure 4.11D with eEF1A2 in red and GAPDH in green (arrows). There were no eEF1A2-specific bands in brain or muscle from the homozygous (-/-) mouse indicating that eEF1A2 was not expressed. Therefore, using founder #9 to establish a new *Eef1a2*-null line was successful.

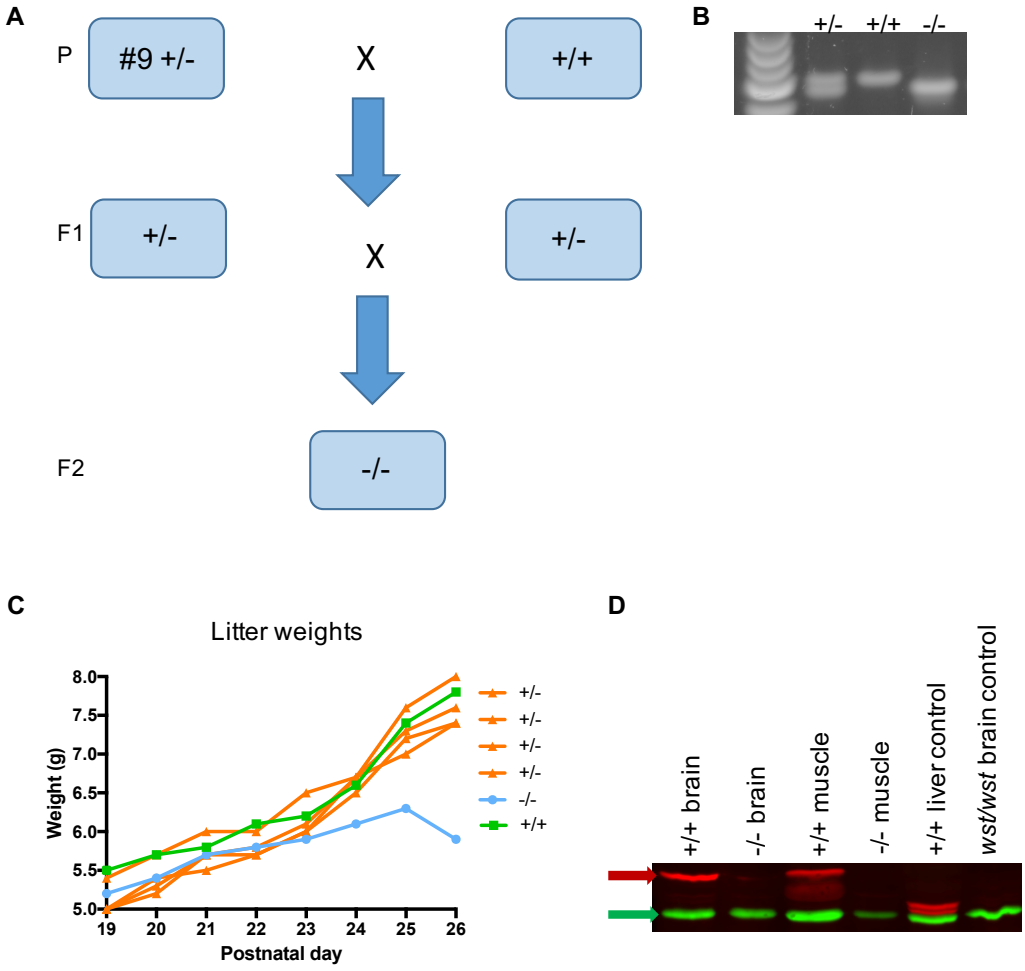

Figure 4.11. Establishing the new Del22.ex3 Eef1a2-null mouse line. *+/+ = wild-type, +/- = heterozygote, -/- = homozygote* ***A.*** *The breeding process. #9 = heterozygous null mouse from the G70S CRISPR/Cas9 experiment.* ***B.*** *Genotyping PCR ran on a 2% agarose gel with Low Molecular Weight DNA Ladder (NEB) (left). +/+ product = 208bp, -/- product = 186bp.* ***C.*** *Weights of F2 generation from P19-P26.* ***D.*** *eEF1A2 protein expression in +/+ and -/- mice from F2 generation. Blots were imaged using the Licor Odyssey FC with eEF1A2 in red (concentration = 1:1000) and GAPDH in green (concentration = 1:2000) and quantified using Image Studio Lite version 4.0. +/+ liver control = wild-type liver negative control, wst/wst brain control = wasted brain negative control.*

4.2.2.2. The Del22.ex3 behaviour cohort

Wild-type (*Eef1a2*$^{+/+}$) and heterozygous (*Eef1a2*$^{+/-}$) mice from the Del22.ex3 line were used to repeat the behavioural tests performed on heterozygous wasted mice. I hypothesised that the variation in results observed with the wasted line would be lower in the Del22.ex3 line and, therefore, testing a lower number of mice would be required to provide robust, reliable behavioural data.

Mice were bred from wild-type x heterozygote matings and were housed in male only cages of mixed genotypes. Mice were housed in groups to avoid any confounding effects of single housing on behaviour. Female mice were excluded from testing due to the potential for results to vary across different phases of the oestrus cycle. Mice were tested in behavioural assays from 9 weeks (2 months) of age. The age of the mice tested ranged only from 2 months to 5 months as there was insufficient time to age mice. This age group provided a comparison for the wasted heterozygous mice tested at 2-6 months. As with the wasted line, data are presented as mean values in the bar graphs and as individual scores for each mouse in the dot plots. The bar graphs allow the means to be observed and compared with ease whilst the dot plots show the spread of data and therefore the variability in scores within genotypes. Testing was performed with assistance from Charlie Cumber (Honours project student).

4.2.2.3. *Eef1a2*$^{+/-}$ mice showed changes in repetitive behaviours in the nest building and marble burying assays

I performed the nest building assay to determine whether *Eef1a2*$^{+/-}$ mice showed changes in repetitive behaviours. This test was performed in the same way as described for the wasted line (Section 4.2.1.2). The results are shown in Figure 4.12.

Figure 4.12A shows the percentage of nestlet shredded for *Eef1a2*$^{+/+}$ and *Eef1a2*$^{+/-}$ mice. *Eef1a2*$^{+/-}$ mice shredded significantly less nestlet than *Eef1a2*$^{+/+}$ mice, shown using an unpaired t-test. Therefore, *Eef1a2*$^{+/-}$ mice were found to show alterations in repetitive behaviours. Figure 4.12B shows the nest building score for *Eef1a2*$^{+/+}$ and *Eef1a2*$^{+/-}$ mice. In contrast to the results for the percentage of nestlet shredded, there

was no significant difference in nest building score between *Eef1a2*$^{+/+}$ and *Eef1a2*$^{+/-}$ mice (Mann-Whitney test). The results of this test are in contrast to those observed for heterozygous wasted mice where there was no significant difference in either parameter between genotypes.

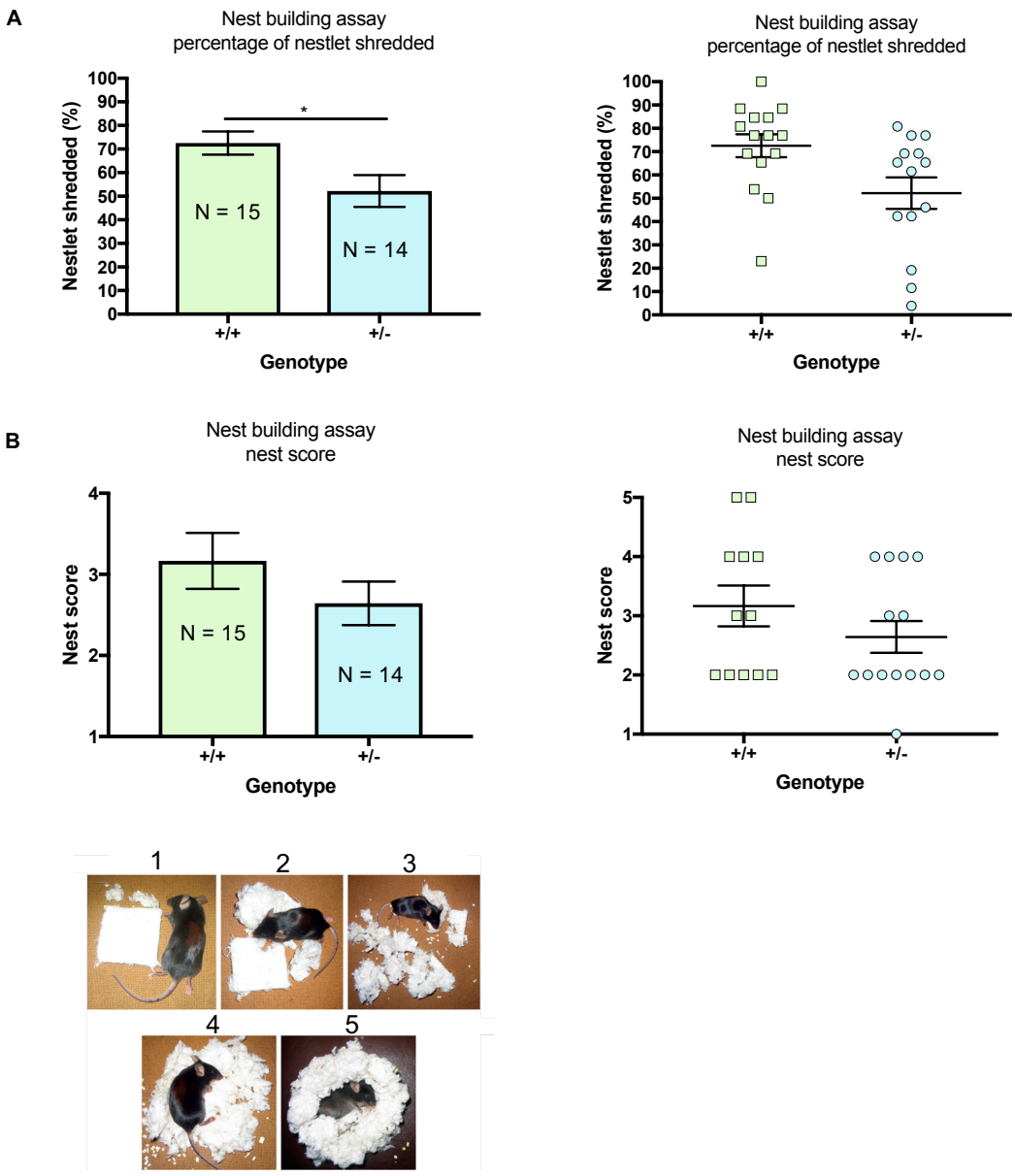

Figure 4.12. Data from Eef1a2$^{+/+}$ and Eef1a2$^{+/-}$ mice in the nest building assay. *Error bars for all graphs show SEM.* ***A.*** *Percentage of nestlet shredded. The asterisk on the bar graph shows a statistically significant difference, unpaired t-test, t = 2.46, DF = 27, p = 0.0207.* ***B.*** *Nest score. The scoring criteria used is shown in the images labelled 1-5 (Deacon, 2006a). There was no significant difference between genotypes (Mann-Whitney test).*

To further explore the effects of *Eef1a2* deletions on repetitive behaviours, *Eef1a2*$^{+/-}$ mice were tested in the marble burying assay. This assay measured the number of marbles, out of 20, buried in 30 minutes as performed on the wasted line (Section 4.2.1.2). The results of this test are shown in Figure 4.13.

The data in Figure 4.13 shows that *Eef1a2*$^{+/-}$ mice buried significantly fewer marbles than *Eef1a2*$^{+/+}$ mice. A similar result was found for *Eef1a2*$^{+/wst}$ mice in that they buried significantly fewer marbles as they aged. However, there was no difference in marble burying scores between genotypes for the wasted line. The marble burying data for the Del22.ex3 line reveals alterations in repetitive digging behaviour. This complements the nest building data which showed that *Eef1a2*$^{+/-}$ mice shredded significantly less nestlet than *Eef1a2*$^{+/+}$ mice, also indicating changes in repetitive behaviour. Curiously, these changes in repetitive behaviours were in the opposite direction from what was expected when considering that most mouse models of autism show an increase in these behaviours (see Section 4.1.4). In addition, some of the patients with missense mutations in *EEF1A2* show an increase in repetitive behaviours, as described in Section 4.1.1.

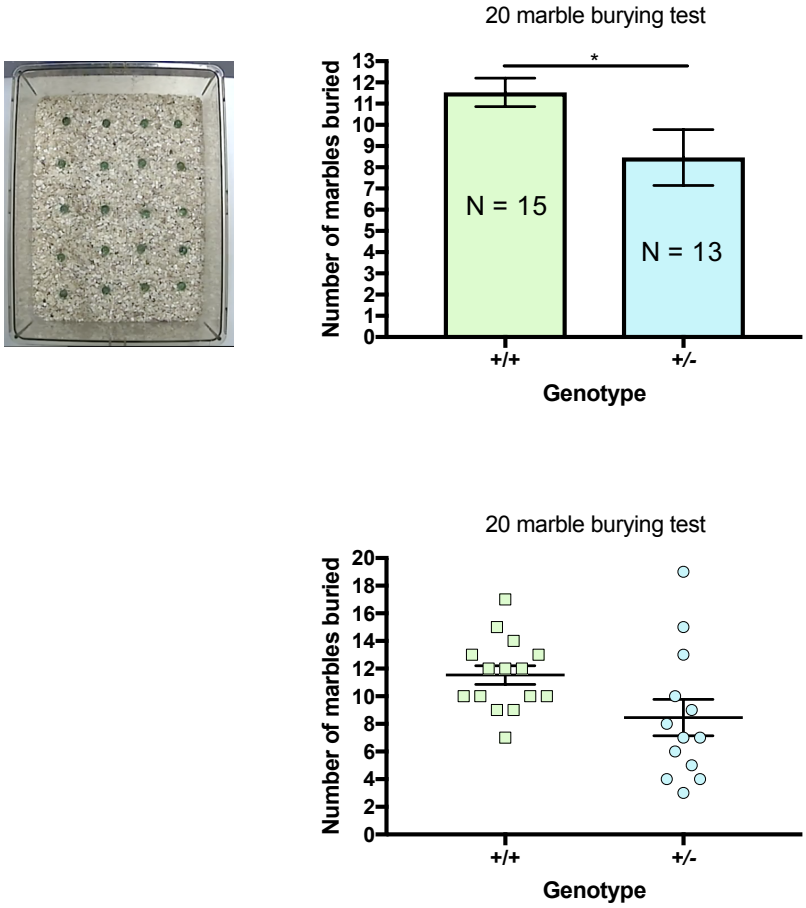

Figure 4.13. Data from Eef1a2$^{+/+}$ and Eef1a2$^{+/-}$ mice in the marble burying assay. *A picture of the apparatus is shown. The graphs show the number of marbles buried for each genotype. Error bars for all graphs show SEM. The asterisk on the bar graph shows a statistically significant difference, unpaired t-test, t = 2.16, DF = 26, p = 0.0399.*

Based on the nest building and marble burying results, it appears that *Eef1a2*$^{+/-}$ mice show a reduction in repetitive behaviours compared with wild-type mice. I performed the digging assay as a further test to analyse repetitive digging behaviour. This test involved observing digging behaviour for 3 minutes as described in Section 4.2.1.2. The results of this test are shown in Figure 4.14.

There was no significant difference in the latency to start digging (Figure 4.14A), the number of digging bouts (Figure 4.14B) or the total duration of digging (Figure 4.14C) between genotypes. Therefore, this test revealed no changes in repetitive

digging behaviour for Del22.ex3 *Eef1a2*$^{+/-}$ mice. The same result was observed for the wasted line (Section 4.2.1.2).

Interestingly, both *Eef1a2*$^{+/+}$ and *Eef1a2*$^{+/-}$ mice from the Del22.ex3 line engaged in very low levels of digging behaviour compared to mice from the wasted line. Mice from the Del22.ex3 line took longer to begin digging, shown by a higher mean latency to start digging than the wasted line. Del22.ex3 mice also had a substantially lower mean number of digging bouts and mean duration of digging than mice from the wasted line (Figure 4.4, Figure 4.14).

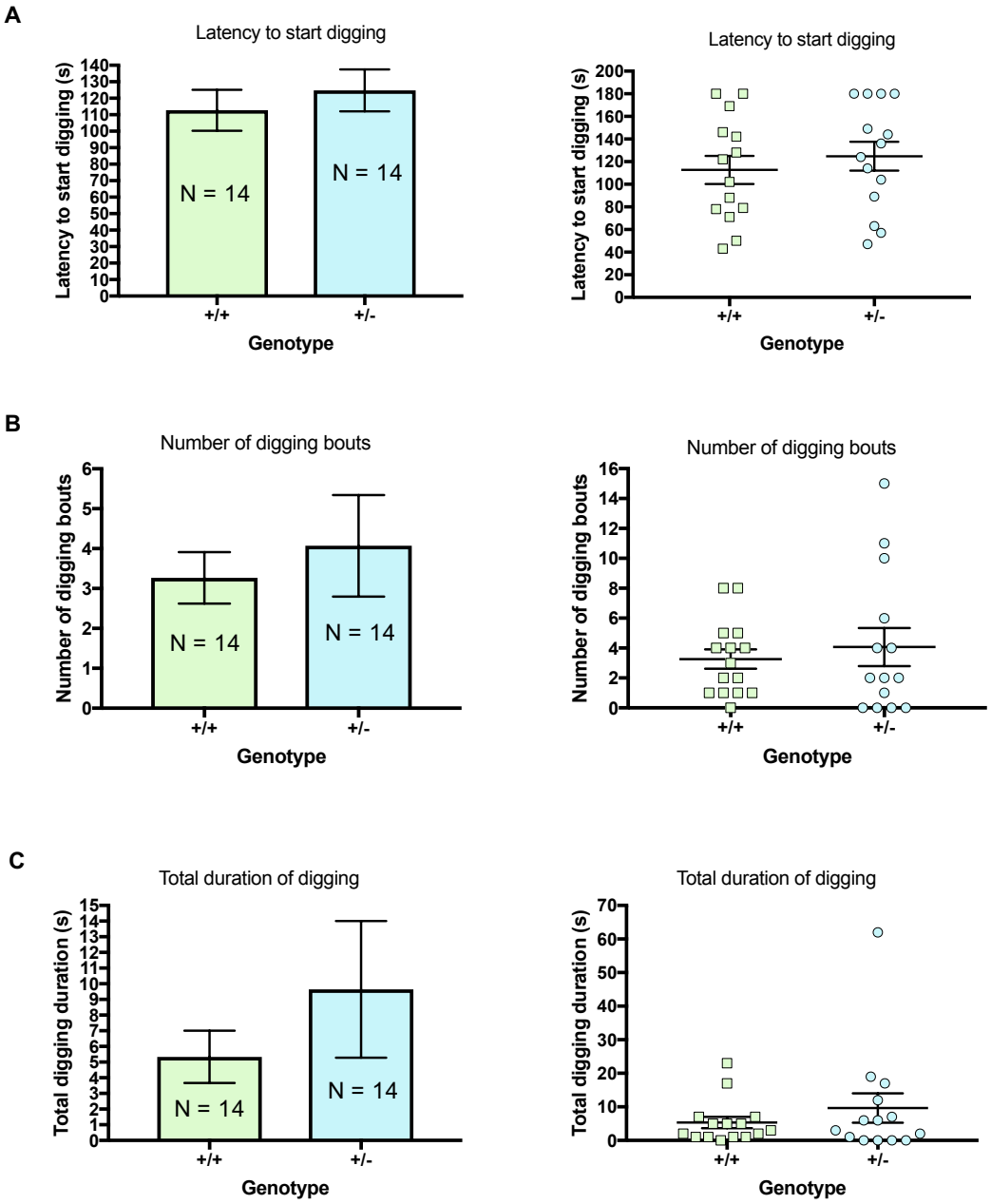

Figure 4.14. Data from Eef1a2$^{+/+}$ and Eef1a2$^{+/-}$ mice in the digging assay. *Error bars for all graphs show SEM.* ***A.*** *Latency to start digging. There was no significant difference between genotypes (unpaired t-test).* ***B.*** *Number of digging bouts. There was no significant difference between genotypes (unpaired t-test).* ***C.*** *Total duration of digging. There was no significant difference between genotypes (unpaired t-test).*

I performed another test for repetitive behaviours on the Del22.ex3 line which had not been tested on the wasted line as the apparatus had not been available earlier. This was the hole-board test. This test involves placing the mouse in a 40cm x 40cm box containing 16 holes and allowing the mouse to explore for a set period of time (Figure 4.15). Changes in repetitive behaviours are indicated by an increase (or decrease) in hole exploration ('head dips') compared with wild-type mice. An image of the apparatus is shown in Figure 4.15A.

Mice with mutations in genes related to autism have shown changes in repetitive behaviours in the hole-board test and, curiously, this has been observed in both directions. Specifically, mice with deletion of *Pten*, a component of the mTOR pathway, show a significantly reduced hole-poke frequency compared with wild-type mice (Lugo *et al*., 2014). Conversely, mice with deletion of *Shank2* specifically in Purkinje cells show an increase in hole-poke frequency compared with wild-type mice (Ha *et al*., 2016).

In my experiment, mice were allowed to explore the hole-board arena for 5 minutes. The results of this test are shown in Figure 4.15B-D. The latency to the first head dip (Figure 4.15B), the total number of head dips (Figure 4.15C) and the total number of holes explored were measured (Figure 4.15D). There were no significant differences in any of these three parameters between *Eef1a2*$^{+/+}$ and *Eef1a2*$^{+/-}$ mice (unpaired t-tests). Therefore, there were no identifiable differences in repetitive behaviours between *Eef1a2*$^{+/+}$ and *Eef1a2*$^{+/-}$ mice in this test.

To summarise, *Eef1a2*$^{+/-}$ mice showed a significant decrease in repetitive behaviours compared with wild-type mice in the nest building and marble burying assays but not in the digging or hole-board tests. These results are in contrast to those for the wasted line for which there were no differences between genotypes.

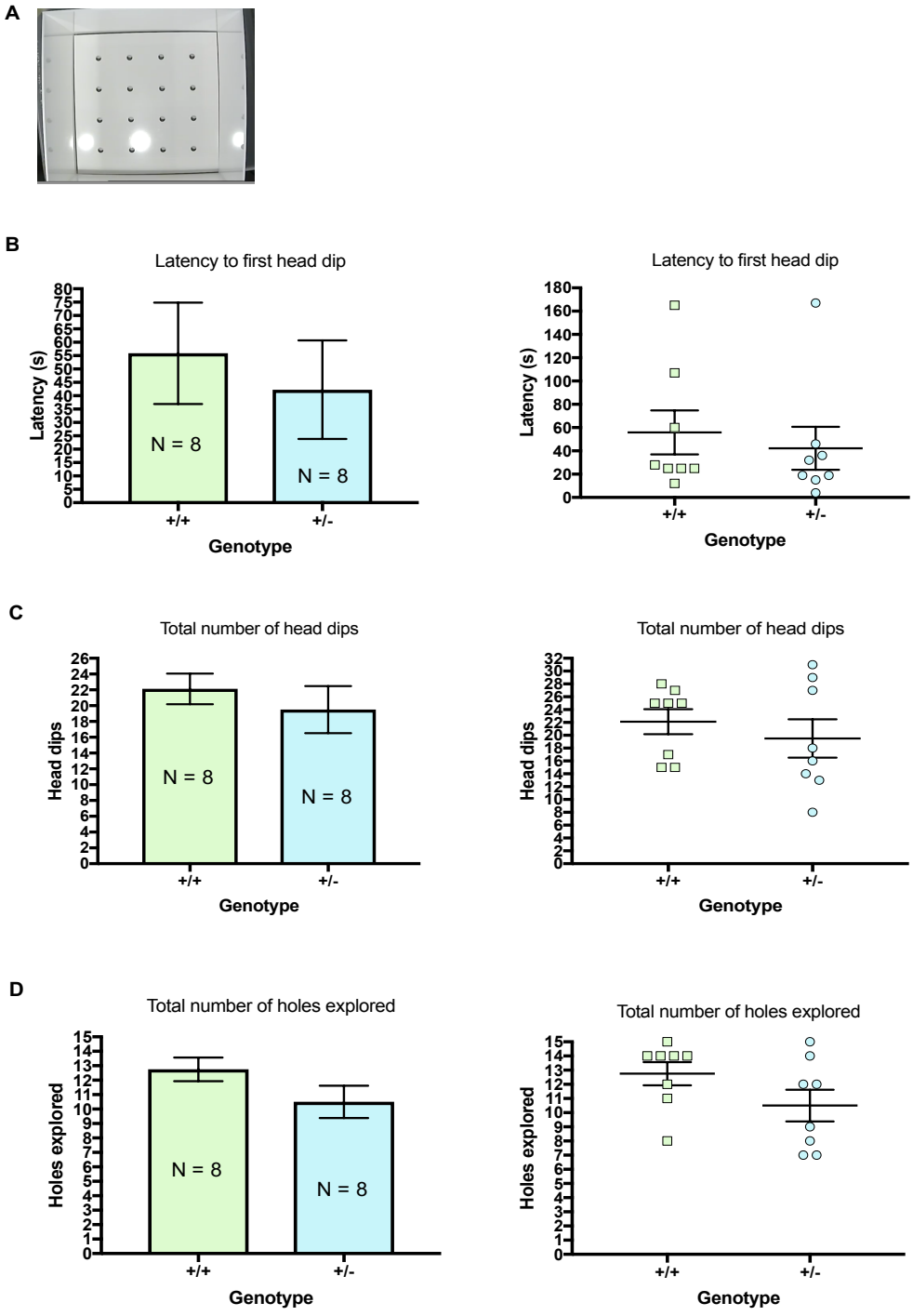

Figure 4.15. Data from Eef1a2$^{+/+}$ and Eef1a2$^{+/-}$ mice in the hole-board test. *Error bars for all graphs show SEM.* ***A.*** *An image of the apparatus.* ***B.*** *Latency to first head dip. There was no significant difference between genotypes (unpaired t-test).* ***C.*** *Total number of head dips. There was no significant difference between genotypes (unpaired t-test).* ***D.*** *Total number of holes explored. There was no significant difference between genotypes (unpaired t-test).*

4.2.2.4. *Eef1a2*$^{+/-}$ mice showed normal sociability and preference for social novelty

Eef1a2$^{+/+}$ and *Eef1a2*$^{+/-}$ mice were tested in the stranger mouse assay to investigate sociability and preference for social novelty as performed on the wasted line (Section 4.2.1.3). Test 1 measured whether the test mouse preferred to spend time alone or with another mouse to assess sociability. The results of this test are shown in Figure 4.16.

Figure 4.16 shows the results for the time spent exploring the mouse vs the empty cage. Both *Eef1a2*$^{+/+}$ and *Eef1a2*$^{+/-}$ mice spent significantly more time exploring the mouse than the empty cage, shown using a two-way ANOVA with Holm-Sidak's multiple comparisons test. The total exploration time did not differ between genotypes, shown using an unpaired t-test (data not shown). These results suggest that *Eef1a2*$^{+/-}$ mice have normal sociability, in agreement with results from *Eef1a2*$^{+/wst}$ mice. However, other tests of social behaviour should be considered in the future.

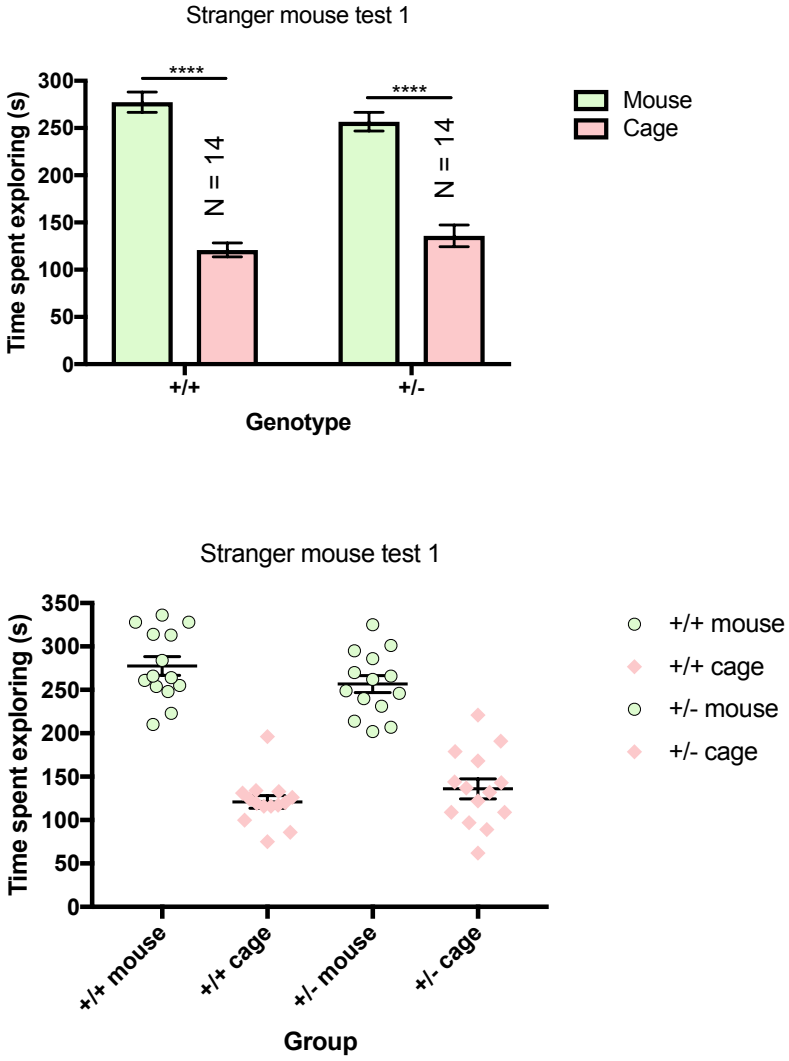

Figure 4.16. Data from Eef1a2$^{+/+}$ and Eef1a2$^{+/-}$ mice in the stranger mouse test stage 1. *Time spent exploring the mouse vs the empty cage. Error bars for all graphs show SEM. Asterisks on the bar graph show statistically significant differences. Two-way ANOVA showed significant effect of stimulus (mouse vs cage): F = 192, DF = 1, 52, p = <0.0001. Holm Sidak's multiple comparisons test: from left to right, p = <0.0001, <0.0001.*

Following this, I performed a second stranger mouse test to determine whether *Eef1a2*$^{+/-}$ mice showed preference for social novelty. This was carried out as described for the wasted line in Section 4.2.1.3. The results of this test are shown in Figure 4.17.

Figure 4.17 shows the results for the time spent exploring the familiar mouse vs the novel mouse. Both *Eef1a2*$^{+/+}$ and *Eef1a2*$^{+/-}$ mice spent significantly more time exploring the novel mouse compared with the familiar mouse, shown using a two-way ANOVA with Holm-Sidak's multiple comparisons test. The total exploration time did not differ between genotypes, shown using an unpaired t-test (data not shown). Therefore, *Eef1a2*$^{+/-}$ mice were phenotypically normal in this test and showed a preference for social novelty. Interestingly, this is in contrast to the behaviour of *Eef1a2*$^{+/wst}$ mice. *Eef1a2*$^{+/wst}$ mice showed no preference for social novelty.

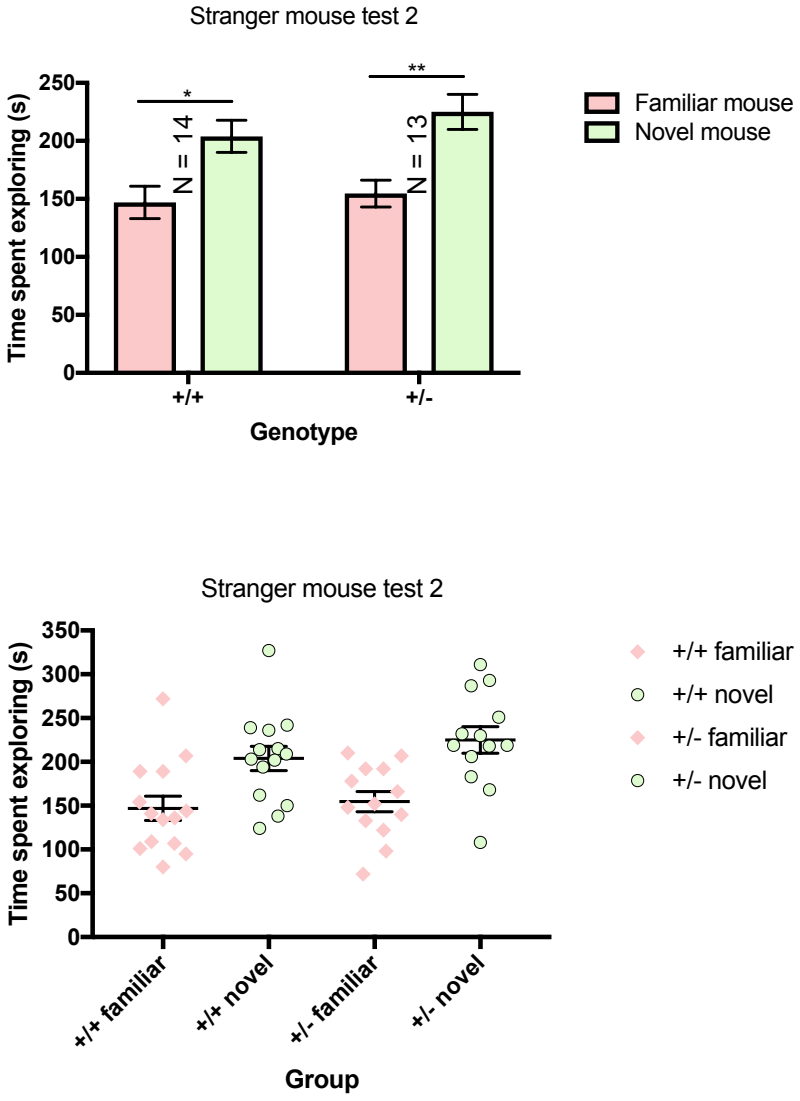

Figure 4.17. Data from Eef1a2$^{+/+}$ and Eef1a2$^{+/-}$ mice in the stranger mouse test stage 2. *Time spent exploring the familiar mouse vs the novel mouse. Error bars for all graphs show SEM. Asterisks on the bar graph show statistically significant differences. Two-way ANOVA showed significant effect of stimulus (familiar vs novel mouse): F = 21.51, DF = 1, 50, p = <0.0001. Holm Sidak's multiple comparisons test: from left to right, p = 0.0172, 0.0041.*

4.2.2.5. *Eef1a2*$^{+/-}$ mice showed no hyperactivity or anxiety phenotypes in the open field test

To detect locomotor and/or anxiety phenotypes in *Eef1a2*$^{+/-}$ mice, I performed the open field test. This was carried out using the same method described for the wasted line in Section 4.2.1.4. The results of this test are shown in Figure 4.18.

The total distance travelled was measured to investigate locomotion (Figure 4.18A), whereas the total time spent freezing (Figure 4.18B) and time spent in each zone (Figure 4.18C) were measured to investigate anxiety. There were no significant differences in the total distance travelled (unpaired t-test), freezing time (unpaired t-test) or time spent in each zone (two-way ANOVA) between genotypes. Therefore, *Eef1a2*$^{+/-}$ mice did not show any locomotor or anxiety phenotypes in this test. The same result was found when testing *Eef1a2*$^{+/wst}$ mice in that there were no significant differences between genotypes. However, locomotor activity decreased in *Eef1a2*$^{+/wst}$ mice with age.

Eef1a2$^{+/+}$ and *Eef1a2*$^{+/-}$ mice spent significantly more time in the outside zone compared with the centre zone (Figure 4.18C). Therefore, *Eef1a2*$^{+/+}$ and *Eef1a2*$^{+/-}$ mice both preferred to spend time in the outside zone. The same result was observed in some but not all of the age groups for the wasted line.

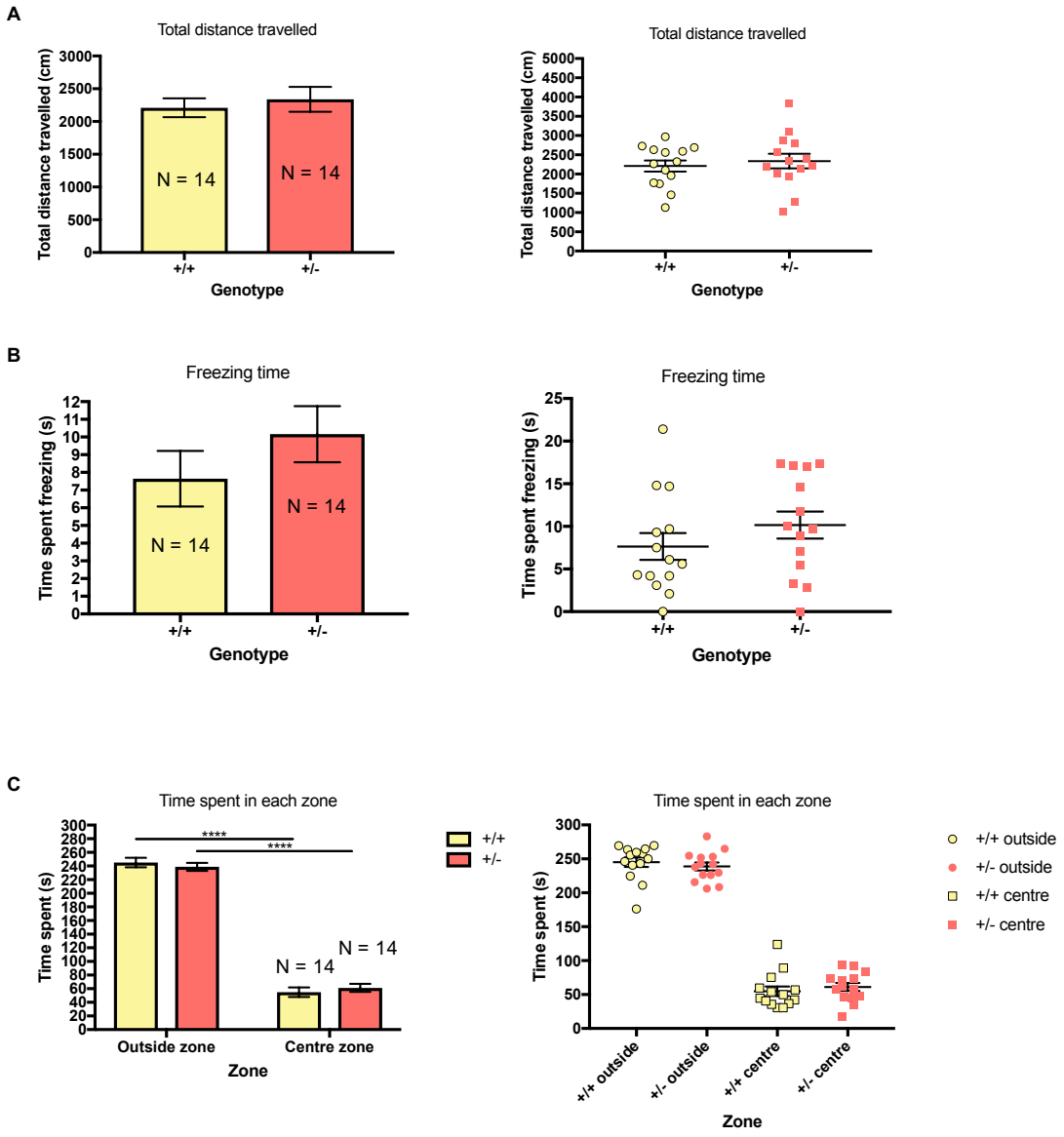

Figure 4.18. Data from Eef1a2$^{+/+}$ and Eef1a2$^{+/-}$ mice in the open field test. *Error bars for all graphs show SEM.* ***A.*** *Total distance travelled. There was no significant difference between genotypes (unpaired t-test).* ***B.*** *Total time spent freezing. There was no significant difference between genotypes (unpaired t-test).* ***C.*** *Time spent in outside and centre zone. Asterisks on the bar graph show statistically significant differences. Two-way ANOVA showed significant effect of zone: F = 821.1, DF = 1, 54, p = <0.0001. Tukey's multiple comparisons test: from left to right, p = <0.0001, <0.0001.*

4.2.2.6. *Eef1a2*$^{+/-}$ mice showed normal spatial memory in a short-ITI Y-maze test

I tested *Eef1a2*$^{+/+}$ and *Eef1a2*$^{+/-}$ mice in the Y-maze to assess spatial memory as performed on the wasted line (Section 4.2.1.5). The results of this test are shown in Figure 4.19.

Figure 4.19 shows the data for arm exploration. Both *Eef1a2*$^{+/+}$ and *Eef1a2*$^{+/-}$ mice spent significantly more time exploring the novel arm compared with the familiar arms indicating normal spatial memory in this particular test after a 15 minute ITI. This was shown using a two-way ANOVA with Tukey's multiple comparisons test. Previously tested *Eef1a2*$^{+/wst}$ mice also showed normal spatial memory in this test.

As mentioned, the implementation of this test with a longer ITI to further assess spatial memory is explored in Chapter 5.

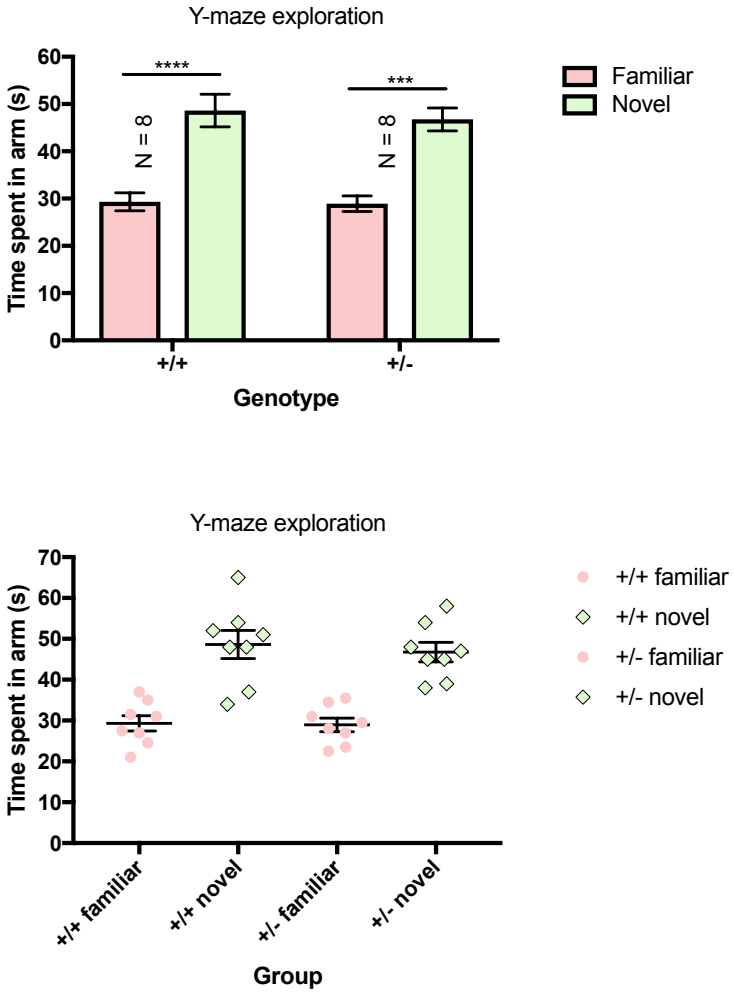

Figure 4.19. Data from Eef1a2$^{+/+}$ and Eef1a2$^{+/-}$ mice in the Y-maze test. *The bar graph shows the mean time spent exploring the Y-maze arms. Familiar = mean of 'start' and 'other' arm. Error bars for all graphs show SEM. Asterisks on the bar graph show statistically significant differences. Two-way ANOVA showed significant effect of arm (familiar vs novel): F = 57.53, DF = 1, 28, p = <0.0001. Tukey's multiple comparisons test: from left to right p = <0.0001, 0.0001.*

4.2.2.7. Requirement for optimisation of the novel object recognition test

Mice with mutations in genes related to autism and intellectual disability have been identified as having impairments in object recognition tasks, including *Fmr1* knockout mice, *Shank3* mutant mice and *Shank1* knockout mice (Bhattacharya *et al*., 2012, Yang *et al*., 2012, Kazdoba *et al*., 2014, Sungur *et al*., 2017). Therefore, I performed the novel object recognition test to assess whether *Eef1a2*$^{+/-}$ mice show an impairment in recognition memory.

The novel object recognition test takes advantage of the innate behaviour of mice to show a preference for novelty and, specifically, explore new objects. In the first phase, the mouse is presented with two identical objects and allowed to explore these for a defined period of time. The mouse is then moved to a holding cage for a set period of time, referred to as the inter-trial interval (ITI). Following this, the second phase begins in which the mouse is allowed to explore one of the objects from phase one and a completely new, or novel, object. Wild-type mice are expected to show a preference to explore the novel object compared with the familiar object. Mice with recognition memory impairments will show no preference for either object (Grayson *et al*., 2015).

I tested Del22.ex3 mice with a short 5 minute ITI. Figure 4.20A shows an image of the apparatus, which was the same Y-shaped maze used in the stranger mouse tests and in the Y-maze test. Figure 4.20B shows the results presented as the mean discrimination ratio (DR) for each genotype (see Section 2.8.4 for discrimination ratio calculation). A score of 1 indicates 100% preference for the novel object, a score of -1 indicates 100% preference for familiar object and a score of 0 indicates no preference for either object. There was no significant difference in DR between genotypes (unpaired t-test). However, as a DR of greater than 0 indicates preference for the novel object, the preference of both *Eef1a2*$^{+/+}$ and *Eef1a2*$^{+/-}$ mice was low (mean = 0.16 and 0.14 respectively). Discrimination ratios for this test are normally approximately 0.5-0.6 for wild-type mice (Lise *et al*., 2012, Mazumder *et al*., 2016).

The dot plot shows that the majority of the mice for each genotype did prefer to investigate the novel object, indicated by scores greater than 1.

I then analysed the first minute only to investigate object exploration during the time when exploration is highest. The results are presented in Figure 4.20C as the mean exploration time for each object rather than DR. Interestingly, wild-type mice spent significantly more time exploring the novel object compared with the familiar object whereas heterozygous mice did not (two-way ANOVA with Tukey's multiple comparisons test). This might suggest that *Eef1a2*$^{+/+}$ mice show learning in this test whilst *Eef1a2*$^{+/-}$ mice do not, however, the test should be optimised such that a DR of 0.5-0.6 is achieved to further investigate this. When the full two-minute test was analysed in the same way, neither genotype showed a significant preference for the novel object (data not shown). There was also no significant difference between genotypes in the total exploration time (data not shown). Therefore, results were not confounded by lower overall exploration of either genotype.

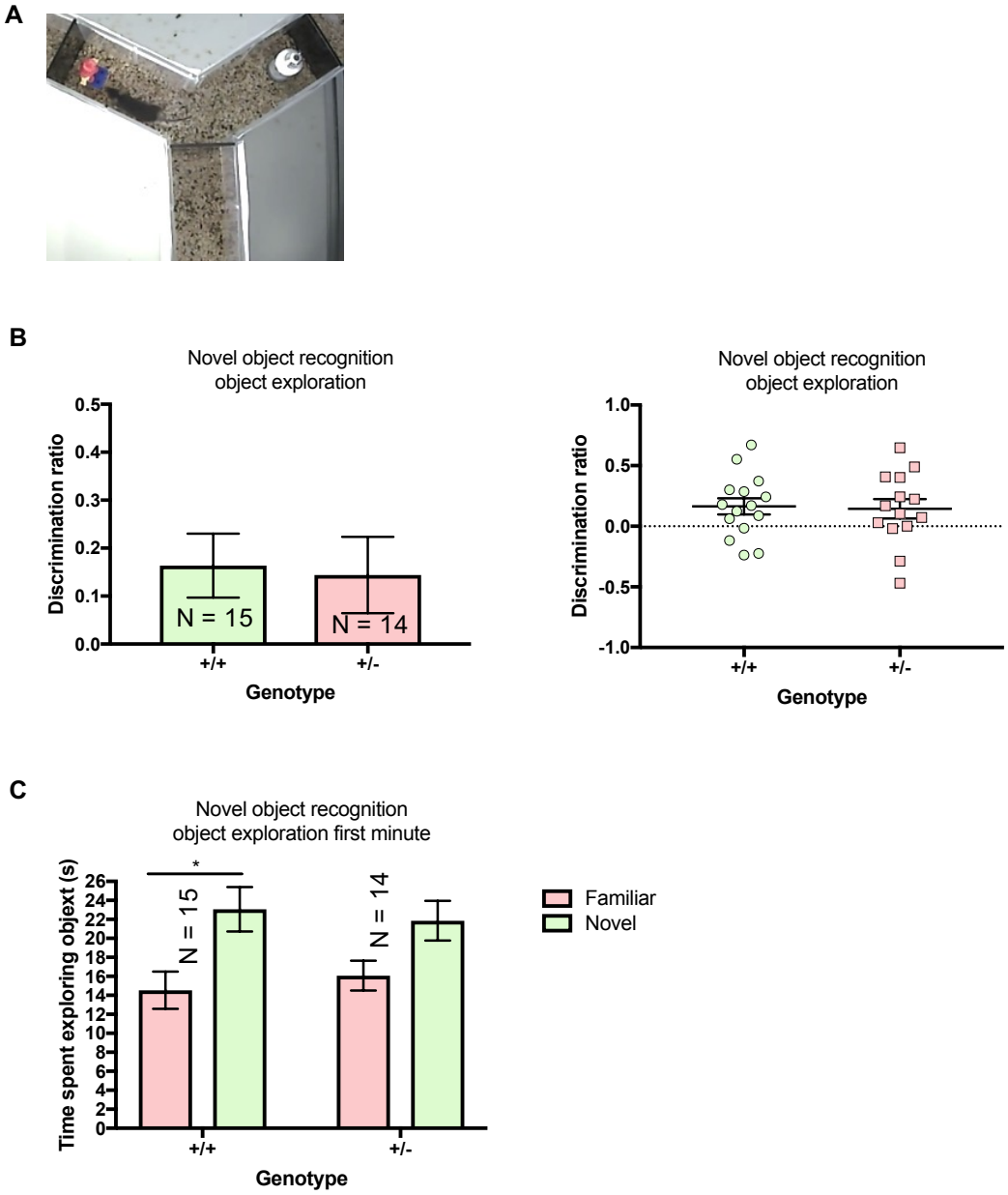

Figure 4.20. Data from Eef1a2$^{+/+}$ and Eef1a2$^{+/-}$ mice in the novel object recognition test. *Error bars for all graphs show SEM.* ***A.*** *Image of apparatus used for novel object recognition. One arm was closed and the other two arms split in half using gates. The objects used were a bulb (right arm) and a Lego® figure (left arm).* ***B.*** *Discrimination ratios. There was no significant difference between genotypes (unpaired t-test).* ***C.*** *Exploration during first minute of test. The asterisk on the bar graph shows a statistically significant difference. Two-way ANOVA showed significant effect of object (familiar vs novel): F = 12.52, DF = 1,54, p = 0.0008. Tukey's multiple comparison's test, p = 0.0188.*

4.2.2.8. No difference in body weight or grip strength between *Eef1a2*$^{+/+}$ and *Eef1a2*$^{+/-}$ mice

Following behavioural testing, *Eef1a2*$^{+/+}$ and *Eef1a2*$^{+/-}$ mice were weighed and grip strength tested to establish whether there were any differences in muscle function between genotypes. Wasted homozygous mice show a significant reduction in weight compared to their wild-type littermates by P23 (Newbery *et al*., 2005) and perform significantly worse than their wild-type littermates in the grip strength test by P20. In contrast, wasted heterozygotes show no significant differences compared with wild-type mice in either of these measurements at all ages tested (Griffiths *et al*., 2012). It was therefore predicted that Del22.ex3 heterozygotes would also be phenotypically normal but it was important to analyse this directly on the experimental cohort under test.

I measured weight and grip strength at 5 months of age. The grip strength test involved measurement of all four limbs and front limbs only, in triplicate. Grip strength measurements were normalised to body weight (Newtons/grams). The results of the weight and grip strength analyses are shown in Figure 4.21. There were no significant differences in weight or grip strength between genotypes. This indicates that Del22.ex3 heterozygotes gain weight normally and do not show any evidence of changes in muscle function compared with wild-type mice. This is in agreement with the phenotypes observed in wasted heterozygotes (Griffiths *et al*., 2012).

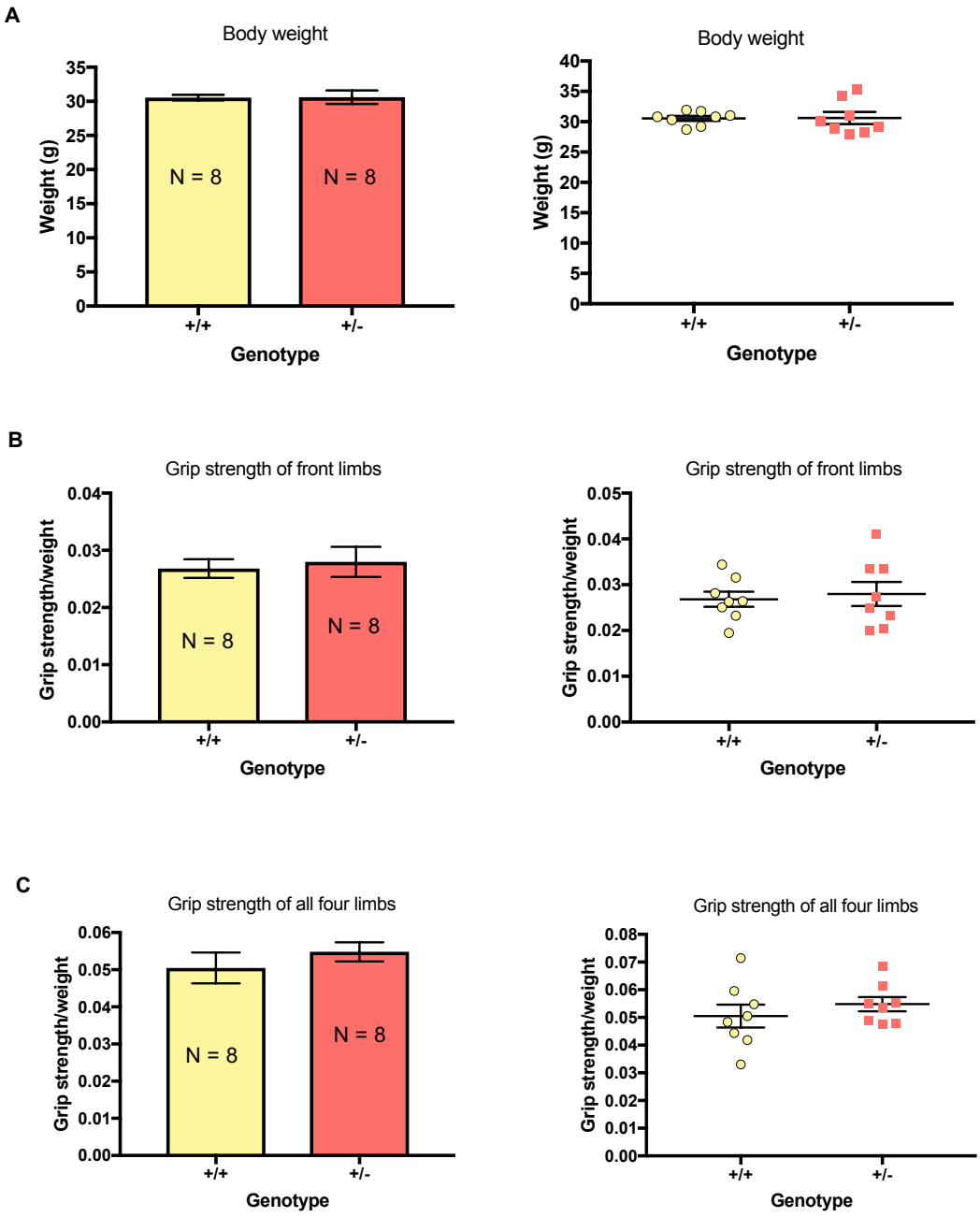

Figure 4.21. Body weight and limb grip strength data from Eef1a2$^{+/+}$ and Eef1a2$^{+/-}$ mice at 5 months. *Error bars for all graphs show SEM.* ***A.*** *Body weight. There was no significant difference between genotypes (unpaired t-test).* ***B.*** *Front (fore) limb grip strength (Newtons) normalised to body weight (grams). There was no significant difference between genotypes (unpaired t-test).* ***C.*** *All four limb grip strength (Newtons) normalised to body weight (grams). There was no significant difference between genotypes (unpaired t-test).*

4.2.2.9. Variation lower in behavioural data from the Del22.ex3 line compared with the wasted line

To compare the level of variation in data from each test between the two lines, I calculated the coefficient of variation (CV). This is the ratio of the standard deviation to the mean and is commonly used to compare the variation in data from two separate experiments. The formula used to calculate the CV is shown in the legend of Table 4.1. The CV is expressed as a percentage and a higher CV indicates more variability in the data.

Table 4.1 shows the CV values for the Del22.ex3 line and the wasted line for each behavioural test. For the wasted line, the 2-6 month old cohort was used for analysis. CV values were calculated using the data from wild-type mice and therefore show the resulting variation from testing mice on a mixed genetic background vs a pure C57BL/6 genetic background. The lower CV values are shown in Table 4.1 in green and it can be seen that the CV is lower for the Del22.ex3 line in all tests apart from the digging assay. The variation in the data for the number of digging bouts and the total duration of digging is higher in the Del22.ex3 line than in the wasted line.

The evidence presented in Table 4.1 suggests that the variation in the Del22.ex3 line is generally lower than the variation in the wasted line and this is likely due to the pure C57BL/6 genetic background.

	Del22.ex3 line	Wasted line
Nest building (% shredded)	26%	47%
Marble burying	23%	29%
Y-maze	20%	34%
Stranger mouse test 1	15%	33%
Stranger mouse test 2	25%	31%
Latency to start digging	41%	65%
Number of digging bouts	76%	36%
Total digging duration	121%	55%
Total distance travelled in open field	24%	63%
Total time spent freezing in open field	77%	117%
Time spent in centre of open field	47%	99%
Mean	45%	55%

Table 4.1. Comparing variation in results from the wasted line and the Del22.ex3 line. *The coefficient of variation for each behavioural test on each mouse line is shown. CV = (SD/mean)*100. Values highlighted in green indicate the line which showed the lowest variation for a given test. The mean CV for each line is given in the final row. There was no significant difference in the mean CV between genotypes (unpaired t-test, t = 0.78, DF = 20, p = 0.4459.*

4.3. Discussion

The aims of this chapter were as follows:

1) To characterise the behavioural phenotype of heterozygous wasted mice and to determine whether phenotype is affected by age.

2) To determine, through protein expression analysis, whether any age-specific effect on behaviour found through aim 1 is accompanied by a dosage of eEF1A2 lower than 50%.

3) To characterise the behavioural phenotype of heterozygous mice from a new *Eef1a2*-null mouse line (Del22.ex3) which, in contrast to the mixed background of wasted mice, is on an inbred C57BL/6J genetic background.

I performed seven behavioural tests on *Eef1a2*$^{+/+}$ and *Eef1a2*$^{+/wst}$ mice which assayed repetitive behaviours, sociability, preference for novelty, locomotor activity and anxiety. In terms of aging, I studied mice up to the age of 18 months and found age-specific changes in behaviour in the marble burying and open field tests.

There were no changes in the repetitive behaviours of *Eef1a2*$^{+/wst}$ mice compared with *Eef1a2*$^{+/+}$ mice in any of the three assays used (nest building, marble burying and digging). However, in the marble burying test, *Eef1a2*$^{+/wst}$ mice buried significantly fewer marbles as they aged. Similarly, *Eef1a2*$^{+/wst}$ mice also travelled a significantly shorter distance and spent more time freezing in the open field test as they aged, despite a lack of significant differences in this test between genotypes. In the marble burying and open field tests, there was no change in the behaviour of *Eef1a2*$^{+/+}$ mice with age, this effect was specific to *Eef1a2*$^{+/wst}$ mice. The reduction in marble burying behaviour and locomotor activity observed here in aging *Eef1a2*$^{+/wst}$ mice may be suggestive of a motor impairment despite the fact that *Eef1a2*$^{+/wst}$ mice show no motor coordination impairments in the rotarod test at 21 months of age (Griffiths *et al*., 2012). It is possible that motor coordination may be intact while general locomotor activity is impaired. In addition, the rotarod test forces activity whereas the open field test allows activity to be optional. Therefore, certain motor impairments which are detectable in the open field test may be undetectable in the rotarod test. Furthermore, pain has never been studied in this

mouse line. It is possible that *Eef1a2*$^{+/wst}$ mice may have reduced motivation for movement due to unidentified muscular pain, however, this is unlikely as pain models have been shown to be impaired in the rotarod test (Ruan *et al*., 2013). Another possibility is that *Eef1a2*$^{+/wst}$ mice have a reduced motivation for activity as they age generally and this may be further tested using an in-cage running wheel which would allow measurement of voluntary activity (Brooks and Dunnett, 2009). In addition, patients with *EEF1A2* mutations present with motor abnormalities (see Table 1.2).

It is curious that *Eef1a2*$^{+/wst}$ mice do not show reduced nestlet shredding or digging behaviour in the digging test with age, as an age-specific motor impairment or motivation change might be expected to reduce these behaviours too. Digging behaviour does appear to decline with age in *Eef1a2*$^{+/wst}$ mice but this was not statistically significant. It is also possible that, rather than the impairments discussed above, *Eef1a2*$^{+/wst}$ mice simply show a reduction in repetitive digging behaviour with age. However, if this was the case, a significant reduction should have been observed in the digging assay as well as the marble burying assay.

The observation that aging *Eef1a2*$^{+/wst}$ mice showed reduced locomotor activity and increased freezing time in the open field test makes it somewhat difficult to disentangle the results. Specifically, this could be due to a motor impairment or reduced motivation as discussed above or it could be due to anxiety. For example, apparent increased freezing could simply represent reduced locomotor activity due to a motor impairment. Or reduced locomotor activity could simply represent increased freezing due to anxiety. No anxiety phenotype was observed when comparing the time spent in the outside of the open field box vs the centre and the 'n' for the 12-18-month group was low resulting in highly variable data and difficulty in drawing conclusions. Further studies of anxiety would be beneficial, such as the elevated plus maze which measures the preference of mice to spend time in open vs closed arms, with more time in the closed arms indicating higher anxiety (Moy *et al*., 2007).

In the stranger mouse test, *Eef1a2*$^{+/wst}$ mice showed normal sociability but reduced preference for social novelty. This was apparent at all ages tested and therefore was not an age-specific impairment. Many mouse models with mutations in autism related genes show impairments in both sociability and social novelty (Won *et al*., 2012, Reith *et al*., 2013), however, impairments in social novelty only have also been observed (Wagnon *et al*., 2015). This reveals that an autism-like phenotype in *Eef1a2*$^{+/wst}$ mice in that they prefer not to spend time with mice with which they are unfamiliar. No specific social impairments have been reported in patients with *EEF1A2* mutations, largely due to the fact that most of the patients are non-verbal (Table 1.2). However, this would be an interesting avenue for future investigation upon identification of any new milder cases, if possible.

Ideally, a larger number of mice would have been used for each behavioural test on the wasted line given the results of the power calculations. However, time limitations and the desire to move on to testing the Del22.ex3 line meant that this was not achieved. In addition, it would have been difficult and time consuming to breed a large cohort of mice at 12-18 months for the aging study; unfortunately, for some tests, there were only 5 mice available per genotype. It was decided that it would be more beneficial to move on to the new line due to the possibility of lower variation and more robust behavioural results. This was a positive decision as the result of comparing the coefficients of variation between the mouse lines showed that the variation was generally lower in the Del22.ex3 line than in the wasted line.

The second aim of this chapter was to determine whether the age-specific effects on behaviour, namely in the marble burying and open field tests, were due to a lower dosage of eEF1A2 in the brains of aging mice. However, I was unable to achieve this aim due to variable Western blot results which was likely due to the use of small amounts of tissue in combination with the Licor detection method. In hindsight, whole brain may have been a better choice for analysis. However, previous work has shown that eEF1A2 expression levels in heterozygous mice are significantly lower than wild-type levels for all age groups that were tested in this study (Griffiths *et al*., 2012).

There was a high level of variation in behavioural data from the wasted line which seemed to be due to the mixed genetic background. To overcome this, I bred a new *Eef1a2*-null mouse line on a C57BL/6J genetic background. My third aim was to characterise the behavioural phenotype of this line and compare this to the behaviour of mice from the wasted line to determine whether genetic background had any influence on the results. Ideally, I would have also analysed the effects of age on behaviour, however, there was insufficient time to age mice. Therefore, mice were tested at 2-5 months and provided a direct comparison for the cohort of heterozygous wasted mice that were tested at 2-6 months.

In the repetitive behaviour analysis, I found that *Eef1a2*$^{+/-}$ mice showed a significant reduction in repetitive behaviours compared with wild-type mice in the nest building and marble burying assays. This reduction was not observed in the digging or hole-board tests. However, the number of digging bouts and the total time spent digging were very low for both genotypes which would make it incredibly difficult to observe any significant differences. Unlike with the wasted line, the reduction in these behaviours cannot be linked to decreased locomotion as there was no significant difference between genotypes in the total distance travelled in the open field test. Commonly, mouse models with mutations in autism-related genes show an increase in repetitive behaviours compared with wild-type mice (Peñagarikano *et al*., 2011, Reith *et al*., 2013, Kazdoba *et al*., 2014, Kazdoba, Leach and Crawley, 2016). However, in some models, a reduction in repetitive behaviours has been observed. For example, mice with deletion of *Pten* have shown a significant reduction in the number of marbles buried and number of head dips in the hole-board test compared with wild-type mice (Lugo *et al*., 2014). However, this is the opposite phenotype from that which is observed in patients with *EEF1A2* mutations who show an increased repetition of behaviours such as hand twisting and finger sucking (Nakajima *et al*., 2014). Therefore, the implications of this change in repetitive behaviours of *Eef1a2*$^{+/-}$ mice are unclear.

There were no other behavioural changes in *Eef1a2*$^{+/-}$ mice compared with *Eef1a2*$^{+/+}$ mice. The novel object recognition test was attempted to investigate recognition memory, however, this was largely unsuccessful due to the observation that wild-type mice showed a very low preference for the novel object. This made it difficult to conclude any differences between genotypes. One possible reason for this may be that the objects selected were not particularly interesting to the mice. Therefore, using the same ITI with more carefully selected objects may be beneficial. Ideas for objects were given by a paper published in Nature whereby a Lego® tower and a flask filled with sand were used (Leger *et al*., 2013). However, similar objects did not work well in my study. Alternatively, choosing to perform this test in the Y-maze may have affected object exploration as mice are required to make two decisions: the first regarding which arm to enter and the second regarding whether or not to explore the object. A further attempt at this test with different objects performed in the open field box rather than the Y-maze is described in Chapter 5. The open field box was chosen as this apparatus is commonly used to perform the novel object recognition test (Antunes and Biala., 2012, Leger *et al*., 2013).

An important part of this chapter involved comparing behaviour results between the wasted line and the Del22.ex3 line. The behaviour results for both lines are summarised in Table 4.2.

	Wasted line	Del22.ex3 line
Repetitive behaviours	N	Y
Reduced locomotion	Y	N
Hyperactivity	N	N
Anxiety	Y?	N
Sociability	N	N
Social novelty preference	Y	N
Spatial memory	N	N

Table 4.2. Comparison of behaviour results from both mouse lines. *Y = heterozygous mice showed a behavioural change. N = heterozygous mice did not show a behavioural change. The wasted line was on a mixed genetic background comprised predominantly of C57BL/6J, C3H/HeH and HRS/J whereas the Del22.ex3 line was on a pure C57BL/6J genetic background.*

There were several differences in the results from the behavioural tests between the two mouse lines. Firstly, *Eef1a2*$^{+/-}$ mice from the Del22.ex3 line showed a significant reduction in repetitive behaviours compared with *Eef1a2*$^{+/+}$ mice, whereas this difference was not observed in the wasted line. Secondly, *Eef1a2*$^{+/wst}$ mice showed reduced locomotion and increased freezing time in the open field test with age. This effect may have also been observed in the Del22.ex3 line had there been sufficient time to investigate aging. Therefore, this cannot be considered a difference between lines as mice above the age of 5 months were not tested for the Del22.ex3 line. As mentioned, it is unclear whether these result in the open field test for *Eef1a2*$^{+/wst}$ mice indicated a locomotor/motivation deficit or anxiety. Therefore, both of these are declared in Table 4.2.

Interestingly, *Eef1a2*$^{+/wst}$ mice showed a lack of preference for social novelty whereas *Eef1a2*$^{+/-}$ mice showed normal preference for social novelty. This behaviour difference between the two lines may have been due to the change in genetic

background, however, other reasons are also possible. For example, the mice that were used as stranger mice for the wasted line came from the same lineage. Therefore, it may have been more difficult for the test mice to distinguish between the familiar mouse and the novel mouse. Following testing of the wasted line, I became aware that that this test is generally carried out with stranger mice that are unrelated to one another (Emma Wood, personal communication). Therefore, I used unrelated stranger mice to test the Del22.ex3 line. In summary, the difference in the results of this test between the two lines may be due to the change in protocol, rather than the change in genetic background.

However, as mentioned, there was also a difference in repetitive behaviour results between the lines. Therefore, it is likely that the genetic background is having an influence on behaviour. This is certainly not uncommon as genetic background has been shown to have an effect on behaviour in many different studies. In a comparison between C57BL/6J and 129/SvJ mice, the 129/SvJ strain were shown to be more anxious in the open field test and the elevated plus maze (Homanics, Quinlan and Firestone, 1998). Different sub-strains can also show differences in behaviour. C57BL/6J, C57BL/6N and C57BL/6C mice have shown significant differences in several behavioural tests including the open field test, elevated plus maze and a radial arm maze which was used to assess spatial working memory. The differences observed in the open field test included differences in the total distance travelled and the time spent in the centre indicating variation in both locomotor activity and anxiety (Matsuo *et al*., 2010). The behaviour of *Fmr1* knockout mice has also been shown to be affected by genetic background. In a study comparing *Fmr1* knockout mice on a FVB and C57BL/6 genetic background, KO mice on the BL/6 background showed more aggression in a direct social interaction task. KO mice on the FVB background showed higher locomotor activity, whereas, KO mice on the BL/6 background spent more time engaging in repetitive grooming behaviour (Pietropaolo *et al*., 2011). In another study comparing *Fmr1* KO mice on six genetic backgrounds, strain-specific differences were observed in several behaviours including open field locomotion and anxiety, repetitive digging behaviour and social novelty preference. The types of social behaviours displayed in a direct social

interaction test also differed between strains (Spencer *et al*., 2011). Other genetic mouse models have also shown variation in behaviour on different genetic backgrounds. One such study compared the anxiety-related behaviours of serotonin transporter (5-HTT) null mice bred on a C57BL/6 or a 129S6 genetic background. In the light/dark exploration and elevated plus-maze tests, they found that only KO mice on the BL/6 background showed increased anxiety and reduced locomotor activity (Holmes *et al*., 2003). Therefore, it is entirely possible that the behavioural differences I observed between the wasted line and the Del22.ex3 line could be explained by the difference in genetic background.

Female mice were excluded from behavioural testing due to potential variability in results caused by different phases of the oestrus cycle. Previous studies have shown that the behavioural performance of female mice differs significantly across different phases of the oestrus cycle (Meziane *et al*., 2007, Kästner *et al*., 2017). Meziane *et al* (2007) showed that this varies between different background strains, with the performance of BALB/cByJ mice showing oestrus-stage dependent variation in more behavioural tests than C57BL/6J mice. Despite this, it may have been worthwhile to test females in my behavioural assays and compare performance with males. If there had been no difference in performance, scores may have been combined and this would have provided an effective means by which to increase the number of mice tested. It is worth considering testing females in the future as *EEF1A2* mutations affect both males and females (Lam *et al*., 2016).

4.4. Conclusion

The aim of this chapter was to determine the effects of aging on the behaviour of heterozygous *Eef1a2*-null mice and to determine how behaviour changes with genetic background. I managed to identify age-related behavioural changes in two of my behavioural tests, however, perhaps it would have been beneficial to test a larger number of mice. Despite this, moving on to test the Del22.ex3 line was a wise decision as I obtained more robust behavioural results due to the lower variation in data from this line. The behavioural results from the two lines did differ which implies that the change in genetic background had an influence. The evidence presented here suggests that heterozygous *Eef1a2*-null mice display social impairments and changes in repetitive behaviours as seen in other autism models. These mouse models provide a valuable tool to study the effects of loss of protein function, however, future research would benefit from a mouse model with one of the human missense mutations. This is explored in Chapter 5.

Chapter 5: Behavioural characterisation of mice with the D252H *Eef1a2* mutation

5.1. Introduction

5.1.1. The D252H mutation

Two patients have been identified so far with a mutation in *EEF1A2* that changes aspartic acid to histidine at position 252 on the protein (D252H). This mutation is in exon 5 of the gene. Based on the clinical evidence available so far, these patients both present with global developmental delay and microcephaly. One of these is a 12-year old female who has generalised tonic-clonic seizures that started at 8 years old, hypotonia, autism, characteristic facial features and atrophy of the cerebrum. In addition, she is unable to walk and is non-verbal (Nakajima *et al*., 2014). There is no further information available regarding the other case, who is also female and was identified through the DDD study. This is all described in Section 1.3.2 and in Table 1.2.

5.1.2. Generation of the D252H mouse line

Generating a mouse line with one of the eEF1A2 missense mutations would provide invaluable insight into the underlying disease mechanisms. This mouse line would greatly benefit research into whether these mutations lead to loss or gain of protein function.

Following the previously unsuccessful attempt to generate a mouse line with the G70S mutation (Chapter 3), another CRISPR/Cas9 experiment was undertaken to generate a mouse line with the D252H mutation. This mutation was chosen because there is more than one human case and the position of the mutation allowed efficient design of repair templates, being far away from exon/intron boundaries. In addition, the D252H mutation causes autism and global developmental delay, making this a relevant and interesting mutation for the study of behaviour.

The reasons for the selection of the CRISPR/Cas9 method to introduce the mutation are described in Section 3.1.2. The gRNAs and repair templates were designed and

cloned into pSpCas9n(BB)-2A-puro plasmids by Faith Davies. RNA was transcribed by Hemant Bengani and microinjected into single-cell stage mouse embryos by staff at the Evans Transgenic Unit, University of Edinburgh. Unlike with the G70S experiment, I was not involved in the genotyping or monitoring of the mice once they had been born. This was performed by Faith Davies.

5.1.3. Importance of comparing behaviour results between the D252H line and the null lines

In Chapter 4, I studied the effects of loss of eEF1A2 function on mouse behaviour. However, it is essential to compare the results with an *Eef1a2*-missense model due to the possibility that human *EEF1A2* mutations may lead to gain of protein function. Therefore, the behaviour of D252H heterozygous mice may provide a more accurate correlate for the intellectual disability and autistic phenotypes observed in humans. Nevertheless, it is interesting and informative to determine the ways in which behaviour changes with different *Eef1a2* mutations in mice. This allows us to better understand the changes in eEF1A2 protein that can and cannot be tolerated in the brain.

5.1.4. Aims

- **To investigate the effects of the *Eef1a2*/D252H missense mutation on mouse behaviour**

1) To establish a new breeding line of mice with the D252H mutation.

2) To characterise the behavioural phenotype of heterozygous *Eef1a2*/D252H mice (*Eef1a2*$^{D252H/+}$) and compare this with the phenotype of heterozygous null mice.

5.2. Results

5.2.1. Establishing the line

Two founders heterozygous for the D252H mutation were born from the CRISPR/Cas9 experiment (mouse #15 and #16, both male). The phenotypes of these two mice were apparently normal at a gross observational level. I bred both of these mice separately with C57BL/6J female mice to establish two new breeding lines. As the D252H change is a point mutation, genotyping solely by PCR was not an option. Therefore, exon 5 of *Eef1a2* was amplified by PCR and products were digested using the restriction enzyme Hin1II. The D252H allele had one more Hin1II restriction site, therefore, the presence of a D252H allele resulted in a different cut pattern from wild-type upon digest. A genotyping example, which also shows the cut pattern for homozygous mice, is shown in Figure 5.1A. Digest of the wild-type allele produced bands of 300bp and 112bp. Digest of the D252H allele produced bands of 202bp, 128bp and 112bp.

Wild-type and heterozygous mice from the first litter from each founder mating were weighed between P20 and P31. The results of this are shown in Figure 5.1B. Wild-type mice are shown in blue and heterozygous D252H mice are shown in orange. The weights of both litters were comparable and therefore they have been plotted together. Due to the low number of mice for the $Eef1a2^{D252H/+}$ group, statistical analysis could not be performed. However, it is clear that $Eef1a2^{D252H/+}$ mice gained weight between P19 and P30 and this weight gain appeared to be comparable to $Eef1a2^{+/+}$ mice. These results are in contrast to the weight analyses described later in this chapter, likely due to the small number of mice tested here.

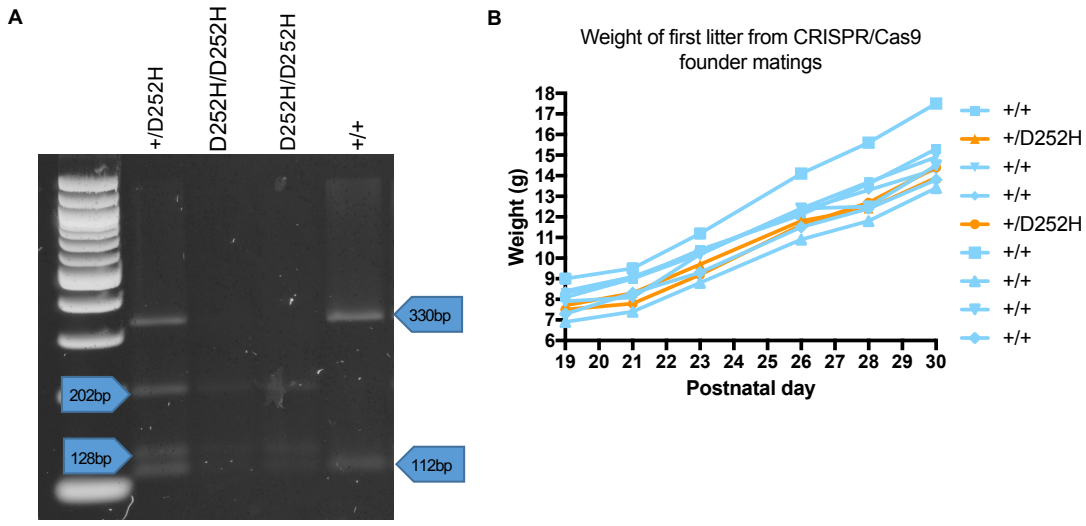

Figure 5.1. Establishing the new Eef1a2/D252H mouse line. ***A.*** *PCR products digested with Hin1II restriction enzyme and ran on a 2% agarose gel with 100bp DNA ladder (NEB) (left). Band sizes are indicated by blue arrows.* ***B.*** *Weights of the F1 generation from P19 to P30.*

5.2.2. The D252H behaviour cohort

The offspring from the two founder breeding pairs along with the offspring from two other wild-type x heterozygote breeding pairs were used for behavioural testing. Therefore, the genotypes used for behavioural testing were *Eef1a2*$^{+/+}$ and *Eef1a2*$^{+/D252H}$. Mice were housed in male only cages of mixed genotypes. All animals were housed in groups to avoid any confounding effects of single housing on behaviour. Female mice were excluded from testing due to the potential for results to vary across different phases of the oestrus cycle. Mice were tested in behavioural assays from 9 weeks (2 months) of age. The age of the mice tested ranged from 2-4 months. Consistent with Chapter 4, data are presented as mean values in the bar graphs and as individual scores for each mouse in the dot plots. The bar graphs allow the means to be observed and compared with ease whilst the dot plots show the spread of data and therefore the variability in scores within genotypes. The background information for each behavioural test has been described in Chapter 4 and all of the tests in this chapter were performed in the same way unless otherwise

stated. Testing was performed with assistance from Charlie Cumber (Honours project student).

5.2.3. *Eef1a2*$^{+/D252H}$ mice showed no evidence of changes in repetitive behaviours compared with *Eef1a2*$^{+/+}$ mice

I tested mice in the nest building assay to detect differences in repetitive behaviours between genotypes. The results are shown in Figure 5.2. There was no statistically significant difference in the percentage of nestlet shredded (Figure 5.2A) or in nest building score (Figure 5.2B) between genotypes, shown using an unpaired t-test for the percentage and a Mann-Whitney test for the score. Therefore, *Eef1a2*$^{+/D252H}$ mice showed no changes in repetitive behaviour in this test.

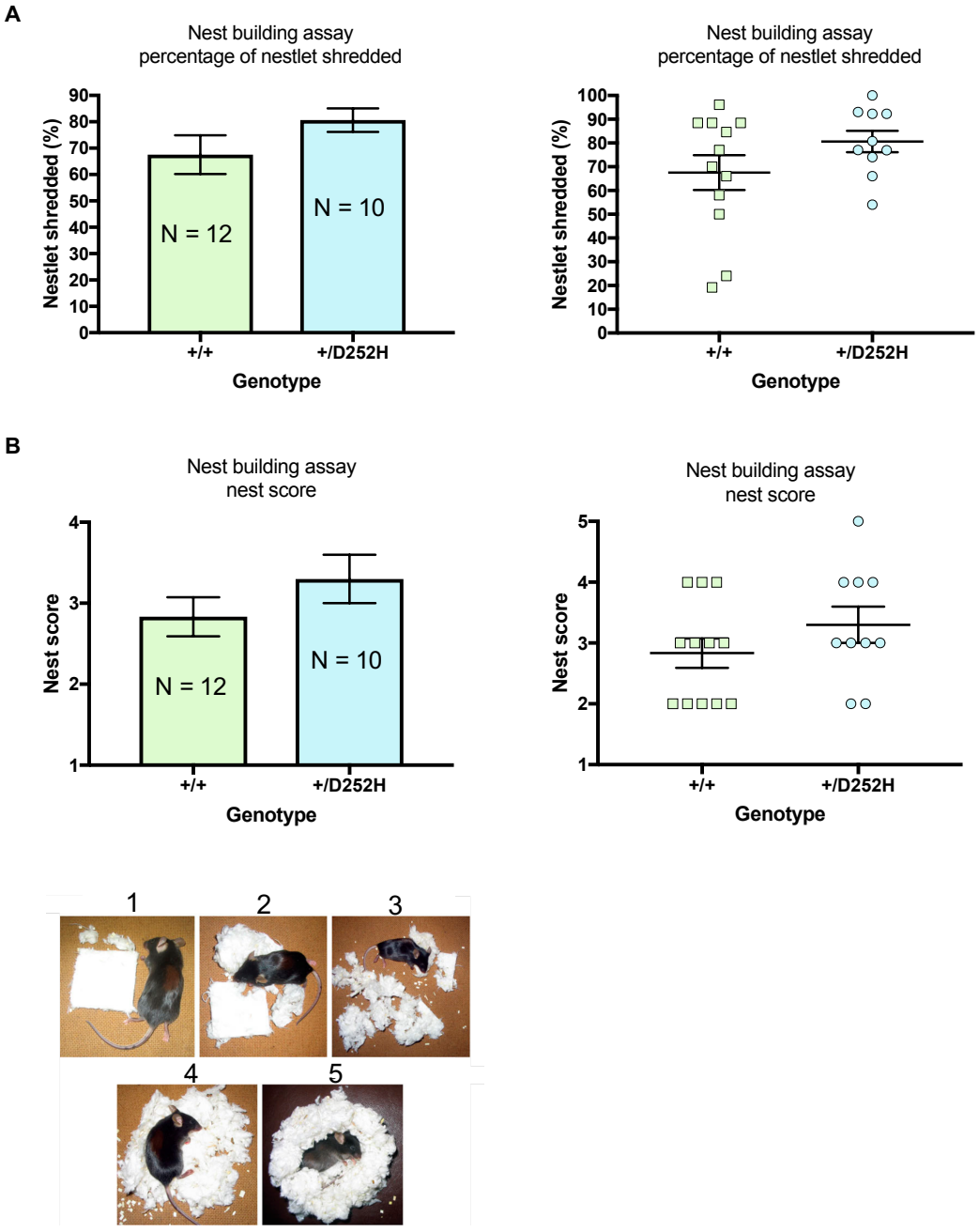

Figure 5.2. Data from Eef1a2$^{+/+}$ and Eef1a2$^{D252H/+}$ mice in the nest building assay. *Error bars for all graphs show SEM.* ***A.*** *Percentage of nestlet shredded. There was no significant difference between genotypes (unpaired t-test).* ***B.*** *Nest score. The scoring criteria used is shown in the images labelled 1-5 (Deacon, 2006a). There was no significant difference between genotypes (Mann-Whitney test).*

To further investigate the effects of the D252H mutation on repetitive behaviours, I assessed the performance of mice in the marble burying assay. The results are shown in Figure 5.3. There was no significant difference in the number of marbles buried between genotypes (unpaired t-test). Although it initially appeared that heterozygous mice buried more marbles, the difference was not statistically significant and the dot plot shows that the data for each genotype was quite variable. Therefore, *Eef1a2*$^{+/D252H}$ mice showed no changes in repetitive digging behaviour in this test.

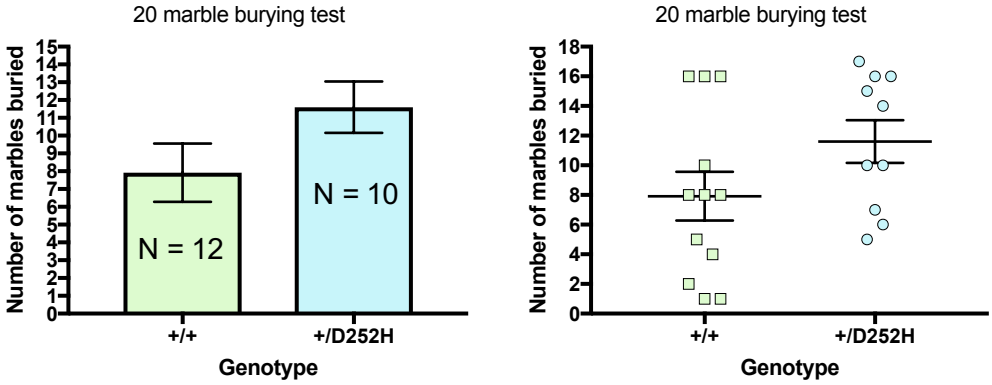

Figure 5.3. Data from Eef1a2$^{+/+}$ and Eef1a2$^{D252H/+}$ mice in the marble burying assay. *The graphs show the number of marbles buried for each genotype. Error bars for all graphs show SEM. There was no significant difference between genotypes (unpaired t-test).*

Following the marble burying test, I performed the digging assay to assess repetitive digging behaviour in *Eef1a2*$^{+/D252H}$ mice further. The results are shown in Figure 5.4. Statistical analysis using unpaired t-tests showed that there were no significant differences in the latency to start digging (Figure 5.4A), the number of digging bouts (Figure 5.4B) or the total digging duration (Figure 5.4C) between genotypes. Therefore, *Eef1a2*$^{+/D252H}$ mice showed no alterations in repetitive digging behaviour.

Both genotypes engaged in very low levels of digging, shown by the high latency to start digging and the low number of digging bouts and total duration of digging. In

addition, the dot plots show that the data for each genotype for all three parameters were quite variable.

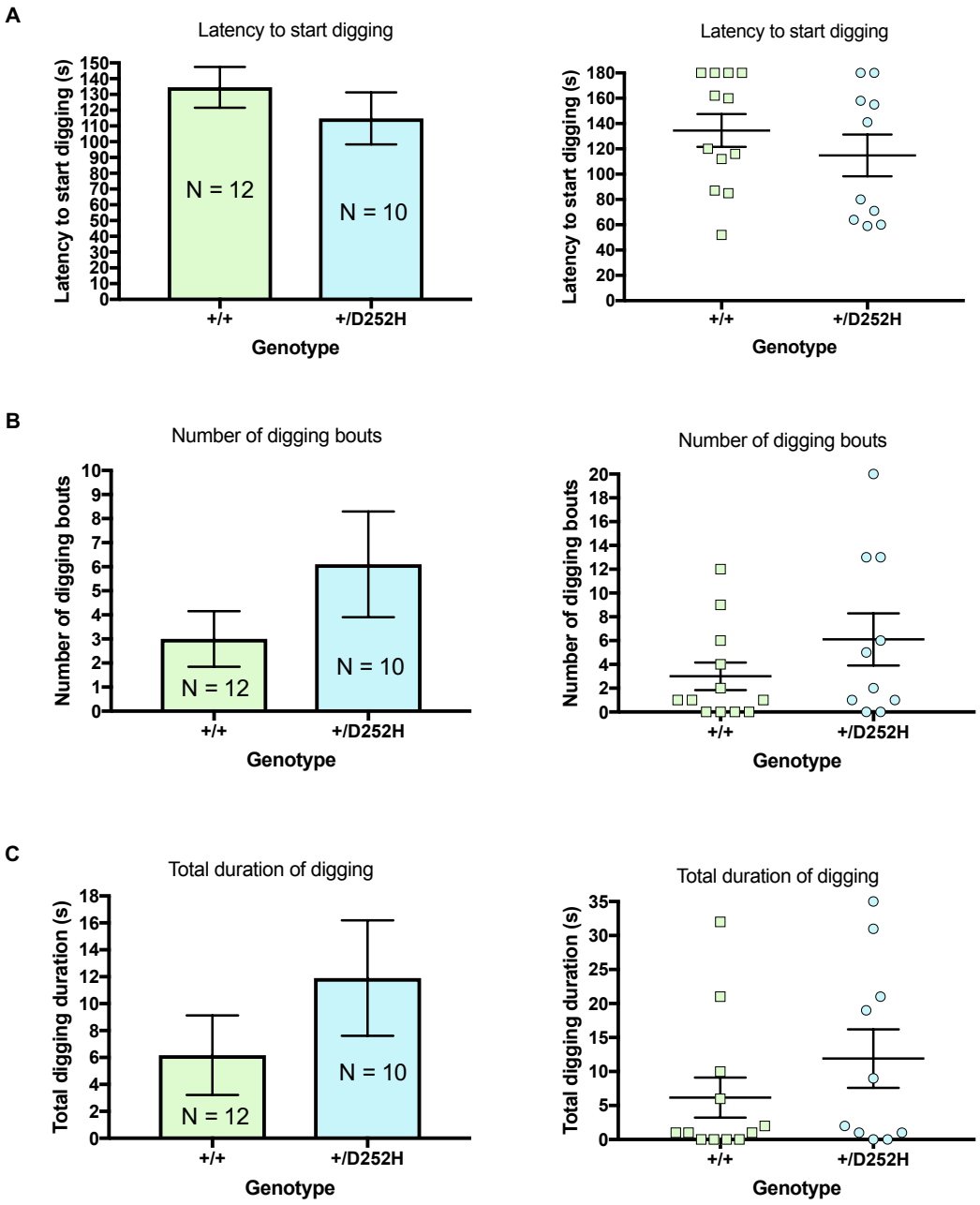

Figure 5.4. Data from Eef1a2$^{+/+}$ and Eef1a2$^{D252H/+}$ mice in the digging assay. *Error bars for all graphs show SEM.* ***A.*** *Latency to start digging. There was no significant difference between genotypes (unpaired t-test).* ***B.*** *Number of digging bouts. There was no significant difference between genotypes (unpaired t-test).* ***C.*** *Total duration of digging. There was no significant difference between genotypes (unpaired t-test).*

As a final test to assess changes in repetitive behaviours, I performed the hole-board test. The results are shown in Figure 5.5. There were no significant differences in the latency to the first head dip (Figure 5.5A), the total number of head dips (Figure 5.5B) or the total number of holes explored (Figure 5.5C) between genotypes. These were determined using unpaired t-tests. The dot plots show that there was a large spread of data for each genotype for all three parameters, although for the total number of head dips the spread of the wild-type data was lower than that for D252H.

Taken together, the results from these four tests suggest that there are no differences in repetitive behaviours between *Eef1a2*$^{+/+}$ and *Eef1a2*$^{+/D252H}$ mice.

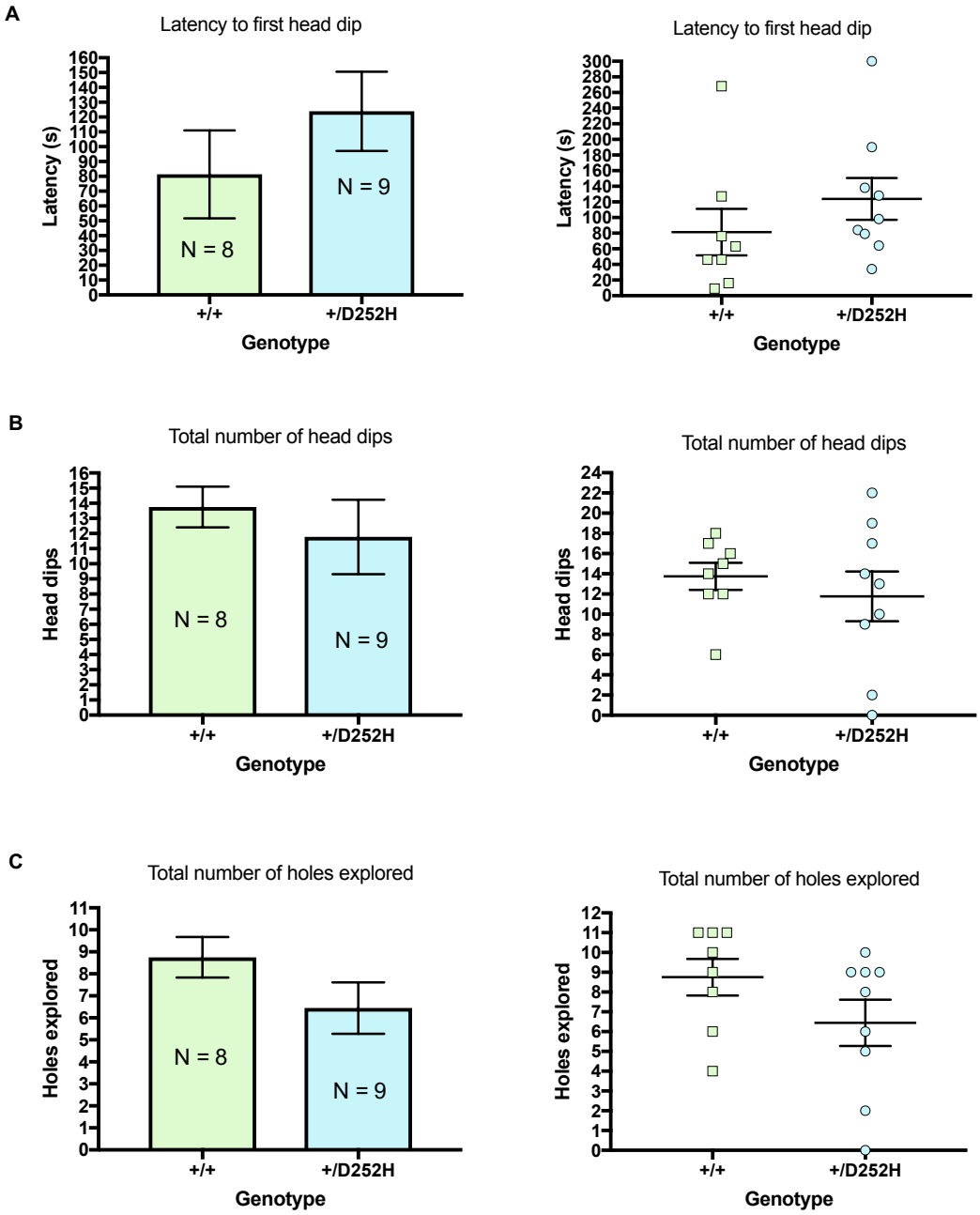

Figure 5.5. Data from Eef1a2$^{+/+}$ and Eef1a2$^{D252H/+}$ mice in the hole-board test. *Error bars for all graphs show SEM.* ***A.*** *Latency to first head dip. There was no significant difference between genotypes (unpaired t-test).* ***B.*** *Total number of head dips. There was no significant difference between genotypes (unpaired t-test).* ***C.*** *Total number of holes explored. There was no significant difference between genotypes (unpaired t-test).*

5.2.4. *Eef1a2*$^{+/D252H}$ mice showed normal sociability and preference for social novelty

I performed the stranger mouse social behaviour test to assess sociability and preference for social novelty in *Eef1a2*$^{+/D252H}$ mice. The results of test 1, which was used to assess sociability, are presented in Figure 5.6. As with the Del22.ex3 line (Chapter 4), the stranger mice used were unrelated to one another.

Data are presented as the time spent exploring the mouse vs the empty cage. Both genotypes spent a significantly larger amount of time exploring the mouse compared with the empty cage, indicating normal sociability. This was shown by a two-way ANOVA with Holm-Sidak's multiple comparisons test. There was no significant difference in the total exploration time between genotypes, shown using an unpaired t-test (data not shown).

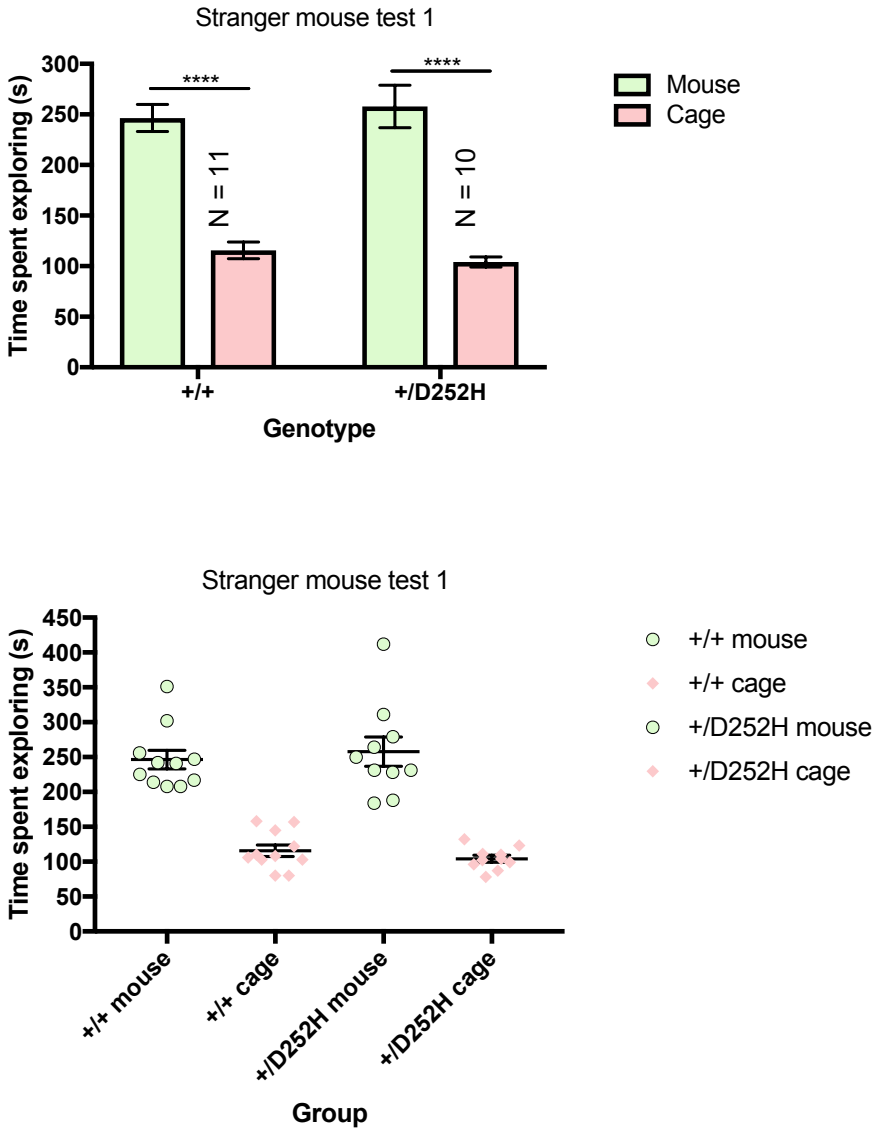

Figure 5.6. Data from Eef1a2$^{+/+}$ and Eef1a2$^{+/D252H}$ mice in the stranger mouse test stage 1. *Error bars for all graphs show SEM. Time spent exploring the mouse vs the empty cage. Asterisks on the bar graph show statistically significant differences. Two-way ANOVA showed significant effect of stimulus (mouse vs cage): F = 116.6, DF = 1, 38, p = <0.0001. Holm-Sidak's multiple comparisons test: from left to right, p = <0.0001, <0.0001.*

I tested *Eef1a2*$^{+/+}$ and *Eef1a2*$^{+/D252H}$ mice in part 2 of the stranger mouse test to assess preference for social novelty. The results for the time spent exploring the novel vs familiar mouse are shown in Figure 5.7.

Both genotypes spent a significantly larger amount of time exploring the novel mouse compared with the familiar mouse, as shown by a two-way ANOVA with Holm-Sidak's multiple comparisons test. In addition, there was no significant difference in the total exploration time between genotypes, shown using an unpaired t-test (data not shown). Therefore, *Eef1a2*$^{+/D252H}$ mice appear to show normal preference for social novelty.

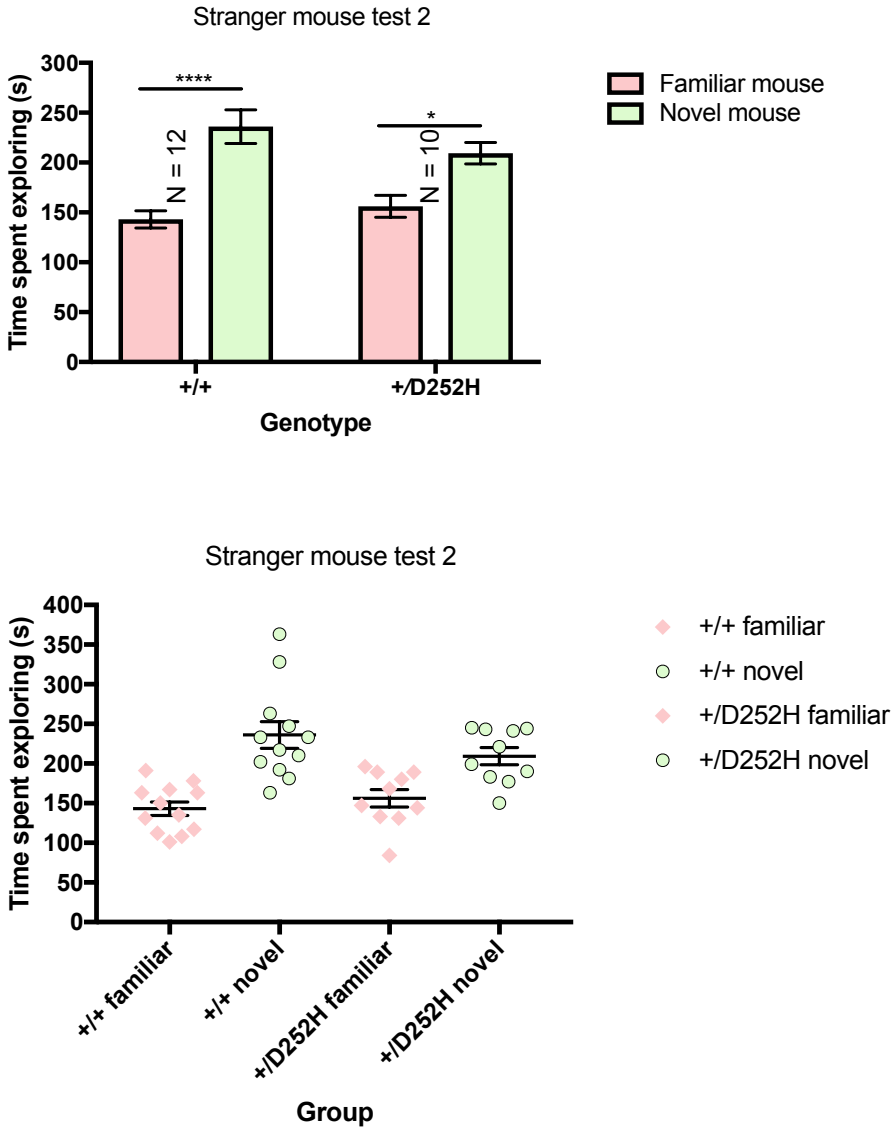

Figure 5.7. Data from Eef1a2$^{+/+}$ and Eef1a2$^{+D252H-}$ mice in the stranger mouse test stage 2. *Error bars for all graphs show SEM. Time spent exploring the familiar mouse vs the novel mouse. Asterisks on the bar graph show statistically significant differences. Two-way ANOVA showed significant effect of stimulus (familiar vs novel mouse): F = 33.66, DF = 1, 40, p = <0.0001. Holm-Sidak's multiple comparisons test: from left to right, p = <0.0001, 0.0201.*

5.2.5. *Eef1a2*$^{+/D252H}$ mice showed no hyperactivity or anxiety phenotypes in the open field test

I assessed the performance of *Eef1a2*$^{+/+}$ and *Eef1a2*$^{+/D252H}$ mice in the open field test to investigate locomotor activity and anxiety. The results are shown in Figure 5.8. There were no significant differences in the total distance travelled (Figure 5.8A), the total time spent freezing (Figure 5.8B) or the time spent in each zone (Figure 5.8C) between genotypes. This was shown using unpaired t-tests for total distance travelled and freezing time and a two-way ANOVA with Tukey's multiple comparisons test for the time spent in each zone. These results indicate that *Eef1a2*$^{+/D252H}$ mice do not show any locomotor or anxiety phenotypes in the open field test. The scores for the total time spent freezing for wild-type mice were quite variable in that two of the mice spent a much higher length of time freezing (25-30s) than the rest of the mice. This resulted in a large SEM error bar on the bar graph and a large difference in mean scores between genotypes, although not significant (+/+ = 9.4, +/D252H = 5.2).

Both genotypes spent a significantly larger amount of time exploring the outside of the arena compared with the centre (two-way ANOVA with Tukey's multiple comparisons test). Therefore, both *Eef1a2*$^{+/+}$ and *Eef1a2*$^{+/D252H}$ mice preferred to spend time in the outside zone.

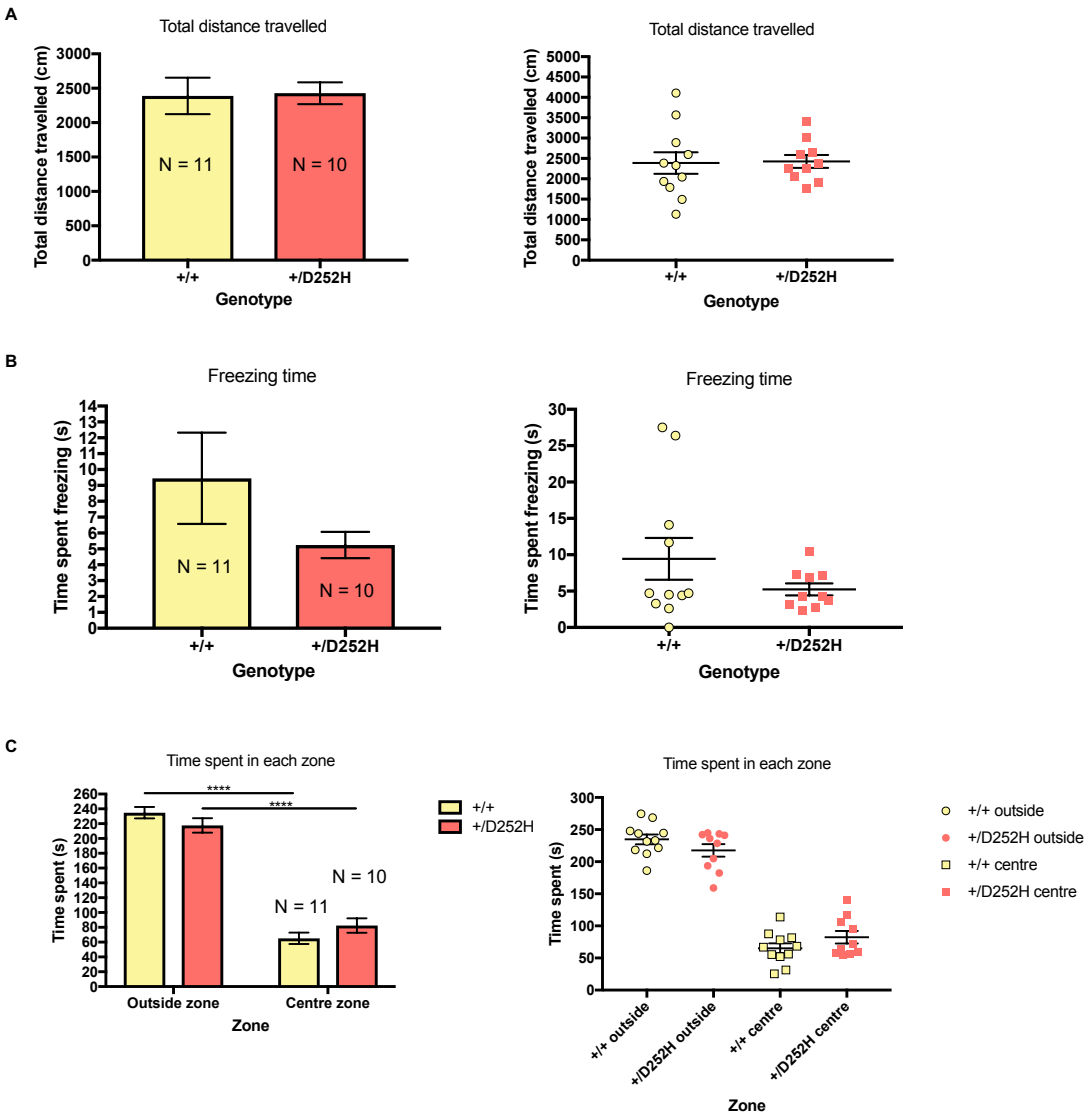

Figure 5.8. Data from Eef1a2$^{+/+}$ and Eef1a2$^{+/D252H}$ mice in the open field test. *Error bars for all graphs show SEM.* ***A.*** *Total distance travelled. There was no significant difference between genotypes (unpaired t-test).* ***B.*** *Total time spent freezing. There was no significant difference between genotypes (unpaired t-test).* ***C.*** *Time spent in outside and centre zone. Asterisks on the bar graph show statistically significant differences. Two-way ANOVA showed significant effect of zone: F = 311.4, DF = 1, 38, p = <0.0001. Tukey's multiple comparisons test: from left to right, p = <0.0001, <0.0001.*

5.2.6. *Eef1a2*$^{+/D252H}$ mice showed normal spatial memory in the Y-maze

I tested *Eef1a2*$^{+/+}$ and *Eef1a2*$^{+/D252H}$ mice in the Y-maze to test spatial memory, a form of memory which is dependent on the hippocampus. Initial testing was performed by following the 15-minute ITI protocol described in Chapter 4. Following this, a different cohort of mice was tested with a longer ITI to assess whether memory for the novel arm was intact after a longer delay. The protocol for this second test was exactly the same except that an ITI of 120 minutes was used. Spatial memory was considered normal when mice were able to remember the familiar arms, indicated by higher exploration of the novel arm. The results of both tests are shown in Figure 5.9.

Figure 5.9A shows the results for the 15-minute ITI test. Both genotypes spent significantly more time exploring the novel arm compared with the familiar arms, shown using a two-way ANOVA with Tukey's multiple comparisons test. This indicates that both *Eef1a2*$^{+/+}$ and *Eef1a2*$^{+/D252H}$ mice show a preference for novelty and normal spatial memory after a short ITI in the Y-maze.

Figure 5.9B shows the results for the 120 minute ITI test. Again, both genotypes spent significantly more time exploring the novel arm compared with the familiar arms, shown using a two-way ANOVA with Tukey's multiple comparisons test. This suggests that *Eef1a2*$^{+/D252H}$ mice also have normal spatial memory after a long ITI, however, other tests of spatial memory should be considered. This is examined in the discussion.

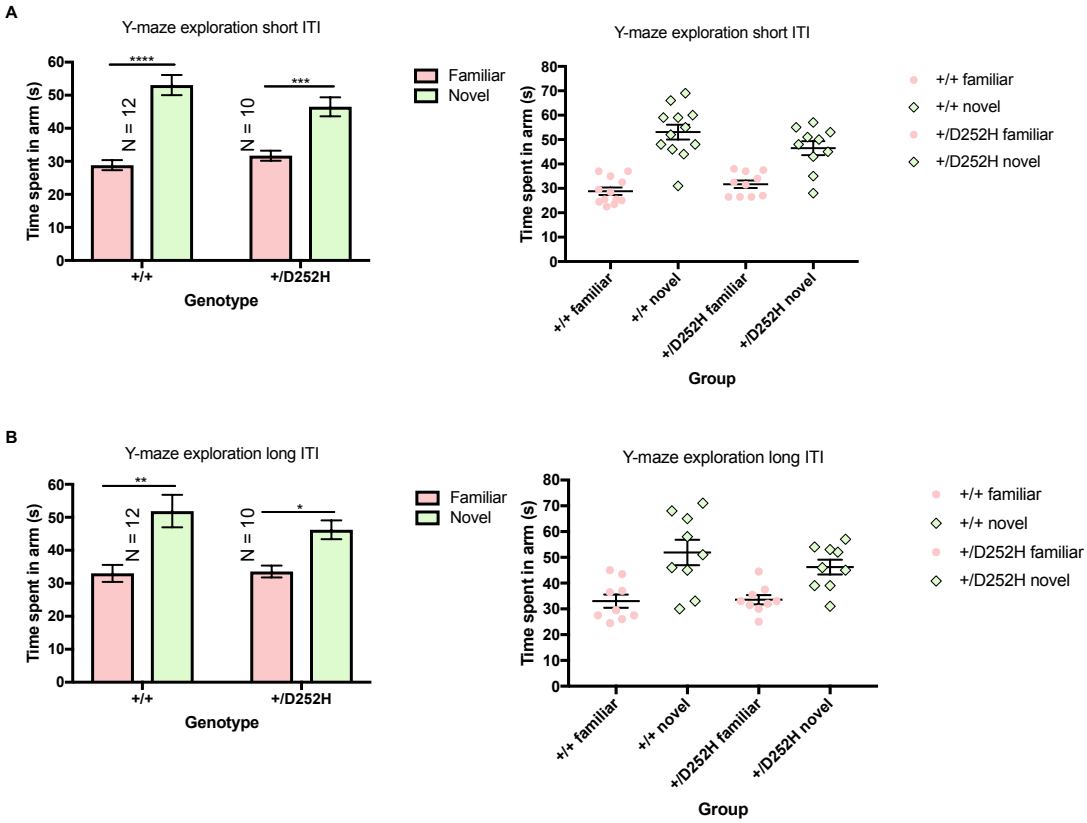

Figure 5.9. Data from Eef1a2$^{+/+}$ and Eef1a2$^{+/D252H}$ mice in the Y-maze test. *Error bars for all graphs show SEM. Familiar = mean of 'start' and 'other' arm.* ***A.*** *15 minute ITI.. Data presented as mean time spent exploring Y-maze arms in the bar graph. Asterisks on the bar graph show statistically significant differences. Two-way ANOVA showed significant effect of arm (familiar vs novel): F = 66.98, DF = 1,40, p = <0.0001. Tukey's multiple comparisons test: from left to right p = <0.0001, 0.0008.* ***B.*** *120 minute ITI. Data presented as mean time spent exploring Y-maze arms in the bar graph. Asterisks on the bar graph show statistically significant differences. Two-way ANOVA showed significant effect of arm (familiar vs novel): F = 23.47, DF = 1, 32, p = <0.0001. Tukey's multiple comparisons test: from left to right p = 0.0014, 0.0456.*

5.2.7. Optimisation of the novel object recognition test was unsuccessful

Following the results of the novel object recognition tests described in Chapter 4 (Section 4.2.2.7) there was a requirement for optimisation. I repeated the test with new sets of objects in the open field box rather than in the Y-maze. The open field box was chosen to perform the novel object recognition test as this apparatus is commonly used for this assay (Antunes and Biala, 2012, Leger *et al*., 2013). The use of this apparatus removed the requirement for mice to select both an arm and an object to explore and ensured that both objects were visible to the mice at all times.

The first attempt at this test involved habituating the mice to the empty open field box for 5 minutes on the 2 days preceding the test. This was followed by a sample phase lasting 5 minutes, a 5-minute ITI and a choice phase lasting 2 minutes. However, the total exploration time for each mouse was very low and the mice were deemed to be very anxious due to the high level of freezing behaviour (data not shown). It was suspected that mice may have been anxious due to the habituation being too short, therefore, the test was repeated with a longer habituation. Mice were habituated to the empty open field box for two 5 minute sessions on the 3 days preceding the test as performed by Leger *et al*., 2013. The results are shown in Figure 5.10A. Coloured pet toys were used as objects as performed by (Deshmukh and Knierim, 2011). The exploration of the familiar object and novel object and the total exploration time in the choice phase is shown for each mouse. The highest total exploration time was 16 seconds which is very low despite the longer habituation. Due to this, it was suspected that the 2-minute choice phase may have been too short. Therefore, the test was repeated with a 5-minute choice phase (Figure 5.10B). A tower and a rocket made from Lego® were used as objects. There was a large improvement in the choice phase exploration time, with a mean of 66 seconds for wild-type and 73 seconds for +/D252H. However, wild-type mice did not show a preference for the novel object, shown by a mean DR below 0. The sample phase exploration time was then analysed to ensure that this was sufficient to allow mice to recognise the novel object. The exploration in the sample phase was low, with a

mean of 48 for wild-type and 33 for +/D252H. Therefore, the ability of the mice to recognise a new object was likely impaired by inadequate learning in the sample phase. In the next attempt, the test was repeated in exactly the same way as in Figure 5.10B but with different objects (Figure 5.10C). In this attempt, Disney® figurines were used as objects. Again, the choice phase exploration time was higher than that of the 2-minute trial (A), with a mean of 37 seconds for wild-type and 48 seconds for +/D252H. However, this was lower than that of the previous trial (B). The exploration in the sample phase was also lower than the previous trial with a mean of 19 for wild-type and 22 for +/D252H. Therefore, the objects appeared to be less interesting to the mice. Unfortunately, as with the previous trial, wild-type mice did not show a preference for the novel object as the mean discrimination ratio was again below 0. As with attempt B, this points towards insufficient learning in the sample phase as a possible explanation for lack of preference for the novel object.

At this point, there was insufficient time to continue optimising this test. A summary table of the above attempts is shown in Figure 5.10D.

A

+/+			+/D252H		
Familiar	Novel	Total	Familiar	Novel	Total
4	12	16	6	1	7
9	5	14	8	8	16
4	6	10	3	3	6
4	6	10	2	4	6
4	8	12	6	6	12
12	4	16	5	4	9
2	7	9	3	7	10
8	1	9	1	3	4
			7	2	9

B

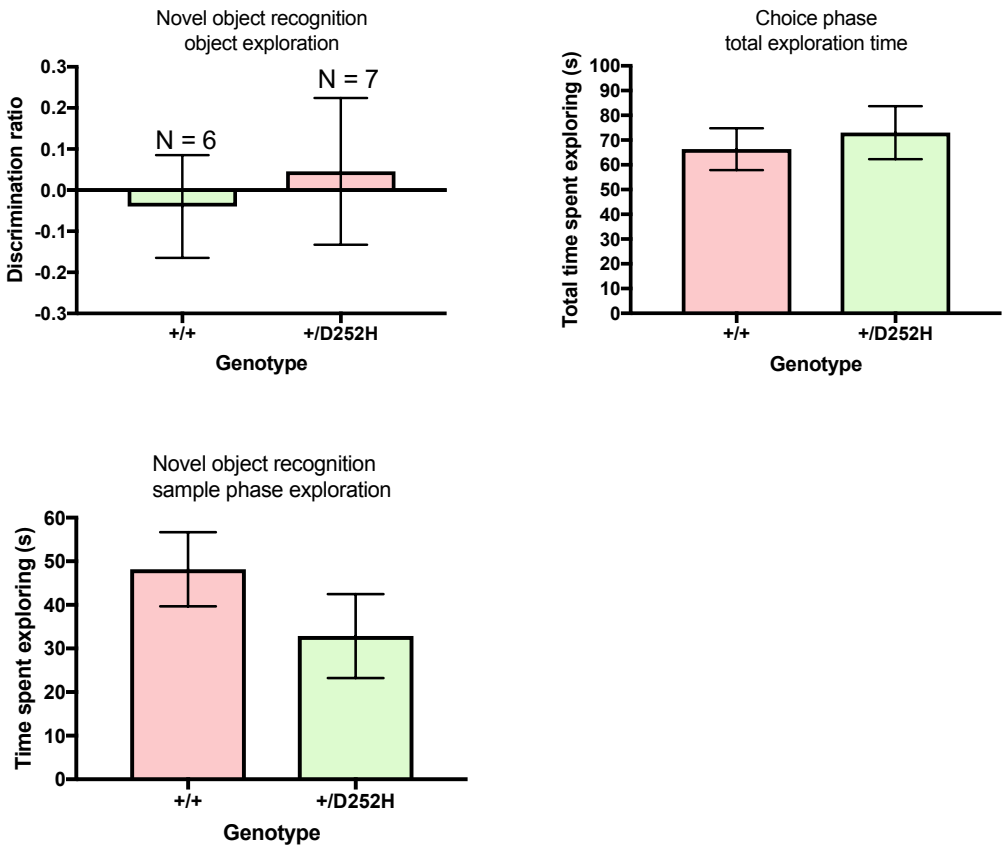

C

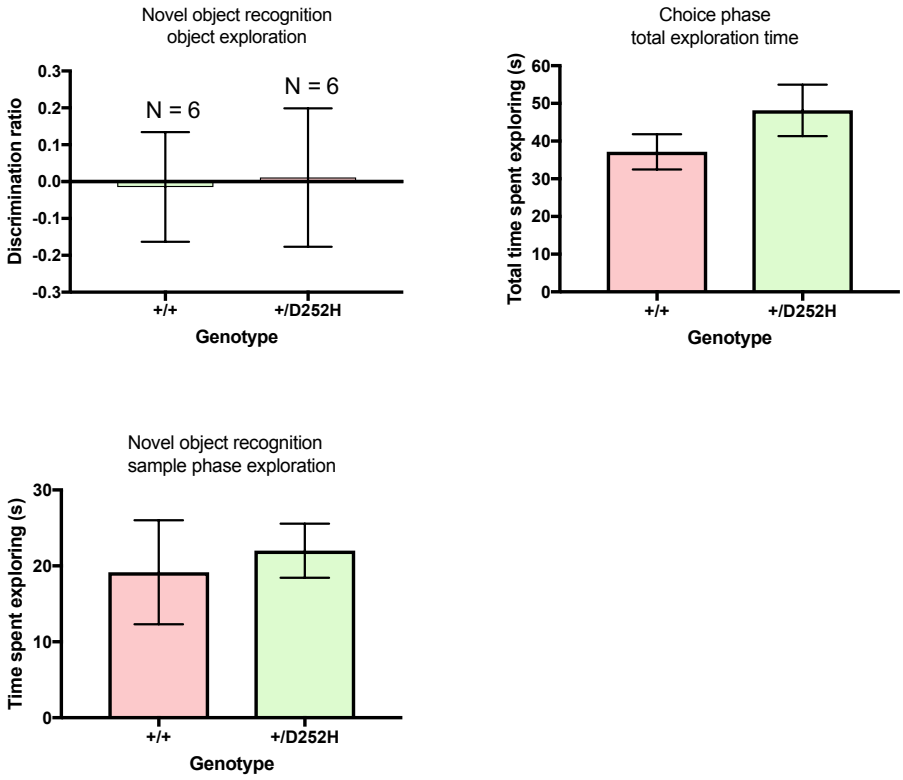

D

	ITI length	Trial length	Habituation length	Problems
Attempt 1 (not shown)	5 minutes	2 minutes	1 x 5 min for 2 days	No/little exploration, mice anxious
Attempt 2 (A)	5 minutes	2 minutes	2 x 5 min for 3 days	Low exploration
Attempt 3 (B)	5 minutes	5 minutes	2 x 5 min for 3 days	Wild-type show no preference for novel object
Attempt 4 (C)	5 minutes	5 minutes	2 x 5 min for 3 days	Wild-type show no preference for novel object

Figure 5.10. Steps taken to optimise the novel object recognition test in the open field box. *Error bars for all graphs show SEM.* ***A.*** *Table showing the results of attempt 2. Each row represents scores from an individual mouse. Mice highlighted in red had a total exploration time of less than 10 seconds. N = 8 +/+, 9 +/D252H.* ***B.*** *Attempt 3. There was no significant difference in the DR, sample phase exploration time or choice phase exploration time between genotypes (unpaired t-tests).* ***C.*** *Attempt 4. There was no significant difference in the DR, sample phase exploration time or choice phase exploration time between genotypes (unpaired t-tests).* ***D.*** *Summary table of each attempt.*

5.2.8. Body weight of *Eef1a2*$^{+/D252H}$ mice significantly lower than that of *Eef1a2*$^{+/+}$ mice

Eef1a2$^{+/D252H}$ and *Eef1a2*$^{+/+}$ mice were weighed and grip strength tested at 4 months of age. This was performed to determine whether *Eef1a2*$^{+/D252H}$ mice are able to gain weight normally and in order to assess muscle strength. This is important due to the fact that homozygous *Eef1a2*-null mice have a well studied skeletal muscle atrophy phenotype, characterised by weight loss and reduced performance in the grip strength test (Newbery *et al*., 2005, Griffiths *et al*., 2012). The effects of the heterozygous D252H mutation on skeletal muscle function are unknown, however, the skeletal muscle function of heterozygous null mice is completely normal (Griffiths *et al*., 2012) (Section 4.2.2.8). Comparing weight profiles and skeletal muscle function between mouse lines will help us to determine whether the missense mutations result in loss or gain of protein function.

The result of the weight analysis is shown in Figure 5.11A. The weight of *Eef1a2*$^{+/D252H}$ mice was significantly lower than that of *Eef1a2*$^{+/+}$ mice, shown using an unpaired t-test. However, the difference in weight was very small, with a mean of 29.9 for wild-type and 27.9 for heterozygote resulting in a difference of 2g. The results of the grip strength tests are shown in Figure 5.11B and C. These were performed as described for the Del22.ex3 line (Section 4.2.2.8). There were no significant differences in the grip strength of front limbs (B) or all four limbs (C) between genotypes (unpaired t-tests). Therefore, adult *Eef1a2*$^{+/D252H}$ mice have normal muscle strength but weigh less than wild-type mice.

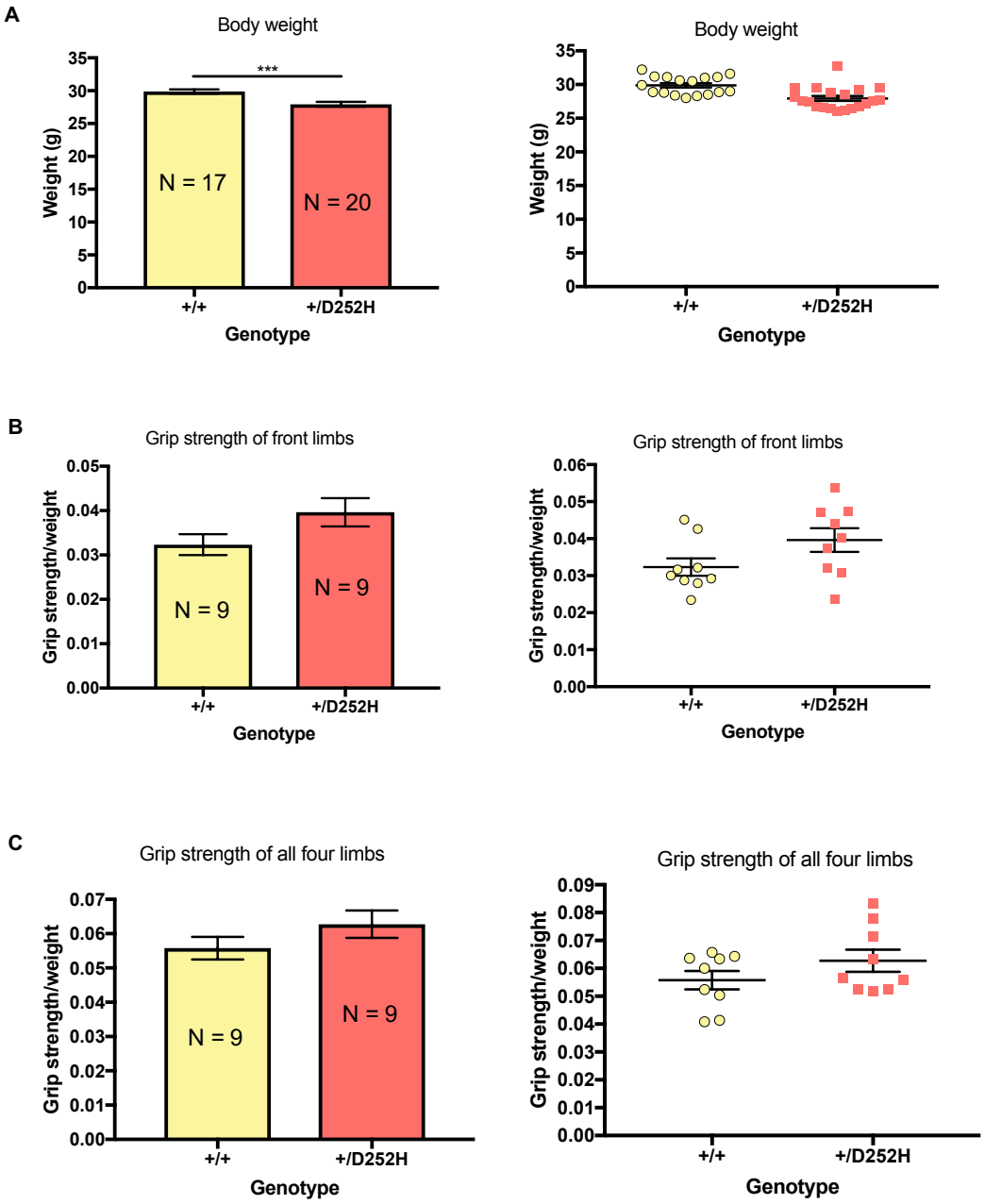

Figure 5.11. Body weight and limb grip strength data from Eef1a2$^{+/+}$ and Eef1a2$^{+/D252H}$ mice at 4 months. *Error bars for all graphs show SEM.* ***A.*** *Body weight. Asterisks on the bar graph show a statistically significant difference. Unpaired t-test: t = 3.91, DF = 35, p = 0.0004.* ***B.*** *Front (fore) limb grip strength (Newtons) normalised to body weight (grams). There was no significant difference between genotypes (unpaired t-test).* ***C.*** *All four limb grip strength (Newtons) normalised to body weight (grams). There was no significant difference between genotypes (unpaired t-test).*

5.2.9. *Eef1a2*$^{D252H/D252H}$ mice showed evidence suggestive of excessive grooming behaviour

A repetitive behaviour which is commonly reported to be excessive in autism models is self-grooming (Silverman *et al*., 2010). Mice with mutations in genes including *Cntnap2*, *Shank2/3* and *Fmr1* have been shown to engage in high levels of grooming behaviour compared with wild-type mice (Pietropaolo *et al*., 2011, Peñagaricano *et al*., 2011, Kazdoba, Leach and Crawley, 2016). A common phenotype which is indicative of increased grooming in mice is the loss of fur.

On collection of tissue from three homozygous D252H mice (*Eef1a2*$^{D252H/D252H}$) for expression analysis at P24, I observed loss of fur on the neck. An example is shown in the image in Figure 5.12A with a wild-type mouse for comparison. Tissue was also collected from heterozygous D252H mice at 4 months of age post-behaviour. Images were taken of these mice as a comparison for the homozygotes. An example is shown in the image in Figure 5.12B with a wild-type mouse for comparison. There was no evidence of fur loss for *Eef1a2*$^{+/D252H}$ mice at 4 months of age. This data highlights the possibility that *Eef1a2*$^{D252H/D252H}$ mice may be engaging in excessive grooming behaviour, however, this must be assessed by observing and analysing various grooming parameters and comparing this with wild-type mice. In addition, it would be interesting to observe whether there is a difference in grooming behaviour between *Eef1a2*$^{+/D252H}$ and *Eef1a2*$^{D252H/D252H}$ mice as the images suggest that this is possible.

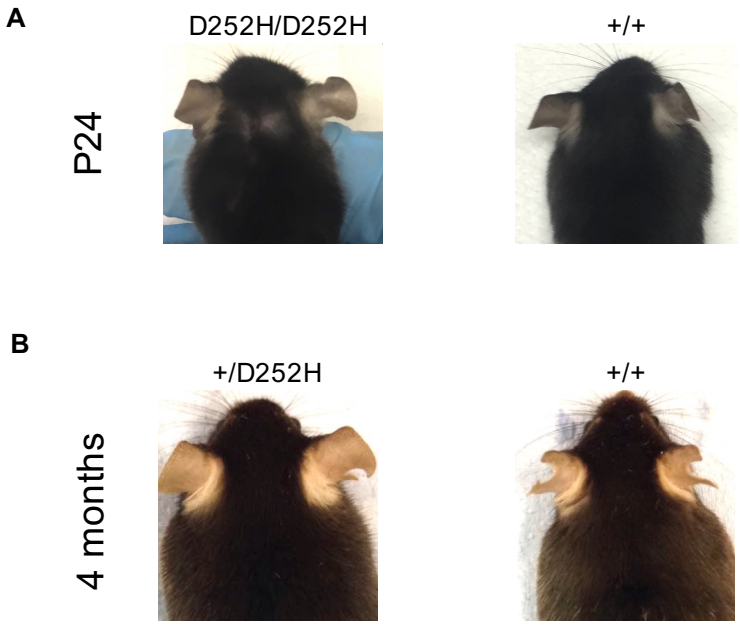

Figure 5.12. Images of mice from the D252H line showing evidence of fur loss. A. *A homozygous mouse at P24 (left) and an age-matched wild-type mouse (right).* ***B.*** *A heterozygous mouse at 4 months (left) and an age-matched wild-type mouse (right).*

5.2.10. Protein and RNA expression analysis showed that the D252H eEF1A2 protein is unstable

As a mouse line with a D252H mutation in *Eef1a2* has never before been made or characterised, it was unknown whether D252H eEF1A2 is expressed and how the expression levels compare to wild-type mice. It is important to determine whether D252H eEF1A2 protein is expressed to better understand whether the mutation leads to loss or gain of protein function. If the protein is not expressed, this indicates that the disease phenotype is as a result of loss of protein function. However, If the protein is expressed, both loss and gain of function remain possible. It was hypothesised that D252H eEF1A2 would be expressed at the protein level as this was found to be the case for G70S eEF1A2 (Section 3.2.5). It is important to determine the level of expression to assess the stability of the protein. For example, homozygous and/or heterozygous D252H mice may express eEF1A2 at the same level as wild-type mice, or the level may be significantly lower. This may be either due to a lower level of synthesis of the mutant protein or due to degradation if the protein is unstable.

I analysed eEF1A2 expression in the brains of wild-type, heterozygous and homozygous littermates at P24 and in wild-type and heterozygous littermates from my behaviour cohort at 4 months. These are the mice mentioned in Section 5.2.9. Brain tissue was collected from the mice and RNA and protein were extracted. Protein lysates were run on a Western blot with antibodies specific to eEF1A2 and GAPDH as a loading control. Note that prior to running the qPCR for RNA expression analysis, samples were amplified by RT-PCR and run on an agarose gel with appropriate controls (see Section 2.5.4) to ensure that there was no contamination. An image of the gel is shown in Appendix A.

The Western blot for the mice at P24 is shown in Figure 5.13A with eEF1A2 shown in red and GAPDH in green. Three samples per genotype were used for analysis. The presence of eEF1A2-specific bands in the *Eef1a2*$^{D252H/D252H}$ samples showed that D252H eEF1A2 was being expressed. The quantification results are shown in the bar graph below the blot, showing that eEF1A2 expression was significantly lower in the

brains of *Eef1a2*$^{D252H/D252H}$ mice compared with *Eef1a2*$^{+/+}$ mice. This was shown using a one-way ANOVA with Tukey's multiple comparisons test. To check whether the lower levels were reflected at the transcriptional level, RNA expression was quantified by qPCR. The results of this analysis are shown in the second bar graph in Figure 5.13A. There was no significant difference in RNA expression between genotypes (one-way ANOVA). These results suggest that the levels of eEF1A2 expression are equal in the brains of *Eef1a2*$^{+/+}$ and *Eef1a2*$^{D252H/D252H}$ mice at the RNA level and that the lower protein level seen is the result of decreased stability of the D252H protein.

As mentioned, expression was also analysed in twelve randomly selected mice from the behaviour cohort (six per genotype). The results are shown in Figure 5.13B with eEF1A2 shown in red and GAPDH in green on the Western blot. The quantified protein expression shown in the bar graph indicates that eEF1A2 expression was significantly lower in the brains of *Eef1a2*$^{+/D252H}$ mice compared with *Eef1a2*$^{+/+}$ mice (unpaired t-test). Subsequently, RNA expression was quantified by qPCR to assess eEF1A2 transcription. The results are shown in the second bar graph in Figure 5.13B. There was no significant difference in RNA expression levels between *Eef1a2*$^{+/D252H}$ and *Eef1a2*$^{+/+}$ mice (unpaired t-test). As with the homozygotes at P24, these results suggest that in the brains of heterozygous mice from the behaviour cohort, eEF1A2 protein is unstable. In contrast, a significant reduction in eEF1A2 protein expression was not observed for *Eef1a2*$^{+/D252H}$ mice at P24 (A), however, analysing a greater number of mice would be beneficial here.

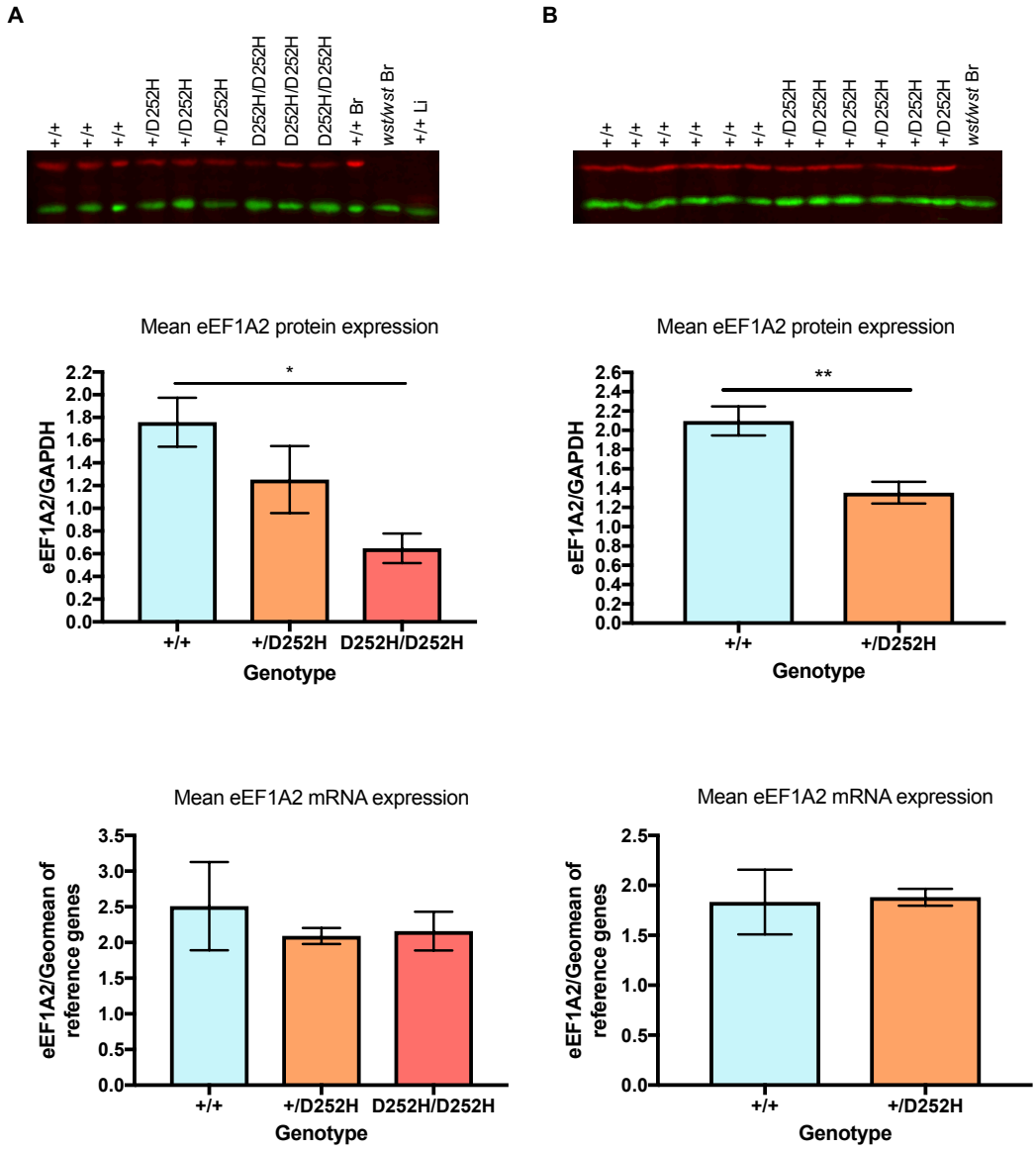

Figure 5.13. eEF1A2 RNA and protein expression in the brains of D252H mice. *Blots were imaged using the Licor Odyssey FC with eEF1A2 in red (concentration = 1:1000) and GAPDH in green (concentration = 1:2000) and quantified using Image Studio Lite version 4.0. +/+ Br = wild-type brain positive control, wst/wst Br = wasted brain negative control, +/+ Li = wild-type liver negative control.* ***A.*** *RNA and protein expression in mice at P24. The asterisk on the top bar graph shows a statistically significant difference. One-way ANOVA F = 6.18, DF = 2, 6, p = 0.0349. Tukey's multiple comparisons test, p = 0.0293.* ***B.*** *RNA and protein expression in mice at 4 months post-behaviour. The asterisk on the top bar graph shows a statistically significant difference. Unpaired t-test, t = 3.97, DF = 8, p = 0.0041.*

5.3. Discussion

The aims of this chapter were as follows:

1) To establish a new breeding line of mice with the D252H mutation.

2) To characterise the behavioural phenotype of *Eef1a2*$^{D252H/+}$ mice and compare this with the phenotype of heterozygous null mice.

I successfully established two new breeding lines of *Eef1a2*/D252H mice using the two *Eef1a2*$^{D252H/+}$ founders from the CRISPR/Cas9 experiment. These two founders were phenotypically normal at a gross observational level and were able to breed normally, making it easy to establish the lines. The *Eef1a2*/D252H mice will provide an invaluable opportunity to study the effects of eEF1A2 missense mutations on both protein function at the cellular and tissue level and phenotype at the whole organism level. Comparing the phenotypes of null mice and D252H mice will provide insight into whether the missense mutations lead to loss or gain of protein function.

I used a mixture of mice bred from both founders for my behavioural experiments. This was necessary as this set of experiments was performed at the end of my project and therefore it was vital to breed a large enough number of mice in a short space of time. The presence or absence of off-target mutations has not been assessed in these lines and therefore it is possible that one or both may have other mutations that could confound results. In the future, both lines should be analysed for off-target effects and phenotypically compared but this was not in the scope of my project. Ideally, it would have been useful to compare behaviour results of mice bred from each founder, however, there were not enough mice to perform this analysis. It is, however, worth noting that off-target mutations are unlikely to be on the same chromosome as *Eef1a2* and therefore would segregate away from the D252H mutation.

In contrast to the situation observed in humans, the behaviour of mice that were heterozygous for the D252H missense mutation was normal. These mice showed no evidence of changes in repetitive behaviours, normal sociability and preference for social novelty, no hyperactivity, no increase in anxiety and no evidence of

hippocampal memory deficits. These are the results of the tests that were implemented, however, there are other tests that have not been considered. These are discussed throughout this section.

It is interesting that mice with heterozygous null mutations in *Eef1a2* showed changes in behaviour (Chapter 4) while mice with a D252H missense mutation did not. The normal behaviour phenotype of *Eef1a2*$^{+/D252H}$ mice is inconsistent with the autism and intellectual disability phenotypes observed in patients with D252H *EEF1A2* mutations. This indicates that *Eef1a2* missense mutations are better tolerated in mice than in humans and points to a mouse-human difference in pathology. My behaviour results suggest that, in mice, *Eef1a2* missense mutations are tolerated better than *Eef1a2* null mutations.

Further analysis of hippocampal spatial memory was of interest because mice with mutations in genes known to cause autism and intellectual disability in humans have shown hippocampal memory deficits. For example, mice with mutations in *Fmr1, Tsc1/2* and *Cntnap2* show impairments in the Morris water maze with *Fmr1* and *Tsc1/2* mutants also showing deficits in contextual fear conditioning tests (Goorden *et al*., 2007, Peñagaricano *et al*., 2011, Kirschstein, 2012, Kazdoba *et al*., 2014). The results of the Y-maze test provided insight into the hippocampal memory of *Eef1a2*$^{+/D252H}$ mice, however, further testing is required to determine whether hippocampal memory is completely normal. In line with the mouse models described above, it would be beneficial to test *Eef1a2*$^{+/D252H}$ mice in the Morris water maze and in hippocampal-dependent contextual fear conditioning tests to determine whether there are similar phenotypes. This is an interesting avenue for future investigation.

Unfortunately, I was unable to resolve the problems associated with the novel object recognition test due to lack of sufficient time. The trials described in this chapter were performed with a very short ITI of 5 minutes to ensure that wild-type mice were able to remember the familiar objects. Despite this, wild-type mice showed no preference for the novel object in any of the attempts. An increase in habituation and choice phase length did not improve the results, nor did any change of objects.

Perhaps a longer sample phase would have been necessary to improve familiarisation with the objects and increase exploration of the novel object in the choice phase as exploration in the sample phase was very low. In addition, the use of a smaller arena might have encouraged mice to explore the objects. Furthermore, the possibility that there was an unforeseen stressor in the test room affecting performance cannot be ruled out. This might have included sub-optimal temperature and/or lighting, environmental noise or odours.

As alluded to in section 4.3, it may have been worthwhile to test females as well as males in the behavioural assays. If there had been no difference in performance between males and females, scores may have been combined. This would have increased the number of mice tested, making results more robust.

I observed loss of fur on the neck of three homozygous D252H mice at P24 but not any of the six heterozygous D252H mice at 4 months whilst collecting tissue. This suggests that *Eef1a2*$^{D252H/D252H}$ mice might engage in excessive grooming behaviour although other causes, such as fighting, must not be overlooked. To assess grooming, behaviour should be observed and scored. Assessment should be carried out by spraying mice with a fine mist to induce the behaviour, placing in a cage and recording for a set period of time. Different types of grooming can be scored, including nose/face grooming, head and neck washing, body grooming and tail/genital grooming which can involve a combination of scratching and licking. Measurements such as the latency to start grooming, the total duration of grooming, the number of grooming bouts and the pattern of grooming should be taken and compared with wild-type mice (Kalueff *et al*., 2007). Age matched *Eef1a2*$^{D252H/D252H}$ and *Eef1a2*$^{+/D252H}$ mice at around P24 should also be compared to assess any differences between homozygotes and heterozygotes. It would also be interesting to assess older heterozygotes, at 4 months and above, to determine whether there are any changes in grooming behaviour with age.

I found that male *Eef1a2*$^{+/D252H}$ mice weighed significantly less than male *Eef1a2*$^{+/+}$ mice, with a small but robust difference of 2g at 4 months of age. In addition, recent

data from our laboratory showed that mixed male and female *Eef1a2*$^{+/D252H}$ mice weighed significantly less than their *Eef1a2*$^{+/+}$ littermates between P14 and P24 (unpublished data). One possible reason for reduced weight may be due to a potentially altered metabolism in *Eef1a2*$^{+/D252H}$ mice. In a study of mice null for the *Kcnma1* BK potassium channel, male KO mice weighed significantly less than their wild-type littermates between 7 and 18 weeks postnatal. Measurement of body composition by quantitative magnetic resonance revealed that KO mice had a higher fat and water composition that their wild-type littermates, indicating differences in metabolism (Halm *et al*., 2017). Other possibilities include a reduced appetite of *Eef1a2*$^{+/D252H}$ mice or heightened stress levels which may be the cause of a reduced appetite or could result in weight loss. It is possible that reduced weight could occur as a result of altered function of the hypothalamic-pituitary-adrenal (HPA) axis and therefore it would be interesting to study the role of eEF1A2 in the hypothalamus. As a next step, it will be important to monitor weight gain weekly, ideally up to 18 weeks as performed by Halm *et al*., 2017, to determine whether this weight difference is present continuously throughout postnatal development in both male and female mice.

eEF1A2 protein expression was significantly lower in the brains of *Eef1a2*$^{D252H/D252H}$ mice at P24 and *Eef1a2*$^{+/D252H}$ mice at 4 months compared with their wild-type littermates. As there was no difference in expression at the RNA level, this suggests that the D252H protein is unstable and is susceptible to degradation as a result. At P24, there was no significant difference in eEF1A2 expression between *Eef1a2*$^{+/+}$ and *Eef1a2*$^{+/D252H}$ mice, although expression in *Eef1a2*$^{+/D252H}$ mice was slightly lower. As it is known than eEF1A2 can homodimerise, this introduces the possibility that wild-type eEF1A2 is able to stabilise mutant eEF1A2 in the heterozygote (Bunai *et al*., 2006). Since there is no wild-type eEF1A2 protein in *Eef1a2*$^{D252H/D252H}$ brain, the protein is unable to be stabilised resulting in degradation and significantly lower expression levels. However, as mentioned, expression in the brains of *Eef1a2*$^{+/D252H}$ mice was significantly lower than *Eef1a2*$^{+/+}$ mice at 4 months in the behaviour cohort. This result argues against the hypothesis that wild-type eEF1A2 stabilises mutant eEF1A2 in heterozygous mice. There were two main differences between the

Eef1a2$^{+/D252H}$ mice at P24 and at 4 months: age and the fact that the 4-month cohort had been through behavioural testing. Either of these may have affected protein expression but the specific reason for the difference in expression at P24 and 4 months is currently unclear.

These experiments have provided insight into the effects of missense mutations on eEF1A2 function, with a particular focus on behaviour. Future experimentation on this mouse line will be hugely beneficial in improving our knowledge of human disease.

Chapter 6: Discussion

6.1. Project summary

The experiments conducted in my PhD project were based on the recent discovery of twenty *de novo* heterozygous missense mutations in *EEF1A2* in over forty patients with intellectual disability, epilepsy and in some cases autism. The main aim of my project was to phenotype mouse models with different mutations in *Eef1a2*, with a particular focus on behaviour. These behavioural analyses were intended to provide a correlate for the intellectual disability and autism observed in patients and to address the question of whether the mutations operate through a gain or loss of function mechanism. For my behavioural experiments, I characterised heterozygous null mice by studying the effects of age and genetic background on behaviour. I compared the behaviour of these null lines to heterozygous mice from a new line, generated by CRISPR/Cas9, with a D252H missense mutation in *Eef1a2*. I also, separately, characterised mice with a G70S missense mutation in *Eef1a2* that were generated using CRISPR/Cas9 technology. Although we were unable to generate a G70S breeding line, the founder mice provided a wealth of information on the effects of the G70S mutation on eEF1A2 function. In this discussion, I will examine the aims of my project by chapter with a focus on the wider context of my work, its limitations and possible future directions.

6.2. Chapter 3 aim: To characterise mice with the *Eef1a2*/G70S missense mutation with an aim to better understand the mechanisms underlying the human phenotype

The restriction enzyme digest protocol I developed provided an accurate prediction of genotype prior to sequencing, with a success rate of 84%. This allowed early prediction of mice that had G70S incorporation and/or large indels, providing an indication of mice that should be particularly closely monitored in terms of phenotype. The utilisation of specific restriction enzyme digests to predict genotype is widely used in studies such as this and has proven to be valuable here (Singh, Schimenti and Bolcun-Filas, 2015).

Using RT-PCR and specific restriction enzyme digests in combination with Fiona McLachlan's western blot results, I was able to show that six mice expressed G70S eEF1A2. Five of these mice were *Eef1a2*$^{G70S/-}$ and the other *Eef1a2*$^{G70S/G70S}$. The phenotype and survival of the *Eef1a2*$^{G70S/-}$ mice was comparable to that of *Eef1a2*-null wasted mice, showing that G70S eEF1A2, although expressed, was unable to compensate for loss of wild-type protein. This result pointed towards loss of function as a mechanism for human disease, however, the one *Eef1a2*$^{G70S/G70S}$ mouse had a more severe phenotype. This suggested that the G70S protein might also gain some toxic functions that contribute to the disease phenotype. It is vital that missense mutations in eEF1A2 are studied further to determine whether loss of function, gain of function, or both, are at play. It is unfortunate that only one G70S homozygote was generated and conclusions regarding gain of function most certainly cannot be based on this mouse alone. Therefore, it will be necessary to correlate phenotype and protein expression in a larger cohort of mice and the D252H line will be ideal for this analysis. However, it is worth bearing in mind that all of the mutations might not operate through the same mechanism as suggested by the different phenotypic manifestations in the patients.

Audiogenic seizures were observed in eight *Eef1a2*$^{-/-}$ mice, however, unfortunately, these were not under controlled conditions. In addition, although four mice with a G70S allele were exposed to the same sound stimulus, none of them had seizures.

However, it is true that the G70S mice were in lower cages and therefore were arguably more sheltered from the sound. Due to the low number of G70S mice exposed, it was not possible to determine whether mice of this genotype are susceptible to audiogenic seizures as a larger cohort would be required. It will be important to determine whether mice with missense mutations in *Eef1a2* are susceptible to audiogenic seizures under controlled conditions. This could be performed using D252H heterozygotes as a correlate for the genotypes of the patients. Audiogenic seizure activity could be closely monitored and scored by exposing mice to sound of around 120dB in a Perspex box (Ross and Coleman, 2000). Wireless telemetry could also be used to record EEG signals in awake behaving mice (Zayachikivsky, Lehmkuhle and Dudek, 2015). Finally, mice could be monitored in-cage using video recording to detect spontaneous seizures.

My aims to predict genotypes prior to sequencing and to determine whether mice carrying a G70S allele expressed G70S eEF1A2 were largely successful and the G70S CRISPR/Cas9 experiment has improved understanding of the effects of missense mutations on eEF1A2 function. In addition, this study showed for the first time that mice with mutations in *Eef1a2* are susceptible to seizures.

6.3. Chapter 4 aim: To determine the effects of age and genetic background on the behaviour of heterozygous *Eef1a2*-null mice

In my behavioural analysis of heterozygous *Eef1a2*-null mice, I found that heterozygous wasted mice showed reduced marble burying behaviour, decreased locomotor activity and an increased freezing response with age. These results pointed towards three main possibilities: a motor impairment, reduced motivation for movement or increased anxiety. In addition, a robust lack of preference for social novelty was identified at all ages tested, a behaviour which has been identified in other autism models (Wagnon *et al*., 2014). The behaviour of heterozygous *Eef1a2*-null mice from the Del22.ex3 line was different from that of heterozygous wasted mice suggesting that the change in genetic background may have had an influence on behaviour. Del22.ex3 *Eef1a2*$^{+/-}$ mice showed a reduction in repetitive behaviours

compared with wild-type mice and normal preference for social novelty. In addition, there was lower variation in results from the Del22.ex3 line, thought to be due to the pure C57BL/6 genetic background in contrast to the mixed genetic background of the wasted line. To summarise, I showed for the first time that heterozygous null mutations in *Eef1a2* result in changes in behaviour.

For future experimentation, it would be more beneficial to study the Del22.ex3 line than the wasted line due to the lower variability of results. Therefore, robust behaviour results could be obtained by testing a much lower number of mice. Ideally, power calculations should be performed either prior to testing or post-hoc after testing a small cohort of mice to determine the number of mice that should be tested.

It would be interesting to repeat the stranger mouse test on the Del22.ex3 line using stranger mice from the same lineage as performed on the wasted line. This would reveal whether the lack of impairment in this task in the Del22.ex3 line was due to the change in protocol or the difference in genetic background. Since I identified a social impairment in heterozygous null mice, it would also be interesting to determine whether mice of this genotype show any other social behaviour deficits, particularly in behaviours that have shown to be affected by other autism-related mutations. For example, *Cntnap2* knockout mice show abnormal social behaviour in the juvenile play test. This test involves allowing direct interaction between the test mouse and an unfamiliar mouse in a cage for 10 minutes and measuring the time spent interacting (Peñagaricano *et al*., 2011). Communication deficits could also be studied by measuring ultrasonic vocalisations (USVs) (Wöhr and Scattoni., 2013).

As there was insufficient time to age mice from the Del22.ex3 line, investigating the effects of age on the behaviour of these mice would be an interesting avenue for future investigation. It would be particularly beneficial to determine whether heterozygous mice from this line show the same age-related behavioural changes as heterozygous mice from the wasted line. Subsequent western blotting could be performed on whole brain tissue to determine eEF1A2 expression levels.

Unfortunately, I was unable to optimise the novel object recognition test which meant that learning and memory was not studied as extensively as desired. It would be valuable to study further the role of eEF1A2 in learning and memory as eEF1A2 has been shown to be important for the maintenance of LTP at hippocampal synapses (Tsokas *et al*., 2005). Firstly, it would be interesting to repeat the Y-maze test with a longer ITI of 120 minutes as performed on the D252H line to study hippocampal spatial memory. Another hippocampal memory test which would be beneficial and easy to implement is the contextual fear conditioning test (Curzon, Rustay and Browman, 2009). Other types of memory should also be studied as behaviours related to brain areas other than the hippocampus may be affected by deletion of *Eef1a2*. For example, *Fmr1* knockout mice show impairments in reversal learning in a water based Y-maze test when the escape platform is moved to the other arm (Bhattacharya *et al*., 2012). This task involves functions of the prefrontal cortex and is used as a correlate for the behavioural inflexibility that is observed in humans with autism (Santos, Kanellopoulos and Bagni, 2014).

As mentioned, my work shows behavioural changes in mice with mutations in *Eef1a2* for the first time. The results from Chapter 4 show that presumed 50% levels of eEF1A2 in the brain are not sufficient to elicit normal behavioural responses. However, interestingly, apart from the observed changes in behaviour, these mice are phenotypically normal (Griffiths *et al*., 2012, Chapter 4). The observation that heterozygous *Eef1a2*-null mice show similar behavioural deficits to other mouse models of autism suggests that eEF1A2 interacts with common pathways, including the ERK1/2 and mTOR pathways, and there is evidence to suggest that this is the case (Tsokas *et al*., 2005, Bluem *et al*., 2007, Khwanraj *et al*., 2016). It has also been shown that eEF1A2 is a target of FMRP, the product of the gene which is mutated in Fragile X syndrome (Darnell *et al*., 2011). However, various lines of evidence, both through the G70S CRISPR/Cas9 experiment and testing of the D252H mouse line (see Chapter 5 aim) suggest that the human missense mutations may lead to gain of protein function. If this appears to be the case after further investigation, further behavioural testing of the D252H line will be more valuable than continuing with the

Del22.ex3 line. Despite this, the new *Eef1a2*-null Del22.ex3 line generated in my project will be useful for future investigation of eEF1A2 function.

6.4. Chapter 5 aim: To investigate the effects of the *Eef1a2*/D252H missense mutation on mouse behaviour

The results of my behavioural analysis on *Eef1a2*$^{+/D252H}$ mice showed that the mice were phenotypically normal, in contrast to the results of heterozygous null mice, suggesting that, in terms of behaviour, the missense mutation is better-tolerated. Weight data revealed that *Eef1a2*$^{+/D252H}$ mice weighed significantly less than *Eef1a2*$^{+/+}$ littermates at 4 months, complementing results gathered between P14 and P24. Finally, expression analysis results showed that D252H eEF1A2 protein is expressed in brain but appears to undergo degradation due to instability.

Other recent data from our laboratory, collected by Laura Kaminioti-Dumont, indicates that there may be a gain of function of the D252H protein (unpublished data). Due to the well-characterised neurodegenerative phenotype of homozygous wasted mice (Newbery *et al*., 2005), homozygous D252H mice and homozygous null mice from the Del22.ex3 line were tested for signs of neuromuscular degeneration. Mice were given a daily phenotypic score based on gait, kyphosis, hindlimb clasping and balance with a higher score indicating a more severe disease phenotype (Guyenet *et al*., 2012). The scores for *Eef1a2*$^{D252H/D252H}$ mice were significantly higher than the scores for *Eef1a2*$^{-/-}$ mice from P18-P24. Between P15 and P24, *Eef1a2*$^{D252H/D252H}$ mice weighed significantly less than *Eef1a2*$^{-/-}$ mice. These results show that the D252H protein has a more severe effect on particular phenotypes than complete absence of eEF1A2. This builds upon data generated through the G70S CRISPR/Cas9 experiment showing the missense protein was insufficient to protect against neurodegeneration and that the homozygous missense mutant had a more severe phenotype than homozygous null mutants. However, it is important to bear in mind that these mutations may work through different mechanisms.

None of the behavioural tests I performed on *Eef1a2*$^{+/D252H}$ mice revealed any evidence for phenotypic abnormalities; however, this does not mean that these mice

do not show changes in behaviour. It would be very interesting to perform the behavioural tests of social behaviour and learning and memory suggested in Section 6.3 on this line. In addition, there was evidence to suggest that *Eef1a2*$^{D252H/D252H}$ mice engage in repetitive grooming behaviour and this could be followed up as described in Chapter 5. Despite repeated attempts to optimise the novel object recognition protocol on both this line and the Del22.ex3 line, the problems could not be resolved. If possible, it would be beneficial to resolve these problems in the future as mice with mutations in autism-related genes have shown impairments in this test, including *Fmr1* knockout mice and *Shank3* mutant mice (Bhattacharya *et al*., 2012, Yang *et al*., 2012).

The observation that *Eef1a2*$^{+/D252H}$ mice show reduced weight compared with their *Eef1a2*$^{+/+}$ littermates is interesting and the reason for this is currently unknown. One possible way to determine whether this could be due to increased stress is by measuring corticosterone metabolites and other stress hormones in blood and/or fecal samples (Touma, Palme and Sachser, 2004). Mouse behaviour and general phenotype could also be observed to determine whether *Eef1a2*$^{+/D252H}$ mice show increased stress responses. This may involve simple observations of coat condition, respiration, motor posture, movement, alertness, feeding, changes in urine/feces and vocalisations. Behavioural tasks such as the elevated plus maze and the light-dark choice test could also be used as measurements of stress and anxiety (Takao and Miyakawa, 2006). However, it is also possible that *Eef1a2*$^{+/D252H}$ mice have either fewer cells or cells of reduced size compared with *Eef1a2*$^{+/+}$ mice and that this may be the reason for the difference in weight. Finally, as mentioned in the discussion for this chapter, differences in body composition may underlie the difference in weight and this would be another interesting avenue for future investigation.

Due to the expression results suggesting that the D252H protein is unstable, drugs that act to stabilise proteins could, possibly, be used therapeutically. However, this is not likely to be beneficial for patients with *EEF1A2* mutations as results from mice suggest that missense mutations in *Eef1a2* lead to gain of toxic functions. Further research into the effects of these mutations on eEF1A2 function is necessary,

however, targeting eEF1A2 using small molecule drugs may be a more efficient strategy as this has been shown to work well in diseases caused by gain of function mutations (Chen and Altman, 2017). Boosting wild-type levels of eEF1A2 using gene therapy is also an option, however, the effectiveness of this approach whilst the toxic protein remains is unknown. In addition, eEF1A2 is an oncogene which is overexpressed in many tumour types (Anand *et al*., 2002, Lee and Surh, 2009), therefore, boosting wild-type levels should be treated with caution. Gene silencing is another potential treatment option. This approach uses single stranded DNA or RNA molecules which are complementary to and bind the mutant mRNA, reducing its translation into protein. This approach has been extensively studied as a potential treatment option for patients with Huntington's disease with success in rodent models and human clinical trials currently ongoing (Godinho *et al*., 2015). However, it is currently unknown whether 50% levels of eEF1A2 are compatible with normal function in humans and therefore the effectiveness of this strategy remains undetermined.

6.5. Conclusion

In my project, I have successfully shown behavioural changes in mice with heterozygous mutations in *Eef1a2* and shown a difference in phenotype between null and missense mutants which suggests that *Eef1a2*-null mutations are less well-tolerated than missense mutations in mice. The number of human cases with missense mutations in *EEF1A2* is increasing and, based on results from the DDD study, there are predicted to be 5-6 new cases in the UK each year, with a birth incidence of approximately 1/100,000 (personal communication). This increase in the number of cases has not occurred because of a rise in mutation frequency but because of the development and widespread use of new sequencing methods. Therefore, genetic causes of developmental disorders are being identified more quickly in a substantially larger number of undiagnosed individuals.

It is important to determine the effects of missense mutations on eEF1A2 function and phenotype using multiple different model systems with the aim to test therapeutics in the future. Cell models are a valuable tool which can be used to study

every human *EEF1A2* mutation by simple and effective mutagenesis and transfection of plasmids. However, studies in cell lines are confounded by co-expression of eEF1A1. Zebrafish models are also being explored, with the hope of screening small molecules for therapy. Mouse models provide a correlate for human physiology and are extremely useful to study the effects of these mutations on phenotype at a whole organism level. Future studies using the D252H mouse model generated in our laboratory will increase understanding of the human phenotype. An interesting avenue for future investigation of D252H mice would be proteomic analysis of brain tissue by mass spectrometry to identify pathways that are involved in disease pathogenesis. Changes to interactions of eEF1A2 with synaptic proteins and ion channel subunits would be interesting to follow up. In the future, a mouse model with another of the human missense mutations, perhaps one identified in patient(s) with different clinical features from the D252H patients, would be a valuable comparator. This would provide insight into the ways in which different missense mutations in *EEF1A2* lead to differences in pathology. Together, these strategies will help to increase our understanding of normal eEF1A2 function and how this changes in disease.

Appendices

Appendix A – qPCR on D252H mouse brain: controls, melting curves and standard curves

A1. Agarose gel showing lack of contamination in controls

Prior to the qPCR experiments presented in Section 5.2.10, cDNA samples were amplified using RT-PCR and run on a 2% agarose gel to ensure that there was no contamination using the protocol shown in Section 2.5.5. The gel images are shown in Figure A1.1.

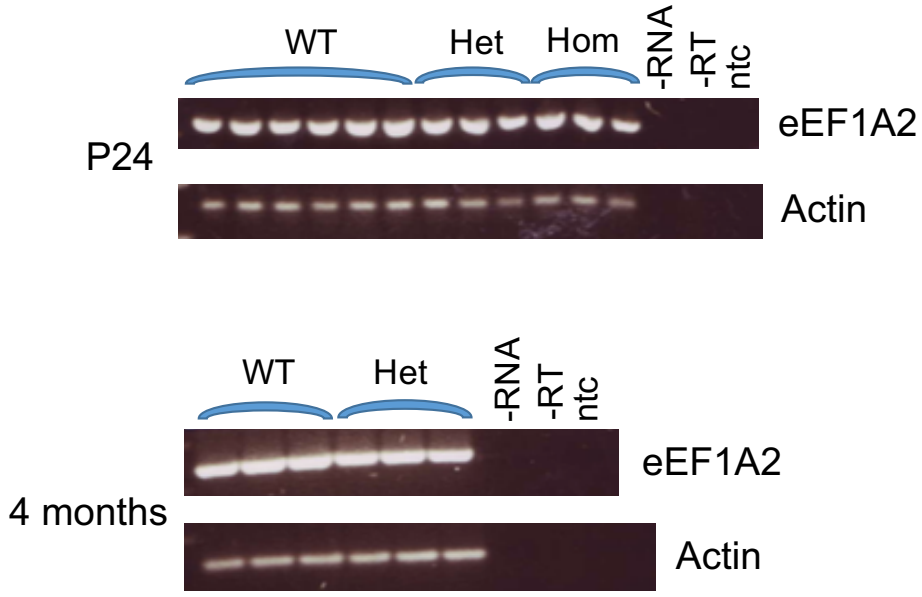

Figure A1.1. cDNA samples run on a 2% agarose gel. *ntc = no template control, -RT = no reverse transcriptase cDNA synthesis control, -RNA = no RNA cDNA synthesis control (see Section 2.5.4).*

A2. Melting curves and standard curves

Serial dilutions of cDNA were used to produce standard curves following the protocol outlined in Section 2.5.7. cDNA was diluted in dH_2O at 1:4, 1:16, 1:64,

1:256, 1:1024, 1:4096 and 1:16384. Melting curves (Figure A2.1) and standard curves (Figure A2.2) were generated using SDS software.

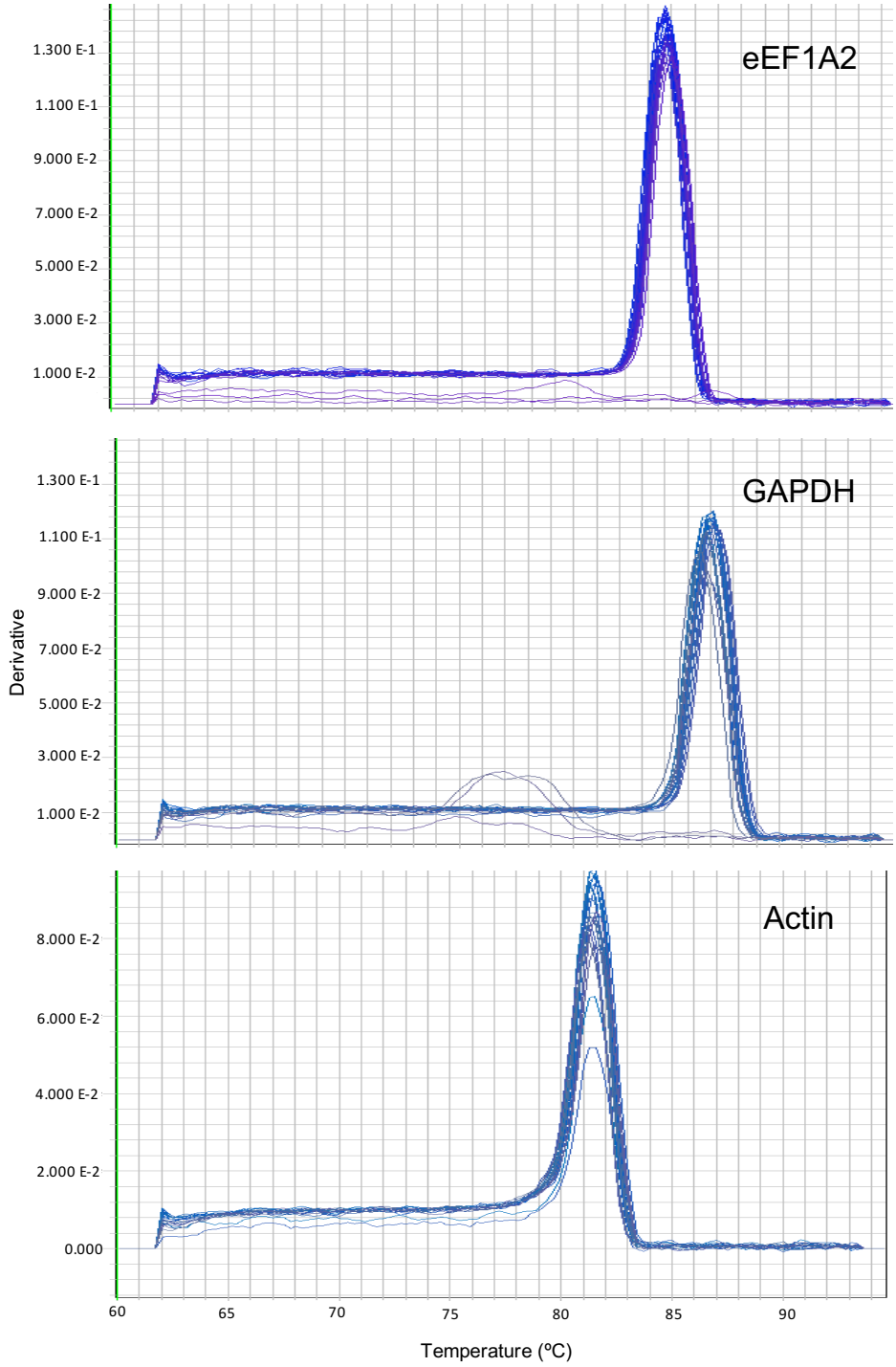

Figure A2.1. qPCR melting curves for eEF1A2 and the reference genes GAPDH and Actin. *These were generated in order to ensure primer specificity. A single peak indicates single amplicon detection.*

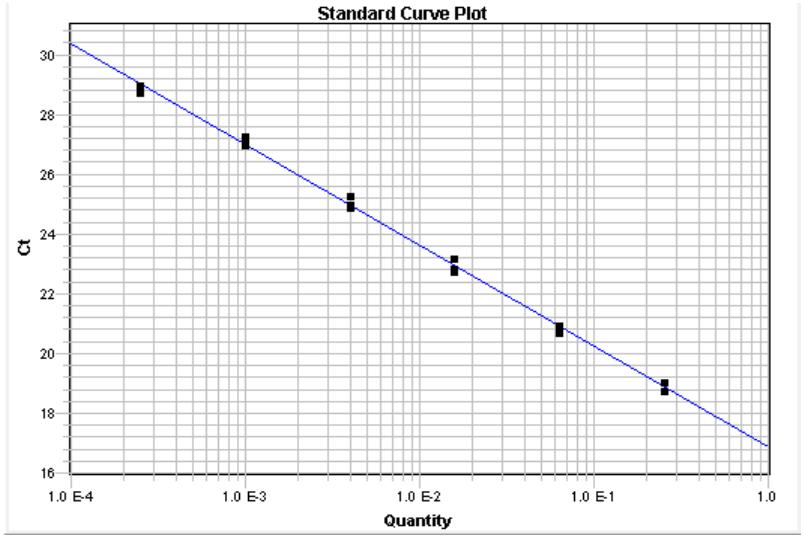

eEF1A2

Slope = -3.3762577
Y-inter = 16.852448
R2 = 0.9973509

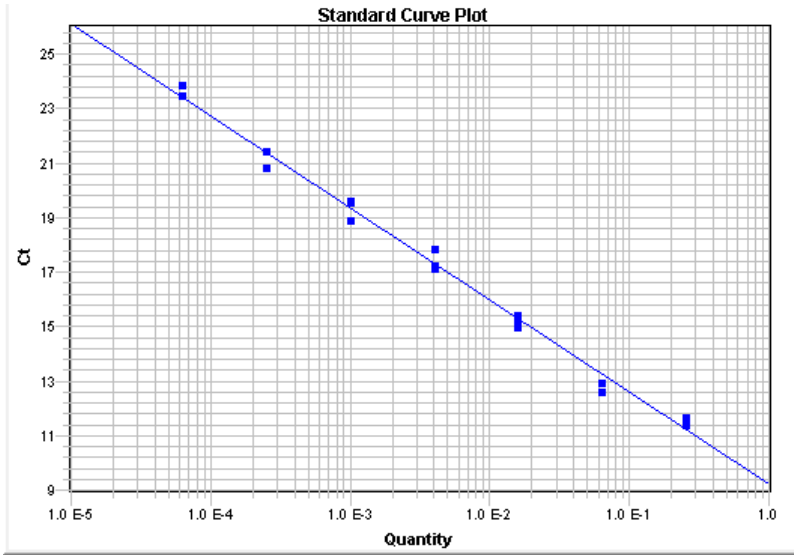

GAPDH

Slope = -3.380188
Y-inter = 9.219257
R2 = 0.99329835

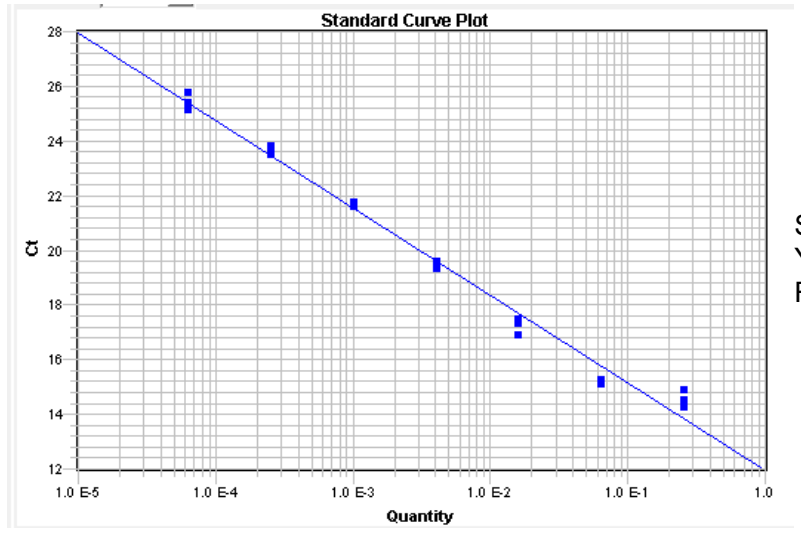

Actin

Slope = -3.1954546
Y-inter = 11.968351
R2 = 0.9869733

Figure A2.2. qPCR standard curves for eEF1A2 and the reference genes GAPDH and Actin. *Primer sets with R2 > 0.98 were considered acceptable for further analysis.*

Appendix B – Correlating behaviour score with age for mice in the wasted line

Behaviour scores were correlated with age to confirm whether scores increased or declined as mice aged. Correlation plots are shown in Figure B1. A summary table of the statistical results for these analyses is also shown (Table B1).

The results of these correlation analysis are largely in agreement with the results of the aging studies presented in Chapter 4. Firstly, there is a significant negative correlation of marble burying score with age for *Eef1a2*$^{+/wst}$ mice (Figure B1. C, Table B1) which complements the result in Figure 4.3 showing that *Eef1a2*$^{+/wst}$ mice bury significantly fewer marbles at 12-18 months compared with 2-6 months. Similarly, there is a significant negative correlation of the total distance travelled in the open field arena with age for *Eef1a2*$^{+/wst}$ mice (Figure B1. G, Table B1) which is in agreement with the result in Figure 4.7A showing that *Eef1a2*$^{+/wst}$ mice cover a significantly shorter distance at 12-18 months compare with at 2-6 months. In addition, the significant positive correlation for *Eef1a2*$^{+/wst}$ mice for time spent freezing in the open field test (Figure B1. H, Table B1) complements data shown in Figure 4.7B whereby *Eef1a2*$^{+/wst}$ mice spend a significantly larger amount of time freezing at 12-18 months compared with 2-6 months.

However, some of the correlations are significant despite the lack of significant differences in the age group analyses shown in Chapter 4. There were two significant correlations for *Eef1a2*$^{+/wst}$ mice in the digging assay: a significant negative correlation for the number of digging bouts (Figure B1. D, Table B1) and a significant positive correlation for the latency to start digging (Figure B1. E, Table B1). In Chapter 4, there was no significant difference in the number of digging bouts of the latency to start digging between *Eef1a2*$^{+/wst}$ age groups (Figure 4.4 A and B). The lack of significance in the data presented in Chapter 4 compared with the significant correlations shown here is thought to be due to the standard error values associated with the Chapter 4 results. Standard error has no influence on correlation results and therefore statistical significance can be reached even when data is

variable. In the correlation analyses, a significant positive correlation was found for *Eef1a2*$^{+/wst}$ mice for the time spent in the centre of the open field arena (Figure B1. I, Table B1). Again, the reason for obtaining a significant result from this analysis but not from the analysis in Chapter 4 (Figure 4.7C) is thought to be due to the standard error values in the Chapter 4 analyses. It can be seen from the correlation plot that the variability in scores from the mice at 16 months is very large which explains why significance was not achieved when comparing age groups in Chapter 4. This result makes sense when considering that *Eef1a2*$^{+/wst}$ mice cover a significantly smaller distance and spend significantly more time freezing in the open field test as they age. The data suggests that 12-18 month old *Eef1a2*$^{+/wst}$ mice spent more time freezing in the centre of the apparatus than around the outside walls.

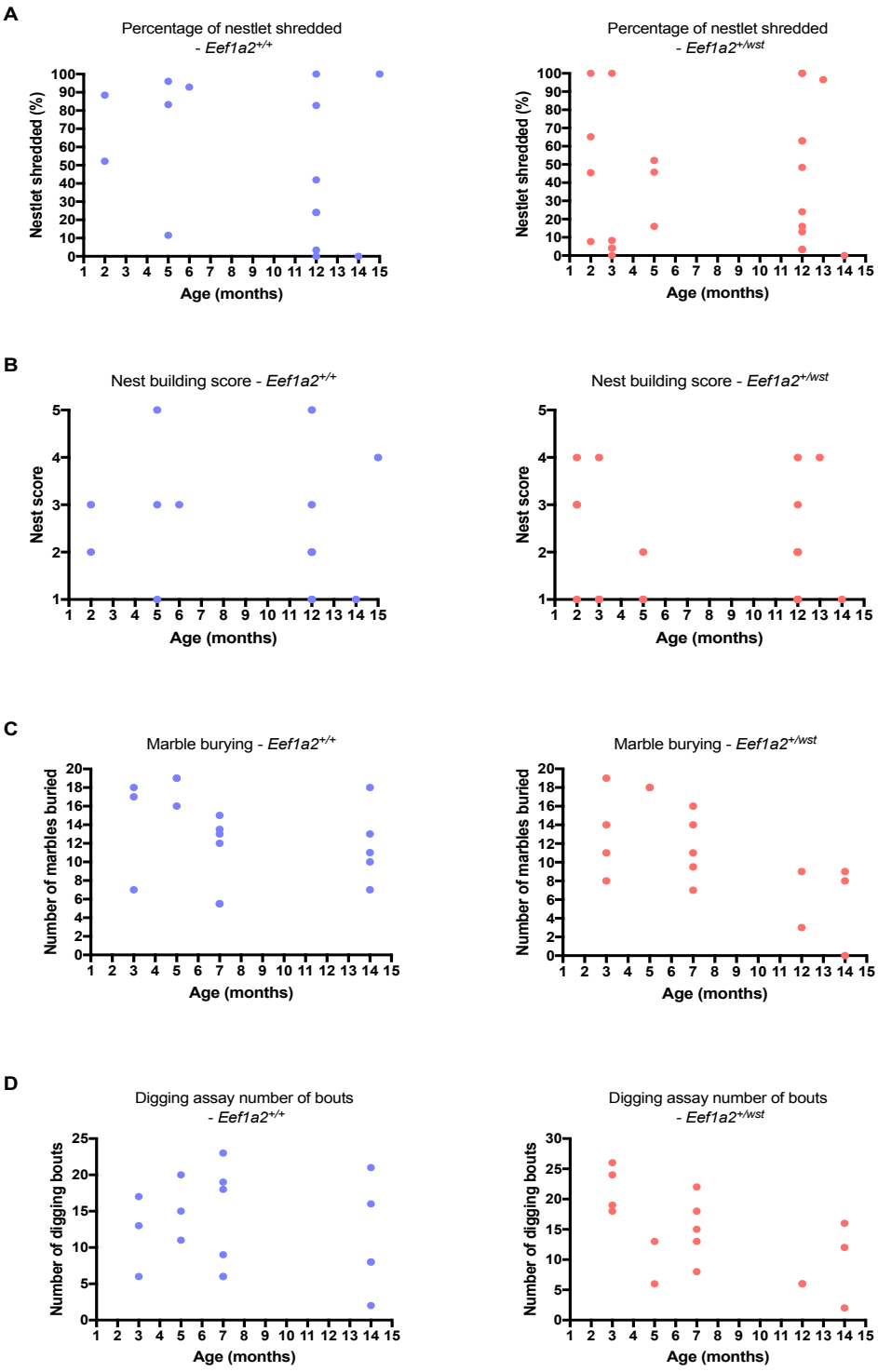
A
Percentage of nestlet shredded
- Eef1a2+/+
Nestlet shredded (%)
Age (months)
Percentage of nestlet shredded
- Eef1a2+/wst
Nestlet shredded (%)
Age (months)
B
Nest building score - Eef1a2+/+
Nest score
Age (months)
Nest building score - Eef1a2+/wst
Nest score
Age (months)
C
Marble burying - Eef1a2+/+
Number of marbles buried
Age (months)
Marble burying - Eef1a2+/wst
Number of marbles buried
Age (months)
D
Digging assay number of bouts
- Eef1a2+/+
Number of digging bouts
Age (months)
Digging assay number of bouts
- Eef1a2+/wst
Number of digging bouts
Age (months)

E

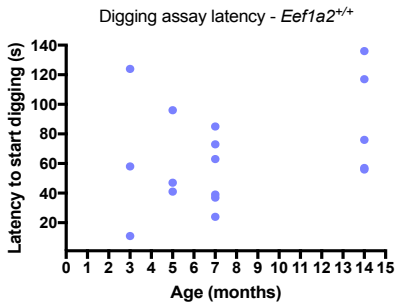
Digging assay latency - Eef1a2+/+
Latency to start digging (s)
Age (months)

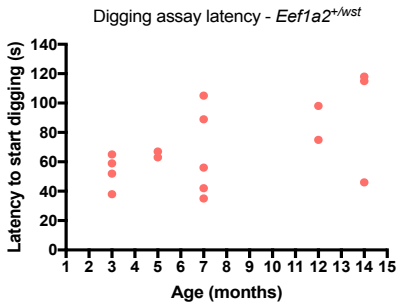
Digging assay latency - Eef1a2+/wst
Latency to start digging (s)
Age (months)

F

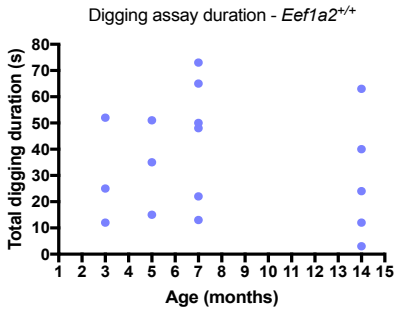
Digging assay duration - Eef1a2+/+
Total digging duration (s)
Age (months)

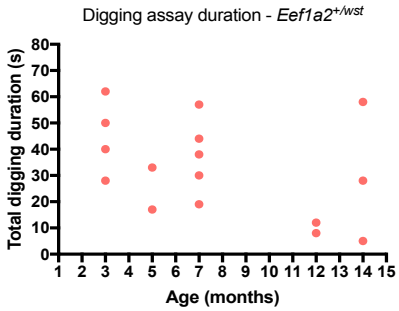
Digging assay duration - Eef1a2+/wst
Total digging duration (s)
Age (months)

G

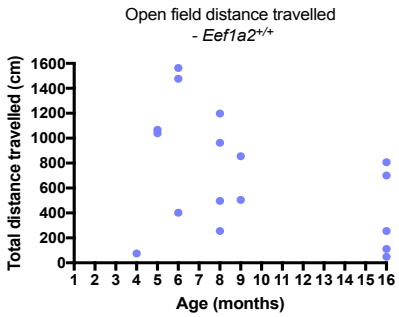
Open field distance travelled
- Eef1a2+/+
Total distance travelled (cm)
Age (months)

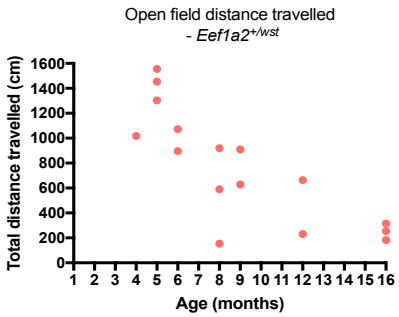
Open field distance travelled
- Eef1a2+/wst
Total distance travelled (cm)
Age (months)

H

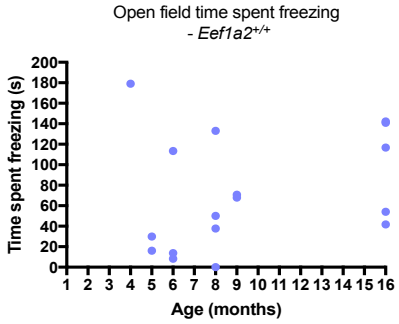
Open field time spent freezing
- Eef1a2+/+
Time spent freezing (s)
Age (months)

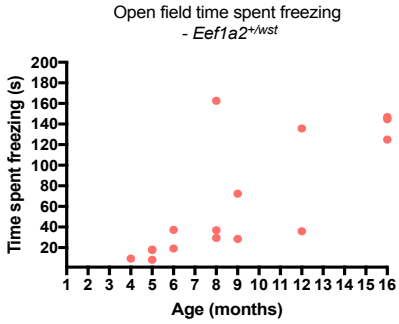
Open field time spent freezing
- Eef1a2+/wst
Time spent freezing (s)
Age (months)

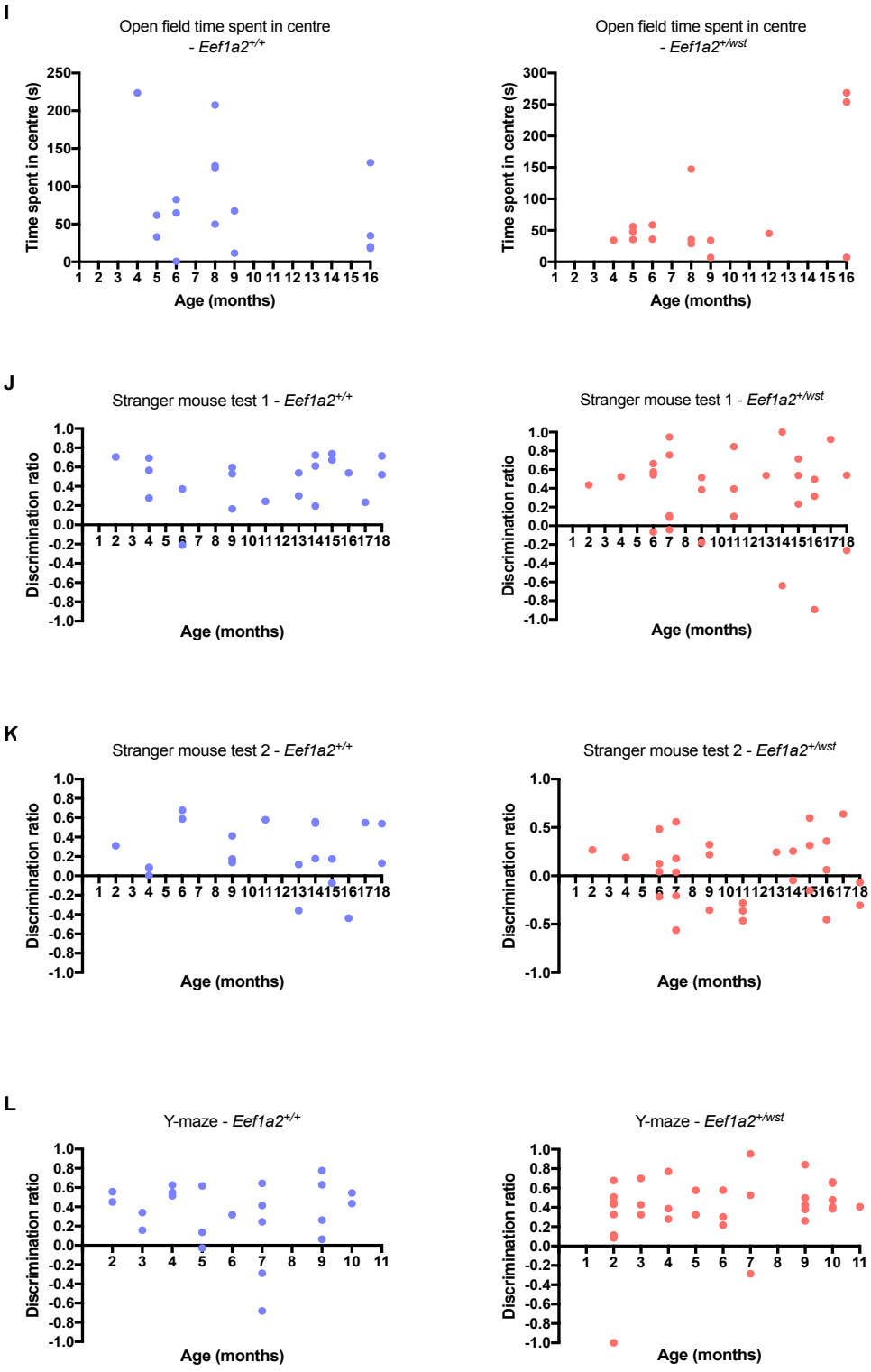

Figure B1. Correlation of age with behaviour score for each test performed on the wasted line. ***A and B.*** *Nest building assay.* ***C.*** *Marble burying test.* ***D, E and F.*** *Digging assay.* ***G, H and I.*** *Open field test.* ***J and K.*** *Stranger mouse test.* ***L.*** *Y-maze test. Results from wild-type analyses are shown with purple data points (left) and results from Eef1a2$^{+/wst}$ analyses are shown with red data points (right).*

	R	R squared	P value	Significant?
Nest building - % nestlet shredded	-0.30	0.09	0.2727	N
Nest building - % nestlet shredded	0.07	0.00	0.7573	N
Nest building - score	-0.13	0.02	0.6565	N
Nest building - score	-0.02	0.00	0.9329	N
Marble burying	-0.26	0.07	0.3136	N
Marble burying	-0.66	0.43	0.0058	Y
Digging – number of bouts	-0.16	0.03	0.5379	N
Digging – number of bouts	-0.61	0.37	0.0120	Y
Digging - latency	0.34	0.12	0.1812	N
Digging - latency	0.55	0.30	0.0283	Y
Digging - duration	-0.11	0.01	0.6629	N
Digging - duration	-0.40	0.16	0.1298	N
Stranger mouse test 1	0.17	0.03	0.4707	N
Stranger mouse test 1	-0.13	0.02	0.5107	N
Stranger mouse test 2	-0.07	0.00	0.7621	N
Stranger mouse test 2	-0.02	0.00	0.9308	N
Y-maze	-0.05	0.00	0.8397	N
Y-maze	0.27	0.07	0.1224	N
Open field – distance travelled	-0.43	0.18	0.0875	N
Open field – distance travelled	-0.80	0.64	0.0002	Y
Open field – time spent freezing	0.28	0.08	0.2772	N
Open field – time spent freezing	0.77	0.59	0.0005	Y
Open field – time in centre	-0.27	0.07	0.3160	N
Open field – time in centre	0.56	0.32	0.0286	Y

Table B1. Statistical analysis of correlations shown in Figure B1. *Pearson's correlations were performed on the data. As with Figure B1, results from wild-type analyses are shown in purple and results from Eef1a2$^{+/wst}$ analyses are shown in red. Statistically significant results are highlighted in yellow. Note: an 'R' of 1 indicates a perfect positive correlation whilst and 'R' of -1indicates a perfect negative correlation.*

Appendix C - Confirming the genotypes of mice from the wasted line behaviour cohort

The genotypes of the mice that were culled for tissue were confirmed by PCR using the protocol shown in Section 2.4.3. DNA was extracted from tissue using the protocol shown in Section 2.4.2. Samples were run on a 2% agarose gel (Figure C1).

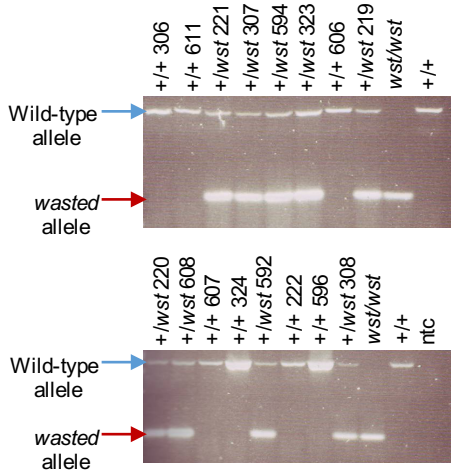

Figure C1. PCR products from the wasted behavioural cohort run on a 2% agarose gel. *+/+ = wild-type, +/wst = wasted heterozygote, wst/wst = wasted homozygote tissue control, ntc = no template control.*

Bibliography

Abbott C, Malas S, Pilz A, Pate L, Ali R, Peters J (1994) Linkage mapping around the Ragged (*Ra*) and wasted (*wst*) loci on distal mouse chromosome 2. Genomics 20:94-98.

Anand N, Murthy S, Amann G, Wernick M, Porter LA, Cukier IH, Collins C, Gray JW, Diebold J, Demetrick DJ, Lee JM (2002) Protein elongation factor EEF1A2 is a putative oncogene in ovarian cancer. Nat Genet 31:301–305.

Angoa-Pérez M, Kane MJ, Briggs DI, Francescutti DM, Kuhn DM (2013) Marble burying and nestlet shredding as tests of repetitive, compulsive-like behaviors in mice. J Vis Exp 82:50978.

Antunes M, Biala G (2012) The novel object recognition memory: neurobiology, test procedure, and its modifications. Cogn Process 13:93–110.

Babinet C, Cohen-Tannoudji M (2001) Genome engineering via homologous recombination in mouse embryonic stem (ES) cells: an amazingly versatile tool for the study of mammalian biology. An Acad Bras Cienc 73(3).

Bagni C, Greenough WT (2005) From mRNP trafficking to spine dysmorphogenesis: the roots of fragile X syndrome. Nat Rev Neurosci 6:376–387.

Baker KB, Wray SP, Ritter R, Mason S, Lanthorn TH, Savelieva K V. (2010) Male and female Fmr1 knockout mice on C57 albino background exhibit spatial learning and memory impairments. Genes, Brain Behav 9:562–574.

Beckelman BC, Day S, Zhou X, Donohue M, Gouras GK, Klann E, Keene CD, Ma T (2016) Dysregulation of Elongation Factor 1A Expression is Correlated with Synaptic Plasticity Impairments in Alzheimer's Disease. J Alzheimer's Dis 54:1–10.

Beckelman BC, Zhou X, Keene CD, Ma T (2015) Impaired Eukaryotic Elongation Factor 1A Expression in Alzheimer's Disease. Neurodegener Dis 16:39–43.

Bhattacharya A, Kaphzan H, Alvarez-Dieppa AC, Murphy JP, Pierre P, Klann E (2012) Genetic Removal of p70 S6 Kinase 1 Corrects Molecular, Synaptic, and Behavioral Phenotypes in Fragile X Syndrome Mice. Neuron 76:325–337.

Bilousova T V, Dansie L, Ngo M, Aye J, Charles JR, Ethell DW, Ethell IM (2009) Minocycline promotes dendritic spine maturation and improves behavioural performance in the fragile X mouse model. J Med Genet 46:94–102.

Bliss T V, Lomo T (1973) Long-lasting potentiation of synaptic transmission in the dentate area of the anaesthetized rabbit following stimulation of the perforant path. J Physiol 232:331–356.

Bluem R, Schmidt E, Corvey C, Karas M, Schlicksupp A, Kirsch J, Kuhse J (2007) Components of the translational machinery are associated with juvenile glycine receptors and are redistributed to the cytoskeleton upon aging and synaptic activity. J Biol Chem 282:37783–37793.

Brooks SP, Dunnett SB (2009) Tests to assess motor phenotype in mice : a user's guide. Nat Publ Gr 10:519–529.

Bunai F, Ando K, Ueno H, Numata O (2006) Tetrahymena eukaryotic translation elongation factor 1A (eEF1A) bundles filamentous actin through dimer formation. J Biochem 140:393–399.

Caban C, Khan N, Hasbani DM, Crino PB (2017) Genetics of tuberous sclerosis complex: implications for clinical practice. Appl Clin Genet 10:1–8.

Cao H, Zhu Q, Huang J, Li B, Zhang S, Yao W, Zhang Y (2009) Regulation and functional role of eEF1A2 in pancreatic carcinoma. Biochem Biophys Res Commun 380:11–16.

Carter TC, Phillips RJS (1954) Ragged, a semi-dominant coat texture mutant. Journal of Heredity 45:151-154.

Chambers DM, Peters J, Abbott CM (1998) The lethal mutation of the mouse wasted (wst) is a deletion that abolishes expression of a tissue-specific isoform of translation elongation factor 1alpha, encoded by the Eef1a2 gene. Proc Natl Acad Sci U S A 95:4463–4468.

Chen B, Altman RB (2017) Opportunities for developing therapies for rare genetic diseases: focus on gain-of-function and allostery. Orphanet J Rare Dis 12:61.

Chévere-torres I, Kaphzan H, Bhattacharya A, Kang A, Maki JM, Gambello MJ, Arbiser JL, Santini E, Klann E (2012) Neurobiology of Disease Metabotropic glutamate receptor-dependent long-term depression is impaired due to elevated ERK signaling in the Δ RG mouse model of tuberous sclerosis complex. Neurobiol Dis 45:1101–1110.

Chuang S-M, Chen L, Lambertson D, Anand M, Kinzy TG, Madura K (2005) Proteasome-mediated degradation of cotranslationally damaged proteins involves translation elongation factor 1A. Mol Cell Biol 25:403–413.

Clark BFC, Thirup S, Kjeldgaard M, Nyborg J (1999) Structural information for explaining the molecular mechanism of protein biosynthesis. Febs Lett 452:41–46.

Clipperton-Allen AE, Page DT (2015) Decreased aggression and increased repetitive behavior in Pten haploinsufficient mice. Genes, Brain Behav 14:145–157.

Cowan N (2008) What are the differences between long-term, short-term, and working memory? Prog Brain Res 169:323–338.

Crawley JN (2007) Mouse behavioral assays relevant to the symptoms of autism. Brain Pathol 17:448–459.

Curzon P, Rustay NR, Browman KE (2009) Cued and Contextual Fear Conditioning for Rodents. Methods of Behavior Analysis in Neuroscience, 2nd Edition. CRC Press/ Taylor & Francis.

Dahlhaus R, El-Husseini A (2010) Altered neuroligin expression is involved in social deficits in a mouse model of the fragile X syndrome. Behav Brain Res 208:96–105.

Darnell JC, Van Driesche SJ, Zhang C, Hung KYS, Mele A, Fraser CE, Stone EF, Chen C, Fak JJ, Chi SW, Licatalosi DD, Richter JD, Darnell RB (2011) FMRP stalls ribosomal translocation on mRNAs linked to synaptic function and autism. Cell 146:247–261.

Davies FCJ (2017) The Role of eEF1A Isoforms in Neuritogenesis and Epilepsy. *PhD Thesis*.

Davies FCJ, Hope JE, Mclachlan F, Nunez F, Doig J, Bengani H, Smith C, Abbott CM (2017) Biallelic mutations in the gene encoding eEF1A2 cause seizures and sudden death in F0 mice. Nature Scientific Reports 7.

Deacon R (2012) Assessing burrowing, nest construction, and hoarding in mice. J Vis Exp 59:e2607.

Deacon RM (2006a) Assessing nest building in mice. Nat Protoc 1:1117–1119.

Deacon RMJ (2006b) Digging and marble burying in mice: simple methods for in vivo identification of biological impacts. Nat Protoc 1:122–124.

de Ligt J, Willemsen MH, van Bon BWM, Kleefstra T, Yntema HG, Kroes T, Vulto-van Silfhout AT, Koolen DA, de Vries P, Gilissen C, del Rosario M, Hoischen A, Scheffer H, de Vries BBA, Brunner HG, Veltman JA, Vissers LELM (2012) Diagnostic exome sequencing in persons with severe intellectual disability. N Engl J Med 367:1921–1929.

Deshmukh SS, Knierim JJ (2011) Representation of non-spatial and spatial information in the lateral entorhinal cortex. Front Behav Neurosci 5:69.

Ding Q, Sethna F, Wang H (2014) Behavioral analysis of male and female Fmr1 knockout mice on C57BL/6 background. Behav Brain Res 271:72–78.

Doig J, Griffiths LA, Peberdy D, Dharmasaroja P, Vera M, Davies FJC, Newbery HJ, Brownstein D, Abbott CM (2013) In vivo characterization of the role of tissue-specific translation elongation factor 1A2 in protein synthesis reveals insights into muscle atrophy. FEBS J 280:6528–6540.

Donner EJ, Camfield P, Brooks L, Buchhalter J, Camfield C, Loddenkemper T, Wirrell E (2017) Understanding Death in Children With Epilepsy. Pediatr Neurol 70:7–15.

Duttaroy A, Bourbeau D, Wang X-L, Wang E (1998) Apoptosis Rate Can Be Accelerated or Decelerated by Overexpression or Reduction of the Level of Elongation Factor-1α. Exp Cell Res 238:168–176.

Freudenberg F, Resnik E, Kolleker A, Celikel T, Sprengel R, Seeburg PH (2016) Hippocampal GluA1 expression in Gria1(-/-) mice only partially restores spatial memory performance deficits. Neurobiol Learn Mem 135:83–90.

Garcia-Esparcia P, Hernández-Ortega K, Koneti A, Gil L, Delgado-Morales R, Castaño E, Carmona M, Ferrer I (2015) Altered machinery of protein synthesis is region- and stage-dependent and is associated with α-synuclein oligomers in Parkinson's disease. Acta Neuropathol Commun 3:76.

Godinho BMDC, Malhotra M, O'Driscoll CM, Cryan JF (2015) Delivering a disease-modifying treatment for Huntington's disease. Drug Discovery Today 20(1):50-64.

Gonskikh Y, Polacek N (2017) Alterations of the translation apparatus during aging and stress response. Mech Ageing Dev. http://dx.doi.org/10.1016/j.mad.2017.04.003.

Goorden SMI, van Woerden GM, van der Weerd L, Cheadle JP, Elgersma Y (2007) Cognitive deficits in *Tsc1* $^{+/-}$ mice in the absence of cerebral lesions and seizures. Ann Neurol 62:648–655.

Grayson B, Leger M, Piercy C, Adamson L, Harte M, Neill JC (2015) Assessment of disease-related cognitive impairments using the novel object recognition (NOR) task in rodents. Behav Brain Res 285:176–193.

Griffiths L a, Doig J, Churchhouse AMD, Davies FCJ, Squires CE, Newbery HJ, Abbott CM (2012) Haploinsufficiency for translation elongation factor eEF1A2 in aged mouse muscle and neurons is compatible with normal function. PLoS One 7:e41917.

Gross C, Raj N, Molinaro G, Allen AG, Whyte AJ, Gibson JR, Huber KM, Gourley SL, Bassell GJ (2015) Report Selective Role of the Catalytic PI3K Subunit p110 b in Impaired Higher Order Cognition in Fragile X Syndrome. Cell Rep 11:681–688.

Guyenet SJ, Furrer SA, Damian VM, Baughan TD, La Spada AR, Garden GA (2010) A simple composite phenotype scoring system for evaluating mouse models of cerebellar ataxia. J Vis Exp 39.

Ha S, Lee D, Cho YS, Chung C, Yoo Y-E, Kim J, Lee J, Kim W, Kim H, Bae YC, Tanaka-Yamamoto K, Kim E (2016) Cerebellar Shank2 Regulates Excitatory Synapse Density, Motor Coordination, and Specific Repetitive and Anxiety-Like Behaviors. J Neurosci 36:12129–12143.

Halm ST, Bottomley MA, Almutairi MM, Di Fulvio M, Halm DR (2017) Survival and growth of C57BL/6J mice lacking the BK channel, *Kcnma1* : lower adult body weight occurs together with higher body fat. Physiol Rep 5:e13137.

Helbig KL, Farwell Hagman KD, Shinde DN, Mroske C, Powis Z, Li S, Tang S, Helbig I (2016) Diagnostic exome sequencing provides a molecular diagnosis for a significant proportion of patients with epilepsy. Genet Med 18:898–905.

Holmes a, Li Q, Murphy DL, Gold E, Crawley JN (2003) Abnormal anxiety-related behaviour in serotonin transporter null mutant mice: the influence of genetic background. Genes Brain Behav 2:365–380.

Homanics GE, Quinlan JJ, Firestone LL (1999) Pharmacologic and behavioral responses of inbred C57BL/6J and strain 129/SvJ mouse lines. Pharmacol Biochem Behav 63:21–26.

Huang F, Chotiner JK, Steward O (2005) The mRNA for elongation factor 1alpha is localized in dendrites and translated in response to treatments that induce long-term depression. J Neurosci 25:7199–7209.

Inui T, Kobayashi S, Ashikari Y, Sato R, Endo W (2016) Two cases of early-onset myoclonic seizures with continuous parietal delta activity caused by EEF1A2 mutations. Brain Dev 38:520–524.

Jeste SS, Tuchman R (2015) Autism Spectrum Disorder and Epilepsy: Two Sides of the Same Coin? J Child Neurol 30:1963–1971.

Kahns S, Lund A, Kristensen P, Knudsen CR, Clark BFC, Cavallius J, Merrick WC (1998) The elongation factor 1 A-2 isoform from rabbit: Cloning of the cDNA and characterization of the protein. Nucleic Acids Res 26:1884–1890.

Kaidanovich-Beilin O, Lipina T, Vukobradovic I, Roder J, Woodgett JR (2011) Assessment of social interaction behaviors. J Vis Exp 48.

Kalueff A V, Aldridge JW, LaPorte JL, Murphy DL, Tuohimaa P (2007) Analyzing grooming microstructure in neurobehavioral experiments. Nat Protoc 2:2538–2544.

Kanibolotsky DS, Novosyl'na O V, Abbott CM, Negrutskii BS, El'skaya A V (2008) Multiple molecular dynamics simulation of the isoforms of human translation elongation factor 1A reveals reversible fluctuations between "open" and "closed" conformations and suggests specific for eEF1A1 affinity for Ca2+-calmodulin. BMC Struct Biol 8:4.

Kästner N, Richter SH, Gamer M, Kaiser S, Sachser N (2017) What a difference a day makes - female behaviour is less predictable near ovulation. Royal Society Open Science 4(4):160998.

Kazdoba TM, Leach PT, Crawley JN (2016) Behavioral phenotypes of genetic mouse models of autism. Genes, Brain Behav 15:7–26.

Kazdoba TM, Leach PT, Silverman JL, Crawley JN (2014) Modeling fragile X syndrome in the Fmr1 knockout mouse. Intractable rare Dis Res 3:118–133.

Khacho M, Mekhail K, Pilon-Larose K, Pause A, Côté J, Lee S (2008) eEF1A is a novel component of the mammalian nuclear protein export machinery. Mol Biol Cell 19:5296–5308.

Khalyfa a, Bourbeau D, Chen E, Petroulakis E, Pan J, Xu S, Wang E (2001) Characterization of elongation factor-1A (eEF1A-1) and eEF1A-2/S1 protein expression in normal and wasted mice. J Biol Chem 276:22915–22922.

Khwanraj K, Madlah S, Grataitong K, Dharmasaroja P (2016) Comparative mRNA Expression of eEF1A Isoforms and a PI3K / Akt / mTOR Pathway in a Cellular Model of Parkinson's Disease. Park Dis 2016.

Kim H, Lim C-S, Kaang B-K (2016) Neuronal mechanisms and circuits underlying repetitive behaviours in mouse models of autism spectrum disorder. Behav Brain Funct 12:3.

Kirschstein T (2012) Synaptic plasticity and learning in animal models of tuberous sclerosis complex. Neural Plast 2012:279834.

Knudsen SM, Frydenberg J, Clark BF, Leffers H (1993) Tissue-dependent variation in the expression of elongation factor-1 alpha isoforms: isolation and characterisation of a cDNA encoding a novel variant of human elongation-factor 1 alpha. Eur J Biochem 215:549–554.

Kurien BT, Scofield RH (2006) Western Blotting: A Guide to Current Methods. Methods 38:283–293.

Lam WWK, Millichap JJ, Soares DC, Chin R, McLellan A, FitzPatrick DR, Elmslie F, Lees MM, Schaefer GB, Abbott CM (2016) Novel de novo EEF1A2 missense mutations causing epilepsy and intellectual disability. Mol Genet Genomic Med 4.

Lamberti A, Caraglia M, Longo O, Marra M, Abbruzzese A, Arcari P (2004) The translation elongation factor 1A in tumorigenesis, signal transduction and apoptosis: Review article. Amino Acids 26:443–448.

Lee M-H, Surh Y-J (2009) eEF1A2 as a Putative Oncogene. Ann N Y Acad Sci 1171:87–93.

Lee S, Francoeur a M, Liu S, Wang E (1992) Tissue-specific expression in mammalian brain, heart, and muscle of S1, a member of the elongation factor-1 alpha gene family. J Biol Chem 267:24064–24068.

Leger M, Quiedeville A, Bouet V, Haelewyn B, Boulouard M, Schumann-Bard P, Freret T (2013) Object recognition test in mice. Nat Protoc 8:2531–2537.

Li D, Wei T, Abbott CM, Harrich D (2013) The unexpected roles of eukaryotic translation elongation factors in RNA virus replication and pathogenesis. Microbiol Mol Biol Rev 77:253–266.

Li R, Wang H, Bekele BN, Yin Z, Caraway NP, Katz RL, Stass SA, Jiang F (2006) Identification of putative oncogenes in lung adenocarcinoma by a comprehensive functional genomic approach. Oncogene 25:2628–2635.

Lise S et al. (2012) Recessive mutations in SPTBN2 implicate β-III spectrin in both cognitive and motor development. PLoS Genet 8:e1003074.

Liu G, Tang J, Edmonds BT, Murray J, Levin S, Condeelis J (1996) F-actin sequesters elongation factor 1alpha from interaction with aminoacyl-tRNA in a pH-dependent reaction. J Cell Biol 135:953–963.

Lopes F et al. (2016) Identification of novel genetic causes of Rett syndrome- *like* phenotypes. J Med Genet 53:190–199.

Lugo JN, Smith GD, Arbuckle EP, White J, Holley AJ, Floruta CM, Ahmed N, Gomez MC, Okonkwo O (2014) Deletion of PTEN produces autism-like behavioral deficits and alterations in synaptic proteins. Front Mol Neurosci 7:27.

Lund a, Knudsen SM, Vissing H, Clark B, Tommerup N (1996) Assignment of human elongation factor 1alpha genes: EEF1A maps to chromosome 6q14 and EEF1A2 to 20q13.3. Genomics 36:359–361.

Martin SJ, Grimwood PD, Morris RGM (2000) Synaptic Plasticity and Memory: An Evaluation of the Hypothesis. Annu Rev Neurosci 23:649–711.

Matsuo N, Takao K, Nakanishi K, Yamasaki N, Tanda K, Miyakawa T (2010) Behavioral profiles of three C57BL/6 substrains. Front Behav Neurosci 4:29.

Mazumder AG, Sharma P, Patial V, Singh D (2017) Crocin Attenuates Kindling Development and Associated Cognitive Impairments in Mice via Inhibiting Reactive Oxygen Species-Mediated NF-κB Activation. Basic Clin Pharmacol Toxicol 120:426–433.

Merrick WC (1992) Mechanism and regulation of eukaryotic protein synthesis. Microbiol Rev 56:291–315.

Meziane H, Ouagazzal AM, Aubert L, Wietrzych M, Krezel W (2007) Estrous cycle effects on behaviour of C57BL/6J and BALB/cByJ female mice: implications for phenotyping strategies. Genes, Brain and Behaviour 6:192-200.

Moldave K, Harris J, Sabo W, Sadnik I (1979) Protein synthesis and aging: studies with cell-free mammalian systems. Fed Proc 38:1979–1983.

Morris RG (n.d.) D.O. Hebb: The Organization of Behavior, Wiley: New York; 1949. Brain Res Bull 50:437.

Moy SS, Nadler JJ, Young NB, Perez A, Holloway LP, Barbaro RP, Barbaro JR, Wilson LM, Threadgill DW, Lauder JM, Magnuson TR, Crawley JN (2007) Mouse behavioral tasks relevant to autism: phenotypes of 10 inbred strains. Behav Brain Res 176:4–20.

Nakajima J, Okamoto N, Tohyama J, Kato M, Arai H, Funahashi O, Tsurusaki Y, Nakashima M, Kawashima H, Saitsu H, Matsumoto N, Miyake N (2014) De novo EEF1A2 mutations in patients with characteristic facial features, intellectual disability, autistic behaviors and epilepsy. Clin Genet 87:1–6.

Neu-Yilik G, Amthor B, Gehring NH, Bahri S, Paidassi H, Hentze MW, Kulozik AE (2011) Mechanism of escape from nonsense-mediated mRNA decay of human ß-globin transcripts with nonsense mutations in the first exon. RNA 17(5).

Newbery HJ, Gillingwater TH, Dharmasaroja P, Peters J, Wharton S, Thomson D, Ribchester R, Abbott C (2005) Progressive Loss of Motor Neuron Function in Wasted Mice: Effects of a Spontaneous Null Mutation in the Gene for the eEF1A2 Translation Factor. J Neuropathol Exp Neurol 64:295–303.

Newbery HJ, Loh DH, O'Donoghue JE, Tomlinson V a L, Chau Y-Y, Boyd J a, Bergmann JH, Brownstein D, Abbott CM (2007) Translation elongation factor eEF1A2 is essential for post-weaning survival in mice. J Biol Chem 282:28951–28959.

Osterweil EK, Chuang S, Chubykin AA, Sidorov M, Bianchi R, Wong RKS, Bear MF (2013) Report Lovastatin Corrects Excess Protein Synthesis and Prevents Epileptogenesis in a Mouse Model of Fragile X Syndrome. Neuron 77:243–250.

Paradee W, Melikian HE, Rasmussen DL, Kenneson A, Conn PJ, Warren ST (1999) Fragile X mouse: strain effects of knockout phenotype and evidence suggesting deficient amygdala function. Neuroscience 94:185–192.

Peñagarikano O, Abrahams BS, Herman EI, Winden KD, Gdalyahu A, Dong H, Sonnenblick LI, Gruver R, Almajano J, Bragin A, Golshani P, Trachtenberg JT, Peles E, Geschwind DH (2011) Absence of CNTNAP2 leads to epilepsy, neuronal migration abnormalities, and core autism-related deficits. Cell 147:235–246.

Pfeiffer BE, Zang T, Wilkerson JR, Taniguchi M, Maksimova MA, Smith LN, Cowan CW, Huber KM (2010) Fragile X Mental Retardation Protein Is Required for Synapse Elimination by the Activity-Dependent Transcription Factor MEF2. Neuron 66:191–197.

Pietropaolo S, Guilleminot A, Martin B, D'Amato FR, Crusio WE (2011) Genetic-background modulation of core and variable autistic-like symptoms in Fmr1 knock-out mice. PLoS One 6:1–11.

Queenan BN, Ryan TJ, Gazzaniga MS, Gallistel CR (2017) On the research of time past: the hunt for the substrate of memory. Ann N Y Acad Sci 1396:108–125.

Rattan SI, Clark BF (1996) Intracellular protein synthesis, modifications and aging. Biochem Soc Trans 24:1043–1049.

Reis A, Hornblower B, Robb B, Tzertzinis G (2014) CRISPR/Cas9 and Targeted Genome Editing: A New Era in Molecular Biology. URL: https://www.neb.com/tools-and-resources/feature-articles/crispr-cas9-and-targeted-genome-editing-a-new-era-in-molecular-biology [Accessed 7th July 2017].

Reith RM, Mckenna J, Wu H, Hashmi SS, Cho S, Dash PK, Gambello MJ (2013) Neurobiology of Disease Loss of Tsc2 in Purkinje cells is associated with autistic-like behavior in a mouse model of tuberous sclerosis complex. Neurobiol Dis 51:93–103.

Restivo L, Ferrari F, Passino E, Sgobio C, Bock J, Oostra BA, Bagni C, Ammassari-Teule M (2005) Enriched environment promotes behavioral and morphological recovery in a mouse model for the fragile X syndrome. Proc Natl Acad Sci U S A 102:11557–11562.

Ronemus M, Iossifov I, Levy D, Wigler M (2014) The role of de novo mutations in the genetics of autism spectrum disorders. Nat Rev Genet 15:133–141.

Ross KC, Coleman JR (2000) Developmental and genetic audiogenic seizure models: behavior and biological substrates. Neurosci Biobehav Rev 24:639–653.

Ruan MZC, Patel RM, Dawson BC, Jiang M-M, Lee BHL (2013) Pain, motor and gait assessment of murine osteoarthritis in a cruciate ligament transection model. Osteoarthr Cartil 21:1355–1364.

Ruest L-B, Marcotte R, Wang E (2002) Peptide elongation factor eEF1A-2/S1 expression in cultured differentiated myotubes and its protective effect against caspase-3-mediated apoptosis. J Biol Chem 277:5418–5425.

Sandbaken MG, Culbertson MR (1988) Mutations in elongation factor EF-1 alpha affect the frequency of frameshifting and amino acid misincorporation in Saccharomyces cerevisiae. Genetics 120:923–934.

Santos AR, Kanellopoulos AK, Bagni C (2014) Learning and behavioral deficits associated with the absence of the fragile X mental retardation protein: what a fly and mouse model can teach us. Learn Mem 21:543–555.

Sasikumar AN, Perez WB, Kinzy TG (2012) The many roles of the eukaryotic elongation factor 1 complex. Wiley Interdiscip Rev RNA 3:543–555.

Schlaeger C, Longerich T, Schiller C, Bewerunge P, Mehrabi A, Toedt G, Kleeff J, Ehemann V, Eils R, Lichter P, Schumacher P, Radlwimmer B (2008) Etiology-dependent molecular mechanisms in human hepatocarcinogenesis. Hepatology 47:511–520.

Schmeisser MJ et al. (2012) Autistic-like behaviours and hyperactivity in mice lacking ProSAP1/Shank2. Nature 486:256–260.

Seibenhener ML, Wooten MC (2015) Use of the Open Field Maze to measure locomotor and anxiety-like behavior in mice. J Vis Exp 96:e52434.

Shanks DR, John MFS (1994) Characteristics of dissociable human learning systems. Behav Brain Sci 17:367–447.

Sharma A, Hoeffer CA, Takayasu Y, Miyawaki T, McBride SM, Klann E, Zukin RS (2010a) Dysregulation of mTOR signaling in fragile X syndrome. J Neurosci 30:694–702.

Sharma S, Rakoczy S, Brown-Borg H (2010b) Assessment of spatial memory in mice. Life Sci 87:521–536.

Shepherd JC, Walldorf U, Hug P, Gehring WJ (1989) Fruit flies with additional expression of the elongation factor EF-1 alpha live longer. Proc Natl Acad Sci U S A 86:7520–7521.

Shikama N, Ackermann R, Brack C (1994) Protein synthesis elongation factor EF-1 alpha expression and longevity in Drosophila melanogaster. Proc Natl Acad Sci U S A 91:4199–4203.

Shultz LD, Sweet HO, Davisson MT, Coman DR (1982) "Wasted", a new mutant of the mouse with abnormalities characteristic to ataxia telangiectasia. Nature 297:402–404.

Silar P, Picard M (1994) Increased longevity of EF-1 alpha high-fidelity mutants in Podospora anserina. J Mol Biol 235:231–236.

Silverman JL, Yang M, Lord C, Crawley JN (2010) Behavioural phenotyping assays for mouse models of autism. Nat Rev Neurosci 11:490–502.

Singh P, Schimenti JC, Bolcun-Filas E (2015) A mouse geneticist's practical guide to CRISPR applications. Genetics 199:1–15.

Soares DC, Abbott CM (2013) Highly homologous eEF1A1 and eEF1A2 exhibit differential post-translationalmodification with significant enrichment around localised sites of sequence variation. Biol Direct 8:29.

Soares DC, Barlow PN, Newbery HJ, Porteous DJ, Abbott CM (2009) Structural models of human eEF1A1 and eEF1A2 reveal two distinct surface clusters of sequence variation and potential differences in phosphorylation. PLoS One 4.

Spencer CM, Alekseyenko O, Hamilton SM, Thomas AM, Serysheva E, Yuva-Paylor LA, Paylor R (2011) Modifying behavioral phenotypes in Fmr1KO mice: genetic background differences reveal autistic-like responses. Autism Res 4:40–56.

Squire LR (2009) The Legacy of Patient H.M. for Neuroscience. Neuron 61:6–9.

Srivastava AK, Schwartz CE (2014) Intellectual disability and autism spectrum disorders: Causal genes and molecular mechanisms. Neurosci Biobehav Rev 46:161-174.

Subramanian M, Timmerman CK, Schwartz JL, Pham DL, Meffert MK (2015) Characterizing autism spectrum disorders by key biochemical pathways. Front Neurosci 9:313.

Sung YJ, Dolzhanskaya N, Nolin SL, Brown T, Currie JR, Denman RB (2003) The fragile X mental retardation protein FMRP binds elongation factor 1A mRNA and negatively regulates its translation in vivo. J Biol Chem 278:15669–15678.

Sungur AÖ, Jochner MCE, Harb H, Kılıç A, Garn H, Schwarting RKW, Wöhr M (2017) Aberrant cognitive phenotypes and altered hippocampal BDNF expression related to epigenetic modifications in mice lacking the post-synaptic scaffolding protein SHANK1: Implications for autism spectrum disorder. Hippocampus 27:906–919.

Svobodová K, Horák P, Stratil A, Bartenschlager H, Van Poucke M, Chalupová P, Dvořáková V, Knorr C, Stupka R, Čítek J, Šprysl M, Palánová A, Peelman LJ, Geldermann H, Knoll A (2015) Porcine EEF1A1 and EEF1A2 genes: genomic structure, polymorphism, mapping and expression. Mol Biol Rep 42:1257–1264.

Sweet H (1984) Wasted linkage. Mouse News Letter 71:31.

Takao K, Miyakawa T (2006) Light/dark transition test for mice. J Vis Exp 1:104.

Timchenko AA, Novosylna O V, Prituzhalov EA, Kihara H, El'skaya A V, Negrutskii BS, Serdyuk IN (2013) Different oligomeric properties and stability of highly homologous A1 and proto-oncogenic A2 variants of mammalian translation elongation factor eEF1. Biochemistry 52:5345–5353.

Tomlinson V AL, Newbery HJ, Wray NR, Jackson J, Larionov A, Miller WR, Dixon JM, Abbott CM (2005) Translation elongation factor eEF1A2 is a potential oncoprotein that is overexpressed in two-thirds of breast tumours. BMC Cancer 5:113.

Topol A et al. (2015) Increased abundance of translation machinery in stem cell–derived neural progenitor cells from four schizophrenia patients. Transl Psychiatry 5:e662.

Touma C, Palme R, Sachser N (2004) Analyzing corticosterone metabolites in fecal samples of mice: A noninvasive technique to monitor stress hormones. Horm Behav 45:10–22.

Tsai N-P, Wilkerson JR, Guo W, Maksimova MA, DeMartino GN, Cowan CW, Huber KM (2012) Multiple autism-linked genes mediate synapse elimination via proteasomal degradation of a synaptic scaffold PSD-95. Cell 151:1581–1594.

Tsokas P, Grace EA, Chan P, Ma T, Sealfon SC, Iyengar R, Landau EM, Blitzer RD (2005) Local Protein Synthesis Mediates a Rapid Increase in Dendritic Elongation Factor 1A after Induction of Late Long-Term Potentiation. J Neurosci 25:5833–5843.

Veeramah KR, Johnstone L, Karafet TM, Wolf D, Sprissler R, Salogiannis J, Barth-Maron A, Greenberg ME, Stuhlmann T, Weinert S, Jentsch TJ, Pazzi M, Restifo LL, Talwar D, Erickson RP, Hammer MF (2013) Exome sequencing reveals new causal mutations in children with epileptic encephalopathies. Epilepsia 54:1270–1281.

Ventura R, Pascucci T, Catania M V, Musumeci SA, Puglisi-Allegra S (2004) Object recognition impairment in Fmr1 knockout mice is reversed by amphetamine: involvement of dopamine in the medial prefrontal cortex. Behav Pharmacol 15:433–442.

Vera M, Pani B, Griffiths LA, Muchardt C, Abbott CM, Singer RH, Nudler E (2014) The translation elongation factor eEF1A1 couples transcription to translation during heat shock response. Elife 16:1–19.

Verkerk AJMH et al. (1991) Identification of a gene (FMR-1) containing a CGG repeat coincident with a breakpoint cluster region exhibiting length variation in fragile X syndrome. Cell 65:905–914.

Vlasenko DO, Novosylna O V, Negrutskii BS, El A V (2015) Truncation of the A , A／, A 0 helices segment impairs the actin bundling activity of mammalian eEF1A1. FEBS Lett 589:1187–1193.

Vorstman JAS, Parr JR, Moreno-De-Luca D, Anney RJL, Nurnberger Jr JI, Hallmayer JF (2017) Autism genetics: opportunities and challenges for clinical translation. Nat Rev Genet 18:362–376.

Wagnon JL, Korn MJ, Parent R, Tarpey TA, Jones JM, Hammer MF, Murphy GG, Parent JM, Meisler MH (2015) Convulsive seizures and SUDEP in a mouse model of SCN8A epileptic encephalopathy. Hum Mol Genet 24:506–515.

Wang X, Snape M, Klann E, Stone JG, Singh A, Petersen RB, Castellani RJ, Casadesus G, Smith MA, Zhu X (2012) Activation of the extracellular signal-regulated kinase pathway contributes to the behavioral deficit of fragile x-syndrome. J Neurochem 121:672–679.

Webster GC, Webster SL (1983) Decline in synthesis of elongation factor one (EF-1) precedes the decreased synthesis of total protein in aging Drosophila melanogaster. Mech Ageing Dev 22:121–128.

Wöhr M, Scattoni ML (2013) Behavioural methods used in rodent models of autism spectrum disorders: current standards and new developments. Behav Brain Res 251:5–17.

Won H, Lee H-R, Gee HY, Mah W, Kim J-I, Lee J, Ha S, Chung C, Jung ES, Cho YS, Park S-G, Lee J-S, Lee K, Kim D, Bae YC, Kaang B-K, Lee MG, Kim E (2012) Autistic-like social behaviour in Shank2-mutant mice improved by restoring NMDA receptor function. Nature 486:261–265.

Yang M, Bozdagi O, Scattoni ML, Wohr M, Roullet FI, Katz a. M, Abrams DN, Kalikhman D, Simon H, Woldeyohannes L, Zhang JY, Harris MJ, Saxena R, Silverman JL, Buxbaum JD, Crawley JN (2012) Reduced Excitatory Neurotransmission and Mild Autism-Relevant Phenotypes in Adolescent Shank3 Null Mutant Mice. J Neurosci 32:6525–6541.

Yang Y et al. (2014) Molecular Findings Among Patients Referred for Clinical Whole-Exome Sequencing. Jama 312:1870–1879.

Zayachkivsky A, Lehmkuhle MJ, Dudek FE (2015) Long-term Continuous EEG Monitoring in Small Rodent Models of Human Disease Using the Epoch Wireless Transmitter System. J Vis Exp 101:e52554.

Zhong J, Zhang T, Bloch LM (2006) Dendritic mRNAs encode diversified functionalities in hippocampal pyramidal neurons. BMC Neurosci 7:17.

Zhou J, Blundell J, Ogawa S, Kwon C-H, Zhang W, Sinton C, Powell CM, Parada LF (2009) Pharmacological Inhibition of mTORC1 Suppresses Anatomical, Cellular, and Behavioral Abnormalities in Neural-Specific Pten Knock-Out Mice. J Neurosci 29:1773–1783.

Zoghbi HY, Bear MF (2012) Synaptic Dysfunction in Neurodevelopmental Disorders Associated with Autism and Intellectual Disabilities. Cold Spring Harb Perspect Biol 4.